



Design, Synthesis and Applications of Chiral Functionalized  
Phosphapalladacycles

**Li Xi-Rui**

School of Physical and Mathematical Sciences

Nanyang Technological University

**2018**

## Statement of Originality

I hereby certify that the work embodied in this thesis is the result of original research, is free of plagiarised materials, and has not been submitted for a higher degree to any other University or Institution.

15 Jan. 2019

Date

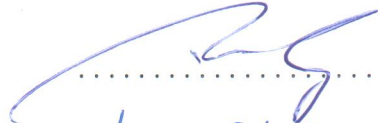


Li Xirui

## Supervisor Declaration Statement

I have reviewed the content and presentation style of this thesis and declare it is free of plagiarism and of sufficient grammatical clarity to be examined. To the best of my knowledge, the research and writing are those of the candidate except as acknowledged in the Author Attribution Statement. I confirm that the investigations were conducted in accord with the ethics policies and integrity standards of Nanyang Technological University and that the research data are presented honestly and without prejudice.

15/1/2019  
.....  
Date

  
.....  
Leung Pak-Hing

## Authorship Attribution Statement

This thesis contains material from 3 papers published in the following peer-reviewed journal(s) where I was the first author.

Chapter 2 is published as X.-R. Li, R. J. Chew, Y. Li, and P.-H. Leung. Investigation of Functional Group Effects on Palladium Catalysed Asymmetric P-H Addition. *Australian Journal of Chemistry* **69(5)**, 499-504 (2016). DOI: 10.1071/CH15577.

The contributions of the co-authors are as follows:

- Prof. Leung and Dr. Chew provided the initial project.
- I designed the study scheme and leded the all experiments.
- Dr. Li Yongxin assisted in the interpretation of the X-ray absorption spectroscopy data and carried out the spectral interpretation.

Chapter 3 is published as X.-R. Li, X.-Y. Yang, Y. Li, S. A. Pullarkat, and P.-H. Leung. Efficient access to a designed phosphapalladacycle catalyst via enantioselective catalytic asymmetric Hydrophosphination. *Dalton Transactions* **46(4)**, 1311-1316 (2017). DOI: 10.1039/C6DT04447F.

The contributions of the co-authors are as follows:

- Prof. Leung and I provided the initial project and design the whole project.
- I designed the study scheme and leded the all the expanding experiments.
- Dr. Li Yongxin assisted in the interpretation of the X-ray absorption spectroscopy data and carried out the spectral interpretation.
- Dr. Yang drafted the manuscript.
- Dr. Pullarkat assisted in submission of the manuscript draft.

Chapter 4 is published as X.-R. Li, Y. Chen, P. B. Pang, J. Tan, Y. Li, S. A. Pullarkat, and P.-H. Leung. Efficient Synthesis of Malonate Functionalized Chiral Phosphapalladacycles and their Catalytic Evaluation in Asymmetric

Hydrophosphination of Chalcone. *European Journal of Inorganic Chemistry* **39**, 4385-4390 (2018). DOI: 10.1002/ejic.201800720

The contributions of the co-authors are as follows:

- Prof. Leung and I provided the initial project and design the whole project.
- I designed the study scheme and leded the all the expanding experiments.
- Dr. Li Yongxin assisted in the interpretation of the X-ray absorption spectroscopy data and carried out the spectral interpretation.
- Prof. Chen drafted the manuscript.
- Dr. Pullarkat assisted in submission of the manuscript draft.
- Mr. Pang and Miss Tan assisted in preparing some materials.

15 Jan. 2019

.....  
Date

LXin

.....  
Li Xirui

## Acknowledgement

I'm very much obliged to my supervisor Leung Pak-Hing for his great help in chemistry and kind hearted. For these four years of pursuing the Doctor of Philosophy, knowledgeable Prof. Leung always enlightened me in the world of chemistry during the projects and showed me how to be a qualified researcher. I really appreciate that Prof. Leung was so nice to trust me in chemistry, allowed me to do project I want, and gave me lots of freedom to achieve me own aim. I'm very grateful to have Prof. Leung's support when my projects were in trouble. Thanks to my supervisor professor Leung Pak-Hing for introducing me the research, encouraging me when I was down in research or life, and showing me what the life should be.

Special thanks to Prof. Chen Yu, who is a visiting professor from the City University of New York in our lab. He is so generous to share lots of experience in research, teach me how to have a nice writing of article, and help me to revise the article. I truly appreciate that professor Chen is so nice and kind hearted to help me and show me how to select the journals and the history of them.

I would be grateful to my seniors, Drs. Sumod A. Pullarkat, Yuan Mingjun, Chew Renta Jonathan, Li Binbin, Jia Yuxiang, Yang Xiangyuan, Kennard Gan, and Jeremy Chen Houguang for the kind suggestion and advice. I also would like to show my gratitude to my lab mates, Balazs Laszlo Bertalan, Katona David, Abdul Sadeer Bin Abd Salam, Tay Wee Shan, and Wong Zheng-Zing Jonathan for encouragement and communications about the projects and experiments. The harmonious circumstance they created in the lab really help me to focus on my research. The friendship between us made me focused on life and research better. Special thanks to Dr. Jeremy and Mr. Laszlo, who gave me lots of suggestions and help in research and life. They are so kind hearted and generous that we would like to be lifelong friend with them.

Special mention goes to my family and all my friends, they always were on my side whenever I need help and delighted me all the time. They gave me the strength and

power to live, and the happiness of them is the meaning of life for me. Thanks to them for creating the very nice and beautiful world for me. The love, beauty, responsibility, satisfaction, and compassion filled in my heart because of them.

I also must thank the staffs in general office, Dr. Li Yongxin, Ms. Seow Ai Hua, Goh Eeling, Zhu Wen Wei, Koh Su Ping, and Lee Yean Chin for the kind assistance of X-ray crystallography, NMR, MS, teaching lab facilities and other matters in the office. Thanks to them to help me to get my research so smooth.

Last but not least, I would like to thank the Division of Chemistry and Biological Chemistry, School of Physical and Mathematical Sciences, Nanyang Technological University, and the Graduate Assistantship Programme in Singapore for supporting my research as well as the scholarship.

## CONTENT

Acknowledgement .....	I
Summary .....	V
Abbreviations and Symbols .....	IX
List of Tables .....	XI
List of Schemes .....	XIII
List of Figures .....	XVII
Chapter 1. Introduction.....	1
1.1. The mechanism and features of cyclopalladation of amines .....	1
1.2. CN <i>ortho</i> -palladacycles complexes with five-membered ring .....	2
1.2.1. The development and applications of 5-membered benzylic CN <i>ortho</i> -palladacycles .....	2
1.2.2. The development and applications of 5-membered naphthyl CN <i>ortho</i> -palladacycles .....	13
1.2.3. The synthesis and applications of 5-membered optically active CN palladacycles .....	14
1.3. CP palladium complexes.....	20
1.3.1. The development of CP complexes.....	20
1.3.2. The chiral CP palladium complexes.....	21
1.3.3. The application of CP palladium complexes.....	24
1.4. Recent development in our group .....	25
1.4.1. The design and synthesis of cyclopalladated complexes .....	25
1.4.2. Chiral CN palladacycles promoted the cycloaddition .....	29
1.4.3. The chiral CN palladacycle as the template for P-H addition ....	30
1.4.4. The catalytic asymmetric hydrophosphination of the activated unsaturated multiple bond.....	33
1.4.5. Asymmetric hydroarsination .....	35
1.5. Objectives of projects .....	35

Chapter 2. Investigation of Functional Group Effects on Palladium Catalyzed Asymmetric P-H Addition .....	37
2.1. Introduction.....	37
2.2. Results and Discussion .....	40
2.3. Conclusion .....	46
2.4. Experimental section.....	47
Chapter 3. Efficient Access to a Designer Phosphapalladacycle Catalyst <i>via</i> Enantioselective Catalytic Asymmetric Hydrophosphination .....	55
3.1. Introduction.....	55
3.2. Results and Discussion .....	58
3.3. Conclusion .....	64
3.4. Experimental section.....	65
Chapter 4. Efficient Synthesis of Malonate Functionalized Chiral Phosphapalladacycles and Their Catalytic Evaluation in Asymmetric Hydrophosphination of Chalcone .....	93
4.1. Introduction.....	93
4.2. Results and discussion .....	95
4.3. Conclusions.....	102
4.4. Experimental section.....	103
Chapter 5. Asymmetric Catalytic P-H Addition Reaction of $\alpha,\beta$ -Unsaturated Sulfonyl Fluoride	131
5.1. Introduction.....	131
5.2. Results and discussion .....	132
5.3. Conclusion .....	138
5.4. Experimental section.....	138
References.....	147
Publications and Conferences .....	173

## Summary

This thesis is focused on the design, synthesis and application of a series of C-stereogenic functionalized naphthyl CP phosphapalladacycles with five-membered organometallic ring within its framework *via* a stepwise asymmetric hydrophosphination and metalation procedure.

According to the effective catalytic properties and tedious synthesis procedures of the chiral CP palladacycle derived from 1-(1-naphthyl)ethyldiphenylphosphine, it is urgent to design new catalysts. We designed and synthesized its analogues with catalytic methods through atom economic green way and saving the chiral auxiliaries to proceed the resolution. The optically active phosphine ligands for the palladacycles were synthesized *via* the asymmetric catalytic P-H addition of diphenylphosphine across activated double bonds. The optimization of the conditions was conducted by screening the solvents, temperature, base, catalysts and functional group. The enantiomeric excess values of the chiral phosphine ligands were determined by  $^{31}\text{P}\{^1\text{H}\}$  NMR spectroscopy upon coordination of the ligands to chiral CN palladium complexes forming a pair of diastereomers or by HPLC after sulfuration of the free air-sensitive ligands. The conversion of the phosphine ligands was determined by  $^{31}\text{P}\{^1\text{H}\}$  NMR spectroscopy. Normally polar solvents tend to accelerate the reaction rates and shorten the reaction time. A lower temperature induced better enantiomeric excess albeit with long time. The base was necessary to activate the P-H bond. The mechanism of the P-H addition was also explained in this thesis in Chapter 5. The conditions of metalation were optimized by screening the base, solvent, palladium source, and purify procedures.

In Chapter 1, an introduction to the synthesis and application of CN and CP cyclopalladated five-membered complexes with/without the chiral center is presented. In the end, the works of our lab in the past decade were classified and discussed. The CN complexes and their CP and CAs analogues have similar synthetic pathway and

properties as they belong to the same main group in the periodic table, and all of them have a lone pair electron that can coordinate to the metal such as Pd, Ir, Pt, Fe *etc.* However, they are different with each other as the phosphorus and arsenic have the vacant orbitals, which can back-donating from the metal.

In Chapter 2, the intricate reason of how various functional groups borne on the substrate can influence the performance of selected palladacycle catalysts is explored in this study, providing valuable insights on the choice of catalyst for structurally distinct substrates. The employment of a mono-coordination site palladium pincer catalyst circumvents catalyst inactivation by the starting material, facilitating the first known asymmetric preparation of phosphines bearing a diketone functionality. While the *ee* values obtained are at best moderate, modifications to the pincer catalyst could potentially engender improvements in the obtained results. A plausible mechanistic cycle has been proposed for the asymmetric hydrophosphination reaction.

In Chapter 3, a chiral phosphine auxiliary was generated quantitatively with excellent *ee* via catalytic asymmetric hydrophosphination of 3-(naphthalen-1-ylmethylene)pentane-2,4-dione. The subsequent metal complexation of the monophosphine yielded two different coordination complexes depending on the reaction conditions. The ortho-palladation of both coordination complexes resulted in the formation of a single dimeric phosphapalladacycle complex that could be further converted to the monomeric bisacetonitrile derivative. Moreover, the palladium complex exhibits interesting oxophilicity as the stable bisquo derivative could be isolated and characterized crystallographically. The catalytic potential of the phosphapalladacycle was also demonstrated. The main factor preventing the advancement of bidentate phosphapalladacycles in asymmetric catalysis has been overcome successfully. The simple catalytic protocol (**Scheme 38**, **Table 6**) is attractive due to the efficiency in preparing chiral phosphine auxiliaries quantitatively without the need for classical resolution techniques. A preliminary investigation on the catalytic potential of the new palladacycle was promising, yielding the desired product with excellent *ee*. It was kept

a positive outlook towards the prospects of the new phosphapalladacycle catalyst. In light of previous experience, the benefits of installing an ester functional group as opposed to a simple methyl group in the palladacycle backbone should be highlighted. It was reported that a P-H bond addition reaction did not proceed in the presence of a pincer catalyst with methyl substituents, but the same reaction could be conducted with an analogous pincer catalyst with ester functionalities. Further developments in the architecture of the palladacycle complexes will be conducted and their application in other transformation reactions will be examined.

In Chapter 4, four functionalized chiral phosphapalladacycle complexes have been efficiently prepared by sequential asymmetric hydrophosphination (P-H reaction) and cyclometallation reaction. The impact of installation of malonate moiety at the chiral carbon as well as the modification of the naphthalene ring system was studied for the asymmetric hydrophosphination reaction. These preliminary results will serve as a guide for the rational design of other functionalized phosphapalladacycles using this alternate synthetic methodology.

In Chapter 5, an optically active fluorosulfonyl-phosphine ligand has been prepared *via* cyclopalladated complex catalyzed asymmetric P-H addition reaction in technically quantitative yield with up to 90% *ee* under mild conditions. Several readily available CP-palladacycles could be employed as catalysts with similar efficiency for the asymmetric addition reaction. Currently, the synthetic applications and biological properties of the novel chiral sulfonyl-substituted phosphine and its metal complexes are studied in our group.



## Abbreviations and Symbols

°	degree of angles
$\delta$	NMR chemical shift in ppm
$[\alpha]_D$	specific rotation measured at sodium D line (589 nm)
Å	angstrom(s)
Ar	aryl group
BINAP	2,2'-bis(diphenylphosphino)-1,1'-binaphthyl
Bn	benzyl group
°C	degree Celsius
calcd.	calculated
conc.	concentrated
d	day(s)
d	doublet (NMR)
dba	dibenzylideneacetone
DCM	dichloromethane
<i>de</i>	diastereomeric excess
DMF	<i>N,N</i> -dimethylformamide
dppe	1,2-bis(diphenylphosphanyl)ethane
<i>ee</i>	enantiomeric excess
equiv.	equivalent
ESI-MS	electrospray ionization mass spectrometry
Et	Ethyl group
<i>et al.</i>	and others (Latin <i>et alii</i> )
FG	Functional group
g	gram(s)

h	hour(s)
Hz	hertz
m	multiplet(NMR)
min	minute(s)
mL	milliliter
mmol	millimole(s)
Mp	melting point
NMR	Nuclear Magnetic Resonance
ppm	parts per million
Pr	propyl group
<i>R</i>	rectus (Latin right absolute configuration)
rt	room temperature
s	singlet (NMR)
<i>S</i>	sinister (Latin left absolute configuration)
t	triplet (NMR)
T	temperature
THF	tetrahydrofuran
TMS	tetramethylsilane
TON	turn over number

## List of Tables

<b>Table 1:</b> Optimization of reaction conditions for ( <i>S,S</i> )- <b>54e</b> catalyzed asymmetric P-H addition of <b>66c</b> with diphenylphosphine (Ph <sub>2</sub> PH) <sup>a</sup> .....	42
<b>Table 2:</b> Sample and crystal data for leung872s.....	49
<b>Table 3:</b> Data collection and structure refinement for leung872s .....	50
<b>Table 4:</b> Sample and crystal data for leung881 .....	52
<b>Table 5:</b> Data collection and structure refinement for leung881 .....	52
<b>Table 6:</b> Optimization of reaction conditions <sup>a</sup> .....	58
<b>Table 7:</b> Catalytic asymmetric hydrophosphination <sup>a</sup> .....	63
<b>Table 8:</b> Data collection and structure refinement for complex ( <i>S</i> )- <b>87</b> .....	74
<b>Table 9:</b> Bond lengths (Å) for complex ( <i>S</i> )- <b>87</b> .....	75
<b>Table 10:</b> Bond angles (°) for complex ( <i>S</i> )- <b>87</b> .....	76
<b>Table 11:</b> Data collection and structure refinement for complex ( <i>S</i> )- <b>80b</b> .....	77
<b>Table 12:</b> Bond lengths (Å) for complex ( <i>S</i> )- <b>80b</b> .....	78
<b>Table 13:</b> Bond angles (°) for complex ( <i>S</i> )- <b>80b</b> .....	79
<b>Table 14:</b> Data collection and structure refinement for complex ( <i>S</i> )- <b>86a</b> .....	81
<b>Table 15:</b> Bond lengths (Å) for complex ( <i>S</i> )- <b>86a</b> .....	82
<b>Table 16:</b> Bond angles (°) for complex ( <i>S</i> )- <b>86a</b> .....	84
<b>Table 17:</b> Data collection and structure refinement for complex ( <i>S</i> )- <b>89</b> .....	87
<b>Table 18:</b> Bond lengths (Å) for complex ( <i>S</i> )- <b>89</b> .....	88
<b>Table 19:</b> Bond angles (°) for complex ( <i>S</i> )- <b>89</b> .....	89
<b>Table 20:</b> Coordination reaction and optical resolution of palladacycles. ....	96
<b>Table 21:</b> Screening of mixed solvent systems for the asymmetric P-H reaction catalyzed by ( <i>R</i> )- <b>67</b> .....	98
<b>Table 22:</b> The cyclometallation reaction of free ligands.....	99
<b>Table 23:</b> The application of complexes <b>88</b> in catalytic hydrophosphination of chalcone .....	102
<b>Table 24:</b> Data collection and structure refinement for complex ( <i>S</i> )- <b>86d</b> .....	113

<b>Table 25:</b> Bond lengths (Å) for (S)- <b>86d</b> .....	114
<b>Table 26:</b> Bond angles (°) for (S)- <b>86d</b> .....	115
<b>Table 27:</b> Data collection and structure refinement for complex (S)- <b>86e</b> .....	116
<b>Table 28:</b> Bond lengths (Å) for complex (S)- <b>86e</b> .....	118
<b>Table 29:</b> Bond angles (°) for complex (S)- <b>86e</b> .....	119
<b>Table 30:</b> Data collection and structure refinement for complex (S)- <b>86f</b> .....	121
<b>Table 31:</b> Bond lengths (Å) for complex (S)- <b>86f</b> .....	123
<b>Table 32:</b> Bond angles (°) for complex (S)- <b>86f</b> .....	125
<b>Table 33:</b> The Pd catalyzed asymmetric P-H addition reaction of sulfonyl fluoride .....	134
<b>Table 34:</b> Data collection and structure refinement for complex <b>92</b> .....	141
<b>Table 35:</b> Bond lengths (Å) for complex <b>92</b> .....	142
<b>Table 36:</b> Bond angles (°) for complex <b>92</b> .....	143

## List of Schemes

<b>Scheme 1:</b> The mechanism of cyclopalladation .....	1
<b>Scheme 2:</b> Cyclopalladation of azobenzene .....	2
<b>Scheme 3:</b> Cyclopalladation between lithium tetrachloropalladate(II) and tertiary benzylamines.....	3
<b>Scheme 4:</b> Regiocontrolled aromatic palladations .....	4
<b>Scheme 5:</b> <i>Ortho</i> -palladation through silver salt.....	5
<b>Scheme 6:</b> The cyclopalladation by oxidative addition of <i>ortho</i> -bromobenzylamine .....	5
<b>Scheme 7:</b> The palladation of unsubstituted benzylamines.....	6
<b>Scheme 8:</b> Synthesis of dimeric cyclopalladated complex of (2,5- dialkylphenyl)ethylamine .....	8
<b>Scheme 9:</b> Palladation of primary nitrobenzylamine .....	9
<b>Scheme 10:</b> Cyclopalladation without solvent on silica gel.....	10
<b>Scheme 11:</b> The reaction between cyclopalladated amines and <i>para</i> -substituted styrene.....	11
<b>Scheme 12:</b> Insertion of alkynes into palladium-carbon bond of cyclopalladated compounds .....	12
<b>Scheme 13:</b> Depalladation of cyclopalladated complexes .....	13
<b>Scheme 14:</b> Synthesis of optically active CN palladacycles .....	14
<b>Scheme 15:</b> Resolution of racemic cyclopalladated compounds .....	15
<b>Scheme 16:</b> Resolution of CN <i>ortho</i> -palladacycles by chiral phosphine ligands	15
<b>Scheme 17:</b> Cyclopalladated complex as promoter of hydrophosphination .....	16
<b>Scheme 18:</b> Asymmetric hydroamination reaction promoted by chiral palladacycles .....	17
<b>Scheme 19:</b> Template of [4+2] Diels-Alder cycloaddition .....	18
<b>Scheme 20:</b> Claisen rearrangement catalyzed by chiral CN palladacycles.....	19
<b>Scheme 21:</b> palladacycles as resolving agent of phosphines.....	20

<b>Scheme 22:</b> The asymmetric catalytic phosphination .....	21
<b>Scheme 23:</b> The <i>ortho</i> -cyclopalladation of free phosphines directly .....	21
<b>Scheme 24:</b> The cyclopalladation of CP ligands .....	23
<b>Scheme 25:</b> The resolution of CP complexes with potassium <i>L</i> -prolinate.....	23
<b>Scheme 26:</b> the synthesis of chiral phosphines <i>via</i> asymmetric P-H addition .....	24
<b>Scheme 27:</b> CP palladated complexes as the template to give enamines.....	25
<b>Scheme 28:</b> the synthesis of pyridine-N-heterocyclic carbene palladacycle.....	27
<b>Scheme 29:</b> The synthesis and resolution of the CP bidentate complexes.....	29
<b>Scheme 30:</b> Asymmetric catalytic synthesis of CP palladacycle .....	29
<b>Scheme 31:</b> The double P-H addition.....	31
<b>Scheme 32:</b> The P-H addition to benzoquinones .....	35
<b>Scheme 33:</b> Coordination studies revealing keto-enol tautomeric products prior and after coordination to palladacycle ( <i>R</i> )- <b>24a-Cl</b> .....	43
<b>Scheme 34:</b> Silica induced tautomerization of sulphurized phosphine adducts...	45
<b>Scheme 35:</b> Proposed catalytic cycle for the Pd-pincer catalyzed hydrophosphination of 3-benzylidenepentane-2,4-dione.....	46
<b>Scheme 36:</b> Multi-step synthesis of optically pure dimeric complex <b>85</b> .....	57
<b>Scheme 37:</b> Retrosynthetic pathway of complex <b>99b</b> .....	57
<b>Scheme 38:</b> Cyclopalladation of tertiary phosphine ( <i>S</i> )- <b>70a</b> .....	60
<b>Scheme 39:</b> Preparation of monomeric Pd complexes .....	62
<b>Scheme 40:</b> Catalytic asymmetric hydrophosphination of malonate 9 .....	66
<b>Scheme 41:</b> Synthesis of coordination complex ( <i>S</i> )- <b>39a</b> .....	67
<b>Scheme 42:</b> Synthesis of P-O bidentate complex ( <i>S</i> )- <b>80b</b> .....	68
<b>Scheme 43:</b> Synthesis of dimeric complex ( <i>S</i> )- <b>86a</b> .....	69
<b>Scheme 44:</b> Synthesis of monomeric bisacetonitrile complex ( <i>S</i> )- <b>88a</b> .....	69
<b>Scheme 45:</b> Synthesis of monomeric bisquo complex ( <i>S</i> )- <b>89</b> .....	70
<b>Scheme 46:</b> Catalytic asymmetric hydrophosphination of substrates <b>75b</b> and <b>75c</b> .....	71

<b>Scheme 47:</b> Synthesis of gold(I)-phosphine complex ( <i>S</i> )- <b>87</b> .....	72
<b>Scheme 48:</b> Overview of the traditional procedure for the synthesis of phosphapalladacycle ( <i>R</i> )- <b>67</b> .....	95
<b>Scheme 49:</b> Synthesis of ( <i>S</i> )- <b>86</b> from racemic phosphine ligands .....	97
<b>Scheme 50:</b> Stereoselective synthesis of ( <i>S</i> )- <b>86</b> <i>via</i> ( <i>R</i> )- <b>67</b> catalyzed asymmetric hydrophosphination and subsequent cyclometallation .....	97
<b>Scheme 51:</b> Treatment of the <b>86</b> with <i>L</i> -proline to examine the enantiomeric purity .....	101
<b>Scheme 52:</b> Synthesis of the CP catalyst ( <i>S</i> )- <b>88</b> .....	102
<b>Scheme 53:</b> Proposed catalytic cycle involving an intramolecular mechanism.	138



## List of Figures

<b>Figure 1:</b> The monomeric cyclopalladated complexes with triphenylphosphine	10
<b>Figure 2:</b> The structure of naphthyl and phenyl palladacycles .....	13
<b>Figure 3:</b> The optically active CN cyclopalladated complexes <i>via</i> sodium <i>L</i> -prolinate .....	15
<b>Figure 4:</b> Chemical list which synthesized <i>via</i> [4+2] cycloaddition reaction promoted by palladacycles.....	19
<b>Figure 5:</b> List of the amine palladated compounds in our lab.....	26
<b>Figure 6:</b> The list of the pincer complexes in our lab .....	28
<b>Figure 7:</b> The list of Iridium complexes.....	29
<b>Figure 8:</b> The list of the cycloaddition adducts .....	30
<b>Figure 9:</b> The asymmetric promoted synthesis of the bidentate ligands .....	32
<b>Figure 10:</b> List of the products of the catalytic asymmetric hydrophosphination	34
<b>Figure 11:</b> The list of promoted adducts for As-H addition.....	35
<b>Figure 12:</b> General classification of established palladacycles.....	37
<b>Figure 13:</b> Improved efficacy of palladacycle ( <i>R</i> )- <b>24a-Cl</b> as a chiral derivatizing agent versus its benzylamine analogue ( <i>R</i> )- <b>4p-Cl</b> .....	38
<b>Figure 14:</b> Disruption of aromaticity in sterically demanding auxiliary upon complexation with palladium.....	38
<b>Figure 15:</b> Phosphapalladacycles employed in the AHP reaction .....	39
<b>Figure 16:</b> Introduction of activating groups to poorly activated Michael acceptors .....	40
<b>Figure 17:</b> Catalyst inactivation owing to formation of stable chelates between palladacycles <b>64/67</b> and the substrate .....	41

<b>Figure 18:</b> Molecular structure and absolute stereochemistry of chelate <b>80a</b> with 50% thermal ellipsoids shown. Hydrogen atoms except those on the chiral center are omitted for clarity .....	43
<b>Figure 19:</b> Molecular structure of the gold(I)-phosphine adduct <b>90c</b> with 50% thermal ellipsoids .....	44
<b>Figure 20:</b> Cyclopalladated complexes developed by our group .....	56
<b>Figure 21:</b> Catalyst deactivation due to coordination of acetylacetonone moiety ...	57
<b>Figure 22:</b> ORTEP structure of complex ( <i>S</i> )- <b>80b</b> .....	61
<b>Figure 23:</b> ORTEP structure of complex ( <i>S</i> )- <b>88a</b> .....	61
<b>Figure 24:</b> ORTEP structure of complex ( <i>S</i> )- <b>86a</b> .....	62
<b>Figure 25:</b> Molecular structures of PC-catalyst <b>67</b> and NC-catalyst <b>64</b> .....	65
<b>Figure 26:</b> ORTEP structure of chiral phosphine-gold(I) complex ( <i>S</i> )- <b>87</b> .....	73
<b>Figure 27:</b> ORTEP structure of chiral phosphine-palladium complex ( <i>S</i> )- <b>80b</b> ...	77
<b>Figure 28:</b> ORTEP structure of chiral phosphine-palladium complex ( <i>S</i> )- <b>86a</b> ...	81
<b>Figure 29:</b> ORTEP structure of chiral phosphine-palladium complex ( <i>S</i> )- <b>89</b> .....	87
<b>Figure 30:</b> Structures of selected existing cyclopalladated complexes and their functionalized derivatives developed in this study .....	93
<b>Figure 31:</b> X-ray structure of <b>86d-86f</b> .....	100
<b>Figure 32:</b> The sulfonyl substrates and Palladacycle catalysts employed .....	137
<b>Figure 33:</b> The ORTEP of ( <i>R</i> )- <b>92</b> .....	137

## Chapter 1. Introduction

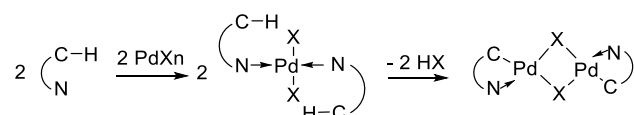
### 1.1. The mechanism and features of cyclopalladation of amines

In the last several decades, a number of reports have been published about the cyclopalladation of amines, *via* the carbon-hydrogen bond activation. In most products, the nitrogen atom is coordinated to the palladium metal, producing the so-called azapalladacycle compounds<sup>1-6</sup>.

According to the kinetic data on the cyclopalladation between palladium acetate and *N,N*-dimethylbenzylamine, Ryabov<sup>7-8</sup> proposed initially the cyclopalladation mechanism having two stages: a) firstly, the amine coordinates to the palladium source to form monomeric intermediates, b) followed by the C-H bond activation to obtain the dimer with *ortho*-attached, covalent Pd-C  $\sigma$  bond and a coordinated Pd-N bond. During the transformation from monomer to dimer, Lewis base is employed to activate the C-H bond and neutralize the by-product HX (X = halide). (**Scheme 1**)

---

**Scheme 1:** The mechanism of cyclopalladation



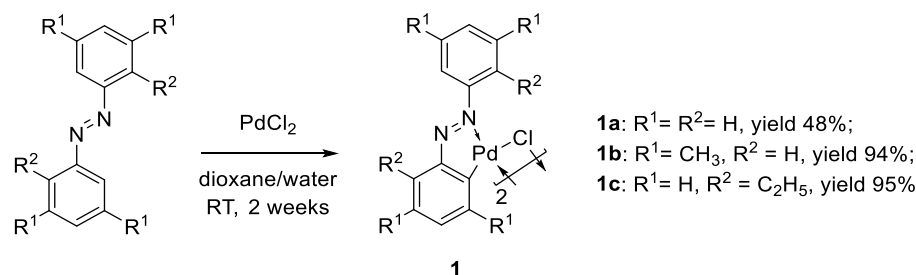
According to the literature reports, the most crucial factors that have significant effect on the reactivity of this reaction are: (a) the substituents on the N atom (primary, secondary or tertiary amines)<sup>9</sup>, (b) the presence of electron-donor or -acceptor functional groups<sup>10</sup>, and (c) the size of ring in the metallacycle ring (four five or six)<sup>2</sup>. The most favorable cyclopalladation requires tertiary amines with electron donors, and five-membered ring product as Cope proposed and reported.<sup>2</sup> There are some theoretical works reported to analyze this empirical rules.<sup>8, 11-16</sup>

Based on Cope's previous reports, the cyclopalladation is favored for the tertiary amines. Two cases, in their calculations including primary amines and tertiary amines, indicated that it is really difficult for primary amines to promote cyclopalladation as the intermediate complex with two primary amines coordinated to the palladium is too stable to undergo the second step. Bosque also found by the calculation of relative energies that the four-membered rings were the most difficult to form palladacycles due to the ring strain. The results also showed that five-membered rings were the more favored, even though the calculations showed that relative energy difference between five- and six-membered rings is very small, less than 0.5 kcal mol<sup>-1</sup>.<sup>8</sup>

### 1.2. CN *ortho*-palladacycles complexes with five-membered ring

The first example of azapalladacycle compounds was reported by Cope in 1965. Azobenzenepalladium complexes **1**<sup>1</sup> were synthesized *via* cyclometallation reaction between aromatic azo compounds and palladium(II) dichloride in the mixture solvent of dioxane and water in 2 weeks (Scheme 2). Since then, a plentiful of compounds with N-Pd-C 5-membered ring complexes, containing both *ortho*-attached covalent Pd-C  $\sigma$  bonding and dative Pd-N bonding, had been obtained in the past few decades.<sup>5, 17-18</sup>

**Scheme 2:** Cyclopalladation of azobenzene



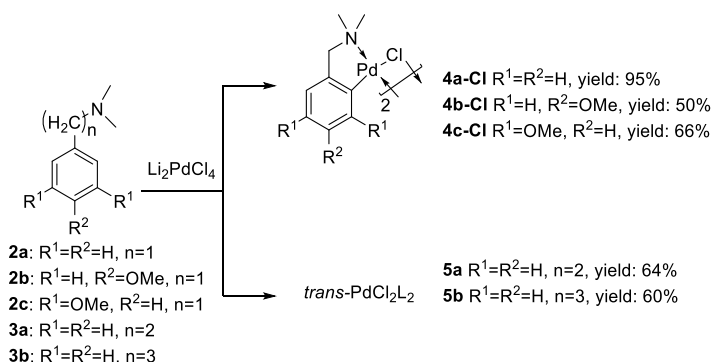
#### 1.2.1. The development and applications of 5-membered benzylic CN *ortho*-palladacycles

Benzylic CN cyclopalladated complexes are among important metallacycles, which can be generated by the *ortho*-metalation of benzylamine derivatives.

These compounds are well established and successfully applied as derivatizing agents<sup>19</sup>, catalysts<sup>20</sup>, palladium sources<sup>21</sup>, promoters<sup>22</sup>, templates<sup>23</sup>, and antiproliferatives<sup>24-25</sup>.

In 1968, Cope<sup>2</sup> reported the reaction between *N,N*-dimethylbenzylamine (**2a**) and  $\text{Li}_2[\text{PdCl}_4]$  in aqueous methanol solvent at room temperature for 48 hours, produced di- $\mu$ -chloro-bis(*N,N*-dimethylbenzylamine-2-*C,N*)dipalladium(II) (**4a-Cl**) in 95 % yield. The report also examined the starting materials *p*-methoxy-*N,N*-dimethylbenzyl amine (**2b**) and 3,5-dimethoxy-*N,N*-dimethylbenzylamine (**2c**), which also gave products **4b-Cl** (50% yield) and **4c-Cl** (66% yield), respectively (**Scheme 3**). On the other hand, the reaction of both *N,N*-dimethyl-2-phenyl-1-ethanamine (**3a**) and *N,N*-dimethyl-3-phenyl-1-propylamine (**3b**), with lithium tetrachloropalladate(II), gave *trans*-dichlorobis(amine)palladium(II) **5a** (64% yield) and **5b** (60% yield), respectively. Different reaction conditions were also investigated in this study and it revealed that lithium tetrachloropalladate(II) (2.0 equiv to amines) was the best Pd source for this transformation. Using palladium(II) chloride, the yield dropped significantly (68%).

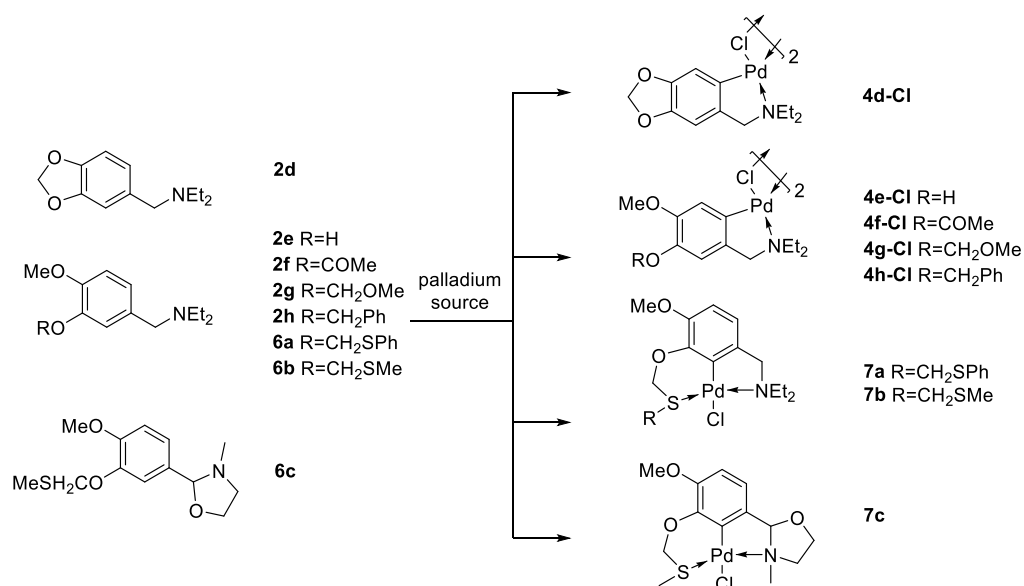
**Scheme 3:** Cyclopalladation between lithium tetrachloropalladate(II) and tertiary benzylamines



Holton also published the cyclopalladation of benzylic amines containing phenolic moiety (**Scheme 4**).<sup>10</sup> The cyclopalladation of **2d-h** and **6a-c** with lithium tetrachloropalladate(II) (1.0 equiv) and excess triethylamine or

diisopropylethylamine in methanol formed creamy yellow crystalline palladacycle complexes **4d-Cl** to **4h-Cl** and **7a-c** in high yields (up to 98%). Benzylic amines **2d-h** reacted with lithium tetrachloropalladate(II) to produce chloro-bridged five-membered dimeric complexes. However, for the substrates **6a-c**, the cyclopalladation gave NCS tridentate pincer complexes after treatment with palladium source, even if the nitrogen atom was a part of another ring, as was the case of the lone pair on sulfur of the **6c**. Because substrates **6a-c** as well as the enhanced stability of tridentate coordination, the NCS pincer complexes **7a-c** were the only products instead of the usual bidentate N-Pd-C cycles.

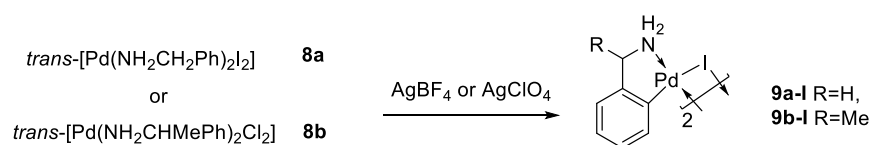
**Scheme 4:** Regiocontrolled aromatic palladations



According to the reports about the cyclometallation of primary amines, it is difficult to obtain the cyclopalladated complexes because of the stability of the intermediate complex with two primary amines coordinated to the palladium. Based on the reports about the reaction of  $[Pt(NH_3)_2Cl_2]$  and silver(I) salt in aqueous solution to form  $[Pt(NH_3)_2(OH_2)_2]^{2+}$ , Parkins<sup>26</sup> and Vicente<sup>27</sup> carried out the cyclopalladation of *trans*-bis-(benzylamine)di-iodopalladium(II) (**8a**) with silver tetrafluoroborate, and *trans*- $PdCl_2[NH_2CH(Me)Ph]_2$  (**8b**) with silver perchlorate, respectively, to promote the cyclometallation (**Scheme 5**). For the

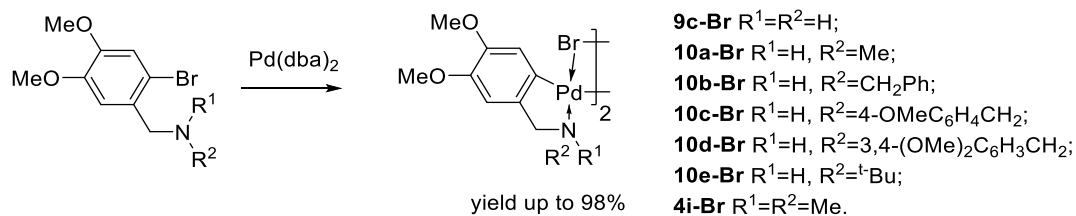
internal *ortho*-palladation of *trans*-[Pd(NH<sub>2</sub>CH<sub>2</sub>Ph)<sub>2</sub>I<sub>2</sub>] (**8a**), two equivalents of silver tetrafluoroborate was applied to break down the Pd-I bond and form the Pd-C bond, followed by treatment with potassium iodide, leading to dimeric *ortho*-palladated CN complexes **9a-I** in common organic solvents. The same procedure was applied to *trans*-PdCl<sub>2</sub>[NH<sub>2</sub>CH(Me)Ph]<sub>2</sub> (**8b**) affording **9b-I**. According to the previous literature<sup>28-29</sup>, the cyclopalladation was preferred in case of the iodide complexes over chloride derivatives, because of the better solubility of silver chloride than silver iodide.

**Scheme 5:** *Ortho*-palladation through silver salt



Another method for the synthesis of *ortho*-cyclopalladated complexes, which were published by Dyke, was the coordination of amines to palladium and subsequent oxidative-addition of *ortho*-halogenated amines containing the *ortho*-Br in methanol (**Scheme 6**).<sup>9</sup> This reaction involved the insertion of palladium into the X-C(sp<sup>2</sup>) bond assisted by primary, secondary, and tertiary amines, and change of the valence of the palladium from 0 to +2, affording the cyclopalladated complexes **9c**, **10a-e**, and **4i** with the bromo-bridge.

**Scheme 6:** The cyclopalladation by oxidative addition of *ortho*-bromobenzylamine

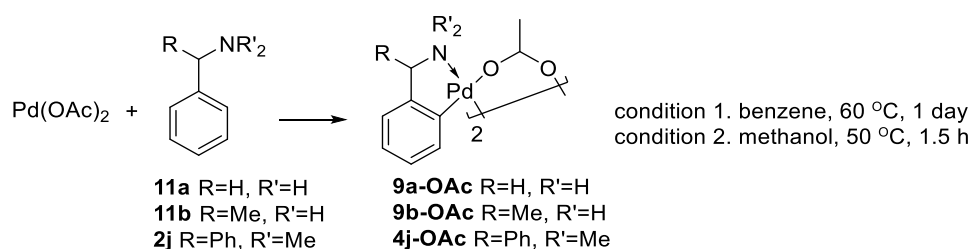


Regardless of the difficulty of cyclopalladation of primary/secondary amines, Fuchita reported the *ortho*-palladation of unsubstituted primary and secondary benzylamine. In their method, direct C-H bond activation of primary/secondary amines was observed with stoichiometric amounts of

palladium(II) acetate<sup>30</sup> as the palladium source in benzene at 60 °C for 1 day to give yellow crystals **9a-OAc** and **9b-OAc**. The final dimeric product in the form of *syn*- and *anti*-isomers could be only isolated by recrystallization because of its insolubility in common organic solvents (**Scheme 7**, condition 1).<sup>31-33</sup> They also reported that the reactivity of palladium(II) acetate was much better than PdCl<sub>4</sub><sup>2-</sup> for this reaction, because of the enhanced electrophilicity of palladium(II) acetate.

Dunina reported the *ortho*-palladation of *N,N*-dimethyldiphenylmethylamine **2j** with palladium(II) acetate in methanol at 50 °C for 1.5 hour, affording cyclopalladated complex **4j-OAc** with phenyl substituent at the  $\alpha$ -carbon stereocenter in a yield of 85% (**Scheme 7**, condition 2).<sup>34</sup> The acetate bridge in the binuclear complex could be transformed into a chloro-bridge when it was treated with sodium chloride or lithium chloride.

**Scheme 7:** The palladation of unsubstituted benzylamines



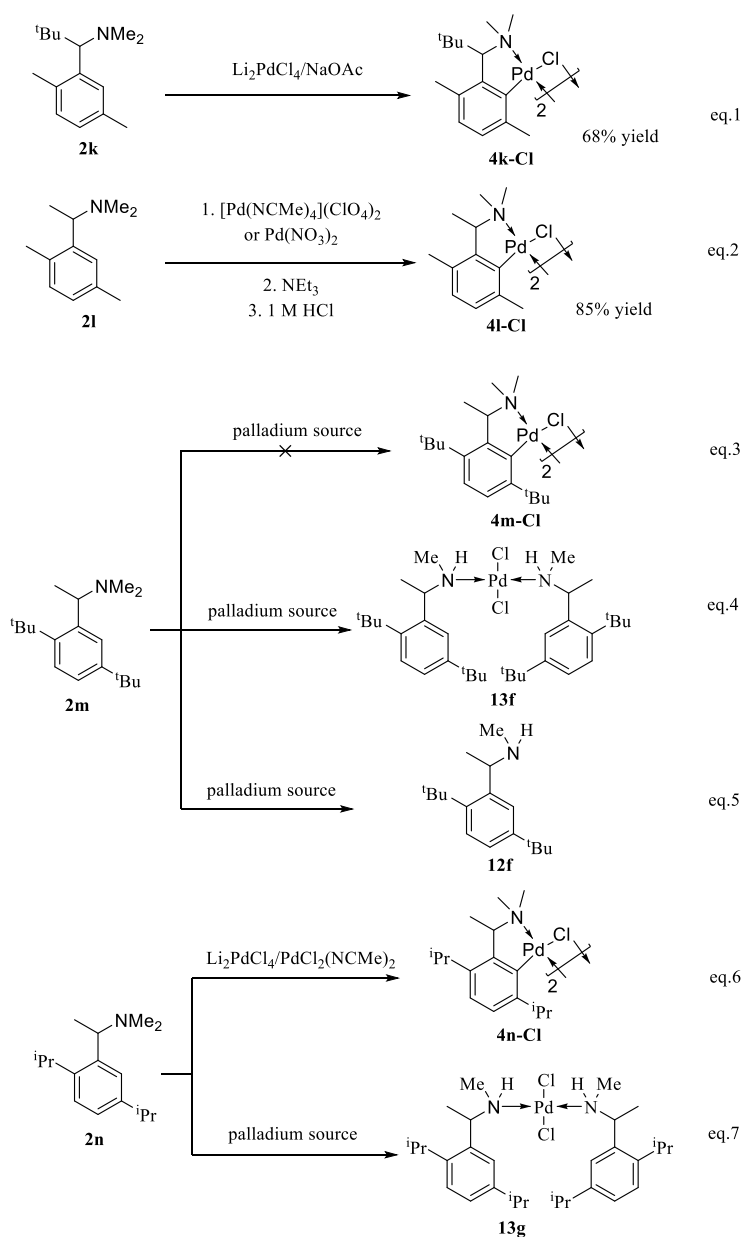
1-(2,5-Dimethylphenyl)-*N,N*,2,2-tetramethylpropan-1-amine **2k** reacted with Li<sub>2</sub>[PdCl<sub>4</sub>] affording dimeric cyclopalladated complex **4k-Cl** in 68% yield (**Scheme 8**, eq.1).<sup>35</sup> Compared with unsubstituted benzylamine, phenylethylamine, and 1-(2,5-dimethylphenyl)-*N,N*,2,2-tetramethylpropan-1-amine **2k**<sup>35</sup>, treatment of (2,5-dimethylphenyl)ethylamine **2l** with Li<sub>2</sub>[PdCl<sub>4</sub>] afforded dimeric complex **4l-Cl**. However, [Pd(MeCN)<sub>4</sub>](ClO<sub>4</sub>)<sub>2</sub> was used as the palladium source in acetonitrile for *ortho*-cyclopalladation of (2,5-dimethylphenyl)ethylamine **2l** in the presence of 1.0 equivalent of NEt<sub>3</sub> followed by 1 M HCl solution in 85% isolated yield (**Scheme 8**, eq.2).<sup>36</sup>

Pd(NO<sub>3</sub>)<sub>2</sub> is also a potential palladium source for this cyclopalladation. However, when the amine was changed to bulkier amine **2m** bearing two tert-

butyl groups on the benzene ring, the cyclopalladation reaction became more challenging and failed to give the complex **4n-Cl** (Scheme 8, eq.3).<sup>37</sup> In this case, complexes **13f** and **12f** was formed *via N*-demethylation.

Cyclopalladation reaction of amine 1-(2,5-diisopropylphenyl)-*N,N*-dimethylethylamine **2n** with the bulkier isopropyl group was investigated (Scheme 8).<sup>38</sup> Depending on the reaction conditions such as the applied palladium agent, solvent, temperature and base, either cyclopalladation or demethylation can occur, resulting in the corresponding products **4n-Cl** and/or **13g**. Palladium agents  $\text{Li}_2[\text{PdCl}_4]$  and  $\text{PdCl}_2(\text{NCMe})_2$  gave the pure cyclopalladated product **4n-Cl** in methanol with sodium acetate as the applied base.  $\text{PdCl}_2$  gave almost equal amounts of **4n-Cl** and **13g** in methanol at 55 °C or 80 °C.  $\text{Pd}(\text{OAc})_2$  in methanol at 55 °C, and  $\text{PdCl}_2$  in benzene at 55 °C resulted in the bidentate **4n-Cl**.  $\text{Pd}(\text{NCMe})_4(\text{ClO}_4)_2$  could not undergo the cyclopalladation reaction. The main product was monodentate complex **13g** if  $\text{PdCl}_2$  was used in methanol at 80 °C. However, the authors got the pure bidentate product **4n-Cl** when the  $\text{PdCl}_2$  was applied in DMF at 55 °C. It was notable that elevated temperature afforded higher yield.

**Scheme 8:** Synthesis of dimeric cyclopalladated complex of (2,5-dialkylphenyl)ethylamine

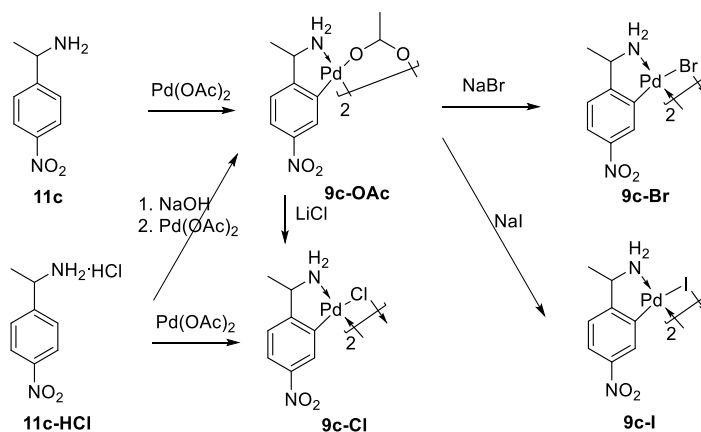


Vicente reported the cyclopalladation of  $\alpha$ -methyl-4-nitrobenzylamine hydrochloride (**11c-HCl**) with palladium(II) acetate (1.0 equivalent). The reaction provided the palladated complexes (**9c-Cl**) in the form of orange powder after refluxing in acetone for 6 hours. Vicente investigated the reaction between  $\alpha$ -methyl-4-nitrobenzylamine **11c** and palladium source, proving his ability one more time to metalate the challenging primary amine. The complex (**9c-OAc**) could also be obtained by treatment of **11c-HCl** with aqueous NaOH, followed

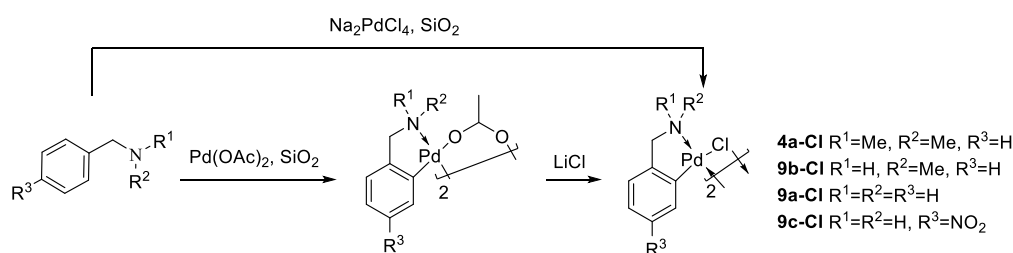
by palladium(II) acetate (1.0 equivalent). Refluxing the mixture of **11c** and palladium(II) acetate (1.0 equivalent) in acetone afforded **9c-OAc** as well. Complex **9c-Cl** was observed when **9c-OAc** was treated with lithium chloride. Addition of NaBr or NaI to the solution of **9c-OAc** resulted in the formation of the bromo- (**9c-Br**) or iodine-bridge complexes (**9c-I**) respectively (**Scheme 9**).

39

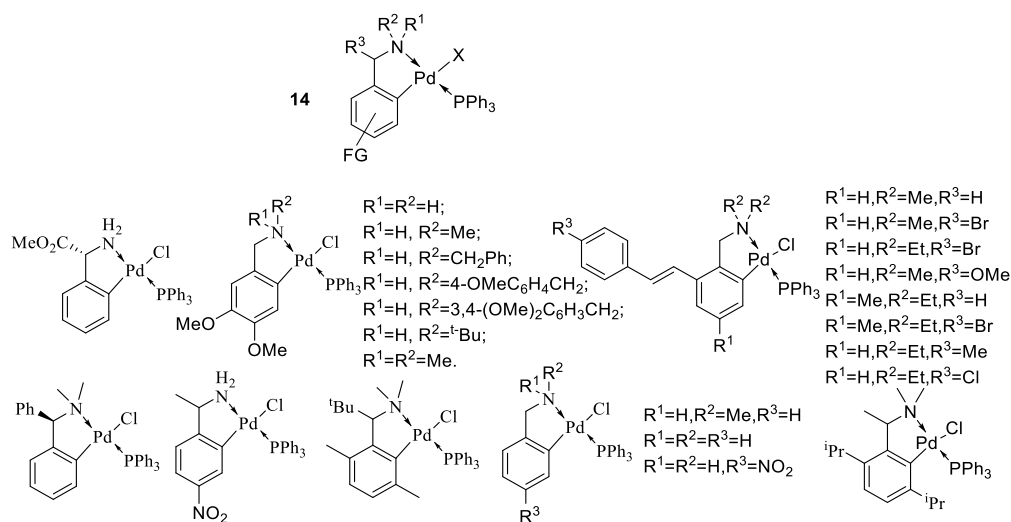
**Scheme 9:** Palladation of primary nitrobenzylamine



The *ortho*-cyclopalladation was also investigated between the amines and palladium(II) acetate or Na<sub>2</sub>PdCl<sub>4</sub> on silica gel (0.375g of silica gel per 1.0 mmol of amines) at 85 °C for 8 hours without the solvent. The product was obtained in moderate to high (45-98%) yield (**Scheme 10**).<sup>40</sup> The amines, including primary, secondary, and tertiary, underwent cyclopalladation with palladium(II) acetate and silica gel SiO<sub>2</sub> affording the dimeric  $\mu$ -acetates **4a-OAc**, **9b-OAc**, **9a-OAc**, and **9c-OAc** at 85°C for 8 hours in 90% isolated yield. The **4a-Cl**, **9b-Cl**, **9a-Cl**, and **9c-Cl** with  $\mu$ -chloride bridge were formed after the bridge-splitting of Pd-O bond in **4a-OAc**, **9b-OAc**, **9a-OAc**, and **9c-OAc** upon treatment with LiCl. Palladacycles were also attained by the cyclopalladation between amines and Na<sub>2</sub>PdCl<sub>4</sub> with SiO<sub>2</sub> in good yield (92% for **4a**).

**Scheme 10:** Cyclopalladation without solvent on silica gel

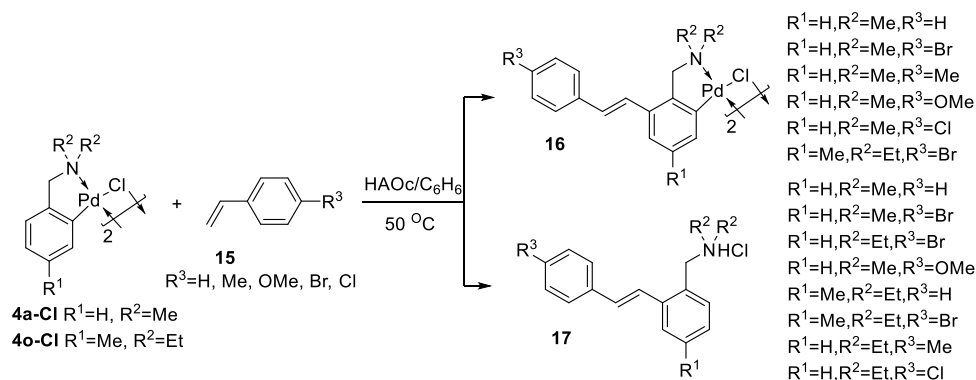
The dimeric *ortho*-palladated benzylic amine compounds with the bridge readily underwent the coordination reaction of donor ligand, resulting in the bridge-splitting monomeric *ortho*-palladated complexes.<sup>24, 27, 32-35, 38-41</sup> Triphenylphosphine proved to be one of the best donor ligands, which can easily coordinate to the palladium of the *ortho*-cyclopalladated complex following the bridge-splitting reaction to form the monomeric complexes **14** (Figure 1).<sup>8-9, 26, 32-35, 38-43</sup> It is also noteworthy, that the complexes **14** often really give X-ray quality crystal.

**Figure 1:** The monomeric cyclopalladated complexes with triphenylphosphine

Ryabov established C-H activation reactions between the *ortho*-cyclopalladated *N,N*-dialkylbenzylamine (**4a-Cl** and **4o-Cl**) and *para*-substituted styrenes **15**. The mixture of acetic acid and benzene (1:1) was stirred at 50 °C for several hour to give the complex **16** and free amine **17** (Scheme 11).<sup>43</sup> The product **17** was dominating if the reaction was protected by argon. However, in the presence of oxygen, the reaction preferentially gave the dimeric product **16**.

The salts  $MClO_4$  ( $M = Na, Li$ ) significantly promoted the reaction and the reaction time was shortened from 8 hours to 1.5 hours. The mechanism involving typical Fujiwara-Moritani or Heck olefin arylation process was proposed. The formation of the dimeric complex **16** likely proceeded through possible two pathways: 1) direct metalation of **17** by reoxidized palladium and 2) the exchange reaction of **4** and **17** to form **16**.

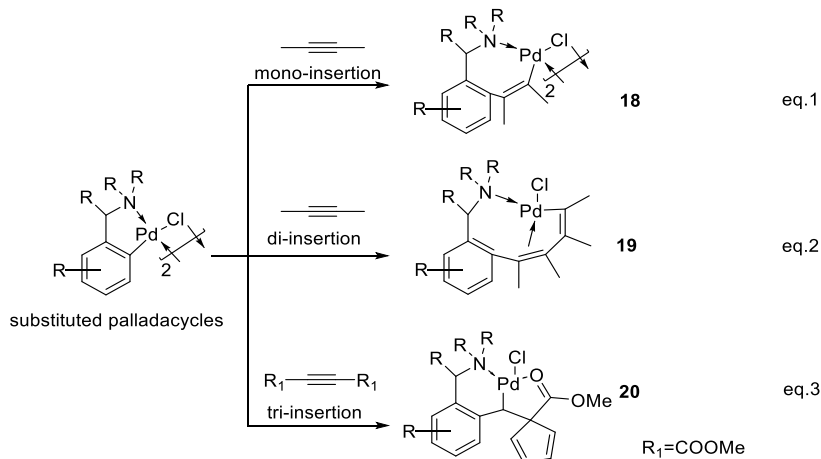
**Scheme 11:** The reaction between cyclopalladated amines and *para*-substituted styrene



*Ortho*-cyclopalladated complexes are relatively reactive towards insertion of one to three alkynes into the Pd-C bond to result in new enlarged cyclopalladated ring.<sup>39, 44-45</sup> The insertion of one equivalent of alkyne into the Pd-C bond of cyclopalladated CN afforded a seven-membered ring **18**, and this reaction preferred alkynes with electron-withdrawing groups (**Scheme 12**, eq.1).<sup>46-48</sup> However, when the reactivity of the Pd-C bond was too high to be stable after the “mono-insertion”, the second alkyne would react with the “mono-inserted” complexes to give rise to the “di-inserted” complexes **19** with nine-membered ring directly, and this always took place when the alkynes with electron-rich substituent were used (**Scheme 12**, eq.2).<sup>49</sup> In this case if the amount of the alkyne was less than two equivalent to the palladated complex, it would result in a mixture of the substrates, the “mono-inserted” product, and the “di-inserted” product. The electron-poor alkynes always afforded “tri-inserted” compounds containing the same five-membered cycles **20** (**Scheme 12**, eq.3). The mechanism of tri-insertion involved mono-insertion and di-insertion first,

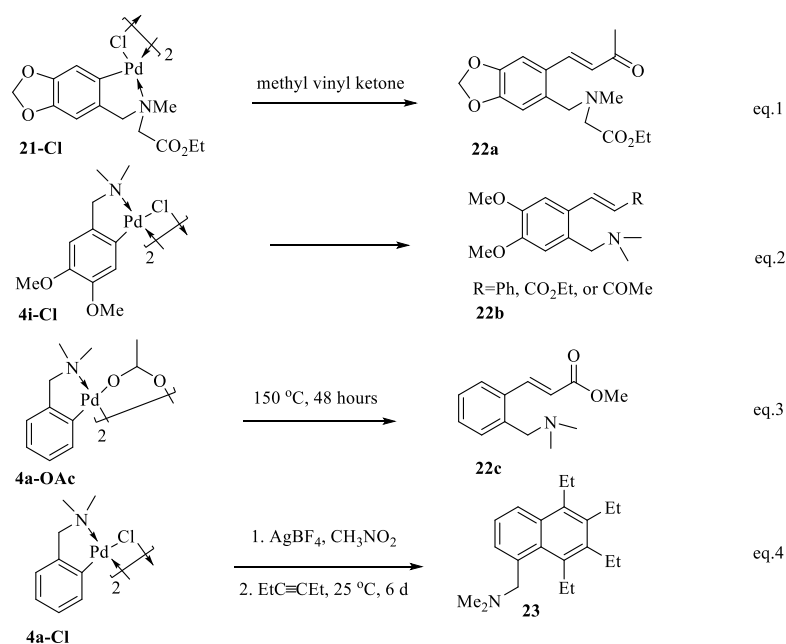
then the last alkyne and the 1,4-diene undergo the addition reaction like [4+2] addition, followed by rearrangement to give the tri-insertion adduct **20**.<sup>39</sup>

**Scheme 12:** Insertion of alkynes into palladium-carbon bond of cyclopalladated compounds



If the inserted complexes were still very reactive, the insertion would give carbocyclic or heterocyclic organic complexes through depalladation reaction (**Scheme 13**).<sup>44</sup> The organic compound **22a** was afforded after the insertion of methyl vinyl ketone into the cyclopalladated complex **21-Cl**, and depalladation in the presence of triethylamine in 73% (**Scheme 13**, eq.1).<sup>50</sup> The cyclopalladated compounds reacted with *para*-substituted styrene at 50 °C under the atmosphere of oxygen to afford the depalladated products **17** (**Scheme 11**).<sup>43</sup> Palladated complexes **4i-Cl** reacted with styrene derivatives followed by the depalladation and coupling reaction to give alkenes **22b** (**Scheme 13**, eq.2).<sup>51</sup> As methyl acrylate was obviously much less reactive to the insertion, the depalladation required elevated temperature, so *trans*-methyl-*o*-dimethylaminomethylcinnamate **22c** was produced when the *ortho*-palladacycle **4a-OAc** was treated with methyl acrylate at 150 °C for 2 days with a 39% yield (**Scheme 13**, eq.3).<sup>52</sup> After the poly-insertion and depalladation, the rearrangement pathway of annulation gave rise to a new carbocyclic ring **23** (**Scheme 13**, eq.4).<sup>53</sup>

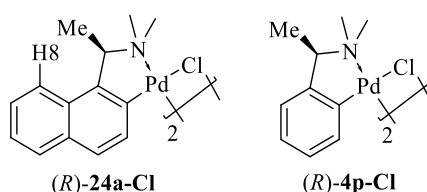
### Scheme 13: Depalladation of cyclopalladated complexes



#### 1.2.2. The development and applications of 5-membered naphthyl CN *ortho*-palladacycles

The resolution of chiral cyclopalladated complexes was carried out after the dimer was coordinated with chiral ligands. Because of the presence of proton H8 in the compound with the naphthyl ring leading to increased conformational rigidity, the resolution of the diastereomers with naphthyl ring (*R*)-**24a-Cl** would be easily to be achieved than the one with benzylic ring such as (*R*)-**4p-Cl**<sup>54</sup>. On account of the increased effective steric hindrance between H8 and  $\alpha$ -Me in (*R*)-**24a-Cl**, the properties of these two kinds of complexes would be a little different such as the synthesis, optical resolution, and application.<sup>30, 55-57</sup>

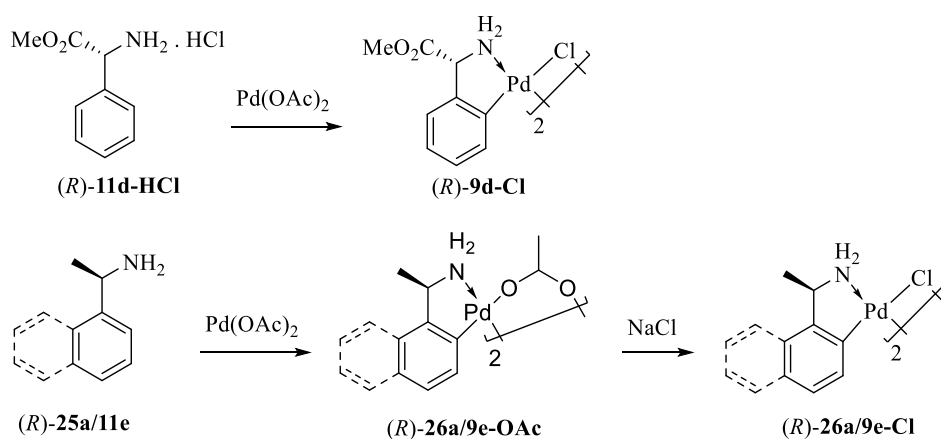
Figure 2: The structure of naphthyl and phenyl palladacycles



### 1.2.3. The synthesis and applications of 5-membered optically active CN palladacycles

The easiest pathway to synthesize chiral CN cyclopalladated complexes, such as *(R)*-**9d-Cl**, *(R)*-**26a-OAc/Cl** and *(R)*-**9e-OAc/Cl**, was to apply the optically active amines *(R)*-**11d-HCl** and *(R)*-**25a/11e** respectively, as the starting material directly *via* the normal procedures to synthesize the racemic ones (**Scheme 14**).<sup>41, 58-59</sup>

**Scheme 14:** Synthesis of optically active CN palladacycles



Resolution of racemic dimeric cyclopalladated CN complexes with sodium *L*-prolinate (prepared by mixing the solution of *L*-proline and NaOH in water) is possible the *L*-prolinate anion coordinates to the palladium to form a pair of diastereomers **27**, which could be separated *via* recrystallization or column chromatography on silica gel (**Scheme 15**).<sup>34-36, 38, 60-62</sup> The separated **27** was treated with 1 M of HCl giving rise to the optically active of dimeric complexes. Examples of optically complexes which were synthesized by resolution of racemic complexes are listed in **Figure 3**.

**Scheme 15:** Resolution of racemic cyclopalladated compounds

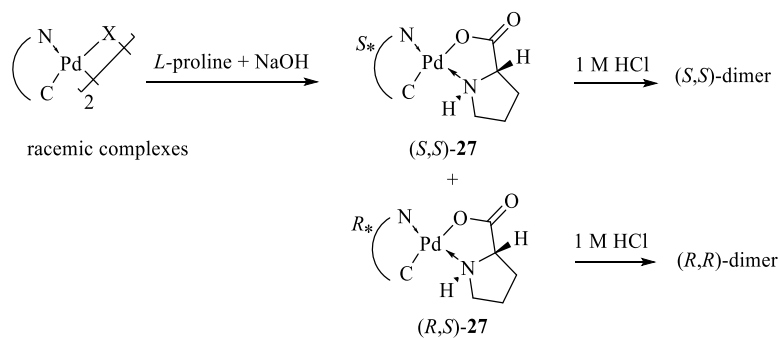
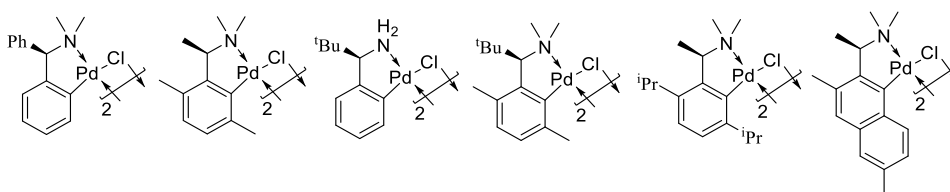
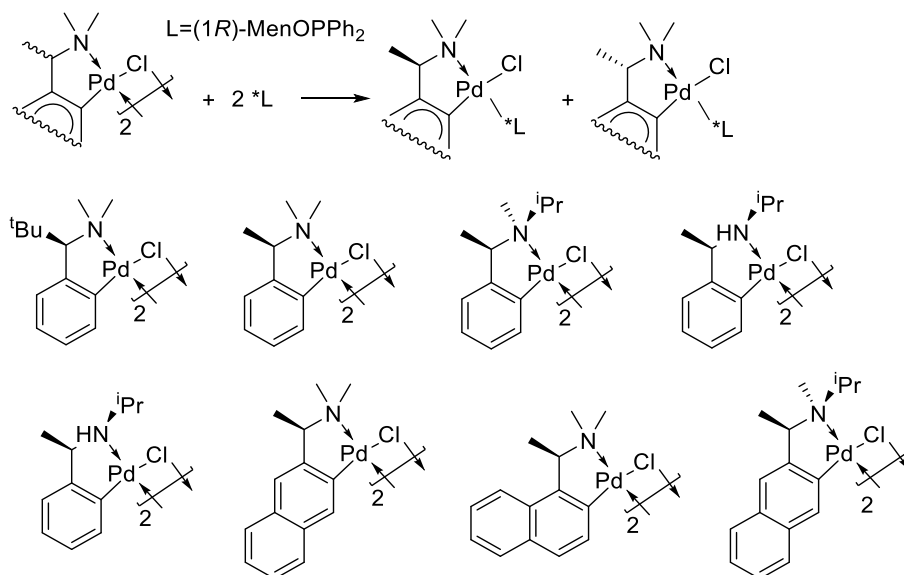


**Figure 3:** The optically active CN cyclopalladated complexes *via* sodium *L*-prolinate



(1*R*,2*S*,5*R*)-Methoxydiphenylphosphine was also used as the chiral derivatizing agent of racemic CN palladacycles (**Scheme 16**).<sup>19</sup> Upon coordination of this ligands, the diastereoisomers were separated by recrystallisation and column chromatography on silica gel followed by decoordination of the phosphine ligand to give optically resolved dimeric CN *ortho*-palladacycles.

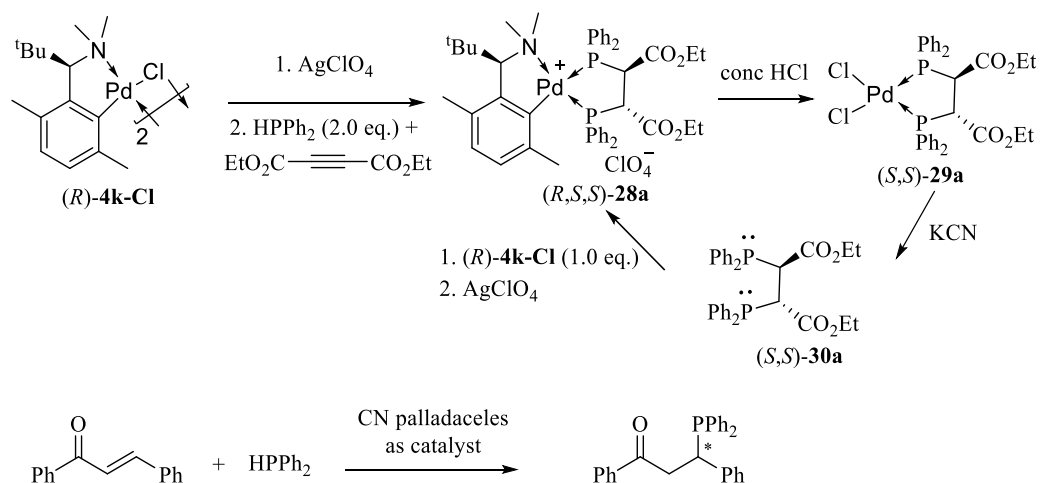
**Scheme 16:** Resolution of CN *ortho*-palladacycles by chiral phosphine ligands



The optically active CN palladacycle (*R*)-**4k-Cl** was used as the promoter of hydrophosphination between 2.0 equivalent of diphenylphosphine and 1.0 equivalent of diethyl acetylenedicarboxylate at -78 °C in the presence of 0.2 equivalent of triethylamine in DCM for 12 h (**Scheme 17**).<sup>35</sup> Cationic product (*R,S,S*)-**28a** was treated with concentrated HCl to remove the CN auxiliary, affording dichlorido palladium complex (*S,S*)-**29a** in 74% isolated yield. The air-sensitive phosphine (*S,S*)-**30a** was liberated from the complex (*S,S*)-**29a** by treatment with aqueous potassium cyanide in 95% yield. The free ligand (*S,S*)-**30a** quantitatively re-coordinated to the isomer (*R*)-**4k-Cl** to reform (*R,S,S*)-**28a**.

CN *ortho*-palladacycles were also used as catalysts for hydrophosphination reaction between diphenylphosphine and some activated alkenes such as chalcone (**Scheme 17**).<sup>30</sup> This kind of reaction was also used to evaluate the stereochemical properties of the newly synthesized catalysts.

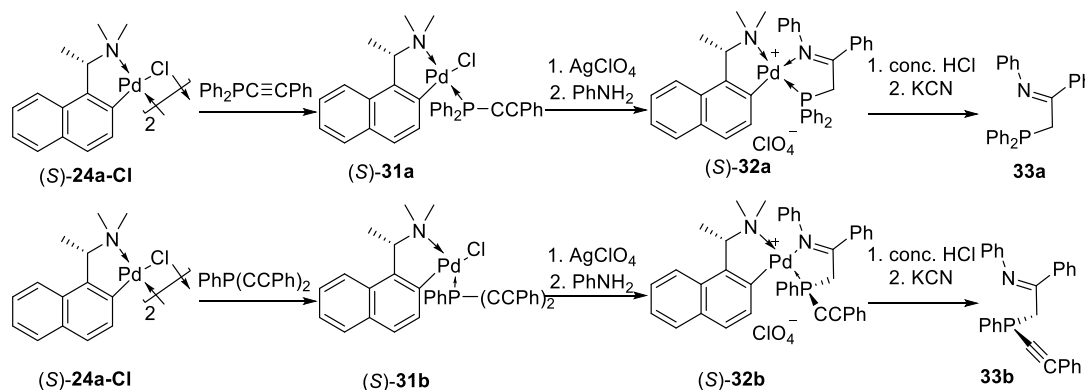
**Scheme 17:** Cyclopalladated complex as promoter of hydrophosphination



Asymmetric hydroamination reaction between aniline and alkenyl phosphines, such as diphenyl(phenylethynyl)phosphine or di(phenylethynyl)phenylphosphine, was promoted by optically active cyclopalladated CN complex (*S*)-**24a-Cl** to afford the corresponding bidentate iminophosphines (*S*)-**32** in high yields (**Scheme 18**).<sup>63</sup> Later, the palladium

complexes were sequentially treated with concentrated HCl and KCN in order to liberate the bidentate ligands **33a/b**.

**Scheme 18:** Asymmetric hydroamination reaction promoted by chiral palladacycles



The insertion of electron-deficient alkynes into the bond of the cyclopalladated complexes occurred even if there was 3,4-dimethyl-1-phenylphosphole (DMPP). On the other hand, [4+2] cycloaddition<sup>64</sup> happened if the electron-deficient alkenes was used (**Scheme 19**).<sup>65</sup> It was one of the important application of the chiral cyclopalladated CN complexes as the template of [4+2] Diels-Alder cycloaddition between diene (DMPP) and dienophiles. The cyclopalladated complexes **34-Cl** with the kinetically stable Pd-Cl bond reacted with dienophiles affording the [4+2] *endo* diastereomeric products (*R*)-**35** and (*S*)-**35**, which could be separated by column chromatography or recrystallisation effectively. The ratio of the two diastereomeric products depended on the reaction system including the substrates, catalysts, and reaction conditions.<sup>17, 36, 38, 48, 55, 66-70</sup> By the treatment of the chloro complexes **34-Cl** with silver perchlorate, the Pd-Cl bond was changed to kinetically labile Pd-OCIO<sub>3</sub> bond. The products **34-OCIO<sub>3</sub>** were able to facilitate the coordination of the dienophiles with lone pair of electrons onto the optically active palladium. The resulting intermediates underwent subsequent intramolecular cycloaddition reaction affording *exo*-cycloadducts (*R*)-**37**.<sup>17, 66-69, 71-74</sup> The enantioselectivity of the intramolecular *exo*-cycloaddition reaction was much better than the

intermolecular *endo*-cycloaddition reaction. Because of the stable structure in **34-OCIO<sub>3</sub>** with bidentate P, E auxiliary forming a cycle P-Pd-E ring, the procedures to liberate the free P-chiral phosphanorbornene ligands were different from each other. The enantiomerically pure compounds (*R*)-**35** or (*S*)-**35** was treated with 1,2-bis(diphenylphosphanyl)ethane (dppe) or KCN<sup>75</sup> to liberate the free phosphine *endo*-ligands (*R*)-**36** or (*S*)-**36**, respectively.<sup>55</sup> On the other hand, sequential treatment with concentrate HCl and KCN to *exo*-cycloadducts **34-OCIO<sub>3</sub>** was used to free the optically active phosphanorbornene ligands (*R*)-**38**.<sup>66</sup> Our group had studied the stereoelectronic properties of a range of cyclopalladated complexes with benzyl, naphthyl, or phenanthryl ring, respectively, for [4+2] Diels-Alder cycloaddition reaction.<sup>76</sup> The results proved that the phenanthrylamine complex showed the best enantioselectivity, and the benzylamine exerted the lowest one. Asymmetric catalyzed [4+2] Diel-Alder cycloaddition reaction was usually used to evaluate the efficiency and stereoselectivity of the CN *ortho*-cyclopalladated compounds.<sup>62</sup> Some cycloadducts were listed in **Figure 4**.

**Scheme 19:** Template of [4+2] Diels-Alder cycloaddition

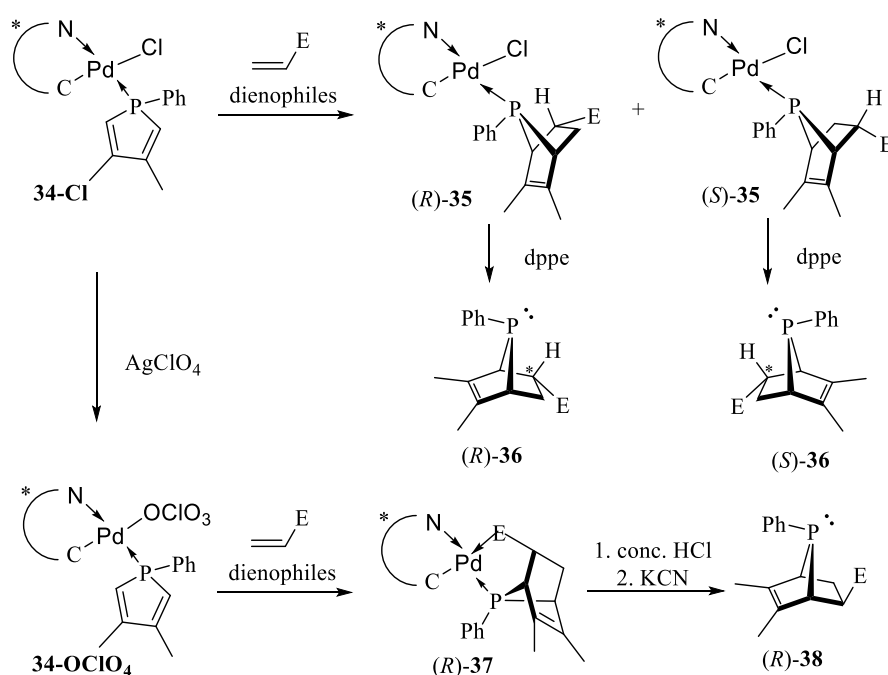
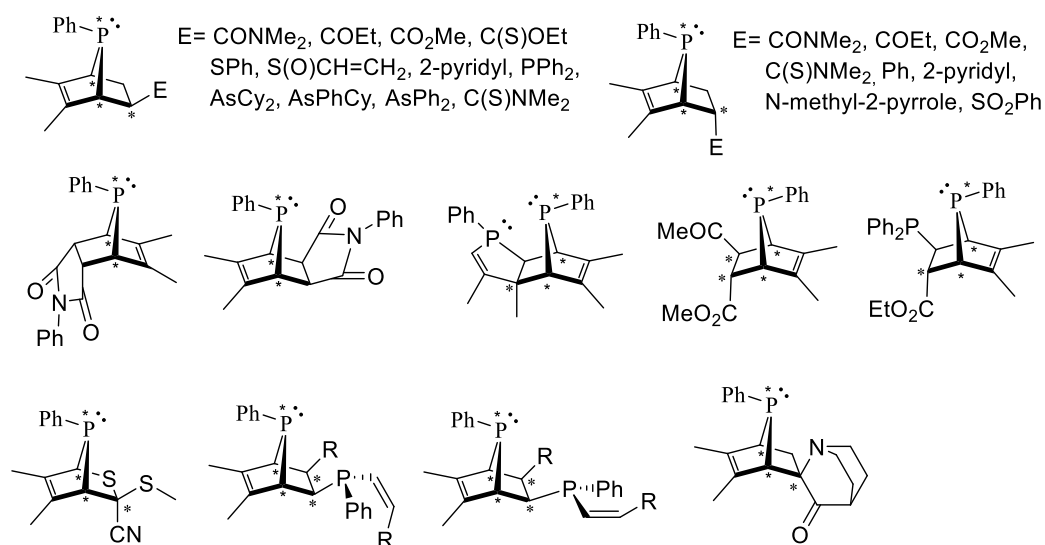
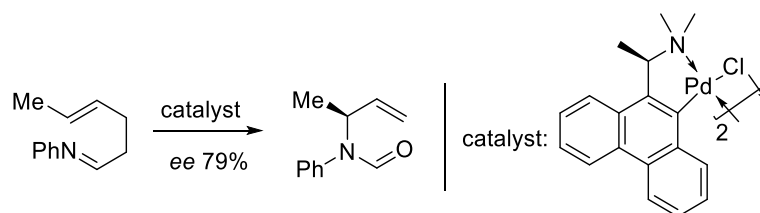


**Figure 4:** Chemical list which synthesized *via* [4+2] cycloaddition reaction promoted by palladacycles



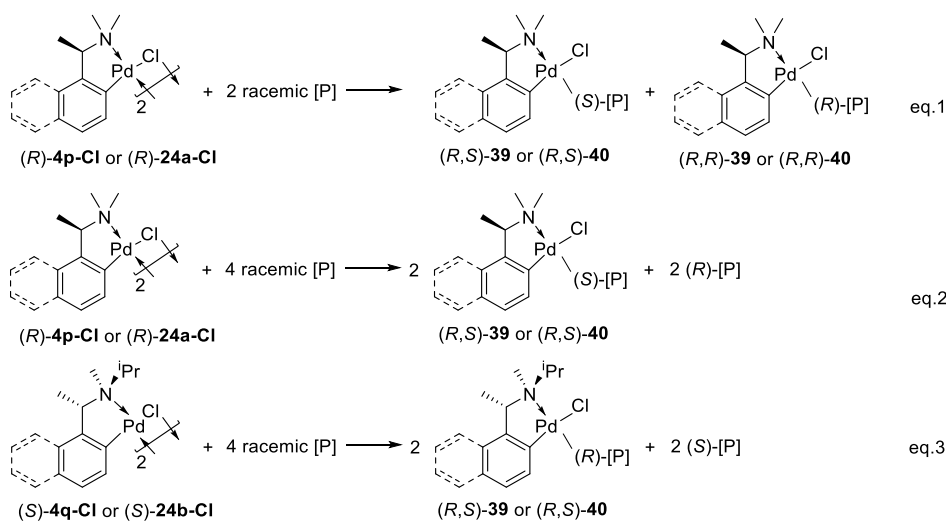
Claisen rearrangement reaction could also be catalyzed by cyclopalladated CN complexes forming the optically active products (**Scheme 20**).<sup>77</sup>

**Scheme 20:** Claisen rearrangement catalyzed by chiral CN palladacycles



Chiral *ortho*-cyclopalladated CN complexes (**(R)**-**4p-Cl** and (**(R)**-**24a-Cl**) were also used as resolving agents<sup>78</sup> after the 2.0 equivalent of racemic free ligands coordinated to the palladium center forming a pair of diastereoisomers (**(R,R)**)/(**(R,S)**-**39** or (**(R,R)**)/(**(R,S)**-**40**), which were separated *via* recrystallisation or column chromatography on silica gel (**Scheme 21**, eq.1).<sup>79-81</sup> On the other hand, palladacycles were also used as resolving agents with 4.0 equivalent of the phosphines based on the solubility difference of coordinated compounds (**Scheme 21**, eq.2 & eq.3).<sup>61, 82-83</sup> After the separation of the diastereoisomers, the free ligands were liberated after coordination of bidentate ligands.

**Scheme 21:** palladacycles as resolving agent of phosphines



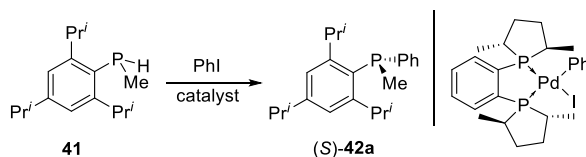
### 1.3. CP palladium complexes

A class of phosphapalladated complexes showed extremely high catalytic ability in hydrovinylation<sup>84-85</sup>, and biaryl coupling reaction such as Heck, Suzuki and Stille reaction with unprecedented turnover numbers and frequencies.<sup>5</sup> The reaction still moved on in high rates and ultimate conversions even though the catalysts were used in very low concentrations (0.0001 mol% catalysts).<sup>86-87</sup> Palladium complexes were also efficient catalysts for carboetherification and carboamination.<sup>88</sup>

#### 1.3.1. The development of CP complexes

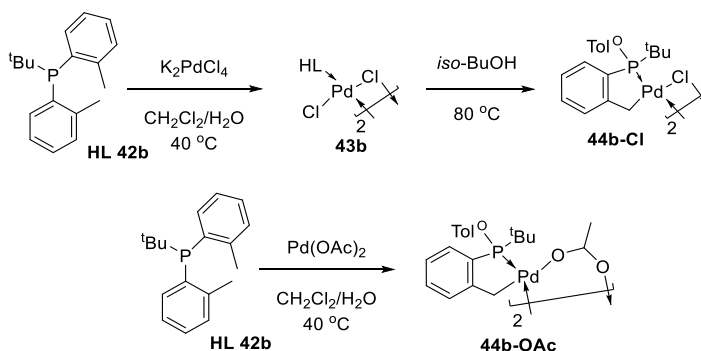
The valuable phosphine compounds have attracted more attention as the ligands for metal-catalyzed asymmetric reactions and organocatalytic reactions. They are usually synthesized by resolution after employing the stoichiometric amounts of chiral auxiliaries.<sup>89</sup> The catalytic asymmetric phosphination is an efficient method for the preparation of chiral phosphines. Glueck reported the enantioselective synthesis of P-chirogenic phosphines (*S*)-42a via palladium catalyzed asymmetric phosphination in yield of 90 % and *ee* of 78 % (Scheme 22).

---

**Scheme 22:** The asymmetric catalytic phosphination

The direct cyclopalladation was conducted between free phosphine ligands and palladium sources such as palladium acetate,  $\text{PdCl}_2$ ,  $[\text{PdCl}]^{2-}_4$ ,  $\text{PdCl}_2(\text{NCMe})_2$ ,  $\text{Pd}(\text{dba})_4$ ,  $\text{Pd}(\text{NCMe})_4(\text{ClO}_4)_2$ , and so on. The bridge ion could be exchanged with each other when the dimer reacted with the agent bearing specified ion. Upon coordination of the free phosphines **HL 42b** palladium source  $\text{K}_2\text{PdCl}_4$ , the  $\mu$ -chloro dimeric palladated complex **44b-Cl** formed directly by intramolecular *ortho*-cyclopalladation of the monodentate complexes **43b**. The reaction was carried out at elevated temperature 80 °C in the *iso*-BuOH as the solvent in high yield up to 94%. The  $\mu$ -acetato analogue **44b-OAc** was prepared by using palladium(II) acetate as the palladium source directly (**Scheme 23**).<sup>90</sup>

---

**Scheme 23:** The *ortho*-cyclopalladation of free phosphines directly

### 1.3.2. The chiral CP palladium complexes

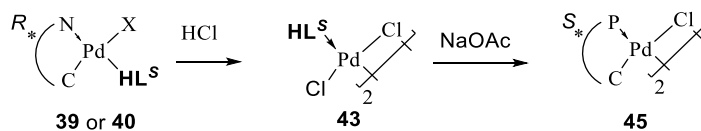
Either as organocatalysts or ligands for transition metal catalysis, enantiopure phosphines had played an important role in the development of enantioselective transformations.<sup>91-93</sup> Until now, optically active phosphines were mainly synthesized either through optical resolution or the employment of

stoichiometric amounts of enantiopure auxiliaries or chiral starting materials. In the past decade, catalytic synthesis of chiral phosphines was also reported.<sup>94-95</sup>

The chiral CP palladated complexes were synthesized directly through the cyclopalladation between chiral phosphine ligands and palladium sources, such as the palladium acetate,  $[\text{PdCl}_4]^{2-}$ ,  $\text{PdCl}_2$ ,  $\text{PdCl}_2(\text{NCMe})_2$ , and so on.<sup>96-97</sup>

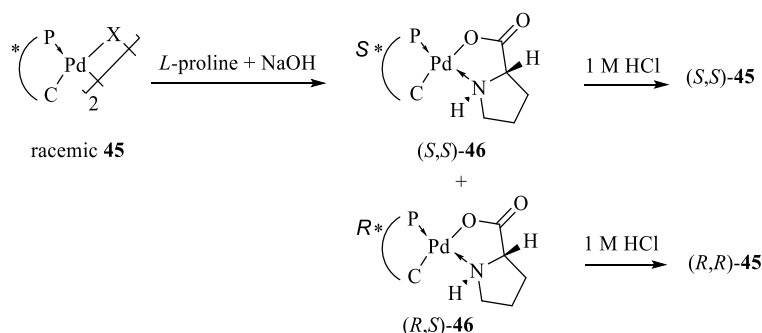
The optical resolution of phosphine ligands was conducted by coordination with stoichiometric amount of optically active transition metal complexes such as the chiral CN palladacycles. A pair of diastereomeric complexes were formed and could be separated using recrystallisation and/or column chromatography on silica gel (**Scheme 21**). As we showed above, liberation of the resolved phosphine ligands was carried out by treating the separated coordinated complexes with KCN solution in water followed by concentrated HCl to remove the auxiliary (**Scheme 19**). The efficiency and selectivity of this process were excellent except the waste of the stoichiometric amount of chiral resolving agent and the agents used for liberation. On the other hand, using the half equivalence of transition metal complexes to the phosphine ligands produced one diastereomer of coordinated adduct and the enantiopure free ligand. This scheme was based on very high level of enantiomeric discrimination in chiral phosphorus bonding in solution, achieved in Tani's approach<sup>42</sup> (**Scheme 21**).<sup>61, 79, 83, 98-102</sup> It should be noted that the CN cyclopalladated complex used here are not only the resolving agent of the CP ligands, but also the palladium source (**Scheme 24**).<sup>100</sup> The resolved complexes **39** or **40** were treated with HCl in acetone at elevated temperature to remove the CN auxiliary forming the monodentate dimeric palladated compounds **43**. Following the extraction of the air-stable compounds **43** with DCM/water, the cyclopalladated dimer **45** was formed when the monodentate **43** was treated with base such as sodium acetate. The details differed depending on the functionalized groups.

**Scheme 24:** The cyclopalladation of CP ligands



As demonstrated for the well-documented CN complexes (**Scheme 15**), the resolution of CP cyclopalladated complexes using *L*-prolinate auxiliary ligand was also established previously. After the coordination of the *L*-prolinate ligand to the Pd atom, the pair of diastereomers **46** were generated. The pair of diastereomers **46** were separated by recrystallization or column chromatography on silica gel depending on the difference of their solubility and polarity. The enantiopure dimeric complexes were obtained by treatment of the separated complex with HCl solution (**Scheme 25**). The absolute configurations of the CP complexes were determined by X-ray measurement of **46**.<sup>60,90</sup>

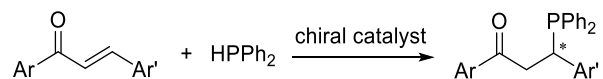
**Scheme 25:** The resolution of CP complexes with potassium *L*-prolinate



Following the asymmetric synthesis of chiral phosphine using stoichiometric optically active reagents, in the asymmetric hydrophosphination, another milestone was the reports by Duan and Leung in 2010. Since then, various substrates and catalysts were studied in this transformation (**Scheme 26**).<sup>57, 103-105</sup> The biggest advantage of this transformation is the simple, one-step synthesis of chiral phosphine ligands using only catalytic amount of metal source. The typical starting materials for these transformations are activated olefins and secondary phosphines in the presence of internal or external base. The most commonly used catalysts for the asymmetric hydrophosphination are the chiral

CP bidentate and PCP tridentate palladacycles. This powerful method allowed to generate chiral trivalent phosphine ligands with excellent enantiomeric excesses (up to 99%) with high reactivity (full conversion for most of the substrates).

**Scheme 26:** the synthesis of chiral phosphines *via* asymmetric P-H addition



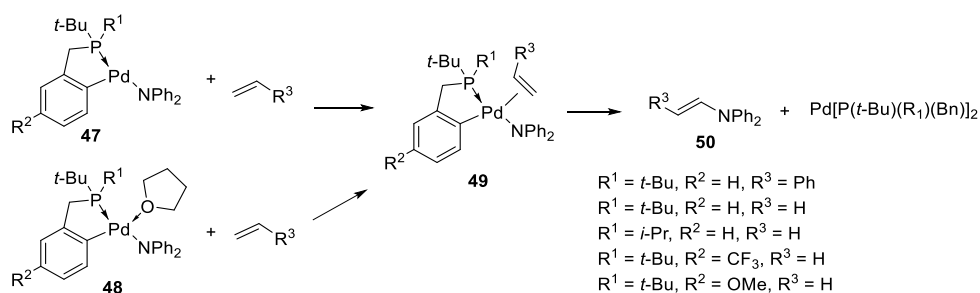
Among optically active phosphines, phosphorus-chiral phosphines have attracted increasing attention as they express great potential for asymmetric catalytic reaction especially, as organocatalysts.

### 1.3.3. The application of CP palladium complexes

Compared to CN palladacycle compounds, analogues cyclopalladated complexes showed significant reactivity and enantioselectivity as the catalysts for asymmetric catalytic hydrophosphination.<sup>106-107</sup> Because of the electronic effect of the strong  $\pi$ -accepting aromatic carbon in the highly conjugated naphthalene ring, the vacant site *trans* to the  $\sigma$ -donating N/P atom preferred the soft donors like phosphorus and arsenic. The replacement of CN to CP cyclopalladated complexes would weaken the Pd-P bond and accelerate the elimination of the phosphine compounds due to the back-donating effect of phosphorus atom. Thus, the catalytic efficiency of CP complexes is superior to the CN compounds.<sup>108</sup> This section introduced the application of the CP palladium complexes.

First, after the alkenes and diarylamides coordinated to the palladium atom, dimeric cyclopalladated chloride-bridge compounds reacted intramolecular migratory insertion with inactivated alkenes into Pd-N bonds generating enamine products **50** in high yield (up to 78%). The authors also studied the mechanism and electronic and steric effects of the auxiliary ligands and alkenes on the rate of the migratory insertion by computing the relative binding energies (**Scheme 27**).<sup>109</sup>

**Scheme 27:** CP palladated complexes as the template to give enamines



When the benzylic ring in the cyclopalladated complexes was replaced with the naphthyl ring, it showed the significance of the lock-and-key principle as the chiral catalyst.<sup>5</sup> Chiral cyclopalladated CP complexes were also used as the catalysts for asymmetric hydrophosphination.<sup>57</sup>

#### 1.4. Recent development in our group

Our group has been working on the synthesis and application of different palladacycle complexes for a few decades. Herein, the biggest milestones and the recent developments are presented.

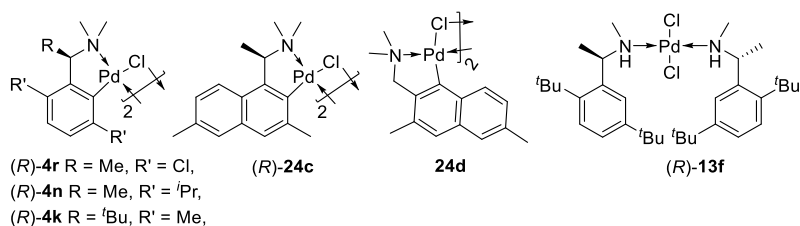
##### 1.4.1. The design and synthesis of cyclopalladated complexes

In the past decade, the chiral cyclophosphapalladated complexes were reported by the researchers as the catalysts in the asymmetric P-H addition with some activated unsaturated organic substrates. In the P-H addition reaction, the optically active phosphine products and diastereomeric cycloadducts were formed.<sup>110</sup> The phosphapalladacycles were classified into two main categories: 1) pincer complexes such as the PCE (E = S, O, P, N and so on) with one vacant coordination site, and 2) the CP cyclopalladated compounds with two coordination sites *trans* to the carbon and phosphorus atom separately. From a purely mechanistic viewpoint, catalytic intermediates derived from the pincer and CP cyclopalladated complexes were quite different from each other. In the case of pincer as the catalyst, the phosphorus atom in the substrates prefers to coordinate to the palladium center in the pincer catalyst at first to activate the P-H bond. The unsaturated substrates would undergo the intermolecular P-H

addition with the P-Pd intermediate. In the case of the CP cyclopalladated complexes as the catalyst, the phosphines and activated unsaturated starting material would coordinate to the catalysts to activate the P-H bond and unsaturated bond to undergo the intramolecular P-H addition reaction. Herein, several new protocols for the synthesis of the cyclopalladated complexes were established by different pathways.

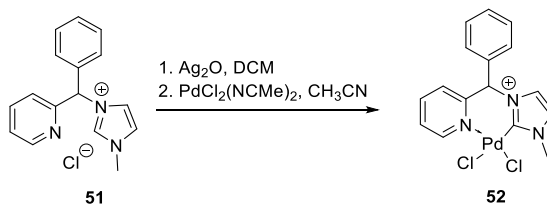
The design and synthesis of chiral bidentate amine–palladacycles were reported in our lab. The racemic substrates amines were prepared through 4 to 6 steps before the metalation. the *ortho*-palladation of the amines and resolution of the cyclopalladated complexes were reported (**Figure 5**).<sup>20-21, 55, 62, 111</sup> The resolution of dimeric *ortho*-palladated complexes **4r**, **4n**, **4k**, **24c**, and **24d** were reported. A pair of the monomeric complexes **27**, which could be separated *via* recrystallization and/or column chromatography on silica gel, were formed after the coordination of chiral bidentate auxiliary *L*-proline to the palladium (**Scheme 15**).<sup>20, 38</sup> Their ability to promote the intramolecular stereoselective Diels–Alder cycloaddition was reported. The reaction was examined between bulky monodentate ligand 3,4-dimethyl-1-phenylphosphole (dmpp) and *N,N*-dimethylacrylamide or ethyl vinyl ketone resulting the ratio of the two diastereomers from 4:1 to 6:1 (**Scheme 19**).<sup>20, 35, 55, 62</sup> The application of the CN cyclopalladated complexes in asymmetric hydrophosphination reactions were also disclosed.<sup>20, 35, 55</sup> Chemoselective *N*-demethylation was reported in the case of the substrate bearing the major steric hindrance, such as **13f**.

**Figure 5:** List of the amine palladated compounds in our lab



It should be noted that an optically active six-membered dimeric bidentate pyridine-*N*-heterocyclic carbene cyclopalladated complex **52** was also synthesized *via* optical resolution of the racemic palladacycles (**Scheme 28**).<sup>111</sup>

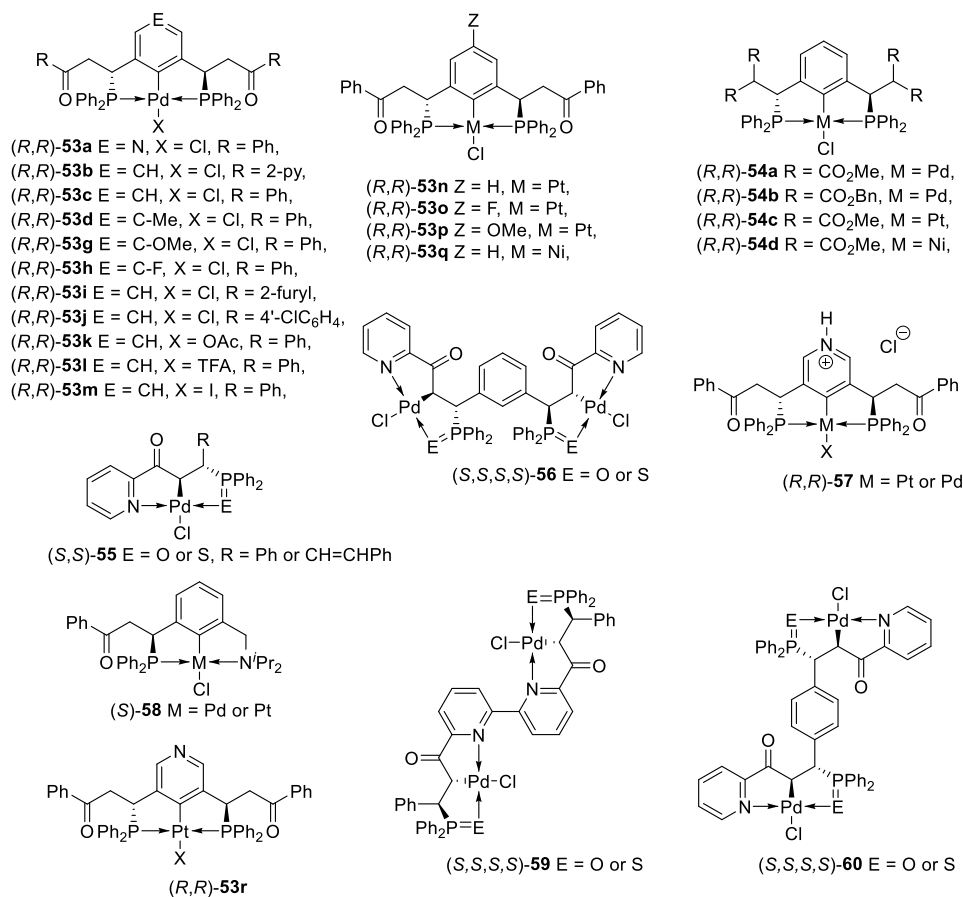
**Scheme 28:** the synthesis of pyridine-*N*-heterocyclic carbene palladacycle



The chiral pincers were obtained by cyclometallation of the phosphine ligands synthesized by asymmetric catalytic hydrophosphination of the multiple bonds (**Figure 6**). The synthesis was started with the asymmetric catalytic mono- or bi-hydrophosphination of the activated unsaturated bond to form the intermediates containing the bidentate phosphine ligands. The regioselectivity and enantioselectivity for the hydrophosphination should be extremely high, so that the next step of resolution would be much better, and the total yield would be higher. The design and synthesis of chiral pincer complexes **55** to **58** was reported. Similar to the phosphorus atom, the nitrogen atom also has a pair of lone electrons which could coordinate to the transition metal. The pincer complexes **55** and **58** were formed after the sequential mono-hydrophosphination and metalation.<sup>112-114</sup> The chiral tridentate phosphine cyclometal pincer **53**, **54**, and **57** were synthesized through sequential bihydrophosphination and metalation.<sup>113-117</sup> The yields of the bihydrophosphination were almost full conversion > 99%, and the *dr* for most of the ligands were better than 95:5. After the P-H addition completed, the cyclometallation was conducted *via* treatment the free ligands with appropriate metal source directly. The compounds **56**, **59**, and **60** bearing two pincer auxiliaries were also reported in our lab. Treatment the diphosphine ligands with palladium source directly formed the complex **53b**. After the sulfurization or oxidation of the air-sensitive free phosphine ligand, the

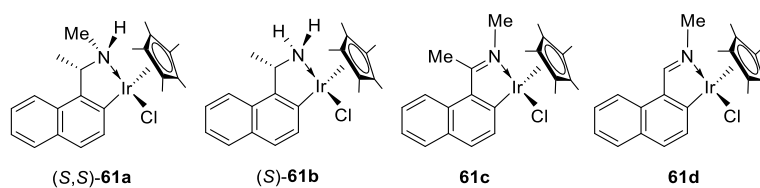
metalation formed the complex **56**, because the two five-membered ring was much more preferred.<sup>113</sup> In the case of the compounds **59** and **60**, it is difficult to get the PCP pincer even if there were two phosphine atoms. Because of the position of the two P- atoms, it is impossible to form the pincer complexes bearing five-membered ring.<sup>113</sup> In this case, the PCN pincer complexes were formed after the coordination of nitrogen atom in the pyridyl group to the metal. The yields of metalation were 68-99% normally. The authors also examined the catalytic properties of the pincer complexes for the asymmetric P-H addition.

**Figure 6:** The list of the pincer complexes in our lab



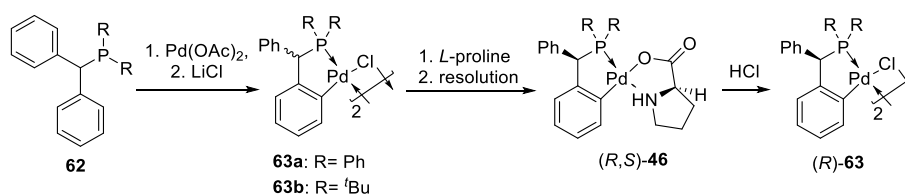
In the presence of sodium acetate as the base, a range of chiral pseudo-tetrahedral five-membered cyclometalated 1-naphthylethanamine Iridium(III) complexes **61a-d** were synthesized through the treatment of the specified amine with the iridium source [IrCp\*Cl<sub>2</sub>]<sub>2</sub>. The authors also examined the catalytic properties of them for asymmetric hydrogen transfer reaction (**Figure 7**).<sup>6</sup>

**Figure 7:** The list of Iridium complexes



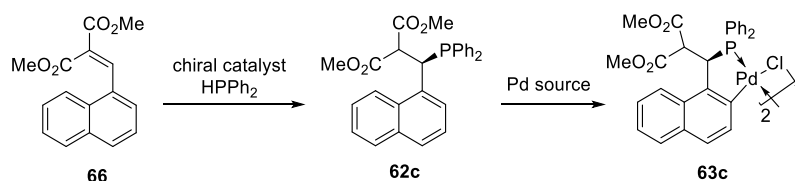
The racemic CP bidentate complexes **63a-b** were prepared by the cyclopalladation of the specified phosphine ligands **62a-b** with palladium acetate. The optical resolution was reported with the *L*-proline auxiliary. The dimeric CP complexes were reformed after the separation of the **46a-b** (Scheme 29).

**Scheme 29:** The synthesis and resolution of the CP bidentate complexes



The CP complex **63c** was prepared by stepwise the catalytic asymmetric hydrophosphination and cyclopalladation without the optical resolution.<sup>118</sup> Compared with the tedious original procedures, this catalytic asymmetric method was easier to synthesize the palladacycles (Scheme 30).<sup>119-120</sup> Stereoelectronic and chemical properties were studied after the coordination of the acetylacetonate (acac) and triphenylphosphine.

**Scheme 30:** Asymmetric catalytic synthesis of CP palladacycle

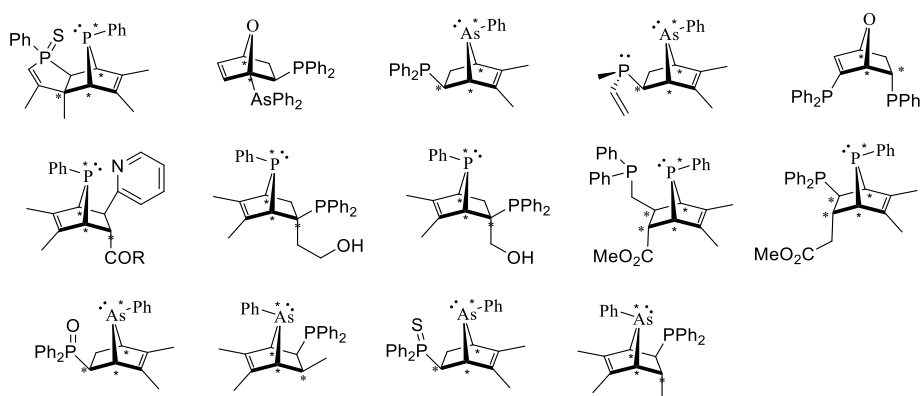


#### 1.4.2. Chiral CN palladacycles promoted the cycloaddition

The asymmetric cycloaddition reaction was promoted by the optically active CN palladacycles forming the individual optically pure *endo*- or *exo*-cycloadducts with very high chemoselectivity and stereoselectivity (Scheme

19).<sup>121-132</sup> The atoms containing the lone pair electrons in the dienes and the dienophiles, such as P, N, S, O, and As, would like to coordinate to the optically active CN palladium. The intramolecular cycloaddition proceeded when the dienes and dienophiles were activated by the palladium. The adducts were sequentially treated with concentrated HCl and KCN to remove the CN palladium auxiliary forming bidentate ligands listed in the **Figure 8**.

**Figure 8:** The list of the cycloaddition adducts

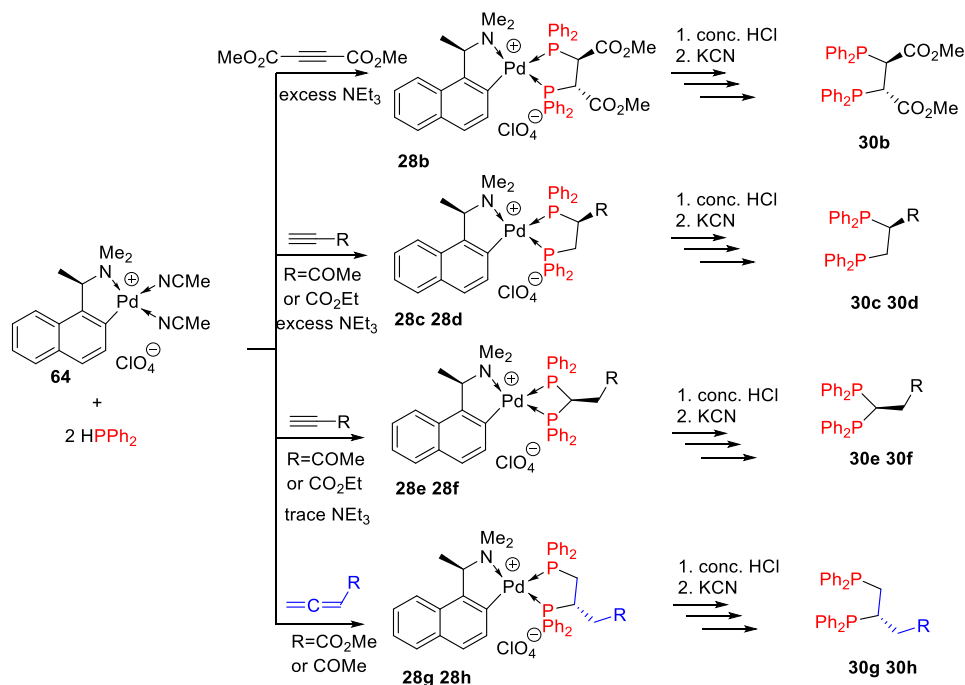


#### 1.4.3. The chiral CN palladacycle as the template for P-H addition

The chiral diphosphine ligands were prepared efficiently through the double P-H addition between the two equivalents of diphenylphosphine and the activated alkynes. The reaction was promoted by organopalladium (II) complex derived from (*S*)-*N,N*-dimethyl-1-(1-naphthyl)ethylamine **64** (**Scheme 31**). There are two types of addition, that is, 1,1- and 1,2-addition, and the chemoselectivity was controlled by the amount of the external base triethylamine. The reaction would not proceed in the absence of triethylamine under the ambient conditions. The alkynes preferred the (1,1)-addition in the presence of 2 mol% of triethylamine give obtain **28e-f**. In the presence of excess of the triethylamine, the reaction proceeded through (1,2)-addition to form the five-membered ring **28b-d**.<sup>133-134</sup> The diphosphine ligands were also synthesized by the double P-H addition. The double P-H addition was promoted by the CN palladium between the ester-or

keto-functionalized allenes in high regio- and stereo-selectivities forming **28g-h** (Scheme 31).<sup>135</sup>

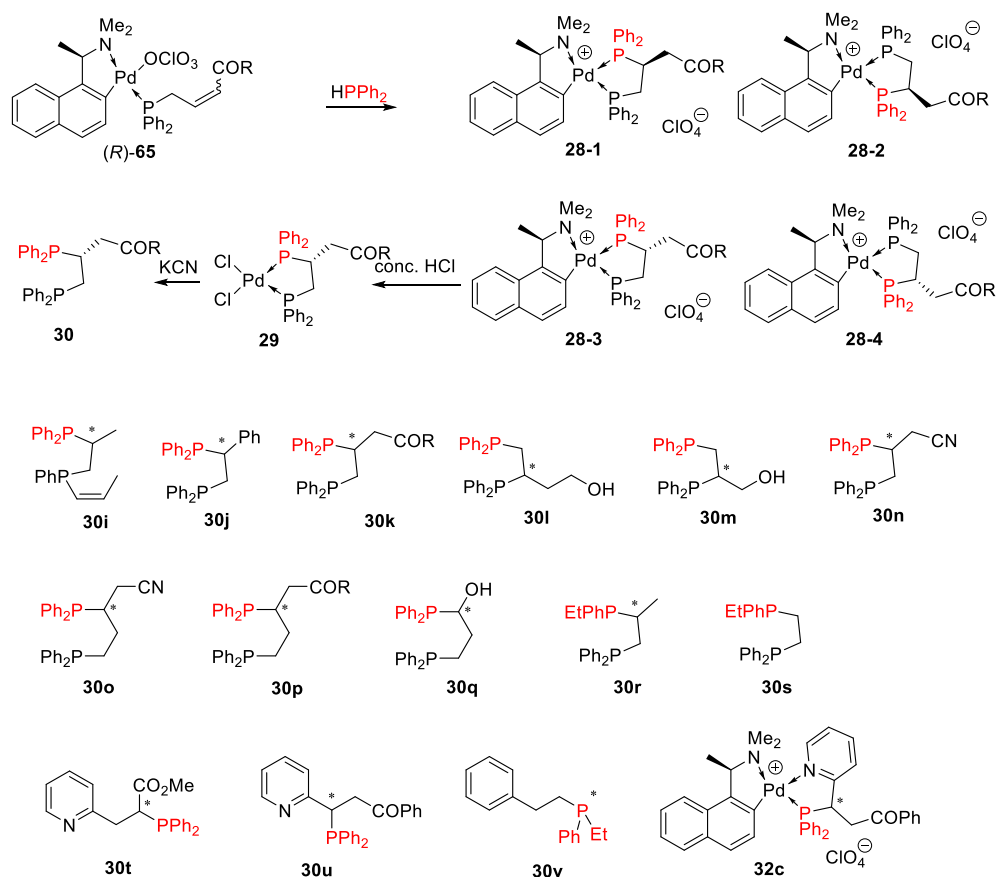
**Scheme 31:** The double P-H addition



Functionalized bidentate PP and PN phosphine ligands containing chiral centers were prepared *via* a two-stage asymmetric transformation of alkenes. The chiral bidentate ligands are usually prepared by very tedious procedure from chiral pool or optical resolution even though they have widespread application. Thus, our lab designed their asymmetric synthesis involving intramolecular P-H addition between the perchlorate monocomplexes **65** and the phosphines at the low temperature. Because of the moderate enantioselectivities for some substrates, the  $^{31}\text{P}\{^1\text{H}\}$  NMR spectrum of the crude mixture of the reaction showed four pairs of doublets for **28-1** to **28-4**. The main product was separated by fractional crystallization. The solution of **28-3** in dichloromethane was subsequently treated with concentrated hydrochloric acid to chemoselectively remove the naphthylamine auxiliary forming the dichloro complex **29**. The chiral free diphosphine ligands were liberated from the palladium after the treatment with the KCN. The intermediates **29** were formed, and its single-crystal X-ray

crystallography was examined.<sup>136-141</sup> It should be noted that ligands **30i** and **30r** have the both of carbon and phosphorus stereogenic centers and diphosphine ligand **30s** just has one phosphines stereogenic center. Diphosphine ligands **30r** and **30s** were prepared by the addition of the prochiral secondary ethylphenylphosphine HPPhEt<sup>142</sup> to the alkene bearing the tertiary prochiral phosphine phenyldi[(Z)-prop-1-enyl]phosphine<sup>138</sup>. Another diphosphine ligand that should be mentioned here is **30q** containing the alcohol which was prepared by the intramolecular promoted P-H addition to the C=O double bond of aldehyde.<sup>143</sup> Compared to the optically active diphosphine ligands **30k** and **30p**, **30n** and **30o**, it revealed that six-membered ring was also favored to the promoted P-H addition as the intermediate. The products **30m** and **30s**, demonstrated that the terminal alkenes were available to react with phosphine.

**Figure 9:** The asymmetric promoted synthesis of the bidentate ligands



Similar with the asymmetric promoted P-H addition to the unsaturated substrate containing the phosphorus, the intramolecular asymmetric promoted P-H addition was still effective with the substrates with pyridyl group.<sup>144</sup> In contrast to synthesis of the diphosphine ligands, which generates two pairs of diastereomers **28-1** and **28-2**, **28-3** and **28-4**, the formation of the NP bidentate ligands just involves one pair of diastereomers. The *trans*- position of the *NMe*<sub>2</sub> group in the (1-(dimethylamino)ethyl)naphthalene auxiliary was occupied by phosphorus, and another site *cis* to the *NMe*<sub>2</sub> group by the nitrogen in the pyridyl ring because of the electronic effect (**Figure 9**).<sup>142, 144-145</sup>

A series of chiral NP bidentate ligands containing 1,2-diester were prepared through *ortho*-palladated (*S*)-(1-(dimethylamino)ethyl)naphthalene. The ligands were obtained by sequential hydrophosphination of diphenylphosphine and hydroamination of different amines with acetylenedicarboxylate in high yields and high stereoselectivity.<sup>22</sup>

#### 1.4.4. The catalytic asymmetric hydrophosphination of the activated unsaturated multiple bond

The catalytic asymmetric P-H addition to the activated unsaturated bond was carried out in our lab forming numerous chiral free phosphine ligands with good regioselectivities and good enantioselectivities (up to 99%).<sup>57, 107, 112-116, 118, 146-154</sup> In the case **69f**, the enantioselectivity was depended on the polarity of the solvent.<sup>148</sup> The chiral phosphine containing the six-membered ring **73** was prepared through stepwise double addition of H-P-H bond to bis(enones) with PhPH<sub>2</sub> in one pot.<sup>106</sup> It should be noted that all products were synthesized with chiral CP complex (*R*)-**67** as the catalyst, except the products **70a** and **70b**. In the case of **70a** and **70b**, the oxygen atoms preferred to coordinate to the CP catalyst, so that the catalyst poison diminished its catalytic property. The catalyst used for P-H addition to prepare **70a** and **70b** was pincer (*S,S*)-**54e** containing just one free coordination site.<sup>118, 155</sup>

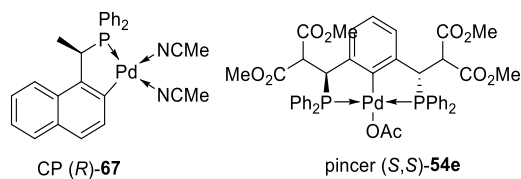
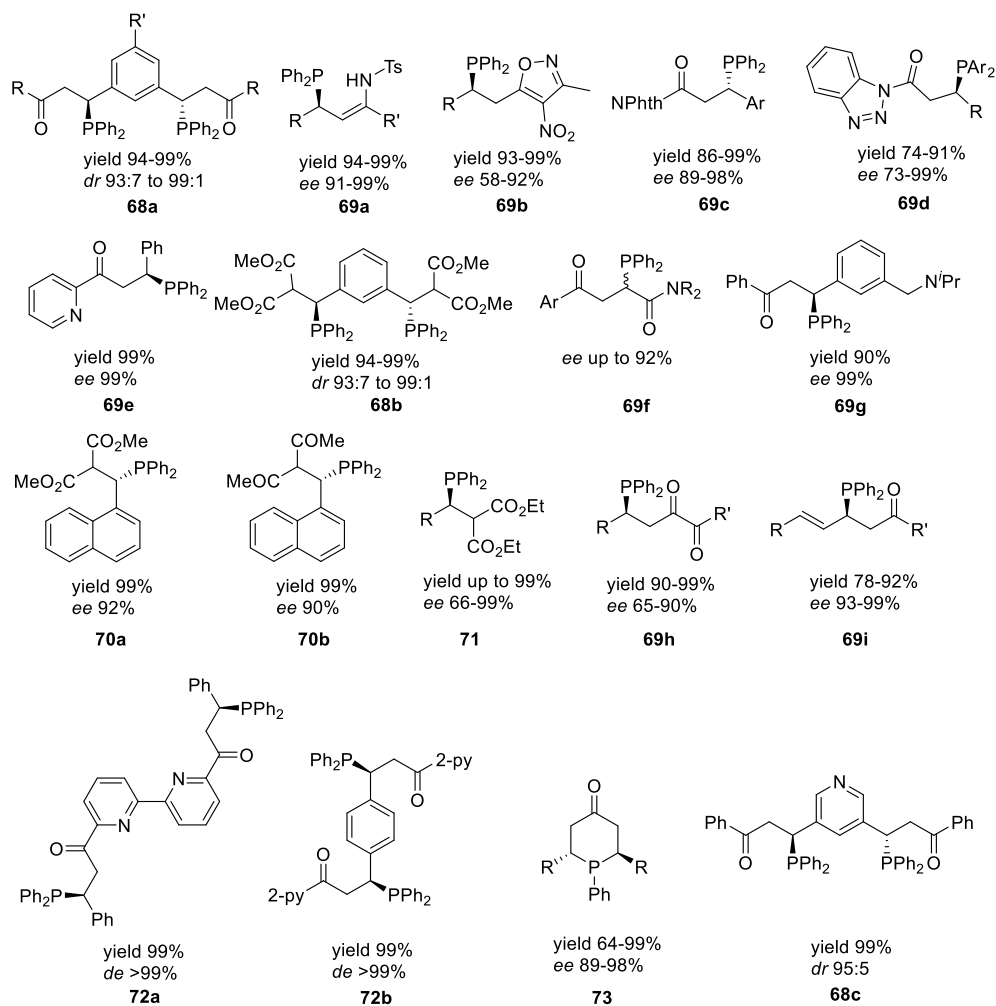
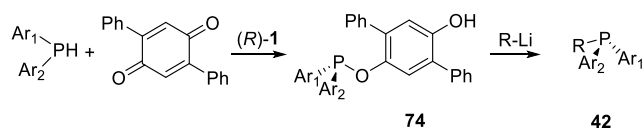


**Figure 10:** List of the products of the catalytic asymmetric hydrophosphination



The reaction of prochiral phosphines with substituted benzoquinones in the presence of an optically active cyclopalladated compound as the organocatalyst and  $\text{NEt}_3$  in  $\text{CHCl}_3$  proceeded in a new type of addition manner. The reaction gave a high yield chiral phosphinites **74** in a high enantioselectivity of 98%. The authors reported the application of **74** as a versatile intermediate readily convertible into a series of phosphines and their derivatives **42** with high enantiomeric purity (Scheme 32).<sup>156</sup>

**Scheme 32:** The P-H addition to benzoquinones

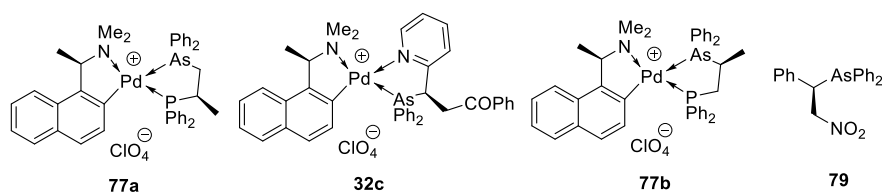


#### 1.4.5. Asymmetric hydroarsination

As the analogue of the phosphines and amines, the arsines containing the lone pair electrons reacted with unsaturated compounds forming new ligands. The reaction was promoted by chiral CN palladacycle. On the other hand, the reaction was carried out in a catalytic fashion with the chiral CP palladacycle as the catalyst forming the optically active adducts (**Figure 11**).<sup>157-159</sup> Unlike hydrophosphination and hydroamination that resulted in *cis*- and *trans*-regioisomers (**Figure 9**), the hydroarsination was 100% regioselective. For P/As ligands, the softer P atom occupied the coordination site *trans* to the N atom of the chiral auxiliary in complexes **77a** and **77b**. On the other hand, for N/As complexes, such as **32c**, the softer As atom occupied the coordination site *trans* to the N atom.

The hydroarsination between (*E*)-nitrostyrene and diphenylarsine was also examined in our group. The reaction was catalyzed by the chiral PCP pincers with Pd, Ni, or Pt transition metal forming the tertiary chiral arsine **79** (**Figure 11**).<sup>160</sup>

**Figure 11:** The list of promoted adducts for As-H addition



#### 1.5. Objectives of projects

Chiral bidentate CP palladacycles and PCE pincers were proved to be the efficient catalysts for asymmetric transformations such as hydrophosphination. However, until now the efficient chiral catalysts for the asymmetric P-H addition

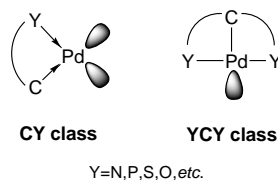
were very few. Herein, we designed the new methods to synthesize chiral catalysts for the asymmetric catalytic hydrophosphination based on the existed methods. Considering the tedious procedures to prepare the CP catalysts **67**, we designed catalytic method to obtain the analogues of **67** and then examined their catalytic properties for the asymmetric hydrophosphination and other reactions. Meanwhile, the conditions of the cyclometallation were also explored depending on the functional group.

## Chapter 2. Investigation of Functional Group Effects on Palladium Catalyzed Asymmetric P-H Addition

### 2.1. Introduction

The past decades have witnessed exponential growth and development of transition metal (TM) complexes in industry and in research.<sup>161</sup> Carbometallated palladium complexes, commonly known as palladacycles, have emerged to be ubiquitous (pre)catalysts and resolving agents. Since the first palladacycle was prepared by Cope in the 1960s,<sup>1-2</sup> there have been substantial reports on their preparation, properties, as well as the classes of reactions in which they mediate.<sup>17, 162-163</sup> To date, they have been demonstrated to be efficient catalysts in a wide variety of reactions, ranging from a) cross coupling reactions including the Suzuki-Miyaura,<sup>164-165</sup> Heck,<sup>166-168</sup> Sonogashira reactions;<sup>169-171</sup> b) rearrangement reactions;<sup>172-174</sup> c) annulations;<sup>175-177</sup> to d) hydrofunctionalizations.<sup>148, 151, 178-180</sup>

**Figure 12:** General classification of established palladacycles



The classes of palladacycles known today are notably the CY type complexes, analogs of the Hermann-Beller palladacycle<sup>181</sup> and the YCY class complexes, better known as pincer complexes (**Figure 12**). One of the first application of chiral CY-type palladacycles was the resolution of P-stereogenic phosphines.<sup>42</sup> Following intensive studies on modification of the structural backbone of the fundamental palladacycle ((*R*)-**4p-Cl**), Wild and co-workers successfully employed a naphthylamine analog ((*R*)-**24a-Cl**) as exceedingly efficient resolving agents for dissymmetric phosphines<sup>182-184</sup> and arsines.<sup>183, 185-186</sup> The enhanced efficiency of (*R*)-**24a-Cl** as a chiral derivatizing agent versus

its benzylamine predecessor was proposed to be due to improved chiral induction to the coordination sites, owing to the rigid conformation of the organometallic ring (**Figure 13**).<sup>62, 187-188</sup> Bosnich *et al.* showed that the aromaticity of highly conjugated and sterically demanding analogs (10,10'-di-hydroxy-9,9'-biphenylanthryl) can be disrupted upon metal complexation (**Figure 14**).<sup>189</sup> Pincer complexes on the other hand were pioneered by Moulten and Shaw in the 1970s. They have proven to be highly versatile as catalysts,<sup>190-191</sup> and chemical sensors, and also in dendrimer chemistry.<sup>192-194</sup>

**Figure 13:** Improved efficacy of palladacycle (*R*)-**24a-Cl** as a chiral derivatizing agent versus its benzylamine analogue (*R*)-**4p-Cl**

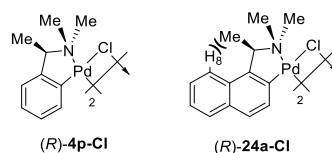
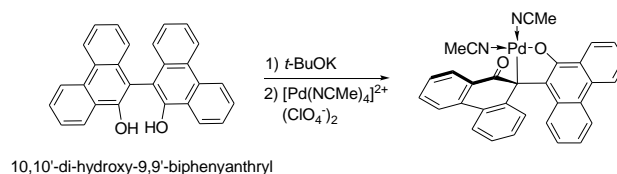


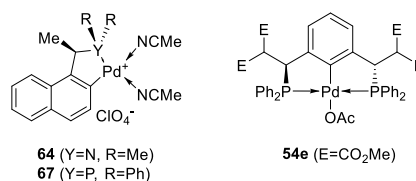
**Figure 14:** Disruption of aromaticity in sterically demanding auxiliary upon complexation with palladium



chiral phosphines, critical elements in metal-mediated asymmetric catalysis, have greatly driven the rapid development of synthetic methodologies over the past century.<sup>195-196</sup> On top of their conventional roles as ligands, they are also efficient organocatalysts in a number of chemical transformations.<sup>197-198</sup> Despite their significance, conventional synthetic methodologies for chiral phosphines rely on often the use of chiral starting materials or auxiliaries, rendering such approaches wasteful and cumbersome. The ideal solution would be their direct preparation *via* catalysis, effectively achieving 100% atom-economy with minimal wastage *via* the addition of phosphines to prochiral substrates. Moreover, this facilitates the syntheses of phosphines bearing various functionalities (esters,

amides, *etc.*) as they are valuable alternatives to typical ligands due to their distinct coordinative and stereoelectronic properties. Realizing the perpetual demand for optically active unprotected phosphines, our group have in recent years achieved the palladacycle (**64** and **67**) catalyzed asymmetric hydrophosphination (AHP) of a variety of Michael acceptors. Substrates including  $\alpha,\beta$ -unsaturated (di)ketones,<sup>106, 150, 154, 199</sup> imines,<sup>153</sup> diesters,<sup>107</sup> ketoamides,<sup>148</sup> phthalimides<sup>151</sup> and alkenylisoxazoles<sup>152</sup> are suitable electrophiles, generating a library of free, enantioenriched phosphines bearing C- and/or P-stereogenic centers. The established methodology could further be utilized in the preparation of optically pure pincer auxiliaries/complexes (**54e**) which require tedious synthetic methodologies or mechanical resolutions according to traditional approaches (Figure 15).<sup>114</sup>

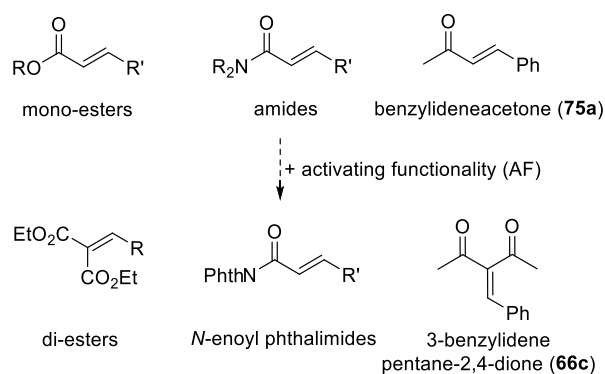
**Figure 15:** Phosphapalladacycles employed in the AHP reaction



Despite the success, there remain certain limitations in the classes of substrates that **64** or **67** can efficiently catalyze. An example would be the addition of phosphorus nucleophiles to poorly activated Michael acceptors. While the AHP of chalcones and its analogs proceeded smoothly,<sup>106, 150, 154, 199</sup> additions to  $\alpha,\beta$ -unsaturated monoesters, amides and benzylideneacetone (**75a**) proved to be challenging. A solution would be the introduction of activating functionalities (AF) (*i.e.* diesters,<sup>107</sup> phthalimides<sup>151</sup>) to increase the electrophilicity of the  $\beta$  carbon, therefore allowing the desired AHP reaction to proceed (Figure 16). Applying the same strategy, an additional acetyl group was introduced to benzylideneacetone **75a** with high hopes of achieving success in the P-H addition reaction. However, it was intriguing to note that the reaction

proceeded sluggishly with palladacycle **64** or **67**; yet gave significantly improved conversions within short reaction times with catalyst **54e**. As such, it was critical to unravel the underlying factors behind the observations so as to gain unprecedented understanding of the influence of functional group(s) on the catalyst and the associated chemical reactivities. The pincer catalyzed asymmetric P-H addition of diphenylphosphine to 3-benzylidene-2,4-pentadione **66c** is herein reported. Albeit successful in catalyzing a series of similar substrates, unexpected chelation of the dione substrate to CP and CN palladacycle catalyst resulted in inactivation of the catalyst with adjacent coordination sites. Protected phosphine adducts were isolated and characterized, providing critical insights to the choice of catalyst for structurally distinct functional groups borne by the substrate.

**Figure 16:** Introduction of activating groups to poorly activated Michael acceptors

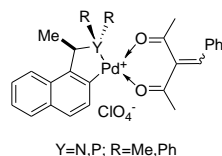


## 2.2. Results and Discussion

From an electronic viewpoint, the di-acetyl activated olefin (**66c**) is considerably more activated than the diester analog (**Figure 16**) as electronic contribution by oxygen to the carbonyl functionality reduces esters' electron withdrawing capabilities. Thus, it was surprising that the latter afforded enantioenriched phosphine adducts at low temperatures with catalytic amounts of **67**<sup>153</sup> while the reaction between diphenylphosphine ( $\text{Ph}_2\text{PH}$ ) and **66c** ironically proceeded sluggishly even with raised temperatures (rt) and prolonged reaction time. It was also intriguing to observe only minute conversions even

when a stoichiometric amount of the azapalladacycle **64** was employed as the promoter. Seeking the underlying factors for the unforeseen outcomes, thorough literature review subsequently revealed the tendency of acetylacetonone (acac) to form kinetically stable *O,O*-chelates with metallacycles in solution and in the solid state.<sup>108</sup> As such, it was evident that CY-type palladacycles (**64/67**) were ineffective in catalyzing or mediating the desired P-H addition owing to **66c** functioning as an effective catalyst poison (**Figure 17**).

**Figure 17:** Catalyst inactivation owing to formation of stable chelates between palladacycles **64/67** and the substrate



Determined to achieve the synthesis of chiral acetylacetonone-functionalized phosphines, a palladacycle bearing a single-coordination site (**54e**) was employed as the catalyst in hope of circumventing potential complications arising from the chelate effect of the substrate. Fortuitously, the reaction proceeded smoothly with (*S,S*)-**54e**, affording distinct signals at 5.8 and -13.8 ppm when subjected to <sup>31</sup>P{<sup>1</sup>H} NMR spectroscopic analysis upon reaction completion. The solvent properties that strongly influence catalysis include dipolarity (or polarity), hydrogen-bond donating ability (proticity) and hydrogen-bond accepting ability (basicity). The performance of a catalyst is strongly influenced by these parameters and therefore finding the right solvent for a catalytic reaction, or determining how a solvent affects the reaction, is important. Optimization of reaction conditions by varying the solvents and temperatures showed that THF produced the best conversion and enantioselectivity (**Table 1**, entry 1). While a reduction in operating temperatures improved the obtained enantiomeric excesses (*ee*), significantly longer reaction time was required for the reaction to

go to completion. In addition, it is observed that the ratios of the obtained products varied depending on the solvents employed.

**Table 1:** Optimization of reaction conditions for (*S,S*)-**54e** catalyzed asymmetric P-H addition of **66c** with diphenylphosphine (Ph<sub>2</sub>PH)<sup>a</sup>

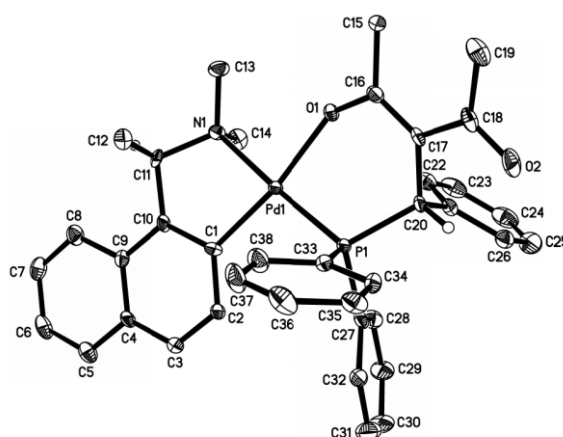
Entry	Solvent	T (°C)	Time (h)	Conv. (%) <sup>b</sup>	<i>ee</i> (%) <sup>c</sup>
1	THF	RT	4	83	58
2	CH <sub>2</sub> Cl <sub>2</sub>	RT	24	82	6
3	acetone	RT	6	83	39
4	CHCl <sub>3</sub>	RT	24	80	5
5	CHCl <sub>3</sub>	-40	120	42	22

<sup>a</sup> Reaction conditions: **66c** (0.1 mmol), Ph<sub>2</sub>PH (0.1 mmol), degassed solvent (5 mL). <sup>b</sup> Conversions are based on the sum of signals of **76** and **70c** arising from the <sup>31</sup>P{<sup>1</sup>H} NMR spectrum of the crude products. <sup>c</sup> Enantiomeric excess (*ee*) are obtained from chiral HPLC analyses of the sulphurized products.

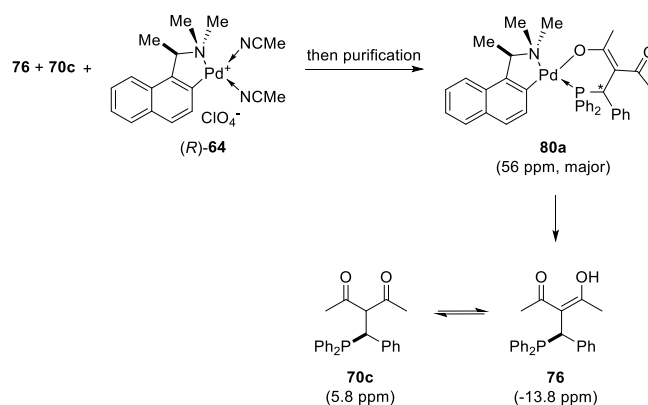
Treatment of the crude product mixture (**76**, **70c**) with enantiopure (*R*)-**64** gave unidentified signals at 44, 46, 48 ppm. However, stirring the mixture with silica subsequently affords diastereomeric adducts (**80a**) with only two apparent signals at 56 and 59 ppm. Crystallization of the diastereomeric mixture followed by X-ray crystallographic analyses revealed a phosphine-enolate chelate, with the newly formed stereogenic center bearing a *R* configuration (**Figure 18**). Comparison of the carbon-oxygen bond lengths in **80a** (C-O = 1.30 Å, C=O = 1.24 Å) reaffirms our observations that tautomers have indeed be obtained. Isolation of the major diastereomer (56 ppm) by flash chromatography and subsequent treatment with aqueous potassium cyanide (KCN) to liberate the bound phosphine surprisingly afforded 2 signals at 5.8 and -13.8 ppm (**Scheme 33**). This provides critical experimental evidence to support our postulations that a tautomeric mixture was obtained after the initial hydrophosphination reaction.

In addition, the observed variation in product ratios in different solvent systems can now be well understood since the degree of tautomerization is dependent on the property of the solvent.

**Figure 18:** Molecular structure and absolute stereochemistry of chelate **80a** with 50% thermal ellipsoids shown. Hydrogen atoms except those on the chiral center are omitted for clarity



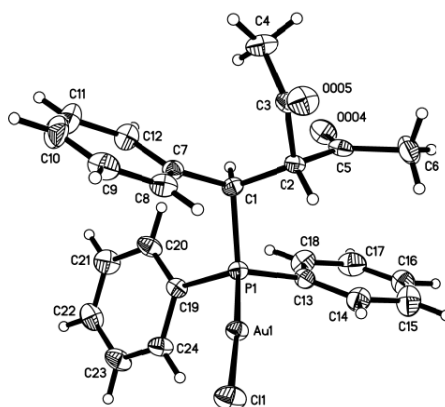
**Scheme 33:** Coordination studies revealing keto-enol tautomeric products prior and after coordination to palladacycle (*R*)-**24a-Cl**



An alternate approach to facilitate isolation and characterization of the phosphine products was the utilization of gold(I) halides as protecting agents. While the approach appears similar to coordination with palladium complexes (*R*)-**24a-Cl**, gold(I) however possess only one coordination site, thus effectively

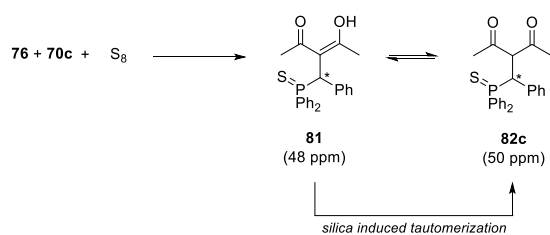
eliminating any potential chelate effects. X-ray analyses of the gold-phosphine complex revealed that the keto isomer was the sole product with no tautomerization observed even after purification with silica chromatography (**Figure 19**). Albeit obtaining racemic crystals, comparisons of the C=O bond lengths in the gold-phosphine complex showed that they are practically identical at 1.21 Å. On the other hand, distinct differences in the carbon-oxygen bond lengths in **80a** (C-O = 1.30 Å, C=O = 1.24 Å) reinforces the experimental findings of product tautomerization and the associated coordination modes with palladium.

**Figure 19:** Molecular structure of the gold(I)-phosphine adduct **90c** with 50% thermal ellipsoids



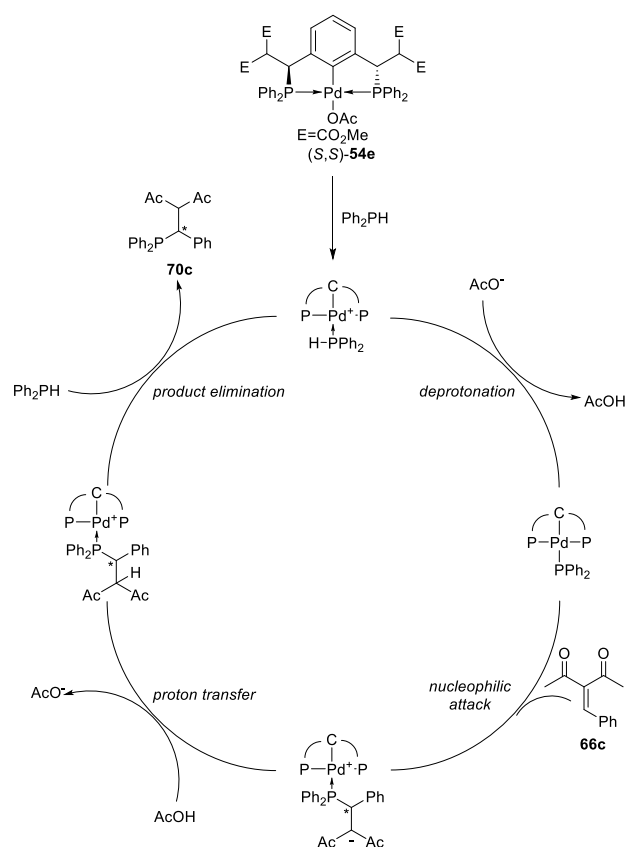
Conversely, protection of the crude phosphine adducts (**76**, **70c**) by sulphurization initially produced signals at 48 and 50 ppm (**81**, **82c**). Compound **81** was transferred to **82c** when treated with silica gel, and pure **82c** tautomerized back to **81** in the presence of HCl. While seemingly analogous to protection *via* complexation with gold(I), it was found that tautomerization of the phosphine-enol adduct to the thermodynamically favorable keto isomer **82c** (50 ppm) ensued upon purification on silica gel (**Scheme 34**). The methine proton (CO-CHC-CO) as observed in the proton NMR of **82c** ( $\delta=5.21$ ) substantiates the formation of the more stable di-keto tautomer.

**Scheme 34:** Silica induced tautomerization of sulphurized phosphine adducts



A mechanistic cycle for the pincer catalyzed hydrophosphination reaction is proposed. As secondary phosphines possess high affinities to palladium, diphenylphosphine readily displaces the weakly bound acetate ion. Unlike palladacycles which possess adjacent coordination sites, pincer **54e** binds preferentially to a single molecule of diphenylphosphine even in the presence of a chelating group. While this may appear insignificant, the unique affinities of various substrates to the catalyst are in fact critical for the desired nucleophilic attack in this study. The free acetate ion subsequently deprotonates the bound phosphine which is acidified due to metal complexation. This generates a highly reactive phosphido species which adds to the olefin *via* an outer sphere mechanism. Proton transfer from acetic acid followed by displacement of the product by unreacted diphenylphosphine regenerates the active catalyst (**Scheme 35**).

**Scheme 35:** Proposed catalytic cycle for the Pd-pincer catalyzed hydrophosphination of 3-benzylidenepentane-2,4-dione



### 2.3. Conclusion

The pincer catalyzed asymmetric P-H addition of diphenylphosphine to 3-benzylidene-2,4-pentadione is herein reported. Albeit successful in catalyzing a series of similar substrates, unexpected chelation of the dione substrate to CP and CN palladacycle catalyst resulted in inactivation of catalyst with adjacent coordination sites. Protected phosphine adducts were isolated and characterized, providing critical insights to the choice of catalyst for structurally distinct functional groups borne by the substrate. The intricate relationship between how various functional groups borne on the substrate can influence the performance of selected palladacycle catalysts is explored in this study, providing valuable insights on the choice of catalyst for structurally distinct substrates. The employment of a mono-coordination site palladium pincer catalyst circumvents

catalyst inactivation by the starting material, facilitating the first known asymmetric preparation of phosphines bearing a diketone functionality. While the *ee* values obtained are at best moderate, modifications to the pincer catalyst could potentially engender improvements in the obtained results. A plausible mechanistic cycle has been proposed for the asymmetric hydrophosphination reaction.

#### 2.4. Experimental section

All reactions were carried out under a positive pressure of nitrogen using standard Schlenk techniques. Commercially available reagents and solvents were purchased and used without further purification. When necessary, solvents should be freshly degassed before use. Column chromatography was conducted on silica gel 60 (Merck or Grace Division Discovery Science's (Davisil)).  $^{31}\text{P}\{^1\text{H}\}$ ,  $^1\text{H}$  and  $^{13}\text{C}\{^1\text{H}\}$  NMR spectra were recorded on Bruker ACF 400 or 500 spectrometers. High Resolution Mass spectroscopy (LC-HRMS) was performed using a Finnigan MAT95XP spectrometer. Chiral HPLC was conducted using a Agilent Technologies Series 1200 spectrometer, equipped with a DIACEL Chiralpak IC column; Conditions: Eluent= Hexane:IPA (19:1), Flow rate= 1 mL/min; temperature= 21.5 °C.

#### **General Procedure for the (*S,S*)-**54e** catalyzed asymmetric hydrophosphination reaction**

3-benzylidene-2,4-pentadione (**66c**) (0.02 g, 0.1 mmol) was added to the solution of PCP pincer catalyst (*S,S*)-**54e** (1.0 mg, 0.03 equiv.) and diphenylphosphine (1.0 equiv.) and stirred in the specified solvent (5 mL), temperature and time. The reaction was monitored by  $^{31}\text{P}\{^1\text{H}\}$  NMR spectroscopy, and the conversions calculated using the sum of integrals of tautomeric products **76** (-13.8 ppm) and **70c** (5.8 ppm).

#### **Characterization of Reaction Products**

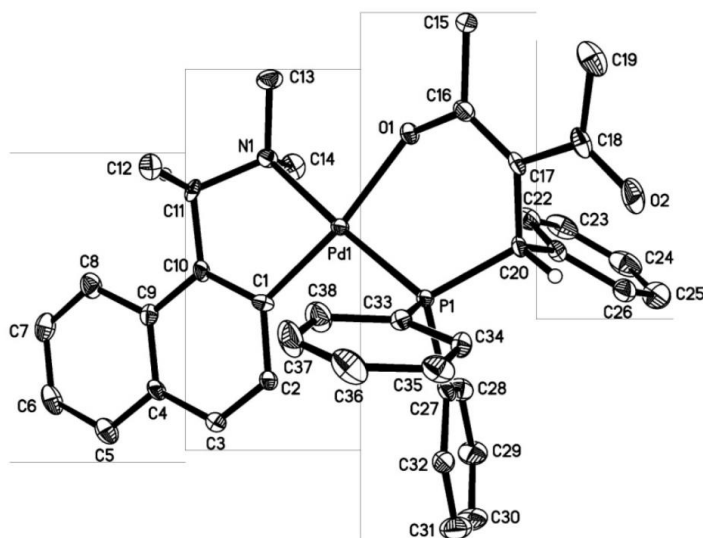
The data of **70c**,  $^{31}\text{P}\{^1\text{H}\}$  NMR (162 MHz,  $\text{CDCl}_3$ ),  $\delta$  50.64.  $^1\text{H}$  NMR (400 MHz,  $\text{CDCl}_3$ ),  $\delta$  6.68-7.55 (m, 21H), 5.17-5.22 (d,  $J = 20.1$  Hz, 1H), 4.48-4.52 (m, 1H), 3.00 – 3.01 (d,  $J = 3.3$  Hz, 3H), 2.86 (s, 3H), 2.36 (s, 3H), 2.24 (s, 3H), 1.94-1.95 (d,  $J = 6.3$  Hz, 3H).  $^{13}\text{C}$  NMR (101 MHz,  $\text{CDCl}_3$ ),  $\delta$  123.98-134.60, 70.96, 50.90, 45.18, 41.18, 30.76, 30.07, 29.79, 24.81, 23.48. HRMS of **80a**: Calculated for  $\text{C}_{38}\text{H}_{39}\text{NO}_2\text{PPd}$ : 678.1753, found: 678.1729.

The data of **82c**:  $^{31}\text{P}\{^1\text{H}\}$  NMR (202 MHz,  $\text{CDCl}_3$ ),  $\delta$  50.64.  $^1\text{H}$  NMR (500 MHz,  $\text{CDCl}_3$ ),  $\delta$  8.14-7.17 (m, 15H), 5.19-5.24 (dd,  $J = 13.1, 10.9$  Hz, 1H), 4.94-5.00 (dd,  $J = 10.8, 9.1$  Hz, 1H), 2.04 (s, 3H), 1.81 (s, 3H).  $^{13}\text{C}$  NMR (126 MHz,  $\text{CDCl}_3$ ),  $\delta$  131.92-127.83, 70.21, 46.70, 31.42, 29.02. HRMS of **82c**: Calculated for  $\text{C}_{24}\text{H}_{24}\text{O}_2\text{PS}$ : 407.1235, found: 407.1231.

The data of Au-phosphine adduct:  $^{31}\text{P}\{^1\text{H}\}$  NMR (162 MHz,  $\text{CDCl}_3$ ),  $\delta$  49.65.  $^1\text{H}$  NMR (400 MHz,  $\text{CDCl}_3$ ),  $\delta$  7.18-8.04 (m, 15H), 4.90-5.01 (m, 2H), 1.92 (s, 3H), 1.80 (s, 3H).  $^{13}\text{C}$  NMR (101 MHz,  $\text{CDCl}_3$ ),  $\delta$  128.46-135.72, 72.59, 43.94, 31.22, 28.79.

### Single Crystal X-ray Diffraction Data

**Figure 18**: Molecular structure and absolute stereochemistry of chelate **80a** with 50% thermal ellipsoids shown. Hydrogen atoms except those on the chiral centre are omitted for clarity.



CCDC 1424966 contains the supplementary crystallographic data for this paper. These data can be obtained free of charge from The Cambridge Crystallographic Data Centre via [www.ccdc.cam.ac.uk/data\\_request/cif](http://www.ccdc.cam.ac.uk/data_request/cif).

### Crystal Structure Report

A yellow block-like specimen of  $C_{38}H_{38}NO_2PPd$ , approximate dimensions 0.180 mm x 0.400 mm x 0.420 mm, was used for the X-ray crystallographic analysis. The X-ray intensity data were measured.

The total exposure time was 0.24 hours. The frames were integrated with the Bruker SAINT software package using a narrow-frame algorithm. The integration of the data using a monoclinic unit cell yielded a total of 60896 reflections to a maximum  $\theta$  angle of  $33.78^\circ$  (0.64 Å resolution), of which 25236 were independent (average redundancy 2.413, completeness = 99.6%,  $R_{int} = 10.73\%$ ,  $R_{sig} = 14.78\%$ ) and 18985 (75.23%) were greater than  $2\sigma(F^2)$ . The final cell constants of  $a = 11.8563(8)$  Å,  $b = 15.4239(10)$  Å,  $c = 17.5713(12)$  Å,  $\beta = 96.314(2)^\circ$ , volume =  $3193.8(4)$  Å<sup>3</sup>, are based upon the refinement of the XYZ-centroids of 5975 reflections above  $20 \sigma(I)$  with  $5.360^\circ < 2\theta < 50.34^\circ$ . Data were corrected for absorption effects using the multi-scan method (SADABS). The ratio of minimum to maximum apparent transmission was 0.798. The calculated minimum and maximum transmission coefficients (based on crystal size) are 0.7670 and 0.8900.

The final anisotropic full-matrix least-squares refinement on  $F^2$  with 924 variables converged at  $R1 = 6.50\%$ , for the observed data and  $wR2 = 14.22\%$  for all data. The goodness-of-fit was 0.989. The largest peak in the final difference electron density synthesis was  $1.476 e^-/\text{Å}^3$  and the largest hole was  $-1.282 e^-/\text{Å}^3$  with an RMS deviation of  $0.139 e^-/\text{Å}^3$ . On the basis of the final model, the calculated density was  $1.410 \text{ g/cm}^3$  and  $F(000)$ , 1400  $e^-$ .

---

**Table 2:** Sample and crystal data for leung872s

<b>Identification code</b>	leung872s
----------------------------	-----------

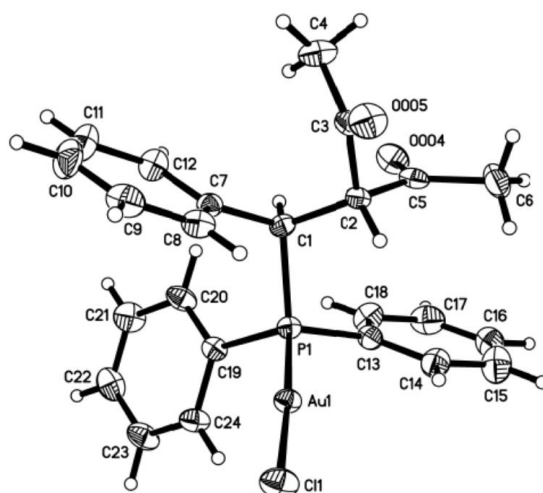
<b>Chemical formula</b>	C <sub>38</sub> H <sub>38</sub> NO <sub>2</sub> PPd	
<b>Formula weight</b>	678.06 g/mol	
<b>Temperature</b>	103(2) K	
<b>Wavelength</b>	0.71073 Å	
<b>Crystal size</b>	0.180 x 0.400 x 0.420 mm	
<b>Crystal habit</b>	yellow block	
<b>Crystal system</b>	Monoclinic	
<b>Space group</b>	P 1 21 1	
<b>Unit cell dimensions</b>	a = 11.8563(8) Å	α = 90°
	β = 96.314(2)°	b = 15.4239(10) Å
	γ = 90°	c = 17.5713(12) Å
<b>Volume</b>	3193.8(4) Å <sup>3</sup>	
<b>Z</b>	4	
<b>Density (calculated)</b>	1.410 g/cm <sup>3</sup>	
<b>Absorption coefficient</b>	0.666 mm <sup>-1</sup>	
<b>F(000)</b>	1400	

**Table 3:** Data collection and structure refinement for leung872s

<b>Theta range for data collection</b>	1.98 to 33.78°	
<b>Index ranges</b>	-18<=h<=18, -24<=k<=24, -26<=l<=27	
<b>Reflections collected</b>	60896	
<b>Independent reflections</b>	25236 [R(int) = 0.1073]	
<b>Coverage of independent reflections</b>	99.6%	
<b>Absorption correction</b>	multi-scan	
<b>Max. and min. transmission</b>	0.8900 and 0.7670	
<b>Refinement method</b>	Full-matrix least-squares on F <sup>2</sup>	
<b>Refinement program</b>	SHELXL-2014/6 (Sheldrick, 2014)	
<b>Function minimized</b>	Σ w(F <sub>o</sub> <sup>2</sup> - F <sub>c</sub> <sup>2</sup> ) <sup>2</sup>	
<b>Data / restraints / parameters</b>	25236 / 806 / 924	
<b>Goodness-of-fit on F<sup>2</sup></b>	0.989	
<b>Δ/σ<sub>max</sub></b>	0.001	
<b>Final R indices</b>	18985 data; I>2σ(I) all data R1 = 0.0942, wR2 = 0.1422	R1 = 0.0650, wR2 = 0.1249
<b>Weighting scheme</b>	w=1/[σ <sup>2</sup> (F <sub>o</sub> <sup>2</sup> )] where P=(F <sub>o</sub> <sup>2</sup> +2F <sub>c</sub> <sup>2</sup> )/3	
<b>Absolute structure parameter</b>	-0.0(0)	

<b>Largest diff. peak and hole</b>	1.476 and -1.282 eÅ <sup>-3</sup>
<b>R.M.S. deviation from mean</b>	0.139 eÅ <sup>-3</sup>

**Figure 19:** Molecular structure of the gold(I)-phosphine adduct with 50% thermal ellipsoids.



CCDC 1424965 contains the supplementary crystallographic data for this paper. These data can be obtained free of charge from The Cambridge Crystallographic Data Centre via [www.ccdc.cam.ac.uk/data\\_request/cif](http://www.ccdc.cam.ac.uk/data_request/cif).

### Crystal Structure Report

A colorless block-like specimen of C<sub>24</sub>H<sub>23</sub>AuClO<sub>2</sub>P, approximate dimensions 0.100 mm x 0.140 mm x 0.200 mm, was used for the X-ray crystallographic analysis. The X-ray intensity data were measured.

The total exposure time was 0.63 hours. The frames were integrated with the Bruker SAINT software package using a narrow-frame algorithm. The integration of the data using a triclinic unit cell yielded a total of 44175 reflections to a maximum  $\theta$  angle of 36.49° (0.60 Å resolution), of which 11409 were independent (average redundancy 3.872, completeness = 99.0%,  $R_{\text{int}} = 10.12\%$ ,  $R_{\text{sig}} = 9.98\%$ ) and 7841 (68.73%) were greater than  $2\sigma(F^2)$ . The final cell constants of  $a = 9.9394(4)$  Å,  $b = 11.1972(4)$  Å,  $c = 11.8538(4)$  Å,  $\alpha = 116.6194(19)^\circ$ ,  $\beta = 92.541(2)^\circ$ ,  $\gamma = 93.610(3)^\circ$ , volume = 1173.18(8) Å<sup>3</sup>, are based upon the refinement of the XYZ-centroids of 4570 reflections above 20

$\sigma(I)$  with  $5.41^\circ < 2\theta < 50.07^\circ$ . Data were corrected for absorption effects using the multi-scan method (SADABS). The ratio of minimum to maximum apparent transmission was 0.715. The calculated minimum and maximum transmission coefficients (based on crystal size) are 0.3580 and 0.5640.

The final anisotropic full-matrix least-squares refinement on  $F^2$  with 264 variables converged at  $R1 = 4.60\%$ , for the observed data and  $wR2 = 9.08\%$  for all data. The goodness-of-fit was 0.971. The largest peak in the final difference electron density synthesis was  $1.429 \text{ e}^-/\text{\AA}^3$  and the largest hole was  $-2.508 \text{ e}^-/\text{\AA}^3$  with an RMS deviation of  $0.233 \text{ e}^-/\text{\AA}^3$ . On the basis of the final model, the calculated density was  $1.718 \text{ g/cm}^3$  and  $F(000)$ , 588  $e^-$ .

**Table 4:** Sample and crystal data for leung881

<b>Identification code</b>	leung881	
<b>Chemical formula</b>	$\text{C}_{24}\text{H}_{23}\text{AuClO}_2\text{P}$	
<b>Formula weight</b>	606.81 g/mol	
<b>Temperature</b>	103(2) K	
<b>Wavelength</b>	0.71073 $\text{\AA}$	
<b>Crystal size</b>	0.100 x 0.140 x 0.200 mm	
<b>Crystal habit</b>	colorless block	
<b>Crystal system</b>	Triclinic	
<b>Space group</b>	P -1	
<b>Unit cell dimensions</b>	$\alpha = 116.6194(19)^\circ$	$a = 9.9394(4) \text{ \AA}$
	$\beta = 92.541(2)^\circ$	$b = 11.1972(4) \text{ \AA}$
	$\gamma = 93.610(3)^\circ$	$c = 11.8538(4) \text{ \AA}$
<b>Volume</b>	$1173.18(8) \text{ \AA}^3$	
<b>Z</b>	2	
<b>Density (calculated)</b>	$1.718 \text{ g/cm}^3$	
<b>Absorption coefficient</b>	$6.468 \text{ mm}^{-1}$	
<b>F(000)</b>	588	

**Table 5:** Data collection and structure refinement for leung881

<b>Theta range for data collection</b>	2.71 to $36.49^\circ$
<b>Index ranges</b>	$-16 \leq h \leq 16$ , $-18 \leq k \leq 18$ , $-19 \leq l \leq 19$
<b>Reflections collected</b>	44175
<b>Independent reflections</b>	11409 [ $R(\text{int}) = 0.1012$ ]

<b>Coverage of independent reflections</b>	99.0%	
<b>Absorption correction</b>	multi-scan	
<b>Max. and min. transmission</b>	0.5640 and 0.3580	
<b>Refinement method</b>	Full-matrix least-squares on $F^2$	
<b>Refinement program</b>	SHELXL-2014/7 (Sheldrick, 2014)	
<b>Function minimized</b>	$\Sigma w(F_o^2 - F_c^2)^2$	
<b>Data / restraints / parameters</b>	11409 / 0 / 264	
<b>Goodness-of-fit on <math>F^2</math></b>	0.971	
<b><math>\Delta/\sigma_{max}</math></b>	0.002	
	7841	
<b>Final R indices</b>	data;	R1 = 0.0460, wR2 = 0.0780
	I > 2 $\sigma$ (I)	
	all data R1 = 0.0865, w	R2 = 0.0908
<b>Weighting scheme</b>	w = 1 / [ $\sigma^2(F_o^2) + (0.0289P)^2$ ] wher	
	e P = (F <sub>o</sub> <sup>2</sup> + 2F <sub>c</sub> <sup>2</sup> ) / 3	
<b>Largest diff. peak and hole</b>	1.429 and -2.508 eÅ <sup>-3</sup>	
<b>R.M.S. deviation from mean</b>	0.233 eÅ <sup>-3</sup>	



## Chapter 3. Efficient Access to a Designer Phosphapalladacycle Catalyst *via* Enantioselective Catalytic Asymmetric Hydrophosphination

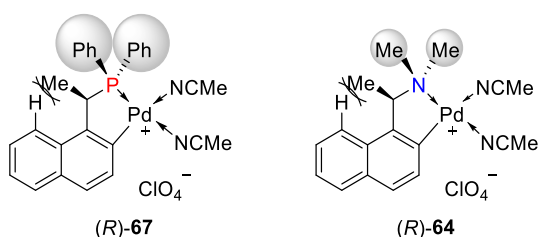
### 3.1. Introduction

Chiral phosphines are an important class of organophosphorus compounds that have found widespread application as ligands in asymmetric catalysis<sup>89, 200</sup> and organocatalysis.<sup>92, 197-198</sup> Similar to other chiral compounds, enantiomerically pure phosphines may be prepared by methods such as classical diastereomeric, chemical kinetic, chromatographic resolutions, asymmetric catalysis or from naturally occurring chiral starting materials.<sup>180, 201-206</sup> Due to the highly oxidizable nature of most phosphines, these compounds are often converted into the corresponding oxides, sulfides or borane derivatives for the ease of handling. In comparison, the direct generation of tertiary phosphines *via* asymmetric catalysis is not only atom-economical, but also attractive as it avoids the traditional protection-resolution-deprotection steps<sup>185, 207-208</sup> which have been known to affect yields and optical purities.<sup>209-212</sup> However, the catalytic asymmetric synthesis of chiral phosphines<sup>57, 104-105, 153, 202, 206, 213-215</sup> is challenging due to the profound affinity of phosphines toward most low valent late transition metal ions.

Palladacycle complexes have been extensively studied for their wide-ranging synthetic applications and in catalysis, especially in the formation of C-C (eg. Heck, Suzuki, Sonogashira, Kumada and Negishi cross couplings) and C-heteroatom (eg. Buchwald-Hartwig amination) bond formations.<sup>216-220</sup> In our group, we have been successful in employing the palladacycle catalysts **67** and **64** (**Figure 20**) toward the generation of chiral tertiary phosphines from asymmetric hydrophosphination of Michael acceptors<sup>57, 104</sup> such as

benzoquinones<sup>156</sup> and imines.<sup>153</sup> In addition, some of the phosphine products have been employed successfully as chiral auxiliaries in transition-metal catalyzed reactions.<sup>112-113, 146, 149, 215</sup> The superior performance of catalysts **67** and **64** in the preparation of valuable chiral phosphines could potentially propel the advancement of the applications of catalytically produced phosphine compounds in many areas such as pharmaceuticals.

**Figure 20:** Cyclopalladated complexes developed by our group

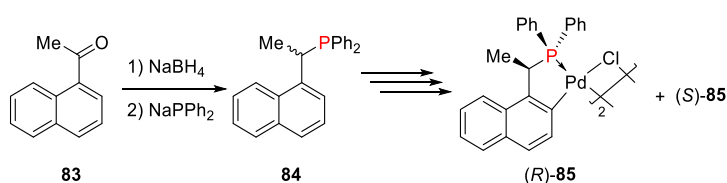


The thermodynamically stable and kinetically inert Pd-C<sub>naphthyl</sub> bond in the *ortho*-metalated chelate offers strong and predictable *trans* electronic influence to the metal center.<sup>61, 108, 187, 221-222</sup> It has been well established that the phosphapalladacycle catalyst **67** outperforms the analogous amine complex **64** in terms of reactivity and stereoselectivity.<sup>150, 154, 223</sup> The N→Pd bond in catalyst **64** offers a favorable *trans* N→Pd←P<sub>product</sub> orientation during the catalytic cycle, resulting in sluggish product dissociation. Furthermore, the smaller prochiral NMe<sub>2</sub> moiety is unable to project the chirality efficiently onto the active catalytic sites of the Pd metal center, leading to diminished stereoselectivity. In addition, the chiral induction process is controlled by the non-interconvertible conformation of the five-membered organometallic ring as a consequence of steric hindrance between the naphthalene proton and the methyl functionality.<sup>55, 62, 224</sup> Despite all these features, the major limitation lies in the synthesis of optically pure complex **67**. The laborious multi-step synthesis involves nucleophilic substitution with NaPPh<sub>2</sub>, optical resolution of racemic phosphine **85** with a chiral amine palladacycle, fractional recrystallization, treatment with conc. HCl, and finally *ortho*-palladation to obtain the optically pure dimeric

complex **85** (precursor of complex **67**) in *ca* 50% overall yield (**Scheme 36**).<sup>102</sup> Consequently, the lengthy protocol restricts the efficient application of analogous chiral phosphapalladacycles in other catalytic scenarios.

Our previous attempt to produce the chiral complex **86b** *via* catalytic asymmetric hydrophosphination of unsaturated diketone **66b** was not successful due to catalyst deactivation arising from the coordination of diketone **66b** to catalyst **67** (**Scheme 37**), forming kinetically stable *O,O*-bidentate chelates (**Figure 21**).<sup>108, 155</sup>

**Scheme 36:** Multi-step synthesis of optically pure dimeric complex **85**



**Scheme 37:** Retrosynthetic pathway of complex **99b**

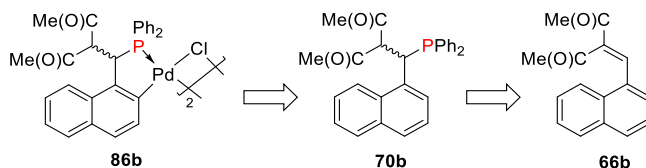
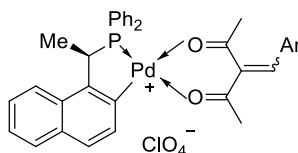


**Figure 21:** Catalyst deactivation due to coordination of acetylaceton moiety



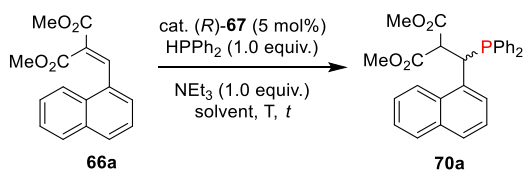
Herein, we report the efficient synthesis, purification, isolation and characterization of an optically active designer phosphapalladacycle catalyst. The catalytic hydrophosphination protocol is efficient in generating the chiral phosphine auxiliary stereoselectively, which negates the need for classical resolution techniques. The efficacy of the new catalyst is demonstrated in the asymmetric hydrophosphination of chalcone. In addition, two oxo-palladium complexes were isolated and characterized crystallographically during this study.

A chiral phosphine auxiliary was generated with excellent *ee* via catalytic asymmetric hydrophosphination of 3-(naphthalen-1-ylmethylene)pentane-2,4-dione. The subsequent metal complexation of the monophosphine yielded two different coordination complexes depending on the reaction conditions. The *ortho*-palladation of both coordination complexes resulted in the formation of a single dimeric phosphapalladacycle complex that could be further converted to the monomeric bisacetonitrile derivative. Moreover, the palladium complex exhibits interesting oxophilicity as the stable bisquo derivative could be isolated and characterized crystallographically. The catalytic potential of the phosphapalladacycle was also demonstrated.

### 3.2. Results and Discussion

From the perspective of catalyst design, earlier studies have revealed the importance of the steric interactions between the chiral moiety and the naphthalene proton (**Figure 20**).<sup>55, 62, 224</sup> As such, it is plausible that increasing the steric bulk of the chiral moiety might have a direct influence on the stereochemical control of the phosphapalladacycle catalyst. Hence, a bulky malonate functionality was installed on substrate **66a** and subjected to asymmetric hydrophosphination in the presence of catalyst (*R*)-**67** (**Table 6**).

**Table 6:** Optimization of reaction conditions<sup>a</sup>



entry	T (°C)	solvent	<i>t</i> (h)	conversion <sup>b</sup> (%)	<i>ee</i> <sup>c</sup> (%)
1 <sup>d</sup>	RT	MeOH	3	99	22 ( <i>S</i> )
2	RT	MeOH	3	99	44 ( <i>S</i> )
3	-80	MeOH	15	99	85 ( <i>S</i> )
4	-80	Acetone	120	54	32 ( <i>S</i> )
5	-80	THF	72	3	62 ( <i>S</i> )
6	-80	DCM	96	26	30 ( <i>S</i> )
7	-80	MeOH/CHCl <sub>3</sub> <sup>e</sup>	48	99	91 ( <i>S</i> ) <sup>f</sup>
8	-80	MeOH/DCM <sup>e</sup>	60	99	83 ( <i>S</i> )

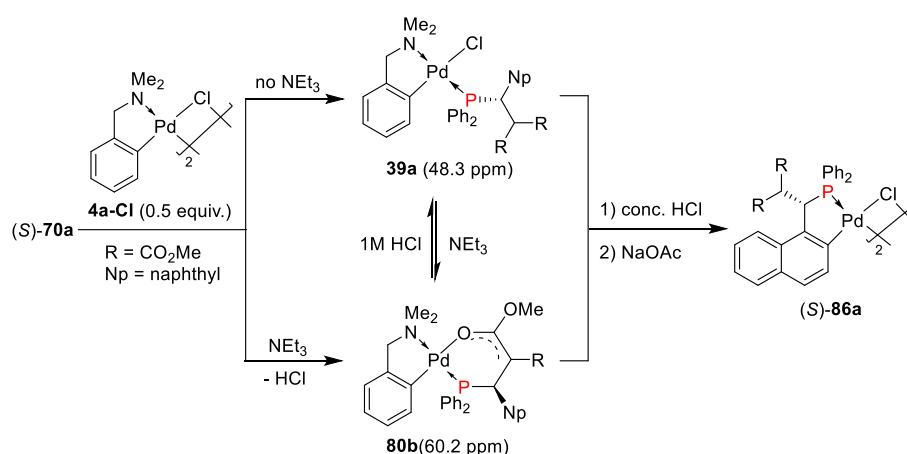
9	-80	MeOH/Acetone <sup>e</sup>	120	90	82 ( <i>S</i> )
10	-80	MeOH/THF <sup>e</sup>	72	7	59 ( <i>S</i> )

<sup>a</sup> Conditions: cat. (*R*)-**67** (3.37 mg, 5.37  $\mu$ mol, 5 mol%), HPPPh<sub>2</sub> (20.0 mg, 0.107 mmol, 1.0 equiv.), NEt<sub>3</sub> (14.9  $\mu$ L, 0.107 mmol, 1.0 equiv.), malonate **66a** (31.9 mg, 0.118 mmol, 1.1 equiv.) in the solvent (6 mL) stirred at the stated temperature. <sup>b</sup> Conversion was monitored by the disappearance of HPPPh<sub>2</sub> (-40.0 ppm) via <sup>31</sup>P{<sup>1</sup>H} NMR spectroscopy. <sup>c</sup> *ee* of phosphine **70c** was established by chiral HPLC after isolating the air sensitive product as the sulfide derivative. The absolute configuration of the major product in parentheses was determined by comparison to entry 7. <sup>d</sup> Cat. (*R*)-**64** (3.37 mg, 5.37  $\mu$ mol, 5 mol%) was used instead of cat. (*R*)-**67**. <sup>e</sup> 50% MeOH. <sup>f</sup> Absolute configuration of the major product was ascertained by X-ray crystallography upon isolation as a phosphine-gold(I) complex (*S*)-**87**.

Overall, the hydrophosphination reaction proceeded smoothly to afford tertiary phosphine **70a** in excellent yields with *ee*'s of up to 91% (**Table 6**). It was found that the stereoselectivity of the hydrophosphination reaction was highest when a mixture of methanol and chloroform was used as the solvent (Entry 7). For the ease of handling and determination of *ee* by chiral HPLC, the air-sensitive tertiary phosphine **70a** was isolated as the sulfide derivative. The absolute configuration of the major enantiomer was ascertained to be *S* by X-ray crystallography upon coordination to Au. With the optimized conditions (Entry 7), the one-pot cyclometallation of the crude tertiary phosphine **70c** was attempted with various Pd sources such as Li<sub>2</sub>PdCl<sub>4</sub>, PdCl<sub>2</sub>(NCMe)<sub>2</sub>, PdCl<sub>2</sub>(NCPh)<sub>2</sub> and the benzylamine complex **4a-Cl**. In these instances, only the reaction between phosphine **70c** and complex **4a-Cl** resulted in a relatively clean reaction mixture as observed from <sup>31</sup>P{<sup>1</sup>H} NMR spectroscopy. Isolation and characterization of the products revealed the formation of complexes **39a** and **80b**. Incidentally, it was discovered that the presence of NEt<sub>3</sub> plays a crucial role in dictating the coordination mode of complex **39a** and **80b** (**Scheme 38**). In the absence of NEt<sub>3</sub>, facile coordination of phosphine **70c** to the Pd center resulted in the formation of the monodentate complex **39a** (<sup>31</sup>P{<sup>1</sup>H} = 48.3 ppm). Upon

addition of  $\text{NEt}_3$ , deprotonation ensued to form the P–O bidentate complex **80b** ( $^{31}\text{P}\{^1\text{H}\} = 60.2 \text{ ppm}$ ). The crystals of complex **80b** suitable for single crystal X-ray diffraction were obtained from a mixture of DCM/*n*-hexane (ORTEP shown in [Figure 22](#)). A comparison of selected bond lengths in complex **80b** with those of analogous complexes shows the presence of delocalization in the O–C–C moiety of the six-membered chelate ring. It was observed that both complexes **39a** and **80b** could be obtained exclusively from their respective pathways (with or without  $\text{NEt}_3$ ). The conversion from complex **39a** to **80b** could be achieved by treatment of complex **39a** with  $\text{NEt}_3$ . On the other hand, addition of dilute HCl to complex **80b** will result in the generation of complex **39a**. This reversible reaction could be monitored by  $^{31}\text{P}\{^1\text{H}\}$  NMR spectroscopy. Subsequently, the benzylamine auxiliary was removed by refluxing either complex **39a** or **80b** with conc. HCl. This was followed by the addition of NaOAc as an external base which will allow the formation of the five-membered chelate ring to afford the *ortho*-palladated complex **86a**. Subsequently, a single recrystallization of the enantioenriched complex **86a** from a solution of DCM/*n*-hexane resulted in the isolation of the optically pure complex (*S*)-**86a** ([Figure 23](#)).

**Scheme 38:** Cyclopalladation of tertiary phosphine (*S*)-**70a**



The bulky ester functional groups on the complex (*S*)-**86a** occupy the axial position, which resembles the characteristic structural feature of this class of

*ortho*-metallated complexes.<sup>55, 62, 102, 224</sup> The optically pure dimer (*S*)-**86a** was then stirred with AgClO<sub>4</sub> in a mixture of MeCN and H<sub>2</sub>O to form the bisacetonitrile complex (*S*)-**88a** according to a literature method (Scheme 39).<sup>154</sup>

Surprisingly, if the same reaction was carried out in a mixture of toluene and H<sub>2</sub>O, the bisaquo complex (*S*)-**89** could be isolated as single crystals from a solution of DCM/*n*-hexane in 84% isolated yield (Figure 24). It is rather rare for a bisaquopalladium complex to be formed due to the oxophobic properties of Pd and in consideration of the fact that oxygen atoms are classic hard donors.<sup>225</sup>

Figure 22: ORTEP structure of complex (*S*)-**80b**

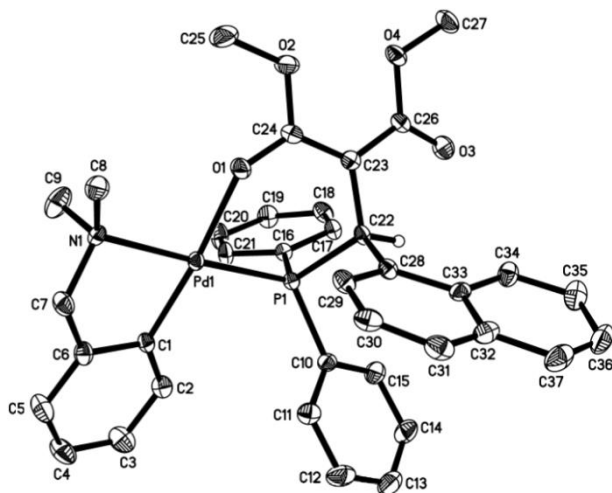
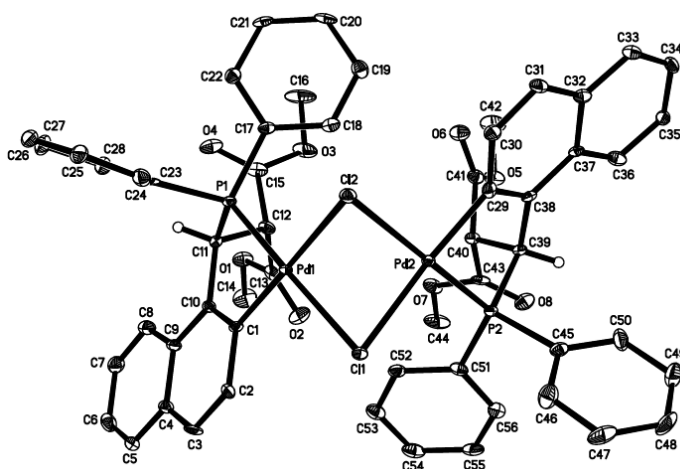
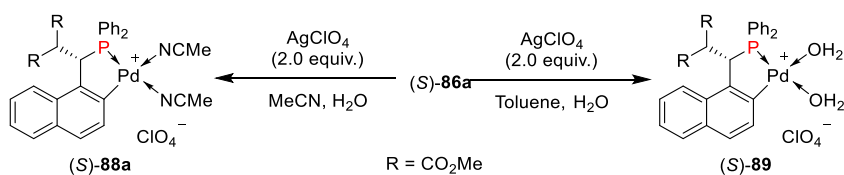


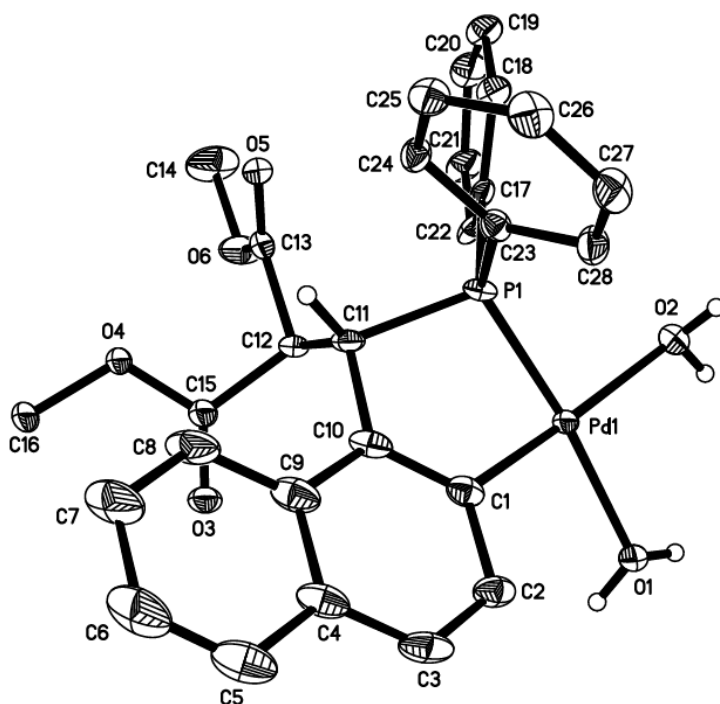
Figure 23: ORTEP structure of complex (*S*)-**88a**



**Scheme 39:** Preparation of monomeric Pd complexes



**Figure 24:** ORTEP structure of complex (S)-86a



We decided to evaluate the catalytic potential and efficiency of the new phosphapalladacycle catalyst (S)-88a against the well-established analogous catalyst (R)-67 in asymmetric hydrophosphination employing chalcone 75b and malonate 75c as model substrates (Table 7). The progress of the reaction was monitored by  $^{31}\text{P}\{^1\text{H}\}$  NMR spectroscopy and in all instances, the reaction proceeded smoothly to afford the desired products in excellent yields. Both catalysts showed similar reactivity toward both substrates. The sterically bulkier ester groups in catalyst (S)-88a do not have any noticeable impact on the chemical reactivity of the organometallic complex. In general, however, the stereoselectivity afforded by the newly designed catalyst (S)-88a is slightly lower than the analogous catalyst (R)-67. Between the two substrates examined, a higher selectivity was observed for the bulkier substrate 75c (entries 1 and 4). It

is noteworthy that it is a common practice to conduct a metal-catalyzed asymmetric reaction by introducing the selected chiral ligand (*S*)-**70a** and the corresponding metal ion directly into the reaction mixture. In order to examine this conventional approach, the phosphine ligand (*S*)-**70a** and PdCl<sub>2</sub>(NCMe)<sub>2</sub> were added simultaneously during the hydrophosphination of chalcone **75a** (entry 3). The reaction progress was slow (ca. 15% conversion after 24 h) and *ee* obtained was moderate (33%). In comparison, a much faster reaction with significantly higher selectivity was observed when the isolated catalyst (*S*)-**88a** was employed (entry 3). This experiment demonstrated that in a stereochemically demanding reaction, it may be essential in some instances to prepare and isolate the catalytically active species prior to its application in the organic synthesis.

**Table 7:** Catalytic asymmetric hydrophosphination<sup>a</sup>

entry	cat.	<b>75b/75c</b>	<i>t</i> (h)	conversion <sup>b</sup> (%)	<i>ee</i> <sup>c</sup> (%)
1	( <i>R</i> )- <b>67</b>	<b>75b</b>	6	99	89 ( <i>S</i> ) <sup>d</sup>
2	( <i>S</i> )- <b>88a</b>	<b>75b</b>	6	99	78 ( <i>R</i> ) <sup>d</sup>
3 <sup>e</sup>	( <i>S</i> )- <b>70a</b> + PdCl <sub>2</sub> (NCMe) <sub>2</sub>	<b>75b</b>	24	15	33 ( <i>S</i> ) <sup>d</sup>
4	( <i>R</i> )- <b>67</b>	<b>75c</b>	96	99	95
5	( <i>S</i> )- <b>88a</b>	<b>75c</b>	96	99	83

<sup>a</sup> Conditions: cat. (5.37 μmol, 5 mol%), HPPPh<sub>2</sub> (20.0 mg, 0.107 mmol, 1.0 equiv.), NEt<sub>3</sub> (14.9 μL, 0.107 mmol, 1.0 equiv.), substrate 16 or 18 (0.118 mmol, 1.1 equiv.) in DCM (6 mL) stirred at -80°C. <sup>b</sup> Conversion was monitored by the disappearance of HPPPh<sub>2</sub> (-40.0 ppm) on <sup>31</sup>P{<sup>1</sup>H} NMR spectroscopy. <sup>c</sup> Determined by chiral HPLC. <sup>d</sup> Absolute configuration of product 17 in parentheses was determined by comparison to literature.<sup>11a</sup> <sup>e</sup> Conditions: ligand (*S*)-**98c**

(4.89 mg, 10.7  $\mu\text{mol}$ , 10 mol%),  $\text{PdCl}_2(\text{NCMe})_2$  (1.39 mg, 5.35  $\mu\text{mol}$ , 5 mol%),  $\text{HPPPh}_2$  (20.0 mg, 0.107 mmol, 1.0 equiv.),  $\text{NEt}_3$  (14.9  $\mu\text{L}$ , 0.107 mmol, 1.0 equiv.) and substrate 16 (24.6 mg, 0.118 mmol, 1.1 equiv.) in  $\text{CHCl}_3$  (6 mL) stirred at  $-40^\circ\text{C}$ .

### 3.3. Conclusion

A chiral phosphine auxiliary was generated with excellent ee via catalytic asymmetric hydrophosphination of 3-(naphthalen-1-ylmethylene)pentane-2,4-dione. The subsequent metal complexation of the monophosphine yielded two different coordination complexes depending on the reaction conditions. The ortho-palladation of both coordination complexes resulted in the formation of a single dimeric phosphapalladacycle complex that could be further converted to the monomeric bisacetonitrile derivative. Moreover, the palladium complex exhibits interesting oxophilicity as the stable bisquo derivative could be isolated and characterized crystallographically. The catalytic potential of the phosphapalladacycle was also demonstrated.

In this work, the main debilitation factor preventing the advancement of bidentate phosphapalladacycles in asymmetric catalysis has been overcome successfully. This simple catalytic protocol is attractive due to the efficiency in preparing chiral phosphine auxiliaries quantitatively without the need for classical resolution techniques. A preliminary investigation on the catalytic potential of the new palladacycle was promising, yielding the desired product with excellent ee. We maintain a positive outlook towards the prospects of the new phosphapalladacycle catalyst. From previous experience, we have noted the benefits of installing an ester functional group as opposed to a simple methyl group in the palladacycle backbone. It was reported that a P-H bond addition reaction did not proceed in the presence of a pincer catalyst with methyl substituents but the same reaction could be conducted with an analogous pincer catalyst with ester functionalities.<sup>116, 214</sup> Further developments in the architecture

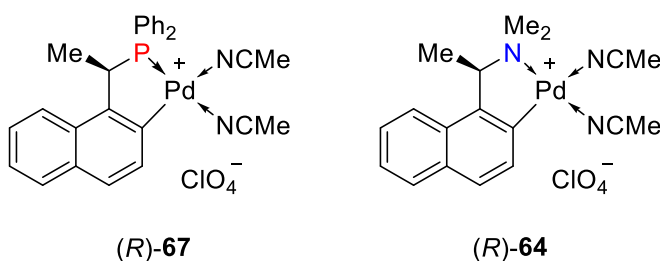
of the palladacycle complexes will be conducted and their application in other transformation reactions will be examined.

### 3.4. Experimental section

#### General Information

All reactions were carried out under a positive pressure of nitrogen using standard Schlenk technique. NMR spectra were recorded on Bruker AV 300, AV500 and BBFO 400 spectrometers. Chemical shifts were reported in ppm and referenced to an internal SiMe<sub>4</sub> standard (0 ppm) for <sup>1</sup>H NMR, chloroform-*d* (77.00 ppm) for <sup>13</sup>C NMR, and an external 85% H<sub>3</sub>PO<sub>4</sub> for <sup>31</sup>P{<sup>1</sup>H} NMR. Dichloromethane, chloroform and acetone and methanol were purchased from their respective companies and used as supplied. Tetrahydrofuran was distilled from sodium/benzophenone prior to use. Solvents were degassed when necessary. A Low Temp Pairstirrer PSL-1800 was used for controlling low temperature reactions. Column chromatography was carried out with Silica gel 60 (Merck). Melting points were measured using SRS Optimelt Automated Point System SRS MPA100. Optical rotations were measured with JASCO P-1030 Polarimeter in the specified solvent in a 0.1 dm cell at 22.0 °C. The enantioselectivities of the hydrophosphination reactions were determined with Agilent 1200 Series High Performance Liquid Chromatography (HPLC) machine fitted with a Daicel Chiralpak IC column and eluted with a mixture of *n*-hexane/2-propanol at 23°C.

**Figure 25:** Molecular structures of PC-catalyst **67** and NC-catalyst **64**

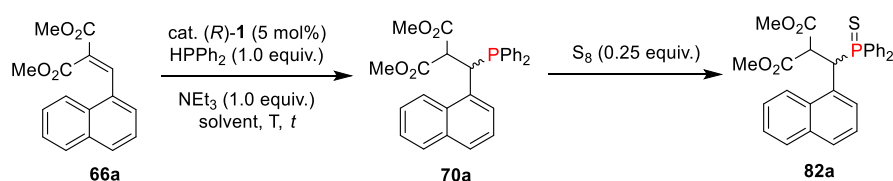


*Caution! Perchlorate salts of metal complexes are potentially explosive compounds and should be handled with care.*

The PC-catalyst **67**<sup>154</sup> NC-catalyst **64**<sup>223</sup> benzylamine palladium complex **4a-Cl**<sup>2</sup> and unsaturated malonate **66a**<sup>226-228</sup> were prepared according to literature methods. All other reactants and reagents were used as supplied without further purification unless stated otherwise.

### General procedure for asymmetric hydrophosphination with PC-catalyst (*R*)-**67**

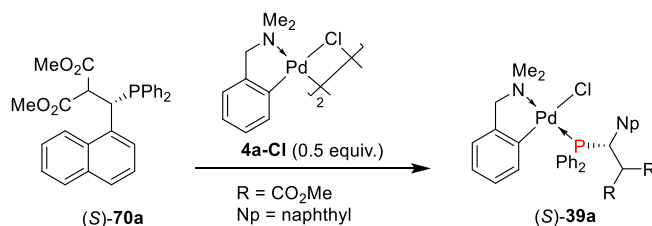
**Scheme 40:** Catalytic asymmetric hydrophosphination of malonate **9**



A Schlenk tube was charged with  $\text{Ph}_2\text{PH}$  (20.0 mg, 0.107 mmol, 1.0 equiv), catalyst (*R*)-**67** (3.37 mg, 5.37  $\mu\text{mol}$ , 5 mol%) in solvent (6 mL) and stirred at the stipulated temperature. The substrate **66a** (31.9 mg, 0.118 mmol, 1.1 equiv) and  $\text{NEt}_3$  (14.9  $\mu\text{L}$ , 0.107 mmol, 1.0 equiv.) was added and stirred. The reaction was monitored for completion by  $^{31}\text{P}\{^1\text{H}\}$  NMR, then allowed to warm up to RT and treated with  $\text{S}_8$  (6.92 mg, 0.027 mmol, 0.25 equiv.). Volatiles were removed under reduced pressure and the crude product was purified by silica gel column chromatography (1 EA : 15 *n*-hexane) to afford white solids of **70a**.  $[\alpha]_{\text{D}} = +10.1$  (*c* 0.68, DCM, Table 1, Entry 7). Mp: 167-168 °C.  $^{31}\text{P}\{^1\text{H}\}$  NMR ( $\text{CDCl}_3$ , 162 MHz),  $\delta$  50.9;  $^1\text{H}$  NMR ( $\text{CDCl}_3$ , 400 MHz),  $\delta$  8.34-6.76 (m, 17H, Ar), 5.76 (dd, 1H,  $J = 10.8, 8.2$  Hz,  $\text{CHCOO}$ ), 4.98 (dd, 1H,  $J = 12.6, 10.8$  Hz,  $\text{CHP}$ ), 3.20 (s, 3H,  $\text{CH}_3$ ), 3.15 (s, 3H,  $\text{CH}_3$ );  $^{13}\text{C}$  NMR ( $\text{CDCl}_3$ , 100 MHz),  $\delta$  167.6-167.2 (2C, COO), 133.4-122.6 (22C, Ar), 54.8 (d, 1C,  $J = 4.5$  Hz,  $\text{CH}_3$ ), 52.4 (d, 2C,  $J = 7.4$  Hz,  $\text{CH}_3$ ), 39.0 (d, 1C,  $J = 50.0$  Hz, PCH). The *ee* was determined on a Daicel Chiralpak IC column with *n*-hexane/2-propanol = 95/5, flow = 0.5 mL/min, wavelength = 280 nm. Retention times: 66.8 min (*R*), 76.6 min (*S*).

### Synthesis of complex (*S*)-**39a**

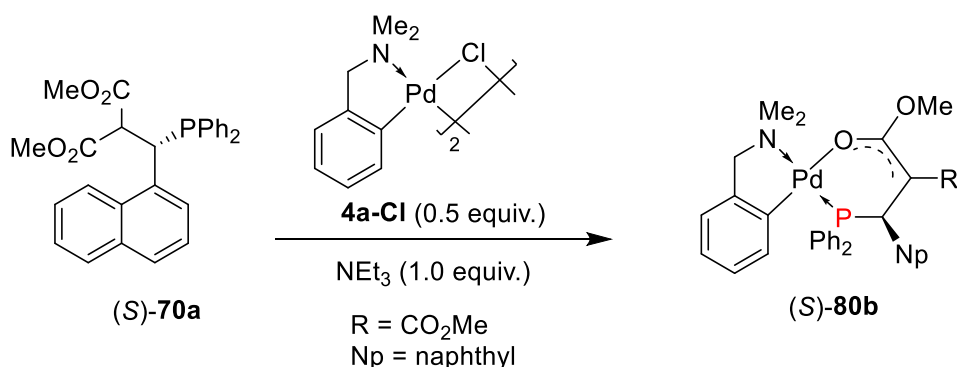
#### Scheme 41: Synthesis of coordination complex (S)-**39a**



The volatiles from the crude reaction mixture containing phosphine **70a** (1.0 equiv.) were removed under reduced pressure. The residue was redissolved in DCM (10 mL), dimeric complex **11** (0.5 equiv.) was added and stirred at RT for 10 mins. The organic product was extracted with DCM (3 x 50 mL), washed with H<sub>2</sub>O (1 x 50 mL), dried over MgSO<sub>4</sub> and filtered. The volatiles were removed by rotary evaporator to afford yellow solids of **39a** in 99% isolated yield.  $[\alpha]_{\text{D}} = -21.9$  (*c* 1.33, DCM). <sup>31</sup>P{<sup>1</sup>H} NMR (CDCl<sub>3</sub>, 162 MHz),  $\delta$  48.3; <sup>1</sup>H NMR (CDCl<sub>3</sub>, 400 MHz),  $\delta$  7.96 (d, 1H, *J* = 8.6 Hz, Ar), 7.89 (dd, 2H, *J* = 11.1, 7.5 Hz, Ar), 7.68-7.64 (m, 3H, Ar), 7.45 (dd, 2H, *J* = 9.9, 8.4 Hz, Ar), 7.31-7.17 (m, 6H, Ar), 6.89 (td, 3H, *J* = 8.0, 2.0 Hz, Ar), 6.84 (d, 1H, *J* = 7.0 Hz, Ar), 6.63 (t, 1H, *J* = 7.2 Hz, Ar), 6.15 (t, 1H, *J* = 7.6 Hz, Ar), 6.09 (t, 1H, *J* = 10.6 Hz, PCH), 5.86 (t, 1H, *J* = 7.0 Hz, Ar), 5.53 (t, 1H, *J* = 10.7 Hz, CH(CO<sub>2</sub>CH<sub>2</sub>)<sub>2</sub>), 4.48 (d, 1H, *J* = 13.2 Hz, NCH<sub>2</sub>), 3.56 (s, 3H, CO<sub>2</sub>CH<sub>3</sub>), 3.59 (dd, 1H, *J* = 13.2, 3.4 Hz, NCH<sub>2</sub>), 3.07-3.05 (m, 6H, NCH<sub>3</sub>), 2.72 (s, 3H, CO<sub>2</sub>CH<sub>3</sub>); <sup>13</sup>C NMR (CDCl<sub>3</sub>, 100 Hz),  $\delta$  169.0 (s, 1C, CO<sub>2</sub>CH<sub>3</sub>), 168.0 (d, 1C, *J* = 14.9 Hz, CO<sub>2</sub>CH<sub>3</sub>), 152.2-121.8 (28C, Ar), 73.3 (s, 1C, NCH<sub>2</sub>), 56.3 (d, 1C, *J* = 9.2 Hz, CH(CO<sub>2</sub>CH<sub>3</sub>)<sub>2</sub>), 52.8 (s, 1C, CO<sub>2</sub>CH<sub>3</sub>), 52.0 (s, 1C, CO<sub>2</sub>CH<sub>3</sub>), 51.4 (s, 1C, NCH<sub>3</sub>), 48.9 (s, 1C, NCH<sub>3</sub>), 40.2 (d, 1C, *J* = 22.5 Hz, PCH). HRMS (+ESI) *m/z*: (M + H)<sup>+</sup> calcd for C<sub>37</sub>H<sub>38</sub>ClNO<sub>4</sub>PPd, 732.1262; found, 732.1296. Anal. Calcd for C<sub>37</sub>H<sub>37</sub>ClNO<sub>4</sub>PPd: C, 60.67; H, 5.09; N, 1.91. Found: C, 60.81; H, 5.56; N, 2.00%.

#### Synthesis of complex (S)-**80b**

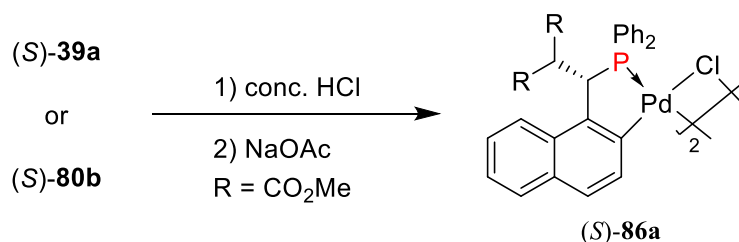
**Scheme 42:** Synthesis of P-O bidentate complex (S)-80b



The dimeric complex **4a-Cl** (0.5 equiv.) was added into the crude reaction mixture containing phosphine **70a** (1.0 equiv.) and stirred for 10 mins. The volatiles were removed under reduced pressure to afford the crude residue which on standing overnight, crystallized to form yellow blocks of complex **80b**.  $[\alpha]_D = -176.8$  (*c* 0.59, DCM). Mp: 121-122 °C (dec.).  $^{31}\text{P}\{^1\text{H}\}$  NMR (CDCl<sub>3</sub>, 162 MHz),  $\delta$  60.2;  $^1\text{H}$  NMR (CDCl<sub>3</sub>, 400 MHz),  $\delta$  8.66 (d, 1H, *J* = 7.2 Hz, Ar), 8.31-8.26 (m, 2H, Ar), 7.84 (d, 1H, *J* = 8.7 Hz, Ar), 7.64-7.54 (m, 5H, Ar), 7.44 (t, 1H, *J* = 7.7 Hz, Ar), 7.17 (t, 1H, *J* = 7.4 Hz, Ar), 7.02 (t, 1H, *J* = 7.5 Hz, Ar), 6.94 (d, 1H, *J* = 7.3 Hz, Ar), 6.88 (t, 1H, *J* = 7.5 Hz, Ar), 6.83-6.78 (m, 3H, Ar), 6.63 (td, 2H, *J* = 7.9, 1.9 Hz, Ar), 6.39-6.29 (m, 2H, Ar), 6.33 (d, 1H, *J* = 29.2 Hz, PCH), 4.43 (d, 1H, *J* = 13.8 Hz, NCH<sub>2</sub>), 3.72 (s, 3H, CH<sub>3</sub>O<sub>2</sub>C), 3.67 (dd, 1H, *J* = 13.9, 3.3 Hz, NCH<sub>2</sub>), 3.56 (s, 3H, CH<sub>3</sub>O<sub>2</sub>C), 3.09 (d, 3H, *J* = 2.9 Hz, NCH<sub>3</sub>), 2.83 (s, 3H, NCH<sub>3</sub>);  $^{13}\text{C}$  NMR (CDCl<sub>3</sub>, 100 MHz),  $\delta$  172.2 (d, *J* = 2.4 Hz, 1C, CO<sub>2</sub>CH<sub>3</sub>), 169.7 (d, *J* = 7.5 Hz, 1C, CO<sub>2</sub>CH<sub>3</sub>), 148.4-122.4 (29C, Ar), 71.1 (d, 1C, *J* = 2.9 Hz, NCH<sub>2</sub>), 51.7 (s, 1C, CH<sub>3</sub>CO<sub>2</sub>), 50.5 (s, 1C, CH<sub>3</sub>CO<sub>2</sub>), 49.8 (d, 1C, *J* = 2.2 Hz, NCH<sub>3</sub>), 48.8 (d, 1C, *J* = 2.4 Hz, NCH<sub>3</sub>), 36.5 (d, 1C, *J* = 29.2 Hz, PCH). HRMS (+ESI) *m/z*: (M + H)<sup>+</sup> calcd for C<sub>37</sub>H<sub>37</sub>NO<sub>4</sub>PPd, 696.1495; found, 696.1514.

**Synthesis of dimeric complex (S)-86a**

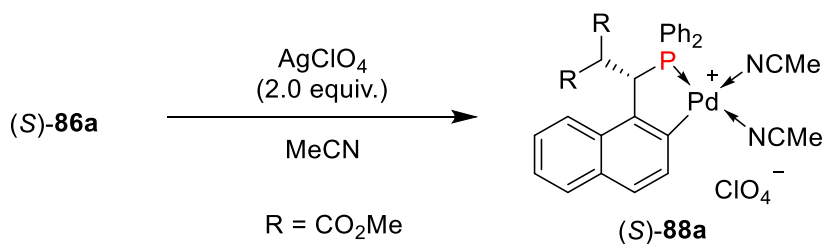
---

**Scheme 43:** Synthesis of dimeric complex (S)-86a

The complex **39a** (0.10 g, 136.5  $\mu\text{mol}$ ) or **80b** (0.10 g, 143.2  $\mu\text{mol}$ ), conc. HCl (0.6 mL) in acetone (6 mL) was refluxed for 90 mins. The solvent was removed, and the residue was extracted with DCM (3 x 25 mL), washed with H<sub>2</sub>O (1 x 25 mL), dried over MgSO<sub>4</sub> and filtered. The volatiles were removed under reduced pressure. The crude residue and NaOAc (0.40 g) were refluxed in EtOH (20 mL) for 30 mins. After removal of the solvent, the organic layer was taken up in DCM (3 x 25 mL), washed with H<sub>2</sub>O (1 x 25 mL), dried over MgSO<sub>4</sub> and filtered. The crude product was purified by column chromatography (1 DCM : 1 *n*-hexane) to afford yellow solids of complex **86a** in 92% isolated yield. Recrystallization of complex **86a** was achieved from a mixture of DCM/*n*-hexane.  $[\alpha]_{\text{D}} = +5.6$  (*c* 0.64, DCM). Mp: 180-181°C (dec.).  $^{31}\text{P}\{^1\text{H}\}$  NMR (CDCl<sub>3</sub>, 162 MHz),  $\delta$  62.9, 62.3;  $^1\text{H}$  NMR (CDCl<sub>3</sub>, 400 MHz),  $\delta$  8.01-7.33 (m, 16H, Ar), 5.69-5.63 (m, 1H, CHCOO), 4.38-4.33 (m, 1H, PCH), 3.2 (s, 3H, CH<sub>3</sub>), 2.8 (s, 3H, CH<sub>3</sub>);  $^{13}\text{C}$  NMR (CDCl<sub>3</sub>, 100 MHz),  $\delta$  167.8 (2C, CO<sub>2</sub>CH<sub>3</sub>), 136.0-124.7 (22C, Ar), 53.4 (s, 2C, CO<sub>2</sub>CH<sub>3</sub>), 52.2 (d, 1C, *J* = 19.0 Hz, PCH). HRMS (+ESI) *m/z*: (*M* + *H*)<sup>+</sup> calcd for C<sub>56</sub>H<sub>49</sub>Cl<sub>2</sub>O<sub>8</sub>P<sub>2</sub>Pd<sub>2</sub>, 1193.0349; found, 1193.0323.

**Synthesis of complex (S)-88a**

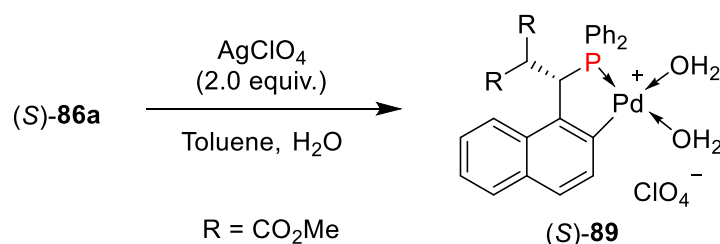
---

**Scheme 44:** Synthesis of monomeric bisacetonitrile complex (S)-88a

The dimeric complex **86a** (0.10 g, 83.7  $\mu\text{mol}$ , 1.0 equiv.) and  $\text{AgClO}_4$  (34.7 mg, 167.4  $\mu\text{mol}$ , 2.0 equiv.) in MeCN (10ml) was stirred for 2 h in the dark. The reaction mixture was filtered through celite and the volatiles were removed. Extraction was performed with DCM (3 x 25 mL), the combined organic layer was washed with  $\text{H}_2\text{O}$  (1 x 25 mL), dried over  $\text{MgSO}_4$  and filtered. The solvent was removed by rotary evaporator to give yellow solids of complex **88a** in 99% isolated yield.  $[\alpha]_{\text{D}} = +357.7$  ( $c$  0.15, DCM). Mp: 81-82  $^{\circ}\text{C}$  (dec.).  $^{31}\text{P}\{^1\text{H}\}$  NMR ( $\text{CDCl}_3$ , 162 MHz),  $\delta$  61.5;  $^1\text{H}$  NMR ( $\text{CDCl}_3$ , 400 MHz),  $\delta$  7.97-7.86 (m, 2H, Ar), 7.75-7.65 (m, 4H, Ar), 7.58-7.35 (m, 10H, Ar), 5.68-5.37 (m, 1H, PCH), 4.17 (dd, 1H,  $J = 17.6, 9.4$  Hz,  $\text{CH}(\text{CO}_2\text{CH}_3)_2$ ), 3.24 (s, 3H,  $\text{CO}_2\text{CH}_3$ ), 2.83 (s, 3H,  $\text{CO}_2\text{CH}_3$ ), 2.22 (m, 6H,  $\text{NCCH}_3$ );  $^{13}\text{C}$  NMR ( $\text{CDCl}_3$ , 100 MHz),  $\delta$  167.2 (s, 1C,  $\text{CO}_2\text{CH}_3$ ), 166.8 (d, 1C,  $J = 15.0$  Hz,  $\text{CO}_2\text{CH}_3$ ), 148.8-123.7 (22C, Ar), 55.3 (d, 1C,  $J = 5.6$  Hz,  $\text{CHCO}_2\text{CH}_3$ ), 52.3 (d, 2C,  $J = 23.7$  Hz,  $\text{CO}_2\text{CH}_3$ ), 48.0 (d, 1C,  $J = 38.0$  Hz, PCH), 2.5 (s, 2C,  $\text{NCCH}_3$ ). HRMS (+ESI)  $m/z$ : ( $\text{M} + \text{H}$ ) $^+$  calcd for  $\text{C}_{32}\text{H}_{31}\text{ClN}_2\text{O}_8\text{PPd}$ , 743.0541; found, 743.0546.

### Synthesis of complex (S)-89

**Scheme 45:** Synthesis of monomeric bisquo complex (S)-89

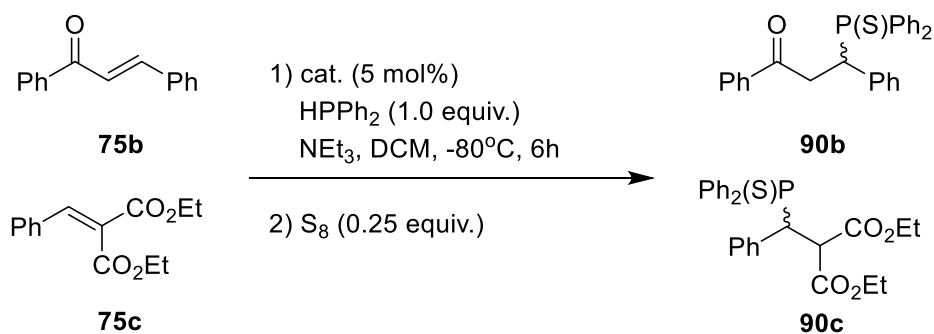


The dimeric complex **86a** (0.10 g, 83.7  $\mu\text{mol}$ , 1.0 equiv.) and  $\text{AgClO}_4$  (34.7 mg, 167.4  $\mu\text{mol}$ , 2.0 equiv.) in toluene (10ml) and  $\text{H}_2\text{O}$  (1 mL) was stirred for 12 h in the dark. The reaction mixture was filtered through celite and the volatiles were removed. Extraction was performed with DCM (3 x 25 mL), the combined organic layer was washed with  $\text{H}_2\text{O}$  (1 x 25 mL), dried over  $\text{MgSO}_4$  and filtered. The solvent was removed by rotary evaporator to give white solids of complex **89**. Recrystallization of complex **89** was achieved from a mixture of DCM/ $n$ -

hexane to afford (*S*)-**89** in 75% isolated yield.  $[\alpha]_D = +223.0$  (*c* 0.85, DCM).  $^{31}\text{P}\{^1\text{H}\}$  NMR ( $\text{CDCl}_3$ , 162 MHz),  $\delta$  63.6;  $^1\text{H}$  NMR ( $\text{CDCl}_3$ , 400 MHz),  $\delta$  7.89-7.83 (m, 3H, Ar), 7.76-7.71 (m, 3H, Ar), 7.58-7.32 (m, 10H, Ar), 5.54 (dd, 1H,  $J = 13.4, 9.8$  Hz, PCH), 4.34 (dd, 1H,  $J = 18.0, 9.7$  Hz,  $\text{CH}(\text{CO}_2\text{CH}_3)_2$ ), 3.82 (brs, 4H,  $\text{OH}_2$ ), 3.27 (s, 3H,  $\text{CO}_2\text{CH}_3$ ), 2.98 (s, 3H,  $\text{CO}_2\text{CH}_3$ );  $^{13}\text{C}$  NMR ( $\text{CDCl}_3$ , 100 MHz),  $\delta$  167.2 (s, 2C,  $\text{CO}_2\text{CH}_3$ ), 135.5-124.6 (22C, Ar), 56.0 (d, 1C,  $J = 7.2$  Hz,  $\text{CH}(\text{CO}_2\text{CH}_3)_2$ ), 54.0 (s, 1C,  $\text{CO}_2\text{CH}_3$ ), 52.9 (s, 1C,  $\text{CO}_2\text{CH}_3$ ), 47.6 (d, 1C,  $J = 39.2$  Hz, PCH). HRMS (+ESI)  $m/z$ : ( $\text{M} + \text{H}$ ) $^+$  calcd for  $\text{C}_{28}\text{H}_{29}\text{ClO}_{10}\text{PPd}$ , 697.0222; found, 697.0231.

### General procedure for asymmetric hydrophosphination of substrates **75b** and **75c**

**Scheme 46:** Catalytic asymmetric hydrophosphination of substrates **75b** and **75c**

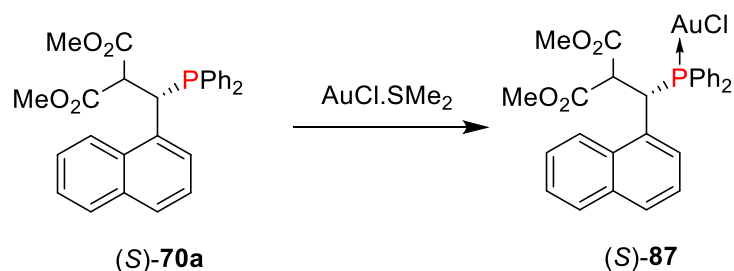


The catalyst (5.37  $\mu\text{mol}$ , 5 mol %), substrate **75b** or **75c** (0.118 mmol, 1.1 equiv.) and  $\text{NEt}_3$  (14.9  $\mu\text{L}$ , 0.107 mmol, 1.0 equiv.) was added to a solution of  $\text{Ph}_2\text{PH}$  (20.0 mg, 0.107 mmol, 1.0 equiv) in DCM (6 mL) and stirred at  $-80^\circ\text{C}$ . The completion of reaction was determined by the disappearance of the signal belonging to  $\text{HPPH}_2$  ( $-40.0$  ppm) on  $^{31}\text{P}\{^1\text{H}\}$  NMR spectroscopy. The crude reaction mixture was treated with  $\text{S}_8$  (6.92 mg, 0.027 mmol, 0.25 equiv.) for 10 min to form the respective products. The volatiles were removed under reduced pressure and the crude product was directly loaded onto silica gel column (1 EA : 15 *n*-hexane) to afford the pure white product **90b** in quantitative yields. The spectroscopic data obtained for product **90b** is consistent with literature. The *ee*

was determined on a Daicel Chiralpak IC column with *n*-hexane/2-propanol = 98/2, flow = 0.3 mL/min, wavelength = 270 nm. Retention times: 40.8 min ((*S*)-**90b**), 56.3 min ((*R*)-**90b**). The product **90c** was purified by silica gel column (1 EA : 30 *n*-hexane) and obtained as a white solid.  $[\alpha]_D = -62.0$  (*c* 0.27, DCM). Mp: 107-108 °C.  $^{31}\text{P}\{^1\text{H}\}$  NMR ( $\text{CDCl}_3$ , 162 MHz),  $\delta$  50.6;  $^1\text{H}$  NMR ( $\text{CDCl}_3$ , 400 MHz),  $\delta$  8.23-8.20 (m, 2H, Ar), 7.60-7.50 (m, 5H, Ar), 7.27-7.03 (m, 8H, Ar), 4.86-4.80 (m, 2H,  $\text{CO}_2\text{CH}_2$ ), 3.82-3.74 (m, 2H,  $\text{CO}_2\text{CH}_2$ ), 3.66-3.57 (m, 1H, PCH), 3.47-3.41 (m, 1H,  $\text{CH}(\text{CO}_2\text{CH}_2\text{CH}_3)_2$ ), 1.01 (t, 3H,  $J = 7.1$  Hz,  $\text{CH}_2\text{CH}_3$ ), 0.82 (t, 3H,  $J = 7.1$  Hz,  $\text{CH}_2\text{CH}_3$ )  $^{13}\text{C}$  NMR ( $\text{CDCl}_3$ , 100 MHz),  $\delta$  166.9 (s, 1C, O=COEt), 166.7(s, 1C, O=COEt), 133.5-127.3 (m, 15C, Ar), 61.4 (d, 2C,  $J = 14.3$  Hz, CH<sub>2</sub>), 53.8 (d, 1C,  $J = 4.3$  Hz, CHPPh<sub>2</sub>), 45.8 (d, 1C,  $J = 49.3$  Hz, CHCOO), 13.3 (d, 2C,  $J = 11.9$  Hz, CH<sub>3</sub>). The *ee* was determined on a Daicel Chiralpak IC column with *n*-hexane/2-propanol = 98/2, flow = 1.0 mL/min, wavelength = 250 nm. Retention times: 31.4 min, 36.8 min.

### Synthesis of gold(I)-phosphine complex (*S*)-**87**.

**Scheme 47:** Synthesis of gold(I)-phosphine complex (*S*)-**87**



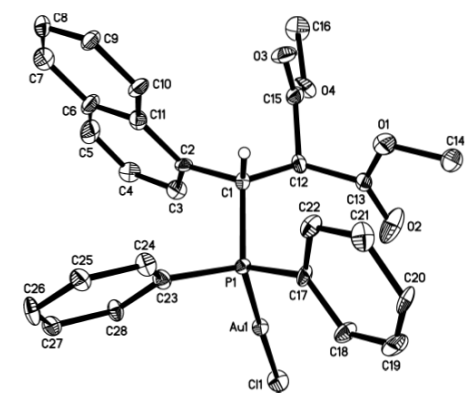
A mixture of chloro(dimethylsulfide)gold(I) chloride (29.5 mg, 0.10 mmol, 1.0 equiv.) and the phosphine ligand (*S*)-**70a** (43.8 mg, 0.10 mmol, 1.0 equiv.) in DCM (20 mL) was stirred at RT for 30 min in the dark. The crude product (*S*)-**87** was purified by silica gel column chromatography (1 EA : 4 *n*-hexane) to afford white solid of complex (*S*)-**87** in 99% isolated yield. Complex (*S*)-**87** was recrystallized from a mixture of DCM/*n*-hexane.  $[\alpha]_D = -33.6$  (*c* 0.76, DCM). Mp: 177-178°C.  $^{31}\text{P}\{^1\text{H}\}$  NMR ( $\text{CDCl}_3$ , 162 MHz),  $\delta$  46.9;  $^1\text{H}$  NMR ( $\text{CDCl}_3$ , 400

MHz),  $\delta$  8.11 (ddd, 2H,  $J = 12.8, 7.1, 2.2$  Hz, Ar), 7.96 (dd, 2H,  $J = 11.9, 7.9$  Hz, Ar), 7.66-7.58 (m, 5H, Ar), 7.42 (d, 1H,  $J = 7.7$  Hz, Ar), 7.34-7.29 (m, 2H, Ar), 7.04 (dd, 2H,  $J = 12.8, 7.4$  Hz, Ar), 6.92 (dd, 1H,  $J = 8.0, 6.3$  Hz, Ar), 6.77 (td, 2H,  $J = 7.8, 2.6$  Hz, Ar), 5.70-5.64 (m, 1H, PCH), 4.67 (t, 1H,  $J = 11.0$  Hz,  $\text{CH}(\text{CO}_2\text{CH}_3)_2$ ), 3.26 (s, 3H,  $\text{CO}_2\text{CH}_3$ ), 3.14 (s, 3H,  $\text{CO}_2\text{CH}_3$ );  $^{13}\text{C}$  NMR ( $\text{CDCl}_3$ , 100 MHz),  $\delta$  167.2 (s, 1C,  $\text{CO}_2$ ), 166.3 (d, 1C,  $J = 17.9$  Hz,  $\text{CO}_2$ ), 134.9-122.5 (22C, Ar), 56.5 (d, 1C,  $J = 13.3$  Hz,  $\text{CH}(\text{CO}_2\text{CH}_3)_2$ ), 52.6 (d, 2C,  $J = 8.2$  Hz,  $\text{CO}_2\text{CH}_3$ ), 36.8 (d, 1C,  $J = 34.7$  Hz, PCH).

From the coordination experiment conducted between complex (*S*)-**88a** and (*S*)-BINAP, the *ee* of the PC-palladacycle complex was determined to be >99% after a single recrystallization. With reference to the  $^{31}\text{P}\{^1\text{H}\}$  NMR spectrum obtained above, the three phosphorus atoms located on the coordination complex may be identified by their coupling constants and chemical shifts. If both enantiomers of the PC-palladacycle complex were present, two sets of similar signals (with different intensities based on the enantiomeric ratio of the isomers) should be obtained. Since that is not observed, it is clear that only one enantiomer of the complex is present after a single recrystallization.

### Crystallographic Data

**Figure 26:** ORTEP structure of chiral phosphine-gold(I) complex (*S*)-**87**



The tertiary phosphine **70a** was coordinated onto AuCl to form complex **87**. Recrystallization of the complex from a mixture of DCM/*n*-hexane afforded single crystals that are suitable for X-ray crystallography. The absolute configuration of the major enantiomer was determined to be *S*.

**Table 8:** Data collection and structure refinement for complex (*S*)-**87**

<b>Chemical formula</b>	C <sub>28</sub> H <sub>25</sub> AuClO <sub>4</sub> P	
<b>Formula weight</b>	688.87 g/mol	
<b>Temperature</b>	103(2) K	
<b>Wavelength</b>	0.71073 Å	
<b>Crystal size</b>	0.120 x 0.320 x 0.410 mm	
<b>Crystal habit</b>	colorless block	
<b>Crystal system</b>	monoclinic	
<b>Space group</b>	P 1 21 1	
<b>Unit cell dimensions</b>	a = 9.1660(5) Å	α = 90°
	b = 16.3269(8) Å	β = 115.576(3)°
	c = 9.5017(5) Å	γ = 90°
<b>Volume</b>	1282.62(12) Å <sup>3</sup>	
<b>Z</b>	2	
<b>Density (calculated)</b>	1.784 g/cm <sup>3</sup>	
<b>Absorption coefficient</b>	5.934 mm <sup>-1</sup>	
<b>F(000)</b>	672	
<b>Theta range for data collection</b>	2.38 to 31.16°	
<b>Index ranges</b>	-13 ≤ h ≤ 13, -23 ≤ k ≤ 23, -13 ≤ l ≤ 13	
<b>Reflections collected</b>	21010	
<b>Independent reflections</b>	7935 [R(int) = 0.1079]	
<b>Coverage of independent reflections</b>	99.8%	
<b>Absorption correction</b>	Multi-Scan	
<b>Max. and min. transmission</b>	0.5360 and 0.1950	
<b>Structure solution technique</b>	direct methods	
<b>Structure solution program</b>	XT, VERSION 2014/5	
<b>Refinement method</b>	Full-matrix least-squares on F <sup>2</sup>	
<b>Refinement program</b>	SHELXL-2014/7 (Sheldrick, 2014)	

<b>Function minimized</b>	$\Sigma w(F_o^2 - F_c^2)^2$
<b>Data / restraints / parameters</b>	7935 / 1 / 318
<b>Goodness-of-fit on F<sup>2</sup></b>	0.905
<b><math>\Delta/\sigma_{\max}</math></b>	0.001
<b>Final R indices</b>	6509 data; I>2 $\sigma$ (I) R1 = 0.0532, wR2 = 0.1112 all data R1 = 0.0708, wR2 = 0.1219
<b>Weighting scheme</b>	w=1/[ $\sigma^2(F_o^2)$ ] where P=(F <sub>o</sub> <sup>2</sup> +2F <sub>c</sub> <sup>2</sup> )/3
<b>Absolute structure parameter</b>	0.016(13)
<b>Largest diff. peak and hole</b>	1.302 and -1.929 eÅ <sup>-3</sup>
<b>R.M.S. deviation from mean</b>	0.219 eÅ <sup>-3</sup>

**Table 9** Bond lengths (Å) for complex (S)- **87**

Au1-P1	2.235(2)	Au1-C11	2.283(2)
C1-C2	1.518(14)	C1-C12	1.558(14)
C1-P1	1.847(11)	C2-C3	1.371(14)
C2-C11	1.436(15)	C3-C4	1.420(17)
C4-C5	1.336(18)	C5-C6	1.380(19)
C6-C11	1.428(17)	C6-C7	1.430(18)
C7-C8	1.355(19)	C8-C9	1.390(18)
C9-C10	1.371(16)	C10-C11	1.432(16)
C12-C15	1.507(17)	C12-C13	1.531(16)
C13-O2	1.209(15)	C13-O1	1.316(15)
C14-O1	1.47(2)	C15-O3	1.182(13)
C15-O4	1.352(13)	C16-O4	1.431(15)
C17-C18	1.378(16)	C17-C22	1.395(15)
C17-P1	1.809(11)	C18-C19	1.357(16)
C19-C20	1.346(18)	C20-C21	1.401(18)
C21-C22	1.411(16)	C23-C24	1.381(14)
C23-C28	1.398(15)	C23-P1	1.826(13)
C24-C25	1.367(16)	C25-C26	1.403(19)
C26-C27	1.37(2)	C27-C28	1.406(16)

**Table 10:** Bond angles (°) for complex (S)-**87**

P1-Au1-C11	178.3(2)	C2-C1-C12	108.8(8)
C2-C1-P1	111.7(7)	C12-C1-P1	113.7(8)
C3-C2-C11	119.4(11)	C3-C2-C1	119.0(10)
C11-C2-C1	121.5(9)	C2-C3-C4	120.9(11)
C5-C4-C3	119.9(11)	C4-C5-C6	121.9(12)
C5-C6-C11	120.2(12)	C5-C6-C7	122.6(12)
C11-C6-C7	117.3(12)	C8-C7-C6	123.0(12)
C7-C8-C9	119.4(12)	C10-C9-C8	121.0(12)
C9-C10-C11	121.1(12)	C6-C11-C10	118.2(11)
C6-C11-C2	117.7(10)	C10-C11-C2	124.1(11)
C15-C12-C13	111.8(9)	C15-C12-C1	106.9(9)
C13-C12-C1	113.8(9)	O2-C13-O1	125.6(12)
O2-C13-C12	122.1(11)	O1-C13-C12	112.3(10)
O3-C15-O4	124.7(11)	O3-C15-C12	125.4(11)
O4-C15-C12	109.9(9)	C18-C17-C22	118.9(10)
C18-C17-P1	120.4(8)	C22-C17-P1	120.6(9)
C19-C18-C17	121.1(11)	C20-C19-C18	121.9(12)
C19-C20-C21	119.3(11)	C20-C21-C22	119.5(10)
C17-C22-C21	119.3(11)	C24-C23-C28	119.0(10)
C24-C23-P1	122.3(8)	C28-C23-P1	118.4(8)
C25-C24-C23	121.8(10)	C24-C25-C26	119.0(11)
C27-C26-C25	120.8(13)	C26-C27-C28	119.5(11)
C23-C28-C27	119.8(9)	C13-O1-C14	114.6(13)
C15-O4-C16	114.8(9)	C17-P1-C23	105.9(5)
C17-P1-C1	106.1(5)	C23-P1-C1	104.2(5)
C17-P1-Au1	113.5(4)	C23-P1-Au1	113.9(4)
C1-P1-Au1	112.4(3)		

**Figure 27:** ORTEP structure of chiral phosphine-palladium complex (*S*)-**80b**

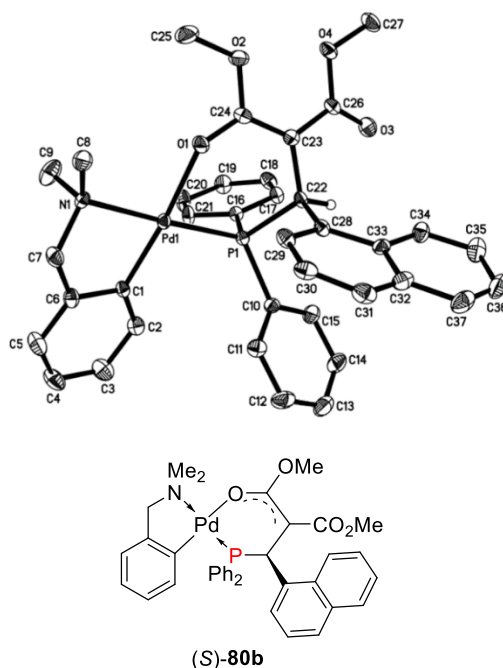


**Table 11.** Data collection and structure refinement for complex (*S*)-**80b**.

<b>Chemical formula</b>	C <sub>38</sub> H <sub>37</sub> Cl <sub>3</sub> NO <sub>4</sub> PPd	
<b>Formula weight</b>	815.40 g/mol	
<b>Temperature</b>	153(2) K	
<b>Wavelength</b>	0.71073 Å	
<b>Crystal size</b>	0.380 x 0.400 x 0.420 mm	
<b>Crystal habit</b>	colorless block	
<b>Crystal system</b>	monoclinic	
<b>Space group</b>	P 1 21 1	
<b>Unit cell dimensions</b>	a = 9.4544(4) Å	α = 90°
	b = 15.4951(6) Å	β = 109.9464(16)°
	c = 12.6849(5) Å	γ = 90°
<b>Volume</b>	1746.82(12) Å <sup>3</sup>	
<b>Z</b>	2	
<b>Density (calculated)</b>	1.550 g/cm <sup>3</sup>	
<b>Absorption coefficient</b>	0.849 mm <sup>-1</sup>	
<b>F(000)</b>	832	
<b>Theta range for data collection</b>	1.71 to 34.03°	
<b>Index ranges</b>	-12 ≤ h ≤ 14, -24 ≤ k ≤ 24, -19 ≤ l ≤ 19	
<b>Reflections collected</b>	38476	

<b>Independent reflections</b>	14147 [R(int) = 0.0777]
<b>Coverage of independent reflections</b>	99.3%
<b>Absorption correction</b>	Multi-Scan
<b>Max. and min. transmission</b>	0.7390 and 0.7170
<b>Structure solution technique</b>	direct methods
<b>Structure solution program</b>	XT, VERSION 2014/5
<b>Refinement method</b>	Full-matrix least-squares on F <sup>2</sup>
<b>Refinement program</b>	SHELXL-2014/7 (Sheldrick, 2014)
<b>Function minimized</b>	$\Sigma w(F_o^2 - F_c^2)^2$
<b>Data / restraints / parameters</b>	14147 / 1 / 437
<b>Goodness-of-fit on F<sup>2</sup></b>	1.024
<b><math>\Delta/\sigma_{\max}</math></b>	0.001
<b>Final R indices</b>	11864 data; R1 = 0.0493, wR2 = 0.1081 I > 2 $\sigma$ (I)
	all data R1 = 0.0656, wR2 = 0.1181
<b>Weighting scheme</b>	$w=1/[\sigma^2(F_o^2)+(0.0424P)^2+0.0709P]$ where $P=(F_o^2+2F_c^2)/3$
<b>Absolute structure parameter</b>	-0.017(17)
<b>Largest diff. peak and hole</b>	0.870 and -1.541 eÅ <sup>-3</sup>
<b>R.M.S. deviation from mean</b>	0.117 eÅ <sup>-3</sup>

**Table 12:** Bond lengths (Å) for complex (*S*)-**80b**

C1-C2	1.400(6)	C1-C6	1.413(6)
C1-Pd1	1.997(4)	C2-C3	1.395(7)
C3-C4	1.367(8)	C4-C5	1.386(7)
C5-C6	1.385(7)	C6-C7	1.503(6)
C7-N1	1.480(6)	C8-N1	1.471(6)
C9-N1	1.487(6)	C10-C11	1.384(7)
C10-C15	1.390(6)	C10-P1	1.823(4)
C11-C12	1.391(7)	C12-C13	1.376(8)
C13-C14	1.386(8)	C14-C15	1.392(7)
C16-C21	1.388(7)	C16-C17	1.390(6)
C16-P1	1.827(4)	C17-C18	1.395(6)
C18-C19	1.385(8)	C19-C20	1.384(7)
C20-C21	1.378(7)	C22-C23	1.510(6)

C22-C28	1.520(6)	C22-P1	1.849(4)
C23-C24	1.397(6)	C23-C26	1.444(6)
C24-O1	1.274(5)	C24-O2	1.355(5)
C25-O2	1.430(6)	C26-O3	1.216(5)
C26-O4	1.367(5)	C27-O4	1.432(6)
C28-C29	1.374(6)	C28-C33	1.445(6)
C29-C30	1.413(7)	C30-C31	1.360(7)
C31-C32	1.422(7)	C32-C37	1.410(7)
C32-C33	1.430(7)	C33-C34	1.420(7)
C34-C35	1.374(7)	C35-C36	1.419(8)
C36-C37	1.350(9)	C38-C13	1.739(6)
C38-C11	1.746(5)	C38-C12	1.777(6)
N1-Pd1	2.144(3)	O1-Pd1	2.123(3)
P1-Pd1	2.2277(10)		

**Table 13:** Bond angles (°) for complex (*S*)-**80b**

C2-C1-C6	117.4(4)	C2-C1-Pd1	130.7(3)
C6-C1-Pd1	111.8(3)	C3-C2-C1	120.9(4)
C4-C3-C2	120.8(5)	C3-C4-C5	119.3(5)
C6-C5-C4	121.1(5)	C5-C6-C1	120.4(4)
C5-C6-C7	121.6(4)	C1-C6-C7	117.9(4)
N1-C7-C6	108.8(4)	C11-C10-C15	119.3(4)
C11-C10-P1	119.3(3)	C15-C10-P1	121.1(4)
C10-C11-C12	120.0(5)	C13-C12-C11	120.7(5)
C12-C13-C14	119.8(5)	C13-C14-C15	119.8(5)
C10-C15-C14	120.5(5)	C21-C16-C17	119.1(4)
C21-C16-P1	117.9(3)	C17-C16-P1	123.0(3)
C16-C17-C18	120.0(4)	C19-C18-C17	120.1(4)
C20-C19-C18	119.7(4)	C21-C20-C19	120.2(4)
C20-C21-C16	120.8(4)	C23-C22-C28	116.0(3)
C23-C22-P1	113.6(3)	C28-C22-P1	109.8(3)
C24-C23-C26	126.1(4)	C24-C23-C22	119.5(4)
C26-C23-C22	114.3(4)	O1-C24-O2	116.1(4)
O1-C24-C23	126.4(4)	O2-C24-C23	117.5(4)

O3-C26-O4	120.3(4)	O3-C26-C23	124.0(4)
O4-C26-C23	115.7(4)	C29-C28-C33	118.5(4)
C29-C28-C22	121.8(4)	C33-C28-C22	119.7(4)
C28-C29-C30	121.9(4)	C31-C30-C29	121.1(5)
C30-C31-C32	119.5(4)	C37-C32-C31	120.4(5)
C37-C32-C33	119.4(5)	C31-C32-C33	120.1(4)
C34-C33-C32	117.4(4)	C34-C33-C28	123.8(4)
C32-C33-C28	118.7(4)	C35-C34-C33	121.7(5)
C34-C35-C36	119.5(5)	C37-C36-C35	120.4(5)
C36-C37-C32	121.4(5)	Cl3-C38-Cl1	111.8(3)
Cl3-C38-Cl2	110.1(3)	Cl1-C38-Cl2	109.9(3)
C8-N1-C7	109.4(4)	C8-N1-C9	109.6(4)
C7-N1-C9	109.9(4)	C8-N1-Pd1	115.4(3)
C7-N1-Pd1	105.2(2)	C9-N1-Pd1	107.3(3)
C24-O1-Pd1	133.6(3)	C24-O2-C25	116.7(4)
C26-O4-C27	114.7(4)	C10-P1-C16	106.2(2)
C10-P1-C22	100.42(19)	C16-P1-C22	106.36(19)
C10-P1-Pd1	122.52(15)	C16-P1-Pd1	109.67(14)
C22-P1-Pd1	110.42(14)	C1-Pd1-O1	173.37(15)
C1-Pd1-N1	82.32(15)	O1-Pd1-N1	91.12(13)
C1-Pd1-P1	98.78(12)	O1-Pd1-P1	87.82(9)
N1-Pd1-P1	176.45(10)		

**Figure 28:** ORTEP structure of chiral phosphine-palladium complex (*S*)-**86a**

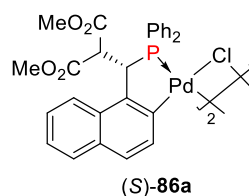
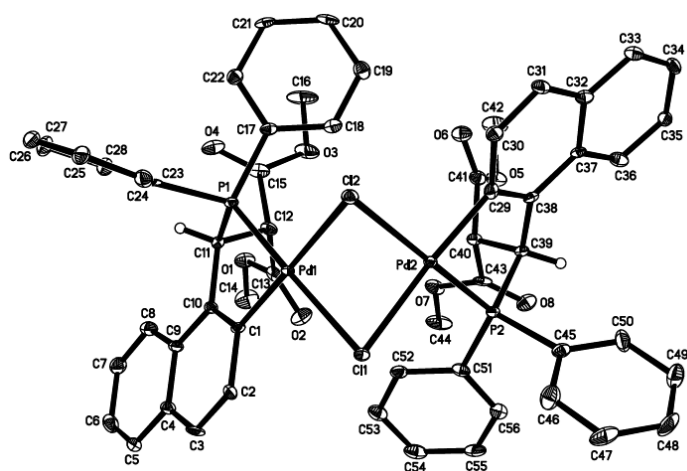


**Table 14:** Data collection and structure refinement for complex (*S*)-**86a**

<b>Chemical formula</b>	C <sub>57</sub> H <sub>50</sub> Cl <sub>4</sub> O <sub>8</sub> P <sub>2</sub> Pd <sub>2</sub>	
<b>Formula weight</b>	1279.51 g/mol	
<b>Temperature</b>	103(2) K	
<b>Wavelength</b>	1.54178 Å	
<b>Crystal size</b>	0.060 x 0.140 x 0.160 mm	
<b>Crystal habit</b>	yellow block	
<b>Crystal system</b>	monoclinic	
<b>Space group</b>	P 1 21 1	
<b>Unit cell dimensions</b>	a = 10.97000(10) Å	α = 90°
	b = 19.8122(2) Å	β = 108.4988(6)°
	c = 12.56070(10) Å	γ = 90°
<b>Volume</b>	2588.89(4) Å <sup>3</sup>	
<b>Z</b>	2	
<b>Density (calculated)</b>	1.641 g/cm <sup>3</sup>	
<b>Absorption coefficient</b>	8.553 mm <sup>-1</sup>	

<b>F(000)</b>	1292		
<b>Theta range for data collection</b>	3.71 to 67.52°		
<b>Index ranges</b>	-12<=h<=13, -23<=k<=23, -14<=l<=14		
<b>Reflections collected</b>	29310		
<b>Independent reflections</b>	8900 [R(int) = 0.0486]		
<b>Coverage of independent reflections</b>	97.8%		
<b>Absorption correction</b>	Multi-Scan		
<b>Max. and min. transmission</b>	0.6280 and 0.3420		
<b>Structure solution technique</b>	direct methods		
<b>Structure solution program</b>	XT, VERSION 2014/5		
<b>Refinement method</b>	Full-matrix least-squares on F <sup>2</sup>		
<b>Refinement program</b>	SHELXL-2014/7 (Sheldrick, 2014)		
<b>Function minimized</b>	$\Sigma w(F_o^2 - F_c^2)^2$		
<b>Data / restraints / parameters</b>	8900 / 200 / 701		
<b>Goodness-of-fit on F<sup>2</sup></b>	1.063		
<b>Final R indices</b>	8525 data; I>2σ(I)	R1 = 0.0325, wR2 = 0.0816	
	all data	R1 = 0.0340, wR2 = 0.0829	
<b>Weighting scheme</b>	$w=1/[\sigma^2(F_o^2)+(0.0422P)^2]$ where $P=(F_o^2+2F_c^2)/3$		
<b>Absolute structure parameter</b>	0.013(8)		
<b>Largest diff. peak and hole</b>	0.587 and -1.454 eÅ <sup>-3</sup>		
<b>R.M.S. deviation from mean</b>	0.142 eÅ <sup>-3</sup>		

**Table 15:** Bond lengths (Å) for complex (S)-**86a**

C1-C10	1.380(9)	C1-C2	1.427(9)
C1-Pd1	2.001(6)	C2-C3	1.370(10)
C3-C4	1.424(11)	C4-C5	1.409(10)
C4-C9	1.433(9)	C5-C6	1.362(11)
C6-C7	1.408(11)	C7-C8	1.374(11)
C8-C9	1.411(10)	C9-C10	1.430(9)
C10-C11	1.518(8)	C11-C12	1.555(10)
C11-P1	1.855(6)	C12-C13	1.527(9)
C12-C15	1.527(9)	C13-O2	1.206(9)
C13-O1	1.348(8)	C14-O1	1.452(9)
C15-O4	1.209(9)	C15-O3	1.332(9)

C16-O3	1.468(9)	C17-C18	1.393(10)
C17-C22	1.396(10)	C17-P1	1.822(6)
C18-C19	1.409(10)	C19-C20	1.377(11)
C20-C21	1.381(11)	C21-C22	1.394(10)
C23-C28	1.391(10)	C23-C24	1.396(10)
C23-P1	1.816(7)	C24-C25	1.393(11)
C25-C26	1.382(11)	C26-C27	1.388(11)
C27-C28	1.402(11)	C29-C38	1.387(10)
C29-C30	1.421(9)	C29-Pd2	2.017(7)
C30-C31	1.378(10)	C31-C32	1.416(10)
C32-C33	1.413(10)	C32-C37	1.429(10)
C33-C34	1.376(10)	C34-C35	1.410(10)
C35-C36	1.380(10)	C36-C37	1.413(10)
C37-C38	1.436(10)	C38-C39	1.506(9)
C39-C40	1.564(9)	C39-P2	1.851(6)
C40-C41A	1.52(2)	C40-C43	1.523(9)
C40-C41	1.528(13)	C41-O6	1.206(15)
C41-O5	1.348(17)	C42-O5	1.470(14)
C41A-O6A	1.20(2)	C41A-O5A	1.33(2)
C42A-O5A	1.47(2)	C43-O8	1.202(9)
C43-O7	1.334(9)	C44-O7	1.444(9)
C45-C46	1.388(11)	C45-C50	1.390(10)
C45-P2	1.804(7)	C46-C47	1.403(11)
C47-C48	1.389(13)	C48-C49	1.392(12)
C49-C50	1.381(11)	C51-C52	1.408(10)
C51-C56	1.421(10)	C51-P2	1.797(7)
C52-C53	1.379(10)	C53-C54	1.404(11)
C54-C55	1.398(11)	C55-C56	1.375(11)
C57-C14	1.755(10)	C57-C13	1.763(8)
C11-Pd1	2.4300(15)	C11-Pd2	2.4322(15)
C12-Pd2	2.4461(17)	C12-Pd1	2.4521(14)
P1-Pd1	2.1983(16)	P2-Pd2	2.2008(17)
Pd1-Pd2	2.9813(6)		

**Table 16:** Bond angles (°) for complex (*S*)-**86a**

C10-C1-C2	119.4(6)	C10-C1-Pd1	123.2(4)
C2-C1-Pd1	117.3(5)	C3-C2-C1	120.9(6)
C2-C3-C4	120.9(6)	C5-C4-C3	121.3(6)
C5-C4-C9	119.8(6)	C3-C4-C9	118.9(6)
C6-C5-C4	121.6(7)	C5-C6-C7	119.3(7)
C8-C7-C6	120.5(7)	C7-C8-C9	121.9(6)
C8-C9-C10	124.4(6)	C8-C9-C4	116.9(6)
C10-C9-C4	118.7(6)	C1-C10-C9	121.2(5)
C1-C10-C11	117.9(5)	C9-C10-C11	120.7(5)
C10-C11-C12	116.6(6)	C10-C11-P1	102.2(4)
C12-C11-P1	109.6(4)	C13-C12-C15	110.7(5)
C13-C12-C11	111.8(5)	C15-C12-C11	109.7(5)
O2-C13-O1	124.2(6)	O2-C13-C12	124.4(6)
O1-C13-C12	111.4(6)	O4-C15-O3	125.1(6)
O4-C15-C12	124.9(6)	O3-C15-C12	110.0(6)
C18-C17-C22	119.5(6)	C18-C17-P1	118.6(5)
C22-C17-P1	121.8(5)	C17-C18-C19	119.8(6)
C20-C19-C18	119.9(7)	C19-C20-C21	120.5(6)
C20-C21-C22	120.2(6)	C21-C22-C17	120.0(6)
C28-C23-C24	120.2(6)	C28-C23-P1	122.1(6)
C24-C23-P1	117.6(5)	C25-C24-C23	120.0(7)
C26-C25-C24	119.6(7)	C25-C26-C27	121.1(7)
C26-C27-C28	119.5(7)	C23-C28-C27	119.6(7)
C38-C29-C30	120.0(6)	C38-C29-Pd2	122.2(5)
C30-C29-Pd2	117.7(5)	C31-C30-C29	120.2(6)
C30-C31-C32	121.3(6)	C33-C32-C31	121.3(6)
C33-C32-C37	119.6(6)	C31-C32-C37	119.0(6)
C34-C33-C32	120.5(6)	C33-C34-C35	120.4(6)
C36-C35-C34	120.1(6)	C35-C36-C37	121.0(6)
C36-C37-C32	118.3(6)	C36-C37-C38	122.8(6)
C32-C37-C38	118.8(6)	C29-C38-C37	120.4(6)
C29-C38-C39	118.2(6)	C37-C38-C39	121.4(6)
C38-C39-C40	113.4(5)	C38-C39-P2	101.7(4)
C40-C39-P2	109.1(4)	C41A-C40-C43	108.(2)

C43-C40-C41	109.9(10)	C41A-C40-C39	115.(4)
C43-C40-C39	110.3(5)	C41-C40-C39	112.0(17)
O6-C41-O5	123.3(15)	O6-C41-C40	125.4(16)
O5-C41-C40	111.1(14)	C41-O5-C42	113.4(14)
O6A-C41A-O5A	129.(3)	O6A-C41A-C40	120.(3)
O5A-C41A-C40	111.(2)	C41A-O5A-C42A	115.(3)
O8-C43-O7	125.0(6)	O8-C43-C40	124.8(6)
O7-C43-C40	110.1(6)	C46-C45-C50	119.4(7)
C46-C45-P2	116.7(5)	C50-C45-P2	123.7(6)
C45-C46-C47	120.1(7)	C48-C47-C46	119.8(7)
C47-C48-C49	119.7(7)	C50-C49-C48	120.3(8)
C49-C50-C45	120.6(7)	C52-C51-C56	118.5(6)
C52-C51-P2	120.9(5)	C56-C51-P2	120.6(5)
C53-C52-C51	120.6(7)	C52-C53-C54	120.2(7)
C55-C54-C53	119.9(7)	C56-C55-C54	120.1(7)
C55-C56-C51	120.7(7)	C14-C57-C13	111.7(5)
Pd1-C11-Pd2	75.64(4)	Pd2-C12-Pd1	74.98(4)
C13-O1-C14	115.1(6)	C15-O3-C16	115.0(7)
C43-O7-C44	114.6(6)	C23-P1-C17	105.5(3)
C23-P1-C11	106.7(3)	C17-P1-C11	109.8(3)
C23-P1-Pd1	115.2(2)	C17-P1-Pd1	115.1(2)
C11-P1-Pd1	104.1(2)	C51-P2-C45	103.8(3)
C51-P2-C39	108.8(3)	C45-P2-C39	107.5(3)
C51-P2-Pd2	118.8(2)	C45-P2-Pd2	113.3(2)
C39-P2-Pd2	104.2(2)	C1-Pd1-P1	79.93(18)
C1-Pd1-C11	95.85(18)	P1-Pd1-C11	170.35(6)
C1-Pd1-C12	177.2(2)	P1-Pd1-C12	100.86(5)
C11-Pd1-C12	83.78(5)	C1-Pd1-Pd2	129.3(2)
P1-Pd1-Pd2	124.43(4)	C11-Pd1-Pd2	52.21(4)
C12-Pd1-Pd2	52.42(4)	C29-Pd2-P2	80.3(2)
C29-Pd2-C11	175.41(19)	P2-Pd2-C11	97.72(6)
C29-Pd2-C12	98.5(2)	P2-Pd2-C12	174.15(6)
C11-Pd2-C12	83.86(5)	C29-Pd2-Pd1	132.32(19)
P2-Pd2-Pd1	124.32(4)	C11-Pd2-Pd1	52.15(4)
C12-Pd2-Pd1	52.60(3)		



**Figure 29:** ORTEP structure of chiral phosphine-palladium complex (*S*)-**89**

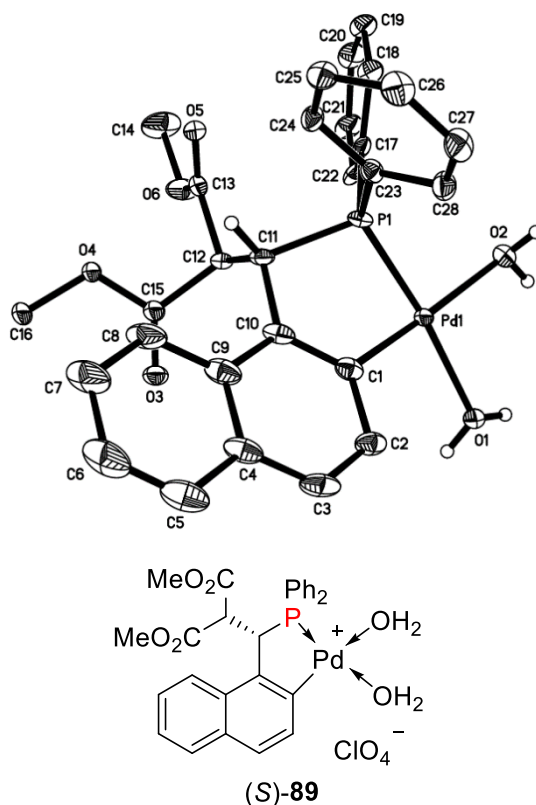


**Table 17:** Data collection and structure refinement for complex (*S*)-**89**

<b>Chemical formula</b>	C <sub>28</sub> H <sub>30</sub> ClO <sub>11</sub> PPd	
<b>Formula weight</b>	715.34 g/mol	
<b>Temperature</b>	103(2) K	
<b>Wavelength</b>	1.54178 Å	
<b>Crystal size</b>	0.080 x 0.100 x 0.200 mm	
<b>Crystal habit</b>	colorless block	
<b>Crystal system</b>	orthorhombic	
<b>Space group</b>	P 21 21 21	
<b>Unit cell dimensions</b>	a = 10.62424(9) Å	α = 90°
	b = 10.81406(10) Å	β = 90°
	c = 25.3404(2) Å	γ = 90°
<b>Volume</b>	2911.39(4) Å <sup>3</sup>	
<b>Z</b>	4	
<b>Density (calculated)</b>	1.632 g/cm <sup>3</sup>	
<b>Absorption coefficient</b>	7.035 mm <sup>-1</sup>	
<b>F(000)</b>	1456	

<b>Theta range for data collection</b>	3.49 to 67.38°		
<b>Index ranges</b>	-12<=h<=12, -12<=k<=11, -29<=l<=30		
<b>Reflections collected</b>	14284		
<b>Independent reflections</b>	5015 [R(int) = 0.0321]		
<b>Coverage of independent reflections</b>	99.0%		
<b>Absorption correction</b>	Multi-Scan		
<b>Max. and min. transmission</b>	0.6030 and 0.3340		
<b>Structure solution technique</b>	direct methods		
<b>Structure solution program</b>	XT, VERSION 2014/5		
<b>Refinement method</b>	Full-matrix least-squares on F <sup>2</sup>		
<b>Refinement program</b>	SHELXL-2014/7 (Sheldrick, 2014)		
<b>Function minimized</b>	$\Sigma w(F_o^2 - F_c^2)^2$		
<b>Data / restraints / parameters</b>	5015 / 953 / 562		
<b>Goodness-of-fit on F<sup>2</sup></b>	1.023		
<b><math>\Delta/\sigma_{\max}</math></b>	0.001		
<b>Final R indices</b>	4886 data; I>2 $\sigma$ (I)	R1 = 0.0308, wR2 = 0.0822	
	all data	R1 = 0.0314, wR2 = 0.0826	
<b>Weighting scheme</b>	$w=1/[\sigma^2(F_o^2)+(0.0564P)^2]$ where $P=(F_o^2+2F_c^2)/3$		
<b>Absolute structure parameter</b>	0.011(4)		
<b>Largest diff. peak and hole</b>	0.435 and -1.178 eÅ <sup>-3</sup>		
<b>R.M.S. deviation from mean</b>	0.153 eÅ <sup>-3</sup>		

**Table 18:** Bond lengths (Å) for complex (S)-**89**

Pd1-C1	1.997(6)	Pd1-O1	2.172(4)
Pd1-P1	2.1786(12)	Pd1-O2	2.205(4)
C1-C10	1.385(8)	C1-C2	1.418(7)
C2-C3	1.362(9)	C3-C4	1.422(9)
C4-C9	1.424(9)	C4-C5	1.429(9)
C5-C6	1.382(10)	C6-C7	1.396(11)
C7-C8	1.379(9)	C8-C9	1.424(9)
C9-C10	1.438(8)	C10-C11	1.504(8)
C11-C12	1.543(7)	C11-P1	1.857(6)
C12-C13	1.523(7)	C12-C15A	1.528(14)
C12-C15	1.532(17)	C13-O5	1.205(7)

C13-O6	1.336(7)	C14-O6	1.451(7)
C15-O3	1.205(17)	C15-O4	1.340(16)
C16-O4	1.456(15)	C15A-O3A	1.205(14)
C15A-O4A	1.337(13)	C16A-O4A	1.454(14)
C17-C18	1.396(12)	C17-C22	1.421(12)
C17-P1	1.809(9)	C18-C19	1.371(13)
C19-C20	1.401(14)	C20-C21	1.399(14)
C21-C22	1.398(12)	C23-C28	1.396(13)
C23-C24	1.397(13)	C23-P1	1.809(8)
C24-C25	1.385(11)	C25-C26	1.390(14)
C26-C27	1.365(14)	C27-C28	1.397(12)
C17A-C18A	1.39	C17A-C22A	1.39
C17A-P1	1.788(11)	C18A-C19A	1.39
C19A-C20A	1.39	C20A-C21A	1.39
C21A-C22A	1.39	C23A-C24A	1.371(18)
C23A-C28A	1.408(19)	C23A-P1	1.836(12)
C24A-C25A	1.391(19)	C25A-C26A	1.39(2)
C26A-C27A	1.366(18)	C27A-C28A	1.401(16)
C11-O9	1.410(10)	C11-O7	1.425(10)
C11-O8	1.436(8)	C11-O10	1.469(9)
C11A-O8A	1.410(17)	C11A-O9A	1.426(15)
C11A-O7A	1.438(17)	C11A-O10A	1.455(16)

**Table 19:** Bond angles (°) for complex (S)-**89**

C1-Pd1-O1	95.30(19)	C1-Pd1-P1	79.32(15)
O1-Pd1-P1	173.80(12)	C1-Pd1-O2	173.14(19)
O1-Pd1-O2	89.05(15)	P1-Pd1-O2	96.60(11)
C10-C1-C2	120.2(5)	C10-C1-Pd1	121.9(4)
C2-C1-Pd1	117.7(4)	C3-C2-C1	120.3(5)
C2-C3-C4	121.3(5)	C3-C4-C9	119.3(5)
C3-C4-C5	121.0(6)	C9-C4-C5	119.8(6)
C6-C5-C4	119.6(7)	C5-C6-C7	121.1(6)
C8-C7-C6	120.2(7)	C7-C8-C9	121.3(7)
C8-C9-C4	118.0(5)	C8-C9-C10	123.6(6)

C4-C9-C10	118.3(6)	C1-C10-C9	120.5(5)
C1-C10-C11	118.3(5)	C9-C10-C11	121.2(5)
C10-C11-C12	116.4(4)	C10-C11-P1	99.9(4)
C12-C11-P1	112.4(3)	C13-C12-C15A	109.8(9)
C13-C12-C15	107.4(11)	C13-C12-C11	110.3(4)
C15A-C12-C11	105.6(11)	C15-C12-C11	116.0(13)
O5-C13-O6	125.1(5)	O5-C13-C12	124.9(5)
O6-C13-C12	110.0(4)	O3-C15-O4	124.(2)
O3-C15-C12	125.(2)	O4-C15-C12	110.3(15)
C15-O4-C16	116.6(12)	O3A-C15A-O4A	124.4(17)
O3A-C15A-C12	124.3(18)	O4A-C15A-C12	111.3(12)
C15A-O4A-C16A	115.9(11)	C18-C17-C22	119.9(8)
C18-C17-P1	125.4(10)	C22-C17-P1	114.7(10)
C19-C18-C17	120.7(10)	C18-C19-C20	119.8(10)
C21-C20-C19	120.6(9)	C22-C21-C20	119.8(9)
C21-C22-C17	118.9(10)	C28-C23-C24	120.0(7)
C28-C23-P1	118.3(7)	C24-C23-P1	121.7(7)
C25-C24-C23	120.2(8)	C24-C25-C26	119.3(8)
C27-C26-C25	121.1(8)	C26-C27-C28	120.5(9)
C23-C28-C27	119.0(8)	C18A-C17A-C22A	120.0
C18A-C17A-P1	117.7(12)	C22A-C17A-P1	122.2(12)
C19A-C18A-C17A	120.0	C18A-C19A-C20A	120.0
C21A-C20A-C19A	120.0	C22A-C21A-C20A	120.0
C21A-C22A-C17A	120.0	C24A-C23A-C28A	120.9(12)
C24A-C23A-P1	119.6(12)	C28A-C23A-P1	119.5(10)
C23A-C24A-C25A	118.9(14)	C26A-C25A-C24A	120.7(15)
C27A-C26A-C25A	120.8(14)	C26A-C27A-C28A	119.6(13)
C27A-C28A-C23A	119.1(12)	C13-O6-C14	115.5(5)
O9-C11-O7	111.5(8)	O9-C11-O8	110.4(7)
O7-C11-O8	108.8(7)	O9-C11-O10	107.9(7)
O7-C11-O10	109.9(7)	O8-C11-O10	108.2(6)
O8A-C11A-O9A	113.4(15)	O8A-C11A-O7A	116.2(16)
O9A-C11A-O7A	105.3(13)	O8A-C11A-O10A	106.9(15)
O9A-C11A-O10A	109.0(12)	O7A-C11A-O10A	105.7(15)
C17-P1-C23	106.8(6)	C17A-P1-C23A	105.9(9)

C17A-P1-C11	112.6(5)	C17-P1-C11	111.8(4)
C23-P1-C11	97.4(4)	C23A-P1-C11	111.9(6)
C17A-P1-Pd1	114.7(6)	C17-P1-Pd1	112.8(4)
C23-P1-Pd1	123.3(3)	C23A-P1-Pd1	108.3(5)
C11-P1-Pd1	103.51(16)		

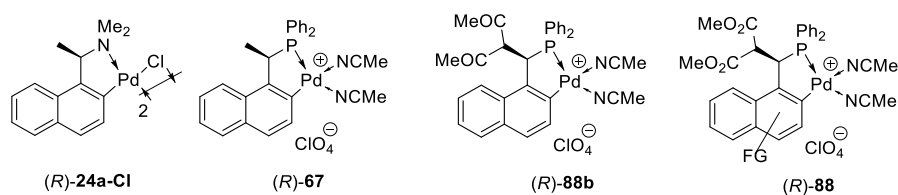


## Chapter 4. Efficient Synthesis of Malonate Functionalized Chiral Phosphapalladacycles and Their Catalytic Evaluation in Asymmetric Hydrophosphination of Chalcone

### 4.1. Introduction

The synthesis and application of *ortho*-palladated C-N complexes have been well established<sup>1-2, 229</sup>. In particular, the N-donor palladacycle initially developed by Wild and co-workers<sup>183, 185, 230</sup> has been employed in a wide variety of catalytic asymmetric reactions, for example, as the catalyst in a Overman rearrangement reaction<sup>174</sup>, as either a catalyst precursor or promoter in hydrophosphination<sup>22, 231</sup>, hydroamination<sup>232</sup>, Heck<sup>233-235</sup>, and Suzuki reaction and as an optical resolution reagent for various chiral ligands<sup>19, 183</sup>. In contrast to the predominantly sigma-donating effect of the nitrogen-metal bond in the azapalladacycle complexes,  $\pi$ -back-bonding effect is well established to be present in the phosphapalladacycle complexes, which leads to different catalytic reactivity of the resulting metal-phosphine complex when compared to the azapalladacycle<sup>108</sup>. However, reports on chiral cyclopalladated C-P compounds, a congener of C-N complexes, are relatively scarce<sup>236-238</sup>, though the phosphine palladium complexes have played an important role in various organic reactions, such as [4+2] cycloadditions<sup>239</sup> Heck<sup>240</sup>, Suzuki<sup>238, 241</sup>, Stille<sup>242</sup>, Sonogashira coupling<sup>243</sup>, Claisen rearrangements<sup>244</sup>, As/P-H addition reaction<sup>112, 118, 152, 160, 231</sup>, and medicinal chemistry<sup>245</sup>.

**Figure 30** : Structures of selected existing cyclopalladated complexes and their functionalized derivatives developed in this study



The application of cyclopalladated complex (*R*)-**24a-Cl** (**Figure 30**) as catalysts in the synthesis of various chiral phosphine compounds *via* asymmetric hydrophosphination reactions of a variety of substrates including  $\alpha$ ,  $\beta$ - and  $\alpha$ ,  $\beta$ ,  $\gamma$ ,  $\delta$ - unsaturated malonate esters<sup>146, 215</sup>,  $\alpha$ ,  $\beta$ -unsaturated carbonyl compounds<sup>246</sup>, enones<sup>105</sup>, and  $\alpha$ ,  $\beta$ -unsaturated N-acylpyrroles<sup>247</sup> has been highlighted recently. The CP compound (*R*)-**67** is known as an excellent catalyst for asymmetric P-H addition reaction of 4-oxo-enamides<sup>148</sup>, *N*-enoyl phthalimides<sup>151</sup>, and benzoquinones<sup>156</sup>.

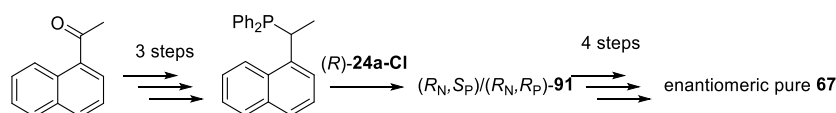
During the course of studying the asymmetric P-H addition, we found that minor modifications of the functional groups present on the phosphorous ligands backbone can help to tune the catalytic properties of the catalyst. On the other hand, considering the laborious synthetic procedure towards complex (*R*)-**67** (**Scheme 48**), we decided to prepare its congeneric complexes (*R*)-**88b** and derivatives represented by (*R*)-**88** by using a protocol that involved asymmetric hydrophosphination followed by regioselective cyclometallation<sup>118</sup>. Besides being electronically different from the traditional methyl moiety, the presence of the diester group at the chiral center in the new complexes also results in greater steric hindrance in the cyclometallated ring system that may potentially be beneficial in enhancing stereocontrol during asymmetric synthesis. In addition to the above argument, the rationale behind our ligand design also took into account the potential electronic effects that can come into play by modification of the naphthalene ring system. We therefore planned to introduce different functional groups, including electron-withdrawing group (F), electron-donating groups (OMe, Me), and greater delocalization (phenanthrenyl), into the aromatic ring to synthesize complexes of the type depicted by **88**. These modifications are expected to have an impact on the nature of the C-Pd bond of the newly designed phosphapalladacycles. This study also has relevance in the greater context of cyclometallation reactions since for cyclopalladation reactions involving free

phosphine ligands, there are only very few examples known in literature involving functionalized chiral aromatic ring-based substrates<sup>81, 90, 102, 118, 248</sup>.

We herein report the preparation of four chiral cyclophosphapalladated complexes of the type depicted by **88**, and their evaluation as chiral catalysts in the asymmetric hydrophosphination reaction. Four chiral phosphapalladacycle complexes functionalized with the malonate moiety at the chiral carbon have been synthesized *via* a consecutive asymmetric hydrophosphination and cyclometallation protocol. High conversions were achieved in the P-H addition reaction, which was itself catalyzed by a phosphapalladacycle. Moderate to good enantioselectivities were obtained for this step depending on the nature of the functional groups present on the naphthalene backbone. In contrast, the outcome of the subsequent cyclometallation reaction relies highly on the character of the functional groups. The catalytic potential of the synthesized phosphapalladacycle complexes was evaluated in the hydrophosphination reaction of chalcone with moderate results.

---

**Scheme 48:** Overview of the traditional procedure for the synthesis of phosphapalladacycle (*R*)-**67**

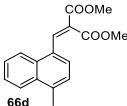
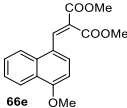
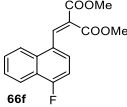


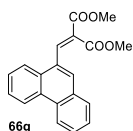
#### 4.2. Results and discussion

We initiated our preliminary investigations by using palladium acetate as the catalyst in the synthesis of the racemic ligands **70** *via* the hydrophosphination reaction between malonate activated substrates **66** and diphenylphosphine in methanol at room temperature (**Scheme 49**). It needs to be noted that based on our previous studies it has been established that the malonate moiety can sufficiently activate C=C bond of substrates such as **66** towards the P-H addition reaction<sup>107</sup>.

The conversions of this reaction were greater than 99% as seen from the  $^{31}\text{P}\{^1\text{H}\}$  NMR. Treatment of racemic phosphine ligands **70** with azapalladacycle (*R*)-**24a-Cl** leads to the formation of diastereoisomers (*R<sub>N</sub>,S<sub>P</sub>*)/(*R<sub>N</sub>,R<sub>P</sub>*)-**91**, which were then separated by either fractional crystallization or column chromatography. With (*R<sub>N</sub>,S<sub>P</sub>*)-**91** in hand, we subsequently explored the synthesis of dimeric phosphapalladacycles (*S*)-**86** by cyclometallation reaction (Table 20). Before the cyclometallation reaction of (*R<sub>N</sub>,S<sub>P</sub>*)-**91d/91e**, concentrated HCl was added to the solution of (*R<sub>N</sub>,S<sub>P</sub>*)-**91d/91e** in acetone at room temperature for 1 hour to remove the CN auxiliary (Scheme 49). Sodium acetate was then added as a base, and C-Pd-P 5-membered ring formation led to the dimeric product (*S*)-**86d/86e** at room temperature after 1 h and 3 h respectively, with yields of 77% and 72%, respectively (Table 20, entries 1 and 2). When the solution of concentrated HCl and (*R<sub>N</sub>,S<sub>P</sub>*)-**91f** in acetone was refluxed for 40 minutes, the final product (*S*)-**86f** was obtained in 81% yield (entry 3). On the other hand, dimeric (*S*)-**86g** was formed in 54% yield upon treatment of (*R<sub>N</sub>,S<sub>P</sub>*)-**91g** with concentrated HCl at 40 °C for 1 hour, followed by treatment of  $\text{NEt}_3$  in degassed DCM (entry 4).

**Table 20:** Coordination reaction and optical resolution of palladacycles.

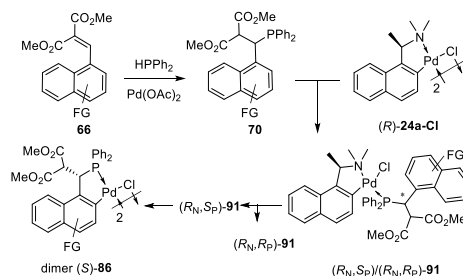
entry	Substrate	Condition <sup>a</sup>	Yield of ( <i>R<sub>N</sub>,S<sub>P</sub></i> )- <b>91</b> from optical resolution (%) <sup>b</sup>	Yield ( <i>R<sub>N</sub>,R<sub>P</sub></i> )- <b>91</b> from optical resolution (%) <sup>b</sup>	Yield ( <i>S</i> )- <b>86</b> from ( <i>R<sub>N</sub>,S<sub>P</sub></i> )- <b>91</b> (%) <sup>b</sup>	Final yields of ( <i>S</i> )- <b>86</b>
1		conc. HCl, RT, 1 h NaOAc, RT, 1 h	35	14	77	27
2		conc. HCl, RT, 1 h NaOAc, RT, 3 h	32	17	72	23
3		conc. HCl, reflux, 40 min	43	12	81	35



conc. HCl, 40 °C, 1 h  
degassed DCM, NEt<sub>3</sub>

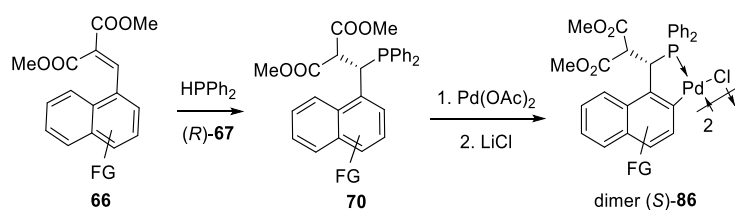
<sup>a</sup> condition of the reaction from **91** to **86**; <sup>b</sup> Isolated yields.

### Scheme 49: Synthesis of (*S*)-**86** from racemic phosphine ligands



The final overall yields of enantiomerically pure dimer (*S*)-**86**, however, were very low (18-35%, **Table 20**). In addition, the usage of stoichiometric amounts of chiral reagent (*R*)-**24a-Cl** is not economical. We, therefore, decided to explore a facile and efficient alternate route for synthesis of the dimer complexes (*S*)-**86** by phosphapalladacycle (*R*)-**67** catalyzed asymmetric hydrophosphination reaction followed by a cyclometallation step (**Scheme 50**).

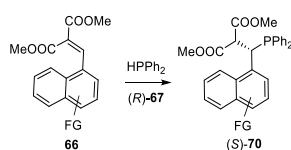
### Scheme 50: Stereoselective synthesis of (*S*)-**86** via (*R*)-**67** catalyzed asymmetric hydrophosphination and subsequent cyclometallation



Following the general conditions established from our previous work<sup>118</sup>, we first examined the reactivity and enantioselectivity of various substrates catalyzed by (*R*)-**67** in the asymmetric P-H addition reaction, at -80 °C in the presence of NEt<sub>3</sub> (**Table 21**). Initial studies established that the use of a single solvent system resulted in either very low conversions, such as in the case of CHCl<sub>3</sub>, THF, acetone, and toluene, or unacceptable enantioselectivities, such as

in the case of MeOH. Therefore, a mixture of two different solvents was employed as shown in **Table 21**. The best reactivity and enantioselectivity were observed on substrate **66f** among the four substrates examined **66** (entries 1-4) (>99% yield, 88% *ee*), hence it was selected as the sample substrate for further optimizing the asymmetric hydrophosphination reaction conditions. The mixture of MeOH and chloroform gave both excellent conversion and enantioselectivity (entries 3, 5-8). Different ratio of methanol and chloroform in the solvent system was also examined, which showed that the best result was obtained when the volume ratio of the two was 1:1 (entries 3, 9-11). This was subsequently selected as the optimum solvent.

**Table 21:** Screening of mixed solvent systems for the asymmetric P-H reaction catalyzed by (*R*)-**67**



Entry	Substrate	Solvent	t (d)	Conversion (%) <sup>a</sup>	<i>ee</i> (%) <sup>b</sup>
1	<b>66d</b>	MeOH:CHCl <sub>3</sub> (v:v=1:1)	4	> 99	58
2	<b>66e</b>	MeOH:CHCl <sub>3</sub> (v:v=1:1)	4	> 99	61
3	<b>66f</b>	MeOH:CHCl <sub>3</sub> (v:v=1:1)	1	> 99	88
4	<b>66g</b>	MeOH:CHCl <sub>3</sub> (v:v=1:1)	5	> 99	78
5	<b>66g</b>	MeOH:Acetone (v:v=1:1)	5	14	35
6	<b>66f</b>	MeOH:THF (v:v=1:1)	3	19	31
7	<b>66f</b>	MeOH:Acetone (v:v=1:1)	3	22	64
8	<b>66f</b>	EtOH:CHCl <sub>3</sub> (v:v=1:1)	2	> 99	19
9	<b>66f</b>	MeOH:CHCl <sub>3</sub> (v:v=2:1)	1	> 99	79
10	<b>66f</b>	MeOH:CHCl <sub>3</sub> (v:v=3:2)	1	> 99	26
11	<b>66f</b>	MeOH:CHCl <sub>3</sub> (v:v=1:2)	1	32	37

<sup>a</sup> The conversions were examined by <sup>31</sup>P{<sup>1</sup>H} NMR; <sup>b</sup> the *ees* were examined by <sup>31</sup>P{<sup>1</sup>H} NMR after coordinating of free phosphine ligands to (*R*)-**24a-Cl**.

With the free phosphine ligands **70** in hand, we then examined the yields of cyclometallation reaction with various palladium sources (**Table 22**). The reaction conditions and palladium sources employed differ depending on the various functional groups present on the aromatic rings. In general, the *ortho*-H on the aromatic ring is activated when the phosphorus ligand coordinates to the palladium centre. Pd(OAc)<sub>2</sub>, Li<sub>2</sub>[PdCl<sub>4</sub>], and PdCl<sub>2</sub>(NCMe)<sub>2</sub> are therefore usually used as the palladium sources for cyclometallation. On the other hand, the C-N palladated compounds similar to **24a-Cl** can be the palladium source too, *via* metal transfer methods followed by removal of the C-N auxiliary. Palladium acetate proved to be the optimal palladium source for the cyclometallation reaction of **70d-g** (entries 1-3, 4-6). Although the enantioselectivities of **66d** and **66e** were only moderate (**Table 21**, entries 1 and 2, 58% for **66d**, 61% for **66e**), the yields of enantiomerically pure product (*S*)-**86** after cyclometallation reaction and fractional crystallization process were still acceptable and better than the one obtained by the previously adopted method (38% and 42% respectively) (**Table 22**, entries 7 and 1). To our delight, enantiomerically pure products (*S*)-**86f/86g** can also be prepared in good yields when **70f** and **70g** were treated with palladium acetate (**Table 23**, entries 4 and 8, 73%, 65% respectively). The molecular structure and the absolute stereochemistry of dimer (*S*)-**86** were determined by X-ray crystallography (**Figure 31**).

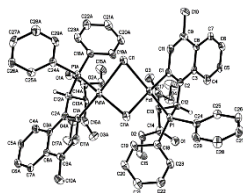
**Table 22:** The cyclometallation reaction of free ligands

Entry	Substrate	Palladium source	Yield (%) <sup>a</sup>
1	<b>70e</b>	Pd(OAc) <sub>2</sub>	42
2	<b>70e</b>	PdCl <sub>2</sub> (NCMe) <sub>2</sub>	22

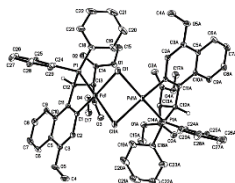
3	<b>70e</b>	Li <sub>2</sub> [PdCl <sub>4</sub> ]	15
4	<b>70f</b>	Pd(OAc) <sub>2</sub>	73
5	<b>70f</b>	PdCl <sub>2</sub> (NCMe) <sub>2</sub>	34
6	<b>70f</b>	Li <sub>2</sub> [PdCl <sub>4</sub> ]	52
7	<b>70d</b>	Pd(OAc) <sub>2</sub>	38
8	<b>70g</b>	Pd(OAc) <sub>2</sub>	65

<sup>a</sup> the yields are the final yields of the enantiomeric pure product (*S*)-**86** after the fractional crystallization.

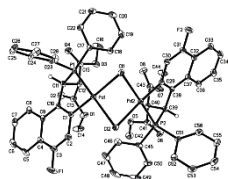
**Figure 31:** X-ray structure of **86d-86f**



X-ray crystal structure of complex (*S*)-**86d**. Selected bond lengths (Å) C2-C12 1.511(14); C12-P1 1.834(10); C1-C2 1.382(13); P1-Pd1 2.192(3); C1-Pd1 2.015(9); Cl1-Pd1 2.422(3); Cl1-Pd1 2.443(2). Selected bond angles (°) C2-C12-P1 103.3(6); C1-C2-C12 117.0(9); C12-P1-Pd1 104.0(4); C2-C1-Pd1 122.7(8); C1-Pd1-P1 80.5(3); Cl1-Pd1-Cl1 83.46(11); Pd1-Cl1-Pd1 74.09(7).



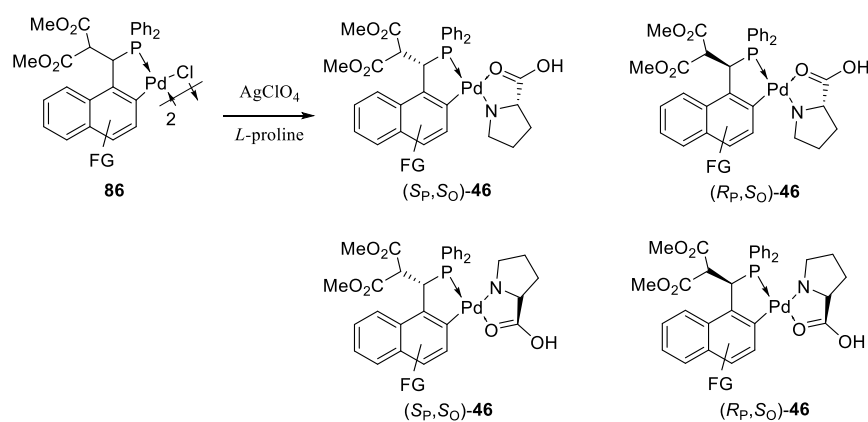
X-ray crystal structure of complex (*S*)-**86e**. Selected bond lengths (Å) C12-P1 1.8456(14); C1-Pd1 2.0105(14); P1-Pd1 2.1914(4); C11-C12 1.5131(19); C1-C11 1.388(2). Selected bond angles (°) C1-Pd1-P1 79.83(4); C12-P1-Pd1 103.39(5); C11-C1-Pd1 121.78(10); Cl1-Pd1-Cl1A 84.17(7); Pd1-Cl1-Pd1A 75.40(5); C1-C11-C12 117.5(5); C11-C12-P1 101.2(4).



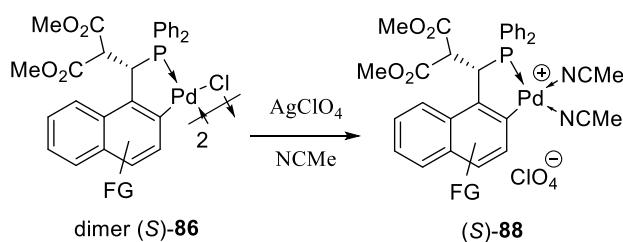
X-ray crystal structure of complex (*S*)-**86f**. Selected bond lengths (Å) C11-P1 1.846(5); Pd1-Cl1 2.001(5); Pd1-P1 2.1926(12); C10-C11 1.516(7); C1-C10 1.391(6). Selected bond angles (°) C1-Pd1-P1 80.70(13); C10-C11-P1 103.0(3); C11-P1-Pd1 103.98(16); C10-C1-Pd1 123.2(3); C11-Pd1-Cl2 83.57(4); Pd1-C11-Pd2 73.57(3); Pd1-Cl2-Pd2 73.68(3); C10-C1-Pd1 123.2(3); C1-C10-C11 116.7(4).

The enantiomeric purity of (*S*)-**86** was examined by exchanging the chloro bridge of the dimeric complex with *L*-proline to form two pairs of diastereoisomers. Treating racemic **86** with *L*-proline led to the formation of two pairs of diastereomeric regio-isomers (*S<sub>P</sub>,S<sub>O</sub>*)-**46**, (*R<sub>P</sub>,S<sub>O</sub>*)-**46** and (*S<sub>P</sub>,S<sub>O</sub>*)-**46**, (*R<sub>P</sub>,S<sub>O</sub>*)-**46**, which displayed four chemical shifts in <sup>31</sup>P{<sup>1</sup>H} NMR (Scheme 51). On the other hand, there were only two chemical shifts observed in <sup>31</sup>P{<sup>1</sup>H} NMR when we added *L*-proline into the CP dimer products **86**, which was obtained after the asymmetric P-H addition reaction and cyclometallation reaction.

**Scheme 51:** Treatment of the **86** with *L*-proline to examine the enantiomeric purity



Derivatives of **88** incorporating an easily leaving moiety such as acetonitrile, suitable for catalytic applications were prepared by removing the chloro bridges with AgClO<sub>4</sub> (Scheme 52). In the absence of the inert Pd-Cl bond, catalysts **88** were more active than **86**.

**Scheme 52:** Synthesis of the CP catalyst (*S*)-**88**

The newly synthesized phosphapalladacycles **88** were subsequently applied in the hydrophosphination reaction and the results showed that all four catalysts gave complete conversions whilst catalyst **88e** gave the best enantioselectivity (**Table 23**). However, their performance, in terms of enantioselectivity was moderate when compared to (*R*)-**67** and (*R*)-**88b** catalysts developed by us previously. We are currently in the process of screening these new complexes for other asymmetric reaction scenarios. Because of the difference of steric hindrance and electronic effect of the catalysts, the results are significantly different.

**Table 23:** The application of complexes **88** in catalytic hydrophosphination of chalcone

Entry	Catalyst	Yield (%) <sup>a</sup>	<i>ee</i> (%) <sup>b</sup>
1	( <i>R</i> )- <b>67</b>	> 99	>99
2	<b>88d</b>	> 99	64
3	<b>88e</b>	> 99	78
4	<b>88f</b>	> 99	70
5	<b>88g</b>	> 99	53
6	( <i>R</i> )- <b>88b</b>	> 99	77

<sup>a</sup> The yield were determined by <sup>31</sup>P{<sup>1</sup>H} NMR spectrum. <sup>b</sup> The *ees* were determined by

<sup>31</sup>P{<sup>1</sup>H} NMR spectrum after the product coordinated to the chiral palladated complexes (*R*)-**24a-CI**.

#### 4.3. Conclusions

Four functionalized chiral phosphapalladacycle complexes have been efficiently prepared by consecutive asymmetric hydrophosphination (P-H

reaction) and cyclometallation reaction. The impact of installation of malonate moiety at the chiral carbon as well as the modification of the naphthalene ring system was studied for the asymmetric hydrophosphination reaction. By analysing the steric hindrance and electronic effect of the catalysts, these preliminary results will serve as a guide for the rational design of other functionalized phosphapalladacycles using this alternate synthetic methodology.

#### 4.4. Experimental section

##### **General Information**

All reactions including the air-sensitive complexes diphenylphosphine and free ligands **70** were carried out under an inert atmosphere of nitrogen employing Schlenk Line and two-neck round bottom flask, and all the solvent contacted the air-sensitive complexes were degassed by blowing with nitrogen. NMR spectra were recorded on Bruker AV 300, AV400, AV 500, and BBFO 400 spectrometers. Chemical shifts were reported in ppm and referenced to an internal SiMe<sub>4</sub> standard (0 ppm) for <sup>1</sup>H NMR, chloroform-*d* (77.16 ppm) for <sup>13</sup>C NMR, and Dimethyl sulfoxide-*d*<sub>6</sub> (39.6 ppm) for <sup>13</sup>C NMR. Dichloromethane, chloroform, tetrahydrofuran, acetone and methanol were purchased from their respective companies and used as supplied. Tetrahydrofuran was distilled from sodium/benzophenone prior to use. Solvents were degassed when necessary. A Low Temp Pairstirrer PSL-1800 was used for controlling low temperature reactions. Column chromatography was carried out with Silica gel 60 (Merck). Melting points were measured using SRS Optimelt Automated Point System SRS MPA100. Optical rotation was measured with JASCO P-1030 Polarimeter in the specified solvent in a 0.1 dm cell at 22.0 °C.

##### **Preparation of substrates **66****

The preparation of substrates **66** was described according to previously report.<sup>249</sup>

##### **Preparation of (*R<sub>N</sub>,S<sub>P</sub>*)-**91** from **66****

To a solution of diphenylphosphine (10.0 mmol, 1.8619 g, 1.0 equiv) in the degassed methanol (30 mL) in the two-neck round bottom flask was added substrate **66** (10.5 mmol, 1.05 equiv) and catalyst Pd(OAc)<sub>2</sub> (0.5 mmol, 0.1123 g, 0.05 equiv), and the resulting mixture was stirred at room temperature for 2 hours to get the air-sensitive crude products **70** (the <sup>31</sup>P{<sup>1</sup>H} NMR chemical shifts were around 4) (yield > 99%). The diastereomeric isomers (*R<sub>N</sub>,S<sub>P</sub>*)/(*R<sub>N</sub>,R<sub>P</sub>*)-**91** were achieved by treating the above system with stoichiometric amounts of chiral reagent (*R*)-**24a-Cl** (5.0 mmol, 3.4016 g, 0.5 equiv) and separated to get enantioselective pure (*R<sub>N</sub>,S<sub>P</sub>*)-**91** and (*R<sub>N</sub>,R<sub>P</sub>*)-**91** by column chromatography on silica gel.

#### **Preparation of dimer (*S*)-**86d/e** from (*R<sub>N</sub>,S<sub>P</sub>*)-**91d/e****

Complex (*R<sub>N</sub>,S<sub>P</sub>*)-**91d/e** (1.0 mmol) was dissolved in acetone (50 mL) and treated with conc. HCl (2.2 mL). The reaction mixture was stirred at room temperature for 1 hour to liberate the C-N auxiliary. The reaction mixture was poured into water (500 mL) and the intermediate compound was filtered and subsequently converted to dimer ((*S*)-**86d/e**) by the treatment with NaOAc (1.6210 g) for 1 hour. Complex ((*S*)-**86d/e**) was purified by column chromatography on silica gel (elution: DCM). The isolated yields were listed in Table 20.

#### **Preparation of dimer (*S*)-**86f** from (*R<sub>N</sub>,S<sub>P</sub>*)-**91f****

The mixture of (*R<sub>N</sub>,S<sub>P</sub>*)-**91f** (1.0 mmol) and conc. HCl was heated in acetone (50 mL) at 60 °C for 40 min. The reaction mixture was cooled to room temperature and then poured into water (500 mL). The crude product was filtered followed by purification with column chromatography on silica gel (elution: DCM) to get the (*S*)-**86f**. The isolated yield was listed in Table 20.

#### **Preparation of dimer (*S*)-**86g** from (*R<sub>N</sub>,S<sub>P</sub>*)-**91g****

The mixture of (*R<sub>N</sub>,S<sub>P</sub>*)-**91g** (1.0 mmol) and conc. HCl was heated in acetone (50 mL) at 60 °C for 1 hour. The resulting mixture was poured into water (500

mL) and the intermediate complex was filtered. The crude product was then stirred with NEt<sub>3</sub> (0.6 mmol) in degassed DCM at room temperature for 1 hour. The crude mixture was extracted with DCM/H<sub>2</sub>O and dried with MgSO<sub>4</sub>, followed by purifying with column chromatography on silica gel (elution: DCM), giving the pure (*S*)-**86g**. The isolated yield was listed in Table 20.

#### **Synthesis of (*S*)-**86** from chiral **70****

Substrate **5** (1.05 mmol, 1.05 equiv) and the chiral catalyst (*R*)-**67** were added a solution of diphenylphosphine (1.0 mmol, 0.1862 g, 1.0 equiv) in the degassed solvent (55 mL) in a 100 mL two-neck round bottom flask. The reaction mixture was then kept in the low temperature bath at the selected temperature for 30 minutes. The external base NEt<sub>3</sub> (1.0 equiv) in degassed solvent (0.5 mL) was added dropwise into the two-neck round bottom flask. The reaction mixture was then kept at the selected temperature for the duration listed in Table 2. The palladium source was then added into the resulting chiral phosphine ligand. The crude cyclopalladated dimer (*S*)-**86** thus obtained was purified by column chromatography on silica gel (elution: DCM). Enantiomerically pure product (*S*)-**86** could be further purified by recrystallization. The isolated yields were listed in Table 22.

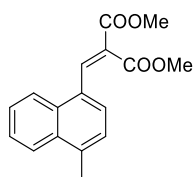
#### **Preparation of **46****

To the solution of **86** (1.0 mmol) in DCM was added the mixture of *L*-proline (1.05 mmol) and KOH (1.05 mmol) in degassed water, then, stirred the resulting mixture at room temperature for 1 hour, giving the product **46**.

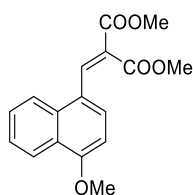
#### **Preparation of **88****

The substrate **86** (1.0 mmol) and AgClO<sub>4</sub> (1.05 mmol) was added to the round bottom flask with acetonitrile (10 mL) as the solvent and stirred for 1 hour. The pure product **88** was obtained after the consequently procedure of removing solvent, extraction, drying, filtration, and removing solvent.

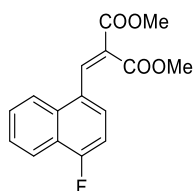
#### **Spectroscopic data of the products**



**Compound 66d:**  $^1\text{H}$  NMR (400 MHz, Chloroform-*d*),  $\delta$  8.52 (s, 1H), 8.04-8.01 (m, 2H), 7.60-7.59 (m, 2H), 7.46 (d,  $J = 7.31$  Hz, 1H), 7.29 (d,  $J = 7.34$  Hz, 1H), 3.90 (s, 3H), 3.69 (s, 3H), 2.71 (s, 3H).  $^{13}\text{C}$  NMR (100 MHz, Chloroform-*d*),  $\delta$  166.99, 164.58, 142.23, 137.79, 132.74, 131.59, 129.13, 127.75, 126.79, 126.45, 126.31, 124.95, 124.62, 52.81, 52.62, 19.88. HRMS ( $m/z$ ): Calculated for  $\text{C}_{17}\text{H}_{16}\text{O}_4\text{H}^+$  ( $\text{MH}^+$ ): 285.1127, Found ( $\text{MH}^+$ ): 285.1133. Melting point: 115.7-115.9  $^\circ\text{C}$ .

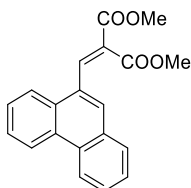


**Compound 66e:**  $^1\text{H}$  NMR (400 MHz, Chloroform-*d*),  $\delta$  8.48 (s, 1H), 8.31 (dd,  $J = 0.88, 8.30$  Hz, 1H), 7.99 (d,  $J = 8.24$  Hz, 1H), 7.59-7.53 (m, 3H), 6.78 (d,  $J = 8.15$  Hz, 1H), 4.02 (s, 3H), 3.89 (s, 3H), 3.73 (s, 3H).  $^{13}\text{C}$  NMR (100 MHz, Chloroform-*d*),  $\delta$  167.43, 164.78, 157.77, 141.60, 132.73, 127.73, 127.67, 126.08, 125.89, 125.63, 123.65, 122.90, 122.81, 103.53, 55.78, 52.72, 52.61. HRMS ( $m/z$ ): Calculated for  $\text{C}_{17}\text{H}_{16}\text{O}_5\text{H}^+$  ( $\text{MH}^+$ ): 301.1076, Found ( $\text{MH}^+$ ): 301.1078. Melting point: 98.1-98.4  $^\circ\text{C}$ .

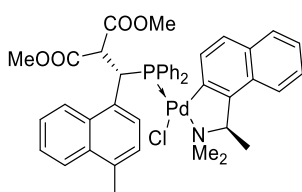


**Compound 66f:**  $^1\text{H}$  NMR (400 MHz, Chloroform-*d*),  $\delta$  8.42 (s, 1H), 8.13 (dd,  $J = 2.38, 7.11$  Hz, 1H), 7.99-7.97 (m, 1H), 7.62-7.59 (m, 2H), 7.51 (dd,  $J =$

5.33, 8.03 Hz, 1H), 7.11 (dd,  $J = 8.09, 10.03$  Hz, 1H), 3.90 (s, 3H), 3.69 (s, 3H).  $^{13}\text{C}$  NMR (100 MHz, Chloroform- $d$ ),  $\delta$  166.68, 164.32, 161.43, 158.88, 140.88, 128.10, 126.91, 126.89, 126.74, 126.65, 124.04, 124.01, 121.35, 109.39, 109.19, 52.85, 52.65.  $^{19}\text{F}\{^1\text{H}\}$  NMR (376 MHz, Chloroform- $d$ ),  $\delta$  -118.35. HRMS ( $m/z$ ): Calculated for  $\text{C}_{16}\text{H}_{13}\text{O}_4\text{FH}^+$  ( $\text{MH}^+$ ): 289.0876, Found ( $\text{MH}^+$ ): 289.0889. Melting point: 60.0-60.2  $^\circ\text{C}$ .

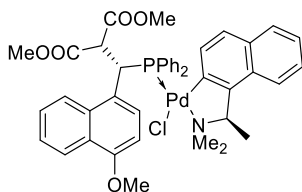


**Compound 66g:**  $^1\text{H}$  NMR (400 MHz, Chloroform- $d$ ),  $\delta$  8.65 (d,  $J = 7.78$  Hz, 1H), 8.60 (d,  $J = 8.20$  Hz, 1H), 8.50 (s, 1H), 8.00 (d,  $J = 7.74$  Hz, 1H), 7.86-7.83 (m, 2H), 7.67-7.57 (m, 4H), 3.95 (s, 3H), 3.65 (s, 3H).  $^{13}\text{C}$  NMR (100 MHz, Chloroform- $d$ ),  $\delta$  166.51, 164.25, 142.24, 130.99, 130.86, 130.22, 129.81, 129.67, 129.29, 128.78, 127.91, 127.75, 127.16, 127.13, 127.06, 124.82, 123.12, 122.57, 52.75, 52.50. HRMS ( $m/z$ ): Calculated for  $\text{C}_{20}\text{H}_{16}\text{O}_4\text{H}^+$  ( $\text{MH}^+$ ): 321.1127, Found ( $\text{MH}^+$ ): 321.1125. Melting point: 115.3-115.4  $^\circ\text{C}$ .

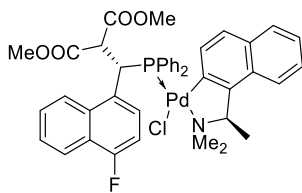


**Compound ( $R_N, S_P$ )-91d:**  $^1\text{H}$  NMR (400 MHz, Chloroform- $d$ ),  $\delta$  8.00-7.96 (m, 3H), 7.86 (d,  $J = 8.09$  Hz, 1H), 7.65 (d,  $J = 8.45$  Hz, 1H), 7.55-7.48 (m, 4H), 7.39-7.31 (m, 3H), 7.29-7.17 (m, 4H), 7.13 (d,  $J = 7.46$  Hz, 1H), 7.05 (t,  $J = 7.24$  Hz, 1H), 6.85 (t,  $J = 6.91$  Hz, 2H), 6.66 (d,  $J = 8.68$  Hz, 1H), 6.24-6.14 (m, 2H), 5.52 (t,  $J = 9.57$  Hz, 1H), 4.32 (p,  $J = 6.24, 6.22$  Hz, 1H), 3.71 (s, 3H), 3.14-3.12 (m, 6H), 2.75 (s, 3H), 2.64 (s, 3H), 2.11 (d,  $J = 6.37$  Hz, 3H).  $^{13}\text{C}$  NMR (100 MHz, Chloroform- $d$ ), 169.27, 168.31, 151.15, 148.05, 137.55, 137.42, 135.64, 135.55, 135.43, 134.23, 134.20, 133.70, 133.67, 132.45, 131.63, 131.57, 131.16,

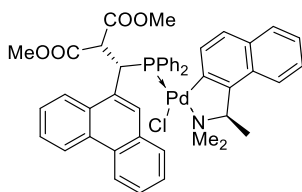
130.84, 130.07, 128.59, 128.41, 127.89, 127.78, 127.09, 126.99, 125.86, 125.52, 125.40, 125.12, 124.56, 124.10, 124.05, 123.99, 123.84, 123.24, 73.31, 56.24, 52.97, 52.14, 51.02, 48.29, 39.88, 22.81, 19.82.  $^{31}\text{P}\{^1\text{H}\}$  NMR (162 MHz, Chloroform-*d*),  $\delta$  47.11. HRMS (m/z): Calculated for  $\text{C}_{43}\text{H}_{43}\text{NO}_4\text{PClPdH}^+$  ( $\text{MH}^+$ ): 812.1735, Found ( $\text{MH}^+$ ): 812.1742. Melting point: 184.9-185.0 °C, decomposed.  $[\alpha]_{\text{D}} = -18.5$  (*c* 0.85, DCM).



**Compound ( $R_N, S_P$ )-91e:**  $^1\text{H}$  NMR (300 MHz, Chloroform-*d*),  $\delta$  8.11 (d,  $J = 8.03$  Hz, 1H), 8.04-8.02 (m, 2H), 7.84 (d,  $J = 8.36$  Hz, 1H), 7.63-7.60 (m, 2H), 7.47-7.44 (m, 3H), 7.33-7.18 (m, 7H), 7.00 (t,  $J = 7.19$  Hz, 1H), 6.80 (t,  $J = 7.10$  Hz, 2H), 6.63 (t,  $J = 7.82$  Hz, 2H), 6.21 (t,  $J = 7.49$  Hz, 1H), 6.00 (t,  $J = 10.58$  Hz, 1H), 5.58 (t,  $J = 10.75$  Hz, 1H), 4.29 (p,  $J = 6.40, 6.28$  Hz, 1H), 3.93 (s, 3H), 3.63 (s, 3H), 3.09 (s, 6H), 2.71 (s, 3H), 2.07 (d,  $J = 6.24$  Hz, 3H).  $^{13}\text{C}$  NMR (75 MHz, Chloroform-*d*),  $\delta$  169.28, 168.16 (d,  $J = 14.9$  Hz), 154.89 (d,  $J = 2.23$  Hz), 151.06, 147.84 (d,  $J = 2$  Hz), 137.22, 137.04, 135.56, 135.40, 135.24, 134.39, 134.35, 130.97, 130.71, 130.48, 129.87, 128.69, 128.46, 128.25, 127.78 (d,  $J = 10.64$  Hz), 126.92, 126.79, 125.26, 125.07, 124.04 (d,  $J = 5.04$  Hz), 124.49, 123.88 (d,  $J = 5.72$  Hz), 123.71, 123.56, 123.08, 121.65, 102.70, 73.16 (d,  $J = 2.90$  Hz), 56.28 (d,  $J = 10.06$  Hz), 55.42, 52.79, 52.02, 50.84, 48.18, 39.51 (d,  $J = 22.63$  Hz), 22.76.  $^{31}\text{P}\{^1\text{H}\}$  NMR (121 MHz, Chloroform-*d*) 48.11. HRMS (m/z): Calculated for  $\text{C}_{43}\text{H}_{43}\text{NO}_5\text{PClPdH}^+$  ( $\text{MH}^+$ ): 826.1680, Found ( $\text{MH}^+$ ): 826.1681. Melting point: 192.9-193.1 °C, decomposed.  $[\alpha]_{\text{D}} = +6276.8$  (*c* 0.85, DCM).

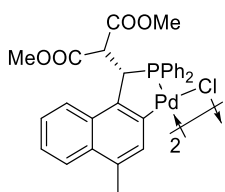


**Compound ( $R_N, S_P$ )-91f:**  $^1\text{H}$  NMR (400 MHz, Chloroform- $d$ ),  $\delta$  8.08-8.06 (m, 2H), 7.94 (t,  $J = 7.39$  Hz, 2H), 7.82-7.80 (m, 1H), 7.62 (d,  $J = 8.37$  Hz, 1H), 7.47-7.44 (m, 3H), 7.34-7.29 (m, 4H), 7.27-7.21 (m, 3H), 6.97 (dt,  $J = 8.21, 18.42$  Hz, 2H), 6.79 (t,  $J = 6.85$  Hz, 2H), 6.65 (d,  $J = 8.70$  Hz, 1H), 6.21 (dd,  $J = 6.52, 8.61$  Hz, 1H), 6.02 (t,  $J = 10.79$  Hz, 1H), 5.70 (s, 1H), 4.30 (p,  $J = 6.11, 6.14$  Hz, 1H), 3.63 (s, 3H), 3.14-3.09 (m, 6H), 2.71 (s, 3H), 2.06 (d,  $J = 6.35$  Hz, 3H).  $^{13}\text{C}$  NMR (100 MHz, Chloroform- $d$ ),  $\delta$  169.28, 168.15, 150.98, 147.99, 137.10, 136.97, 135.61, 135.50, 135.27, 135.15, 134.94, 131.49, 131.21, 130.86, 130.21, 129.34, 128.57, 128.39, 128.07, 127.97, 127.21, 127.12, 127.02, 125.67, 125.46, 124.11, 124.06, 123.93, 123.22, 120.47, 108.43, 108.22, 73.32, 56.20, 52.98, 52.23, 50.96, 48.33, 39.82, 22.96.  $^{31}\text{P}\{^1\text{H}\}$  NMR (162 MHz, Chloroform- $d$ ),  $\delta$  47.46.  $^{19}\text{F}\{^1\text{H}\}$  NMR (376 MHz, Chloroform- $d$ ),  $\delta$  -122.78. HRMS (m/z): Calculated for  $\text{C}_{42}\text{H}_{40}\text{NFO}_4\text{PCIPdH}^+$  ( $\text{MH}^+$ ): 814.1481, Found ( $\text{MH}^+$ ): 814.1505. Melting point: 184.4-184.6  $^\circ\text{C}$ , decomposed.  $[\alpha]_D = -2.0$  ( $c$  0.85, DCM).

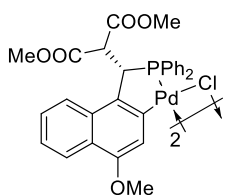


**Compound ( $R_N, S_P$ )-91g:**  $^1\text{H}$  NMR (400 MHz, Chloroform- $d$ ),  $\delta$  8.56 (dd,  $J = 8.11, 13.01$  Hz, 2H), 8.01-8.00 (m, 3H), 7.83 (s, 1H), 7.67-7.52 (m, 6H), 7.44 (dd,  $J = 6.06, 7.43$  Hz, 2H), 7.31-7.27 (m, 3H), 7.27-7.00 (m, 3H), 7.00 (t,  $J = 6.97$  Hz, 1H), 6.80 (t,  $J = 6.65$  Hz, 2H), 6.61 (d,  $J = 8.70$  Hz, 1H), 6.21-6.17 (m, 2H), 5.53 (s, 1H), 4.27 (p,  $J = 6.19, 6.19, 6.15, 6.15$  Hz, 1H), 3.69 (s, 3H), 3.12 (d,  $J = 3.33$  Hz, 3H), 3.05 (s, 3H), 2.73 (d,  $J = 1.04$  Hz, 3H), 1.98 (d,  $J = 6.32$  Hz, 3H).  $^{13}\text{C}$  NMR (100 MHz, Chloroform- $d$ ),  $\delta$  169.17, 168.26 (d,  $J = 14.1$  Hz),

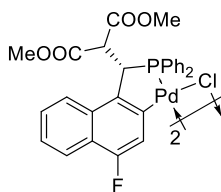
150.99, 148.08 (d,  $J = 1.87$  Hz), 137.54 (d,  $J = 14.3$  Hz), 135.55, 135.43, 132.41, 131.36 (d,  $J = 2.44$  Hz), 131.32, 130.84, 130.76 (d,  $J = 2.02$  Hz), 130.21 (d,  $J = 2.11$  Hz), 129.93, 128.77, 128.57, 128.42, 127.59 (d,  $J = 10.81$  Hz), 127.12 (d,  $J = 10.4$  Hz), 126.92, 126.64 (d,  $J = 16.12$  Hz), 126.03, 125.42, 124.86, 124.07 (d,  $J = 5.88$  Hz), 123.87, 123.23, 122.47 (d,  $J = 2.90$  Hz), 73.35 (d,  $J = 2.91$  Hz), 56.39 (d,  $J = 8.83$  Hz), 53.01, 52.19, 51.05 (d,  $J = 2.67$  Hz), 48.30, 39.77 (d,  $J = 22.36$  Hz), 22.82.  $^{31}\text{P}\{^1\text{H}\}$  NMR (162 MHz, Chloroform- $d$ ),  $\delta$  50.34. HRMS (m/z): Calculated for  $\text{C}_{46}\text{H}_{43}\text{NO}_4\text{PClPdH}^+$  ( $\text{MH}^+$ ): 846.1731, Found ( $\text{MH}^+$ ): 846.1767. Melting point: 167.6-168.2 °C, decomposed.  $[\alpha]_{\text{D}} = -170.5$  ( $c$  0.85, DCM).



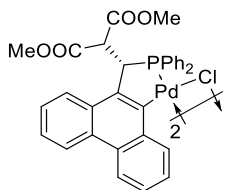
**Compound (S)-86d (there are two diastereomeric isomer: *trans*- and *cis*-):**  $^1\text{H}$  NMR (400 MHz, Dimethyl sulfoxide- $d_6$ ),  $\delta$  7.90-7.76 (m, 6H), 7.57-7.55 (m, 1H), 7.47-7.40 (m, 7H), 5.49 (dd,  $J = 9.87, 13.09$  Hz, 1H), 4.05 (s, 1H), 3.17 (s, 3H), 2.75 (s, 3H), 2.51 (s, 3H).  $^{13}\text{C}$  NMR (100 MHz, Dimethyl sulfoxide- $d_6$ ),  $\delta$  166.85, 166.78, 166.63, 138.41, 135.21, 135.14, 132.11, 132.02, 131.79, 131.46, 131.29, 130.83, 129.84, 129.63, 129.18, 128.05, 128.05, 127.98, 127.58, 127.18, 125.47, 124.96, 124.51, 79.14, 55.35, 55.27, 54.87, 52.24, 51.92, 50.82, 47.33, 46.98, 46.30, 19.33.  $^{31}\text{P}\{^1\text{H}\}$  NMR (162 MHz, Dimethyl sulfoxide- $d_6$ ), 64.27, 58.30. HRMS (m/z): Calculated for  $\text{C}_{58}\text{H}_{52}\text{O}_8\text{P}_2\text{Cl}_2\text{Pd}_2\text{H}^+$  ( $\text{MH}^+$ ): 1223.0666, Found ( $\text{MH}^+$ ): 1223.0684. Melting point: 186.3-186.6 °C, decomposed.  $[\alpha]_{\text{D}} = +224.1$  ( $c$  0.85, DCM).



**Compound (S)-86e (there are two diastereomeric isomer: *trans*- and *cis*-):**  $^1\text{H}$  NMR (400 MHz, Chloroform-*d*),  $\delta$  8.17 (dd,  $J = 0.89$ , 8.27 Hz, 3H), 7.99-7.94 (m, 4H), 7.90-7.85 (t,  $J = 9.67$  Hz, 9H), 7.79-7.74 (m, 2H), 7.55 (s, 1H), 7.45-7.21 (m, 9H), 7.36 (s, 9H), 7.29 (d,  $J = 6.80$  Hz, 4H), 7.23 (t,  $J = 7.10$  Hz, 4H), 5.60 (dd,  $J = 10.34$ , 13.90 Hz, 2H), 5.63-5.29 (m, 1H), 4.31 (dd,  $J = 10.03$ , 17.16 Hz, 2H), 4.34-3.77 (m, 1H), 3.99 (s, 3H), 3.77 (s, 6H), 3.20 (s, 3H), 3.14 (s, 6H), 2.84 (s, 3H), 2.80 (s, 6H).  $^{13}\text{C}$  NMR (100 MHz, Chloroform-*d*),  $\delta$  168.05, 167.83, 153.91, 152.43, 136.44, 136.32, 136.06, 132.88, 132.76, 132.47, 131.67, 131.24, 129.17, 129.06, 128.28, 128.21, 128.10, 127.64, 126.45, 125.12, 124.97, 124.73, 124.13, 122.62, 113.48, 112.40, 55.44, 52.36, 47.67.  $^{31}\text{P}\{^1\text{H}\}$  NMR (162 MHz, Chloroform-*d*), 62.90, 61.54. HRMS (m/z): Calculated for  $\text{C}_{58}\text{H}_{52}\text{P}_2\text{Cl}_2\text{O}_{10}\text{Pd}_2\text{H}^+$  ( $\text{MH}^+$ ): 1255.0551, Found ( $\text{MH}^+$ ): 1255.0565. Melting point: 172.6-172.9 °C, decomposed.  $[\alpha]_{\text{D}} = +439.2$  ( $c$  0.85, DCM).

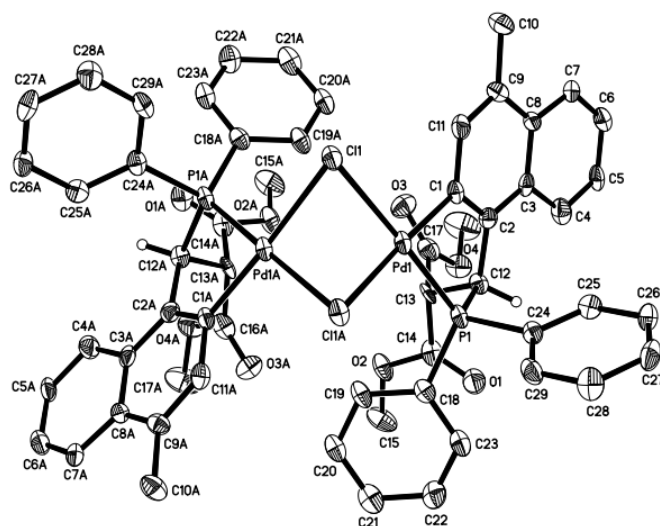


**Compound (S)-86f (there are two diastereomeric isomer: *trans*- and *cis*-):**  $^1\text{H}$  NMR (400 MHz, Chloroform-*d*),  $\delta$  7.87 (m, 6H), 7.62 (m, 1H), 7.45 (m, 8H), 5.55 (dd,  $J = 16.75$ , 23.59 Hz, 1H), 4.30 (dd,  $J = 9.92$ , 16.75 Hz, 1H), 3.22 (s, 3H), 2.82 (s, 3H).  $^{13}\text{C}$  NMR (100 MHz, Chloroform-*d*),  $\delta$  167.87, 167.67, 153.07, 136.20, 136.07, 132.64, 132.53, 132.16, 131.40, 130.92, 129.31, 129.20, 128.62, 128.49, 128.38, 127.42, 127.01, 126.89, 125.22, 125.03, 122.73, 121.29, 117.91, 55.44, 52.53, 52.35, 47.34.  $^{31}\text{P}\{^1\text{H}\}$  NMR (162 MHz, Chloroform-*d*), 62.35, 61.91.  $^{19}\text{F}\{^1\text{H}\}$  (376 MHz, Chloroform-*d*), -122.75, -123.30. HRMS (m/z): Calculated for  $\text{C}_{56}\text{H}_{46}\text{O}_8\text{P}_2\text{Cl}_2\text{F}_2\text{Pd}_2\text{H}^+$  ( $\text{MH}^+$ ): 1231.0165, Found ( $\text{MH}^+$ ): 1231.0175. Melting point: 1175.4-175.9 °C, decomposed.  $[\alpha]_{\text{D}} = +236.3$  ( $c$  0.85, DCM).



**Compound (S)-86g (there are two diastereomeric isomer: *trans*- and *cis*-):**  $^1\text{H}$  NMR (400 MHz, Chloroform-*d*),  $\delta$  9.40 (s, 1H), 8.53 (dd,  $J = 2.78, 6.47$  Hz, 1H), 8.40-8.35 (m, 1H), 8.04-7.97 (m, 3H), 7.73-7.68 (m, 2H), 7.61-7.10 (m, 10H), 5.57 (dt,  $J = 7.65, 15.03$  Hz, 1H), 5.07-5.00 (m, 1H), 3.42-3.31 (m, 3H), 2.91 (s, 3H).  $^{13}\text{C}$  NMR (100 MHz, Chloroform-*d*),  $\delta$  168.45, 168.23, 138.02, 137.84, 136.96, 135.18, 135.12, 135.07, 133.19, 132.45, 132.33, 131.73, 131.13, 130.17, 130.11, 129.41, 129.22, 129.03, 128.92, 128.44, 128.33, 126.65, 126.32, 125.56, 125.43, 124.98, 123.10, 121.93, 55.25, 52.57, 52.46, 49.80.  $^{31}\text{P}\{^1\text{H}\}$  NMR (162 MHz, Chloroform-*d*), 58.30, 57.48. HRMS ( $m/z$ ): Calculated for  $\text{C}_{64}\text{H}_{52}\text{O}_8\text{P}_2\text{Cl}_2\text{Pd}_2\text{H}^+$  ( $\text{MH}^+$ ): 1295.0666, Found ( $\text{MH}^+$ ): 1295.0649. Melting point: 195.2-195.4  $^\circ\text{C}$ , decomposed.  $[\alpha]_{\text{D}} = +4247.0$  ( $c$  0.85, DCM).

### Crystallographic data



CCDC 1835263

**Table 24:** Data collection and structure refinement for complex (S)-**86d**

<b>Chemical formula</b>	C <sub>30</sub> H <sub>28</sub> Cl <sub>3</sub> O <sub>4</sub> PPd	
<b>Formula weight</b>	696.24 g/mol	
<b>Temperature</b>	100(2) K	
<b>Wavelength</b>	0.71073 Å	
<b>Crystal size</b>	0.040 x 0.060 x 0.100 mm	
<b>Crystal habit</b>	yellow block	
<b>Crystal system</b>	Monoclinic	
<b>Space group</b>	C 1 2 1	
<b>Unit cell dimensions</b>	a = 17.5319(10) Å	α = 90°
	b = 13.5222(7) Å	β = 101.162(2)°
	c = 13.0323(8) Å	γ = 90°
<b>Volume</b>	3031.1(3) Å <sup>3</sup>	
<b>Z</b>	4	
<b>Density (calculated)</b>	1.526 g/cm <sup>3</sup>	
<b>Absorption coefficient</b>	0.963 mm <sup>-1</sup>	
<b>F(000)</b>	1408	
<b>Theta range for data collection</b>	2.34 to 31.03°	
<b>Index ranges</b>	-25 ≤ h ≤ 25, -19 ≤ k ≤ 19, -18 ≤ l ≤ 18	
<b>Reflections collected</b>	29565	
<b>Independent reflections</b>	9397 [R(int) = 0.1175]	
<b>Coverage of independent reflections</b>	99.6%	
<b>Absorption correction</b>	Multi-Scan	
<b>Max. and min. transmission</b>	0.9630 and 0.9100	
<b>Structure solution technique</b>	direct methods	
<b>Structure solution program</b>	SHELXT 2014/5 (Sheldrick, 2014)	
<b>Refinement method</b>	Full-matrix least-squares on F <sup>2</sup>	
<b>Refinement program</b>	SHELXL-2016/6 (Sheldrick, 2016)	
<b>Function minimized</b>	Σ w(F <sub>o</sub> <sup>2</sup> - F <sub>c</sub> <sup>2</sup> ) <sup>2</sup>	
<b>Data / restraints / parameters</b>	9397 / 187 / 412	

<b>Goodness-of-fit on <math>F^2</math></b>	1.028	
<b>Final R indices</b>	6165 data; $I > 2\sigma(I)$	R1 = 0.0721, wR2 = 0.1489
	all data	R1 = 0.1297, wR2 = 0.1818
<b>Weighting scheme</b>	$w = 1/[\sigma^2(F_o^2) + (0.0757P)^2 + 3.3868P]$ where $P = (F_o^2 + 2F_c^2)/3$	
<b>Absolute structure parameter</b>	0.00(3)	
<b>Largest diff. peak and hole</b>	1.454 and -1.665 $e\text{\AA}^{-3}$	
<b>R.M.S. deviation from mean</b>	0.174 $e\text{\AA}^{-3}$	

**Table 25:** Bond lengths ( $\text{\AA}$ ) for (*S*)-**86d**

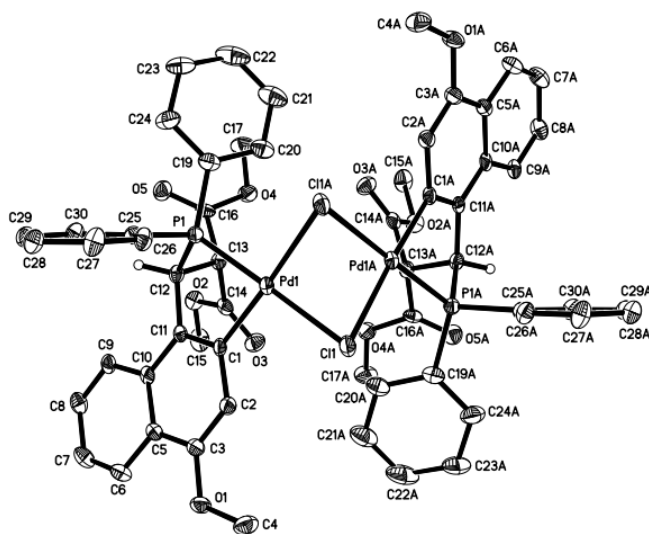
C1-C2	1.382(13)	C1-C11	1.421(14)
C1-Pd1	2.015(9)	C2-C3	1.407(14)
C2-C12	1.511(14)	C3-C8	1.446(14)
C3-C4	1.459(16)	C4-C5	1.370(14)
C5-C6	1.394(15)	C6-C7	1.375(15)
C7-C8	1.394(14)	C8-C9	1.419(14)
C9-C11	1.382(14)	C9-C10	1.491(14)
C12-C13	1.575(13)	C12-P1	1.834(10)
C13-C16	1.503(15)	C13-C14	1.525(15)
C14-O1	1.197(13)	C14-O2	1.329(12)
C15-O2	1.439(13)	C16-O3	1.199(13)
C16-O4	1.321(13)	C17-O4	1.489(14)
C18-C23	1.390(15)	C18-C19	1.395(14)
C18-P1	1.812(10)	C19-C20	1.380(15)
C20-C21	1.384(17)	C21-C22	1.414(16)
C22-C23	1.339(15)	C24-C25	1.400(13)
C24-C29	1.405(15)	C24-P1	1.811(10)
C25-C26	1.388(14)	C26-C27	1.383(15)
C27-C28	1.400(16)	C28-C29	1.369(16)
C30-Cl3	1.80(2)	C30-Cl2	1.82(2)

C30A-C12A	1.79(3)	C30A-C13A	1.80(3)
C14-C33	1.74(3)	C15-C33	1.75(3)
C11-Pd1	2.422(3)	C11-Pd1	2.443(2)
P1-Pd1	2.192(3)	Pd1-Pd1	2.9313(13)

**Table 26:** Bond angles (°) for (*S*)-**86d**

C2-C1-C11	118.1(9)	C2-C1-Pd1	122.7(8)
C11-C1-Pd1	119.1(7)	C1-C2-C3	121.4(9)
C1-C2-C12	117.0(9)	C3-C2-C12	121.6(9)
C2-C3-C8	119.6(9)	C2-C3-C4	122.0(10)
C8-C3-C4	118.3(9)	C5-C4-C3	118.9(11)
C4-C5-C6	122.1(11)	C7-C6-C5	120.1(10)
C6-C7-C8	121.7(10)	C7-C8-C9	122.1(9)
C7-C8-C3	118.9(9)	C9-C8-C3	119.0(9)
C11-C9-C8	118.8(9)	C11-C9-C10	120.9(9)
C8-C9-C10	120.3(9)	C9-C11-C1	123.1(9)
C2-C12-C13	111.8(8)	C2-C12-P1	103.3(6)
C13-C12-P1	110.8(6)	C16-C13-C14	110.3(8)
C16-C13-C12	112.2(8)	C14-C13-C12	110.7(8)
O1-C14-O2	124.1(10)	O1-C14-C13	125.4(10)
O2-C14-C13	110.6(9)	O3-C16-O4	125.2(11)
O3-C16-C13	123.2(10)	O4-C16-C13	111.6(10)
C23-C18-C19	119.4(10)	C23-C18-P1	121.7(8)
C19-C18-P1	118.7(8)	C20-C19-C18	119.9(11)
C19-C20-C21	120.5(11)	C20-C21-C22	118.5(11)
C23-C22-C21	121.0(11)	C22-C23-C18	120.7(10)
C25-C24-C29	119.6(9)	C25-C24-P1	121.9(8)
C29-C24-P1	118.3(7)	C26-C25-C24	119.4(9)
C27-C26-C25	120.5(10)	C26-C27-C28	120.2(10)
C29-C28-C27	119.8(10)	C28-C29-C24	120.5(10)

C13-C30-C12	109.1(13)	C12A-C30A-C13A	111.5(19)
C14-C33-C15	124.(2)	Pd1-C11-Pd1	74.09(7)
C14-O2-C15	116.2(10)	C16-O4-C17	114.3(10)
C24-P1-C18	105.1(5)	C24-P1-C12	108.1(5)
C18-P1-C12	109.0(4)	C24-P1-Pd1	111.7(4)
C18-P1-Pd1	118.5(3)	C12-P1-Pd1	104.0(4)
C1-Pd1-P1	80.5(3)	C1-Pd1-C11	99.0(3)
P1-Pd1-C11	175.49(10)	C1-Pd1-C11	177.0(3)
P1-Pd1-C11	97.24(9)	C11-Pd1-C11	83.46(11)
C1-Pd1-Pd1	130.3(3)	P1-Pd1-Pd1	123.84(7)
C11-Pd1-Pd1	53.28(6)	C11-Pd1-Pd1	52.63(6)



CCDC 1835218

**Table 27:** Data collection and structure refinement for complex (S)-86e

<b>Chemical formula</b>	$C_{58}H_{52}Cl_2O_{10}P_2Pd_2$
<b>Formula weight</b>	1254.63 g/mol
<b>Temperature</b>	100(2) K
<b>Wavelength</b>	0.71073 Å

<b>Crystal size</b>	0.100 x 0.120 x 0.320 mm	
<b>Crystal habit</b>	yellow block	
<b>Crystal system</b>	monoclinic	
<b>Space group</b>	C 1 2 1	
<b>Unit cell dimensions</b>	a = 23.6895(8) Å	$\alpha = 90^\circ$
	b = 9.6156(3) Å	$\beta = 117.2564(13)^\circ$
	c = 13.0926(5) Å	$\gamma = 90^\circ$
<b>Volume</b>	2651.21(16) Å <sup>3</sup>	
<b>Z</b>	2	
<b>Density (calculated)</b>	1.572 g/cm <sup>3</sup>	
<b>Absorption coefficient</b>	0.899 mm <sup>-1</sup>	
<b>F(000)</b>	1272	
<b>Theta range for data collection</b>	2.33 to 31.01°	
<b>Index ranges</b>	-34 ≤ h ≤ 30, -13 ≤ k ≤ 13, -18 ≤ l ≤ 18	
<b>Reflections collected</b>	16907	
<b>Independent reflections</b>	8340 [R(int) = 0.0651]	
<b>Coverage of independent reflections</b>	99.3%	
<b>Absorption correction</b>	Multi-Scan	
<b>Max. and min. transmission</b>	0.9150 and 0.7620	
<b>Structure solution technique</b>	direct methods	
<b>Structure solution program</b>	XT, VERSION 2014/5	
<b>Refinement method</b>	Full-matrix least-squares on F <sup>2</sup>	
<b>Refinement program</b>	SHELXL-2016/6 (Sheldrick, 2016)	
<b>Function minimized</b>	$\Sigma w(F_o^2 - F_c^2)^2$	
<b>Data / restraints / parameters</b>	8340 / 1 / 337	
<b>Goodness-of-fit on F<sup>2</sup></b>	1.022	
<b><math>\Delta/\sigma_{\max}</math></b>	0.001	
<b>Final R indices</b>	6757 data; I > 2σ(I)	R1 = 0.0537, wR2 = 0.0929
	all data	R1 = 0.0761, wR2 = 0.1058

<b>Weighting scheme</b>	$w=1/[\sigma^2(F_o^2)+(0.0279P)^2]$ where $P=(F_o^2+2F_c^2)/3$
<b>Absolute structure parameter</b>	-0.02(3)
<b>Largest diff. peak and hole</b>	1.337 and -1.219 eÅ <sup>-3</sup>
<b>R.M.S. deviation from mean</b>	0.138 eÅ <sup>-3</sup>

**Table 28:** Bond lengths (Å) for complex (*S*)-**86e**

C1-C11	1.391(8)	C1-C2	1.414(8)
C1-Pd1	2.010(6)	C2-C3	1.376(8)
C2-H2	0.95	C3-O1	1.360(7)
C3-C5	1.425(9)	C4-O1	1.436(8)
C4-H4A	0.98	C4-H4B	0.98
C4-H4C	0.98	C5-C10	1.418(9)
C5-C6	1.428(9)	C6-C7	1.356(9)
C6-H6	0.95	C7-C8	1.401(10)
C7-H7	0.95	C8-C9	1.355(9)
C8-H8	0.95	C9-C10	1.424(9)
C9-H9	0.95	C10-C11	1.431(9)
C11-C12	1.512(8)	C12-C13	1.559(8)
C12-P1	1.845(6)	C12-H12	1.0
C13-C16	1.519(8)	C13-C14	1.524(8)
C13-H13	1.0	C14-O3	1.203(7)
C14-O2	1.335(7)	C15-O2	1.457(8)
C15-H15A	0.98	C15-H15B	0.98
C15-H15C	0.98	C16-O5	1.202(7)
C16-O4	1.331(7)	C17-O4	1.432(8)
C17-H17A	0.98	C17-H17B	0.98
C17-H17C	0.98	C19-C24	1.380(9)
C19-C20	1.402(9)	C19-P1	1.804(7)
C20-C21	1.381(10)	C20-H20	0.95
C21-C22	1.369(12)	C21-H21	0.95
C22-C23	1.379(12)	C22-H22	0.95
C23-C24	1.405(10)	C23-H23	0.95
C24-H24	0.95	C25-C30	1.403(8)
C25-C26	1.408(10)	C25-P1	1.799(7)

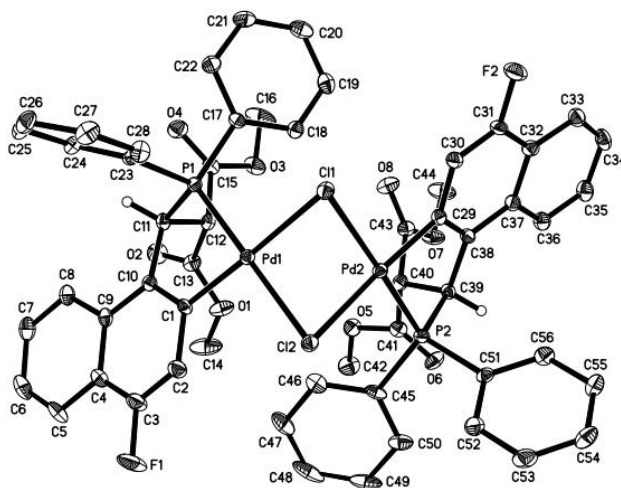
C26-C27	1.374(9)	C26-H26	0.95
C27-C28	1.384(9)	C27-H27	0.95
C28-C29	1.380(9)	C28-H28	0.95
C29-C30	1.387(9)	C29-H29	0.95
C30-H30	0.95	Cl1-Pd1	2.4170(16)
Cl1-Pd1	2.4359(16)	P1-Pd1	2.1921(16)
Pd1-Pd1	2.9677(8)		

**Table 29:** Bond angles (°) for complex (S)-**86e**

C11-C1-C2	119.1(6)	C11-C1-Pd1	121.6(4)
C2-C1-Pd1	119.2(4)	C3-C2-C1	121.2(5)
C3-C2-H2	119.4	C1-C2-H2	119.4
O1-C3-C2	124.4(6)	O1-C3-C5	115.1(5)
C2-C3-C5	120.5(6)	O1-C4-H4A	109.5
O1-C4-H4B	109.5	H4A-C4-H4B	109.5
O1-C4-H4C	109.5	H4A-C4-H4C	109.5
H4B-C4-H4C	109.5	C10-C5-C3	119.3(5)
C10-C5-C6	119.7(6)	C3-C5-C6	121.0(6)
C7-C6-C5	120.4(6)	C7-C6-H6	119.8
C5-C6-H6	119.8	C6-C7-C8	120.3(6)
C6-C7-H7	119.8	C8-C7-H7	119.8
C9-C8-C7	120.7(6)	C9-C8-H8	119.7
C7-C8-H8	119.7	C8-C9-C10	121.7(6)
C8-C9-H9	119.2	C10-C9-H9	119.2
C5-C10-C9	117.2(6)	C5-C10-C11	118.7(5)
C9-C10-C11	124.1(6)	C1-C11-C10	121.1(6)
C1-C11-C12	117.5(5)	C10-C11-C12	121.3(5)
C11-C12-C13	112.4(5)	C11-C12-P1	101.2(4)
C13-C12-P1	109.3(4)	C11-C12-H12	111.2
C13-C12-H12	111.2	P1-C12-H12	111.2
C16-C13-C14	111.2(5)	C16-C13-C12	112.1(5)

C14-C13-C12	112.4(5)	C16-C13-H13	107.0
C14-C13-H13	107.0	C12-C13-H13	107.0
O3-C14-O2	125.5(6)	O3-C14-C13	123.2(6)
O2-C14-C13	111.3(5)	O2-C15-H15A	109.5
O2-C15-H15B	109.5	H15A-C15-H15B	109.5
O2-C15-H15C	109.5	H15A-C15-H15C	109.5
H15B-C15-H15C	109.5	O5-C16-O4	125.4(6)
O5-C16-C13	124.9(6)	O4-C16-C13	109.6(5)
O4-C17-H17A	109.5	O4-C17-H17B	109.5
H17A-C17-H17B	109.5	O4-C17-H17C	109.5
H17A-C17-H17C	109.5	H17B-C17-H17C	109.5
C24-C19-C20	119.6(6)	C24-C19-P1	121.9(6)
C20-C19-P1	118.4(5)	C21-C20-C19	120.1(7)
C21-C20-H20	119.9	C19-C20-H20	119.9
C22-C21-C20	120.0(8)	C22-C21-H21	120.0
C20-C21-H21	120.0	C21-C22-C23	120.9(8)
C21-C22-H22	119.5	C23-C22-H22	119.5
C22-C23-C24	119.6(8)	C22-C23-H23	120.2
C24-C23-H23	120.2	C19-C24-C23	119.7(7)
C19-C24-H24	120.2	C23-C24-H24	120.2
C30-C25-C26	118.1(6)	C30-C25-P1	125.2(6)
C26-C25-P1	116.7(4)	C27-C26-C25	121.1(6)
C27-C26-H26	119.5	C25-C26-H26	119.5
C26-C27-C28	119.9(7)	C26-C27-H27	120.0
C28-C27-H27	120.0	C29-C28-C27	120.3(6)
C29-C28-H28	119.9	C27-C28-H28	119.9
C28-C29-C30	120.4(6)	C28-C29-H29	119.8
C30-C29-H29	119.8	C29-C30-C25	120.3(6)
C29-C30-H30	119.9	C25-C30-H30	119.9
Pd1-C11-Pd1	75.40(5)	C3-O1-C4	117.4(5)

C14-O2-C15	113.7(5)	C16-O4-C17	117.1(5)
C25-P1-C19	107.4(3)	C25-P1-C12	108.0(3)
C19-P1-C12	110.1(3)	C25-P1-Pd1	110.0(2)
C19-P1-Pd1	117.8(2)	C12-P1-Pd1	103.2(2)
C1-Pd1-P1	79.98(17)	C1-Pd1-Cl1	98.76(17)
P1-Pd1-Cl1	178.68(7)	C1-Pd1-Cl1	176.97(17)
P1-Pd1-Cl1	97.10(6)	Cl1-Pd1-Cl1	84.17(7)
C1-Pd1-Pd1	130.56(17)	P1-Pd1-Pd1	128.04(5)
Cl1-Pd1-Pd1	52.59(4)	Cl1-Pd1-Pd1	52.01(4)



CCDC 1835219

**Table 30:** Data collection and structure refinement for complex (S)-86f

<b>Chemical formula</b>	$C_{57}H_{48}Cl_4F_2O_8P_2Pd_2$
<b>Formula weight</b>	1315.49 g/mol
<b>Temperature</b>	100(2) K
<b>Wavelength</b>	0.71073 Å
<b>Crystal size</b>	0.100 x 0.180 x 0.200 mm
<b>Crystal habit</b>	orange block
<b>Crystal system</b>	triclinic

<b>Space group</b>	P 1
<b>Unit cell dimensions</b>	a = 11.0362(3) Å $\alpha = 103.8454(9)^\circ$ b = 11.3363(3) Å $\beta = 110.5773(10)^\circ$ c = 12.8691(4) Å $\gamma = 108.0924(9)^\circ$
<b>Volume</b>	1318.39(7) Å <sup>3</sup>
<b>Z</b>	1
<b>Density (calculated)</b>	1.657 g/cm <sup>3</sup>
<b>Absorption coefficient</b>	1.009 mm <sup>-1</sup>
<b>F(000)</b>	662
<b>Theta range for data collection</b>	2.19 to 35.66°
<b>Index ranges</b>	-18<=h<=18, -18<=k<=18, -21<=l<=21
<b>Reflections collected</b>	78198
<b>Independent reflections</b>	24161 [R(int) = 0.0724]
<b>Coverage of independent reflections</b>	99.5%
<b>Absorption correction</b>	Multi-Scan
<b>Max. and min. transmission</b>	0.9060 and 0.8240
<b>Structure solution technique</b>	direct methods
<b>Structure solution program</b>	XT, VERSION 2014/5
<b>Refinement method</b>	Full-matrix least-squares on F <sup>2</sup>
<b>Refinement program</b>	SHELXL-2016/6 (Sheldrick, 2016)
<b>Function minimized</b>	$\Sigma w(F_o^2 - F_c^2)^2$
<b>Data / restraints / parameters</b>	24161 / 3 / 680
<b>Goodness-of-fit on F<sup>2</sup></b>	1.023
<b>Final R indices</b>	18914 data; I>2 $\sigma$ (I)    R1 = 0.0478, wR2 = 0.0805
	all data    R1 = 0.0799, wR2 = 0.0960
<b>Weighting scheme</b>	w=1/[ $\sigma^2(F_o^2)+(0.0336P)^2+0.1723P$ ] where P=(F <sub>o</sub> <sup>2</sup> +2F <sub>c</sub> <sup>2</sup> )/3
<b>Absolute structure parameter</b>	-0.029(10)
<b>Largest diff. peak and hole</b>	1.442 and -1.277 eÅ <sup>-3</sup>

**R.M.S. deviation from mean**0.155 eÅ<sup>-3</sup>**Table 31:** Bond lengths (Å) for complex (S)-**86f**

Pd1-C1	2.001(5)	Pd1-P1	2.1926(12)
Pd1-Cl1	2.4288(12)	Pd1-Cl2	2.4308(11)
Pd1-Pd2	2.9188(4)	Pd2-C29	2.005(5)
Pd2-P2	2.1900(12)	Pd2-Cl2	2.4373(11)
Pd2-Cl1	2.4454(11)	C1-C10	1.391(6)
C1-C2	1.426(6)	C2-C3	1.357(7)
C2-H2	0.95	C3-F1	1.354(6)
C3-C4	1.403(7)	C4-C5	1.418(7)
C4-C9	1.427(7)	C5-C6	1.361(8)
C5-H5	0.95	C6-C7	1.412(8)
C6-H6	0.95	C7-C8	1.381(7)
C7-H7	0.95	C8-C9	1.414(7)
C8-H8	0.95	C9-C10	1.434(6)
C10-C11	1.516(7)	C11-C12	1.547(6)
C11-P1	1.846(5)	C11-H11	1.0
C12-C13	1.520(6)	C12-C15	1.532(6)
C12-H12	1.0	C13-O2	1.195(6)
C13-O1	1.332(6)	C14-O1	1.456(7)
C14-H14A	0.98	C14-H14B	0.98
C14-H14C	0.98	C15-O4	1.195(6)
C15-O3	1.339(5)	C16-O3	1.452(6)
C16-H16A	0.98	C16-H16B	0.98
C16-H16C	0.98	C17-C22	1.389(6)
C17-C18	1.397(6)	C17-P1	1.814(4)
C18-C19	1.394(7)	C18-H18	0.95
C19-C20	1.372(7)	C19-H19	0.95
C20-C21	1.388(8)	C20-H20	0.95
C21-C22	1.383(7)	C21-H21	0.95

C22-H22	0.95	C23-C24	1.389(7)
C23-C28	1.402(7)	C23-P1	1.812(5)
C24-C25	1.384(6)	C24-H24	0.95
C25-C26	1.388(7)	C25-H25	0.95
C26-C27	1.386(7)	C26-H26	0.95
C27-C28	1.393(7)	C27-H27	0.95
C28-H28	0.95	C29-C38	1.394(6)
C29-C30	1.413(6)	C30-C31	1.356(7)
C30-H30	0.95	C31-F2	1.358(5)
C31-C32	1.410(6)	C32-C33	1.411(7)
C32-C37	1.434(7)	C33-C34	1.364(7)
C33-H33	0.95	C34-C35	1.406(7)
C34-H34	0.95	C35-C36	1.368(7)
C35-H35	0.95	C36-C37	1.419(6)
C36-H36	0.95	C37-C38	1.428(6)
C38-C39	1.510(6)	C39-C40	1.564(6)
C39-P2	1.847(4)	C39-H39	1.0
C40-C41	1.525(6)	C40-C43	1.526(7)
C40-H40	1.0	C41-O6	1.202(6)
C41-O5	1.329(6)	C42-O5	1.459(6)
C42-H42A	0.98	C42-H42B	0.98
C42-H42C	0.98	C43-O8	1.195(6)
C43-O7	1.333(5)	C44-O7	1.446(6)
C44-H44A	0.98	C44-H44B	0.98
C44-H44C	0.98	C45-C46	1.393(7)
C45-C50	1.398(7)	C45-P2	1.807(5)
C46-C47	1.397(7)	C46-H46	0.95
C47-C48	1.372(9)	C47-H47	0.95
C48-C49	1.381(9)	C48-H48	0.95
C49-C50	1.392(8)	C49-H49	0.95

C50-H50	0.95	C51-C56	1.389(7)
C51-C52	1.406(7)	C51-P2	1.804(5)
C52-C53	1.385(7)	C52-H52	0.95
C53-C54	1.387(8)	C53-H53	0.95
C54-C55	1.382(7)	C54-H54	0.95
C55-C56	1.385(7)	C55-H55	0.95
C56-H56	0.95	C57-Cl3	1.759(6)
C57-Cl4	1.767(6)	C57-H57A	0.99
C57-H57B	0.99		

**Table 32:** Bond angles (°) for complex (S)-**86f**

C1-Pd1-P1	80.70(13)	C1-Pd1-Cl1	178.16(13)
P1-Pd1-Cl1	97.47(4)	C1-Pd1-Cl2	98.26(13)
P1-Pd1-Cl2	177.64(4)	Cl1-Pd1-Cl2	83.57(4)
C1-Pd1-Pd2	127.83(13)	P1-Pd1-Pd2	125.82(3)
Cl1-Pd1-Pd2	53.47(3)	Cl2-Pd1-Pd2	53.26(3)
C29-Pd2-P2	80.81(13)	C29-Pd2-Cl2	176.66(14)
P2-Pd2-Cl2	97.39(4)	C29-Pd2-Cl1	98.90(13)
P2-Pd2-Cl1	176.13(5)	Cl2-Pd2-Cl1	83.09(4)
C29-Pd2-Pd1	130.27(13)	P2-Pd2-Pd1	124.46(3)
Cl2-Pd2-Pd1	53.06(3)	Cl1-Pd2-Pd1	52.95(3)
C10-C1-C2	119.2(4)	C10-C1-Pd1	123.2(3)
C2-C1-Pd1	117.6(3)	C3-C2-C1	119.1(5)
C3-C2-H2	120.5	C1-C2-H2	120.5
F1-C3-C2	118.6(5)	F1-C3-C4	117.3(4)
C2-C3-C4	124.2(5)	C3-C4-C5	122.0(5)
C3-C4-C9	117.6(4)	C5-C4-C9	120.4(5)
C6-C5-C4	120.4(5)	C6-C5-H5	119.8
C4-C5-H5	119.8	C5-C6-C7	120.1(5)
C5-C6-H6	119.9	C7-C6-H6	119.9

C8-C7-C6	120.4(5)	C8-C7-H7	119.8
C6-C7-H7	119.8	C7-C8-C9	121.2(5)
C7-C8-H8	119.4	C9-C8-H8	119.4
C8-C9-C4	117.4(4)	C8-C9-C10	124.0(4)
C4-C9-C10	118.6(4)	C1-C10-C9	121.1(4)
C1-C10-C11	116.7(4)	C9-C10-C11	122.1(4)
C10-C11-C12	112.0(4)	C10-C11-P1	103.0(3)
C12-C11-P1	109.2(3)	C10-C11-H11	110.8
C12-C11-H11	110.8	P1-C11-H11	110.8
C13-C12-C15	105.1(4)	C13-C12-C11	110.8(4)
C15-C12-C11	112.0(4)	C13-C12-H12	109.6
C15-C12-H12	109.6	C11-C12-H12	109.6
O2-C13-O1	124.9(5)	O2-C13-C12	123.1(4)
O1-C13-C12	112.0(4)	O1-C14-H14A	109.5
O1-C14-H14B	109.5	H14A-C14-H14B	109.5
O1-C14-H14C	109.5	H14A-C14-H14C	109.5
H14B-C14-H14C	109.5	O4-C15-O3	125.3(4)
O4-C15-C12	125.2(4)	O3-C15-C12	109.5(4)
O3-C16-H16A	109.5	O3-C16-H16B	109.5
H16A-C16-H16B	109.5	O3-C16-H16C	109.5
H16A-C16-H16C	109.5	H16B-C16-H16C	109.5
C22-C17-C18	119.9(4)	C22-C17-P1	122.1(3)
C18-C17-P1	118.0(3)	C17-C18-C19	119.2(4)
C17-C18-H18	120.4	C19-C18-H18	120.4
C20-C19-C18	120.6(5)	C20-C19-H19	119.7
C18-C19-H19	119.7	C19-C20-C21	120.1(5)
C19-C20-H20	119.9	C21-C20-H20	119.9
C22-C21-C20	120.1(5)	C22-C21-H21	120.0
C20-C21-H21	120.0	C21-C22-C17	120.1(4)
C21-C22-H22	119.9	C17-C22-H22	119.9

C24-C23-C28	119.2(4)	C24-C23-P1	124.1(4)
C28-C23-P1	116.7(4)	C25-C24-C23	120.2(5)
C25-C24-H24	119.9	C23-C24-H24	119.9
C24-C25-C26	120.7(5)	C24-C25-H25	119.7
C26-C25-H25	119.7	C25-C26-C27	119.7(4)
C25-C26-H26	120.1	C27-C26-H26	120.1
C26-C27-C28	119.9(5)	C26-C27-H27	120.1
C28-C27-H27	120.1	C27-C28-C23	120.3(5)
C27-C28-H28	119.9	C23-C28-H28	119.9
C38-C29-C30	118.7(4)	C38-C29-Pd2	122.6(3)
C30-C29-Pd2	118.4(3)	C31-C30-C29	120.0(4)
C31-C30-H30	120.0	C29-C30-H30	120.0
F2-C31-C30	119.3(4)	F2-C31-C32	116.7(4)
C30-C31-C32	123.9(4)	C33-C32-C31	123.4(4)
C33-C32-C37	119.8(4)	C31-C32-C37	116.7(4)
C34-C33-C32	120.8(5)	C34-C33-H33	119.6
C32-C33-H33	119.6	C33-C34-C35	119.8(4)
C33-C34-H34	120.1	C35-C34-H34	120.1
C36-C35-C34	121.1(5)	C36-C35-H35	119.4
C34-C35-H35	119.4	C35-C36-C37	120.9(5)
C35-C36-H36	119.6	C37-C36-H36	119.6
C36-C37-C38	123.4(4)	C36-C37-C32	117.5(4)
C38-C37-C32	119.1(4)	C29-C38-C37	121.4(4)
C29-C38-C39	117.7(4)	C37-C38-C39	120.9(4)
C38-C39-C40	113.4(4)	C38-C39-P2	102.3(3)
C40-C39-P2	110.0(3)	C38-C39-H39	110.3
C40-C39-H39	110.3	P2-C39-H39	110.3
C41-C40-C43	109.3(4)	C41-C40-C39	111.9(4)
C43-C40-C39	112.0(4)	C41-C40-H40	107.8
C43-C40-H40	107.8	C39-C40-H40	107.8

O6-C41-O5	124.9(4)	O6-C41-C40	124.9(4)
O5-C41-C40	110.2(4)	O5-C42-H42A	109.5
O5-C42-H42B	109.5	H42A-C42-H42B	109.5
O5-C42-H42C	109.5	H42A-C42-H42C	109.5
H42B-C42-H42C	109.5	O8-C43-O7	125.5(4)
O8-C43-C40	124.0(4)	O7-C43-C40	110.4(4)
O7-C44-H44A	109.5	O7-C44-H44B	109.5
H44A-C44-H44B	109.5	O7-C44-H44C	109.5
H44A-C44-H44C	109.5	H44B-C44-H44C	109.5
C46-C45-C50	119.6(5)	C46-C45-P2	119.7(4)
C50-C45-P2	120.6(4)	C45-C46-C47	120.5(5)
C45-C46-H46	119.7	C47-C46-H46	119.7
C48-C47-C46	119.0(6)	C48-C47-H47	120.5
C46-C47-H47	120.5	C47-C48-C49	121.3(5)
C47-C48-H48	119.3	C49-C48-H48	119.3
C48-C49-C50	120.2(5)	C48-C49-H49	119.9
C50-C49-H49	119.9	C45-C50-C49	119.3(5)
C45-C50-H50	120.4	C49-C50-H50	120.4
C56-C51-C52	119.0(5)	C56-C51-P2	122.6(4)
C52-C51-P2	118.1(4)	C53-C52-C51	120.1(5)
C53-C52-H52	119.9	C51-C52-H52	119.9
C52-C53-C54	120.0(5)	C52-C53-H53	120.0
C54-C53-H53	120.0	C55-C54-C53	120.2(5)
C55-C54-H54	119.9	C53-C54-H54	119.9
C54-C55-C56	120.1(5)	C54-C55-H55	119.9
C56-C55-H55	119.9	C51-C56-C55	120.6(5)
C51-C56-H56	119.7	C55-C56-H56	119.7
Cl3-C57-Cl4	111.9(3)	Cl3-C57-H57A	109.2
Cl4-C57-H57A	109.2	Cl3-C57-H57B	109.2
Cl4-C57-H57B	109.2	H57A-C57-H57B	107.9

Pd1-C11-Pd2	73.57(3)	Pd1-C12-Pd2	73.68(3)
C13-O1-C14	113.6(5)	C15-O3-C16	114.2(4)
C41-O5-C42	114.8(4)	C43-O7-C44	115.8(4)
C23-P1-C17	108.6(2)	C23-P1-C11	107.4(2)
C17-P1-C11	109.9(2)	C23-P1-Pd1	110.84(17)
C17-P1-Pd1	115.79(16)	C11-P1-Pd1	103.98(16)
C45-P2-C51	105.4(2)	C45-P2-C39	108.1(2)
C51-P2-C39	108.4(2)	C45-P2-Pd2	118.05(17)
C51-P2-Pd2	111.74(17)	C39-P2-Pd2	104.82(14)



## Chapter 5. Asymmetric Catalytic P-H Addition Reaction of $\alpha,\beta$ -Unsaturated Sulfonyl Fluoride

### 5.1. Introduction

Chiral phosphines containing selected functional groups are important ligands in synthetic organic chemistry.<sup>6, 250</sup> The phosphorus donors support transition metal ions as catalysts in asymmetric transformations. On the other hand, functional groups having weak interactions with the reacting species are generally selected for the purpose of enhancing reaction selectivity. We have recently reported that gold(I) complexes containing functionalized chiral phosphine ligands are potential anti-cancer agents.<sup>251</sup> Their biological properties are highly dependent on the selected functional groups as well as the ligand chirality.

Previously, we have also disclosed the synthesis of a series of functionalized phosphines such as ketoester-<sup>150</sup>, pyridyl-<sup>113</sup>, keto-<sup>108, 114</sup>, ester-<sup>114, 251</sup>, and amidophosphines<sup>148, 150</sup>. We herein reported the synthesis of an enantioenriched tertiary phosphine containing the sulfoxide group. It is worth noting that sulfonylphosphines have found application in biological, synthetic organic, and medicinal chemistry. Currently we are particularly interested in the synthesis of phosphines containing sulfonyl fluorides. These compounds have demonstrated potential in click chemistry as additives<sup>252-253</sup>, in biological chemistry as probes<sup>254</sup> and in sulfur(VI) fluoride exchange (SuFEx) protocols as coupling partners<sup>255</sup> and in C-C bond forming reactions as chelating groups<sup>256-257</sup>. In the past several decades, small sulfonyl fluoride containing molecules have also attracted attention in biological chemistry as pharmacophores and insecticides *via* inhibition of esterases<sup>258</sup>. Roberta has also reported their other application as nucleoside probes to label the NAD and ATP binding sites specifically in more than 50 proteins, as well as an affinity probe for measuring kinase activities.<sup>259-260</sup> The

sulfonyl fluorides were also employed as Michael acceptors and Diels–Alder dienophiles<sup>261</sup>. In addition, fluorosulfate group functioned as a cheaper triflate alternative. Chiral sulfonyl phosphines also played an important role as silyl or proton activators because of their synthetic stability, accessibility, and responsiveness.

It is worth noting the synthesis of sulfonylphosphines is challenging, as the tertiary phosphorus donors are sensitive to oxidizing agents while the sulfone group is reactive toward reducing agents. The sulfonyl chlorides (ArSO<sub>2</sub>Cl), sulfonyl bromides (ArSO<sub>2</sub>Br), and sulfonyl iodides (ArSO<sub>2</sub>I) are therefore reduced rapidly to the corresponding sulfonyl ester (ArSO<sub>2</sub>OR) irreversibly when they are treated with phosphines. Furthermore, sulfonyl fluorides are susceptible to heterolytic bond cleavage because of the extreme electronegativity of F.<sup>252</sup> These intrinsic properties render challenges to the synthetic manipulation of these molecules. Perhaps due to these synthetic difficulties, there are no optically active sulfonylphosphines reported in the literature to date. We herein report the efficient synthesis of the first C-chiral phosphine containing sulfonyl fluoride function by a palladium catalyzed asymmetric hydrophosphination reaction.

The first example of catalytic synthesis of a chiral sulfonyl-phosphine ligand was achieved via palladium catalyzed asymmetric hydrophosphination under mild conditions in high conversion (> 99%) and moderate to high enantioselectivities (up to 90% *ee*). The air-sensitive phosphine product was subsequently converted to its phosphine-sulfide analogue for structural and stereochemical characterization via X-ray crystallography. The mechanistic cycle was proposed in this Chapter.

## 5.2. Results and discussion

In principle, the direct addition of diphenylphosphine to the sulfone substrates **75j** should be the most efficient approach to generate a racemic mixture of the targeted fluorosulfonyl-phosphine **69j**. Experimentally, however,

no reaction could be observed in the absence of a catalyst, despite long reaction time and strong reaction condition were employed. Clearly the electronic withdrawing fluorine atom in in  $-\text{SO}_2\text{F}$  alone is not able to activate **75j** toward the addition reaction. Therefore, we selected the chiral palladium catalysts **67**, **54e**, and **88** to promote the addition reaction.

We have previously reported that these six catalysts are highly efficient catalysts for the P-H addition reaction for the related enones, such as chalcone.<sup>223</sup> Both enantiomeric forms of these complexes are equally available. Their chiral auxiliaries offer different electronic influences on the respective palladium atoms while projecting their stereochemistry onto the catalytic sites in the well-defined directions. In the current work, 5 mol % of the selected catalyst was used in the selected solvent and in the presence of trimethylamine (**Table 33**).

It was observed that all the C,P-palladacycles **67**, **54e**, and **88** are efficient catalysts for the P-H addition reaction involving  $\alpha,\beta$ -unsaturated sulfonyl fluoride **75j**. When the reaction was conducted in methanol at room temperature, catalysts **88a** and **88f** appeared to be more efficient than other C,P catalysts as the desired product **69j** could be obtained in quantitative yield in 3-5 h with 78 and 73 % *ee*, respectively (entries 10 and 14). The stereoselectivity of **88a** was not improved by lowering the reaction temperature (entry 11). While catalyst **88f** showed an improved selectivity to 85 % *ee* at lower temperature in MeOH, a significantly longer reaction time was required (72 h, entry 15). Indeed, long reaction durations are generally required for all CP-catalysts when the reaction was conducted in polar solvents at low temperature. For example, in THF, the reaction remained incomplete after being kept at  $-80\text{ }^\circ\text{C}$  for 96 h (entry 19). Similar long reaction durations were also recorded when acetonitrile and acetone were employed at low temperature. Interestingly, a very long reaction time but with high (87 %) *ee* were also recorded when toluene, a typical non-polar solvent, was used at  $-80\text{ }^\circ\text{C}$  (entry 9).

On the other hand, all the CP-catalysts show higher catalytic efficiency in dichloromethane as all the addition reactions are completed within 3 h -80 °C to generate the product quantitatively in 71-87 % *ee*. Under these low temperature reaction conditions, **67** gave the highest selectivity of 87 % *ee*. Attempts to further improve the stereoselectivity of **67** by employing chloroform as the alternative solvent indeed showed a slight improvement. At -60 °C, the highest *ee* of 90 % was achieved but the reaction time is noticeably longer than when DCM was used as the solvent (entry 5). Accordingly, among all the CP-catalysts, **67** is the most efficient catalyst for the synthesis of the air-sensitive tertiary phosphine **69j** by using either DCM or chloroform as the solvents at low temperatures. For structural and absolute stereochemistry determination purposes, the product (*R*)-**69j** generated by catalyst (*R*)-**67** was subsequently converted to the corresponding air-stable phosphine-sulfide (*R*)-**92j**, by the addition of elemental Sulphur (**Figure 33**).

**Table 33:** The Pd catalyzed asymmetric P-H addition reaction of sulfonyl fluoride

Reaction scheme:  $\text{Ph-CH=CH-SO}_2\text{F} + \text{HPPH}_2 \xrightarrow[\text{NEt}_3 (1.0 \text{ eq.})]{\text{cat. (5.0 mol\%)}}$   $\text{Ph-CH(PPh}_2\text{)-CH}_2\text{-SO}_2\text{F}$

75j  69j

Entry	catalyst	solvent	T (°C)	Time (h)	Conversion <sup>a</sup> (%)	<i>ee</i> <sup>b</sup> (%)
1	( <i>R</i> )- <b>67</b>	MeOH	RT	1	> 99	59( <i>R</i> )
2	( <i>R</i> )- <b>67</b>	CHCl <sub>3</sub>	RT	6	> 99	66( <i>R</i> )
3	( <i>R</i> )- <b>67</b>	MeOH	-40	16	> 99	67( <i>R</i> )
4	( <i>R</i> )- <b>67</b>	MeOH	-80	16	> 99	80( <i>R</i> )
5	( <i>R</i> )- <b>67</b>	CHCl <sub>3</sub>	-60	24	> 99	90( <i>R</i> )
6	( <i>R</i> )- <b>67</b>	MeCN	-80	72	84	36( <i>R</i> )
7	( <i>R</i> )- <b>67</b>	acetone	-80	72	86	53( <i>R</i> )
8	( <i>R</i> )- <b>67</b>	DCM	-80	3	> 99	87( <i>R</i> )
9	( <i>R</i> )- <b>67</b>	toluene	-80	72	75	87( <i>R</i> )
10	( <i>S</i> )- <b>88a</b>	MeOH	RT	5	> 99	78( <i>S</i> )
11	( <i>S</i> )- <b>88a</b>	MeOH	-80	72	> 99	78( <i>S</i> )
12	( <i>S</i> )- <b>88a</b>	THF	-80	72	64	72( <i>S</i> )
13	( <i>S</i> )- <b>88a</b>	DCM	-80	3	> 99	78( <i>S</i> )
14	( <i>S</i> )- <b>88f</b>	MeOH	RT	3	> 99	73( <i>S</i> )
15	( <i>S</i> )- <b>88f</b>	MeOH	-80	72	> 99	85( <i>S</i> )
16	( <i>S</i> )- <b>88f</b>	DCM	-80	3	> 99	84( <i>S</i> )

17	( <i>S</i> )- <b>88g</b>	MeOH	RT	5	> 99	51( <i>S</i> )
18	( <i>S</i> )- <b>88g</b>	MeOH	-80	72	> 99	61( <i>S</i> )
19	( <i>R</i> )- <b>88g</b>	THF	-80	96	69	86( <i>R</i> )
20	( <i>S</i> )- <b>88d</b>	MeOH	RT	5	> 99	67( <i>S</i> )
21	( <i>S</i> )- <b>88d</b>	MeOH	-80	72	> 99	75( <i>S</i> )
22	( <i>S</i> )- <b>88d</b>	DCM	-80	3	> 99	71( <i>S</i> )
23	( <i>S</i> )- <b>88e</b>	MeOH	RT	5	> 99	59( <i>S</i> )
24	( <i>S</i> )- <b>88e</b>	DCM	-80	3	> 99	76( <i>S</i> )
25	( <i>S</i> )- <b>88e</b>	MeOH	-80	72	> 99	68( <i>S</i> )
26	( <i>R,R</i> )- <b>54e</b>	MeOH	RT	48	--	--

<sup>a</sup> The conversions were determined by <sup>31</sup>P{<sup>1</sup>H} NMR; <sup>b</sup> The *ee* values were determined by HPLC.

It is important to note that, no catalytic effect could be observed from the pincer complex **54e** (Table 33, entry 26). The ineffectiveness of **54e** is surprising as it showed similar high catalytic properties as **67** in the analogous P-H addition reaction involving enones.<sup>114, 262</sup> We believe that this striking observation is attributed to the fact that the CP- and the PCP-catalysts operate *via* different reaction mechanisms.

Due to the structural features, the CP-catalysts allows both diphenylphosphine and the sulfone substrates **75j** to interact simultaneously during the course of the addition reaction, as illustrated in Scheme 53. We have previously reported that the enormous electronic withdrawing effects originated from the highly conjugated *trans* aromatic naphthalene ring is critical for the activation of the reacting substrates in P-H addition reactions.<sup>108</sup> The *trans* P-Pd-P bonds in the catalytic cycle are kinetically labile. Therefore, while the more stable 5-membered CP-auxiliary remained coordinated onto palladium, the less stable 6-membered P-O product is readily eliminated from the catalyst. Such an intramolecular reaction mechanism, however, cannot be adopted by the P-C-P catalyst, as only one catalytic site is available in **54e**.<sup>146</sup>

In order to examine if the sulfonyl oxygen→palladium interaction is indeed a crucial requirement for the activation of the adjacent carbon-carbon bond, the aryl- and alkyl-sulfone substrates **75b** and **75l** were selected for the analogous

catalytic P-H addition reaction. Electronically, the oxygen atoms within the –SO<sub>2</sub>Ph and –SO<sub>2</sub><sup>t</sup>Bu sulfoxide groups are better donor atoms than their counterparts in –SO<sub>2</sub>F, hence they should form stronger oxygen→palladium interactions to promote the addition reaction. However, model studies<sup>117</sup> showed that the S-phenyl and the S-<sup>t</sup>butyl group in **75k** and **75l** will experience severe steric repulsion between the projecting prochiral P-Ph groups originated from the chiral auxiliary. Due to this steric hindrance, model study indicated that **75k** and **75l** cannot form the required intermediates for the intramolecular addition reaction.

Indeed, all catalysts **67**, **54e**, and **88** experimentally failed to activate the addition reaction. In view of these observations, we further examined if the functional group-catalysts interactions could be avoided. For this purpose, the highly reactive nitro-substrate **75m** was selected for the analogous hydrophosphination reaction since electronically **75m** should not require the nitro oxygen→palladium coordination to activate its carbon-carbon double bond. Experimentally, **75m** was indeed found to be highly reactive toward the P-H addition reaction, even without a catalyst. However, the thermal pathway could not be suppressed even at -80 °C. At this low temperature, the non-catalyzed reaction between **75m** and diphenylphosphine was found to be complete in just a few minutes to generate the corresponding Michael addition reaction product **69m** quantitatively. Introduction of the chiral catalysts **67**, **54e**, and **88** into this low temperature reaction only generated the same nitro-substituted product **69m** quantitatively as a racemic mixture. Perhaps an optical resolution process is required should the enantiomerically pure forms of **69m** in demand in the future.

**Figure 32:** The sulfonyl substrates and Palladacycle catalysts employed

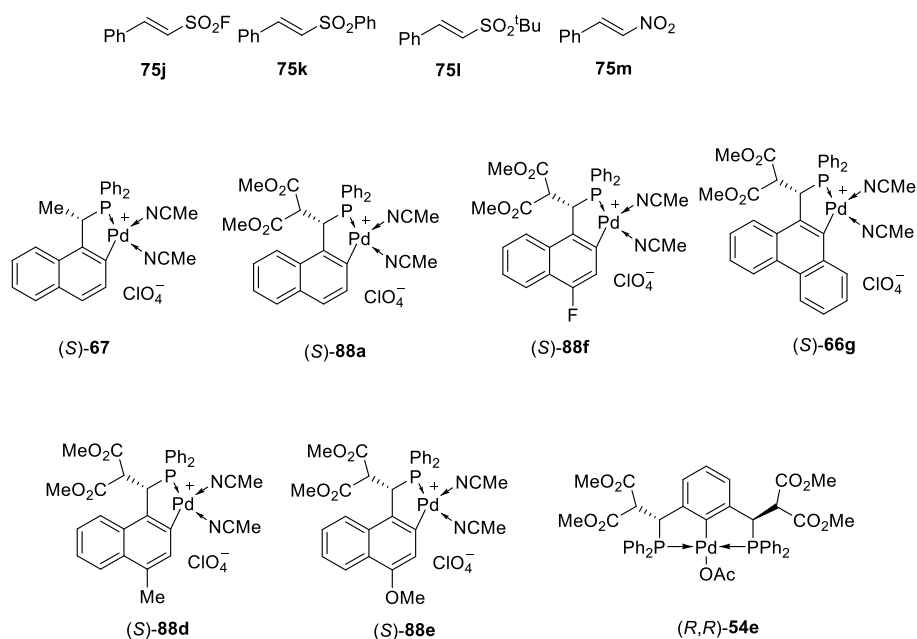
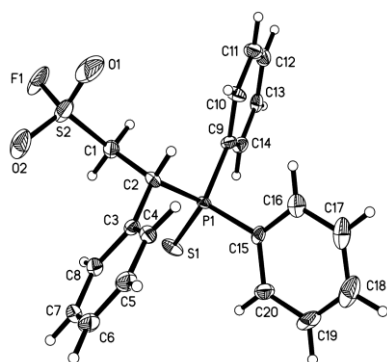
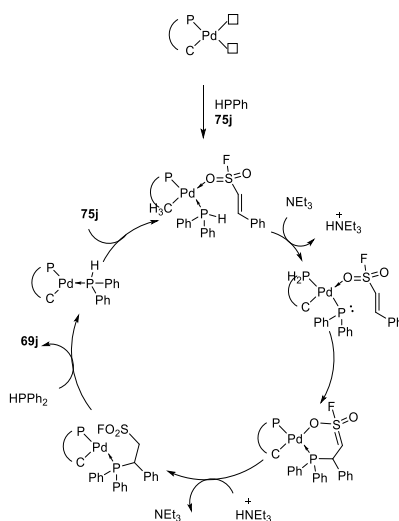


**Figure 33:** The ORTEP of (R)-92



Selected bond lengths (Å) C15- P1 1.801(10); P1-S1 1.949(4); C9-P1 1.817(10); C2-P1 1.858(10); C1-C2 1.528(13); C1-S2 1.758(10); C2-C3 1.500(13); F1-S2 1.561(7); O1-S2 1.385(10); O2-S2 1.400(8). Selected bond angles (°) C2-C1-S2 112.4(7); C3-C2-C1 116.0(8); C3-C2-P1 112.2(7); C1-C2-P1 106.6(6); C15-P1-C9 107.1(4); C15-P1-C2 107.7(4); C9-P1-C2 105.2(4); C15-P1-S1 113.1(4); C9-P1-S1 112.6(3); C2-P1-S1 110.6(3); O1-S2-O2 120.0(6); O1-S2-F1 106.9(6); O2-S2-F1 105.0(5); O1-S2-C1 111.0(5); O2-S2-C1 113.3(5); F1-S2-C1 97.6(4).

**Scheme 53:** Proposed catalytic cycle involving an intramolecular mechanism



### 5.3. Conclusion

We have prepared an optically active fluorosulfonyl-phosphine ligand *via* cyclopalladated complex catalyzed asymmetric P-H addition reaction in technically quantitative yield with up to 90% *ee* under mild conditions. Several readily available CP-palladacycles could be employed as catalysts with similar efficiency for the asymmetric addition reaction. Currently, the synthetic applications and biological properties of the novel chiral sulfonyl-substituted phosphorus **69j** and its metal complexes are being studied in our group.

### 5.4. Experimental section

#### General information

All reactions including the air-sensitive complexes diphenylphosphine and free ligands **69j** were carried out under an inert atmosphere of nitrogen employing Schlenk Line and two-neck round bottom flask, and all the solvent contacted the air-sensitive complexes were degassed by blowing with nitrogen. NMR spectra were recorded on Bruker AV 300, AV400, AV 500, and BBFO 400 spectrometers. Chemical shifts were reported in ppm and referenced to an internal SiMe<sub>4</sub> standard (0 ppm) for <sup>1</sup>H NMR, and chloroform-d (77.16 ppm) for <sup>13</sup>C NMR. Dichloromethane, chloroform, tetrahydrofuran, acetone, toluene, and methanol were purchased from their respective companies and used as supplied.

Tetrahydrofuran was distilled from sodium/benzophenone prior to use. Solvents were degassed when necessary. A Low Temp Pairstirrer PSL-1800 was used for controlling low temperature reactions. Column chromatography was carried out with Silica gel 60 (Merck). Melting points were measured using SRS Optimelt Automated Point System SRS MPA100. Optical rotation was measured with JASCO P-1030 Polarimeter in the DCM in a 0.1 dm cell at 22.0 °C.

### Synthesis and characteristics

#### Procedure of for **75j**

The 50 mL round bottom flash was charged with substrates AgTFA (2.4 mmol, 1.2 eq.), Pd(OAc)<sub>2</sub> (9 mg, 2 mol%), phenyl iodide (2 mmol), and ethenesulfonyl fluoride (220 mg, 1.0 eq.) in the acetone (5 mL), and the resulting mixture was refluxed at 60 °C for 8 hours. The white powder was purified by column chromatography with the eluent of 98: 2 (Hexane: ethyl acetate): yield 87%. <sup>1</sup>H NMR (400 MHz, CDCl<sub>3</sub>), δ 7.82 (d, *J* = 15.5 Hz, 1H), 7.60 – 7.42 (m, 5H), 6.87 (dd, *J* = 15.5, 2.5 Hz, 1H). <sup>19</sup>F{<sup>1</sup>H} NMR (377 MHz, CDCl<sub>3</sub>), δ 62.30 (s). <sup>13</sup>C NMR (101 MHz, CDCl<sub>3</sub>), δ 149.01, 148.99, 132.78, 131.10, 129.54, 129.17, 118.20, 117.92, 77.48, 77.16, 76.84. Melting point: 95.4-95.7 °C. HRMS (m/z): Calculated for C<sub>8</sub>H<sub>7</sub>SO<sub>2</sub>FH<sup>+</sup> (MH<sup>+</sup>): 187.0229, Found (MH<sup>+</sup>): 187.0228.

#### Procedure of **69j** and **92**

The substrates **75j** (1.05 equivalent) and catalysts **67** (5 mol%) were added into the solution of solution of weighted diphenylphosphine in the solvent (5.1 mL) in the degassed and degassing Schlenk flask. The system was put into the appointed temperature for half an hour until the solution was cool down. The triethylamine (1.0 equivalent) solution in the solvent (0.5 mL) was dropwise added into the Schlenk flask. <sup>31</sup>P{<sup>1</sup>H} NMR (162 MHz, CDCl<sub>3</sub>), δ 0.69 (d, *J* = 80.3 Hz). <sup>19</sup>F{<sup>1</sup>H} NMR (162 MHz, CDCl<sub>3</sub>), δ 49.83 (s). When the diphenylphosphine had been consumed (detected by <sup>31</sup>P{<sup>1</sup>H} NMR), the air-sensitive free ligand was quenched by sulfur affording **92**. Melting point: 149.6 -

150.2 °C.  $^1\text{H}$  NMR (400 MHz,  $\text{CDCl}_3$ ),  $\delta$  8.26 – 8.11 (m, 2H), 7.74 – 7.57 (m, 3H), 7.52 – 7.08 (m, 10H), 4.48 (td,  $J = 11.8, 1.7$  Hz, 1H), 4.27 (ddd,  $J = 15.3, 11.7, 3.6$  Hz, 1H), 3.83 – 3.64 (m, 1H).  $^{31}\text{P}\{^1\text{H}\}$  NMR (162 MHz,  $\text{CDCl}_3$ ),  $\delta$  50.43 (d,  $J = 8.0$  Hz).  $^{19}\text{F}\{^1\text{H}\}$  NMR (377 MHz,  $\text{CDCl}_3$ ),  $\delta$  60.07 (d,  $J = 8.2$  Hz).  $^{13}\text{C}$  NMR (101 MHz,  $\text{CDCl}_3$ ),  $\delta$  132.86 (d,  $J = 3.0$  Hz), 132.14 (s), 132.05 (s), 132.02 (s), 131.98 (s), 131.63 (d,  $J = 10.0$  Hz), 131.15 (d,  $J = 4.8$  Hz), 130.18 (s), 129.60 (s), 129.55 (s), 129.48 (s), 129.35 (s), 128.83 (s), 128.78 (d,  $J = 3.1$  Hz), 128.36 (s), 128.24 (s), 52.55 (dd,  $J = 14.9, 7.2$  Hz), 42.69 (d,  $J = 48.9$  Hz). HRMS (m/z): Calculated for  $\text{C}_{20}\text{H}_{18}\text{O}_2\text{S}_2\text{FPH}^+$  ( $\text{MH}^+$ ): 405.0548, Found ( $\text{MH}^+$ ): 405.0566. (*R*)-**92**  $[\alpha]_{\text{D}} = +242.7$  ( $c$  0.85, DCM).

## Crystallographic data

CCDC 1850875

**Table 34:** Data collection and structure refinement for complex **92**

<b>Chemical formula</b>	C <sub>20</sub> H <sub>18</sub> FO <sub>2</sub> PS <sub>2</sub>	
<b>Formula weight</b>	404.43 g/mol	
<b>Temperature</b>	100(2) K	
<b>Wavelength</b>	0.71073 Å	
<b>Crystal size</b>	0.020 x 0.120 x 0.220 mm	
<b>Crystal habit</b>	colorless plate	
<b>Crystal system</b>	monoclinic	
<b>Unit cell dimensions</b>	a = 12.196(3) Å	α = 90°
	b = 6.4854(12) Å	β = 96.086(7)°
	c = 24.125(5) Å	γ = 90°
<b>Volume</b>	1897.4(12) Å <sup>3</sup>	
<b>Z</b>	4	
<b>Density (calculated)</b>	1.414 g/cm <sup>3</sup>	
<b>Absorption coefficient</b>	0.386 mm <sup>-1</sup>	
<b>F(000)</b>	840	
<b>Theta range for data collection</b>	2.55 to 25.01°	
<b>Index ranges</b>	-14 ≤ h ≤ 14, -7 ≤ k ≤ 7, -28 ≤ l ≤ 28	
<b>Reflections collected</b>	24201	
<b>Independent reflections</b>	6348 [R(int) = 0.1385]	
<b>Coverage of independent reflections</b>	99.8%	
<b>Absorption correction</b>	Multi-Scan	
<b>Max. and min. transmission</b>	0.9920 and 0.9200	
<b>Structure solution technique</b>	direct methods	
<b>Structure solution program</b>	XT, VERSION 2014/5	
<b>Refinement method</b>	Full-matrix least-squares on F <sup>2</sup>	
<b>Refinement program</b>	SHELXL-2016/6 (Sheldrick, 2016)	
<b>Function minimized</b>	Σ w(F <sub>o</sub> <sup>2</sup> - F <sub>c</sub> <sup>2</sup> ) <sup>2</sup>	
<b>Data / restraints / parameters</b>	6348 / 409 / 469	
<b>Goodness-of-fit on F<sup>2</sup></b>	1.058	

<b>Final R indices</b>	4561 data; I>2σ(I)	R1 = 0.0757, wR2 = 0.1548
	all data	R1 = 0.1170, wR2 = 0.1782
<b>Weighting scheme</b>	w=1/[σ <sup>2</sup> (F <sub>o</sub> <sup>2</sup> )+(0.0517P) <sup>2</sup> +4.6019P] where P=(F <sub>o</sub> <sup>2</sup> +2F <sub>c</sub> <sup>2</sup> )/3	
<b>Absolute structure parameter</b>	0.01(10)	
<b>Largest diff. peak and hole</b>	1.654 and -0.621 eÅ <sup>-3</sup>	
<b>R.M.S. deviation from mean</b>	0.098 eÅ <sup>-3</sup>	

**Table 35:** Bond lengths (Å) for complex **92**

C1-C2	1.528(13)	C1-S2	1.758(10)
C1-H1A	0.99	C1-H1B	0.99
C2-C3	1.500(13)	C2-P1	1.858(10)
C2-H2	1.0	C3-C4	1.393(13)
C3-C8	1.412(13)	C4-C5	1.386(14)
C4-H4	0.95	C5-C6	1.386(15)
C5-H5	0.95	C6-C7	1.401(15)
C6-H6	0.95	C7-C8	1.385(13)
C7-H7	0.95	C8-H8	0.95
C9-C14	1.385(13)	C9-C10	1.387(13)
C9-P1	1.817(10)	C10-C11	1.384(14)
C10-H10	0.95	C11-C12	1.386(15)
C11-H11	0.95	C12-C13	1.364(14)
C12-H12	0.95	C13-C14	1.395(13)
C13-H13	0.95	C14-H14	0.95
C15-C16	1.387(14)	C15-C20	1.394(14)
C15-P1	1.801(10)	C16-C17	1.373(14)
C16-H16	0.95	C17-C18	1.384(18)
C17-H17	0.95	C18-C19	1.398(19)
C18-H18	0.95	C19-C20	1.396(15)
C19-H19	0.95	C20-H20	0.95
C21-C22	1.568(13)	C21-S4	1.749(10)
C21-H21A	0.99	C21-H21B	0.99
C22-C23	1.525(13)	C22-P2	1.862(10)
C22-H22	1.0	C23-C24	1.364(15)
C23-C28	1.382(16)	C24-C25	1.376(16)

C24-H24	0.95	C25-C26	1.331(18)
C25-H25	0.95	C26-C27	1.366(18)
C26-H26	0.95	C27-C28	1.396(15)
C27-H27	0.95	C28-H28	0.95
C29-C30	1.363(14)	C29-C34	1.381(16)
C29-P2	1.838(10)	C30-C31	1.449(15)
C30-H30	0.95	C31-C32	1.361(15)
C31-H31	0.95	C32-C33	1.387(15)
C32-H32	0.95	C33-C34	1.357(15)
C33-H33	0.95	C34-H34	0.95
C35-C40	1.361(16)	C35-C36	1.377(16)
C35-P2	1.841(11)	C36-C37	1.359(18)
C36-H36	0.95	C37-C38	1.37(2)
C37-H37	0.95	C38-C39	1.37(2)
C38-H38	0.95	C39-C40	1.414(16)
C39-H39	0.95	C40-H40	0.95
F1-S2	1.561(7)	F2-S4	1.566(6)
O1-S2	1.385(10)	O2-S2	1.400(8)
O3-S4	1.439(9)	O4-S4	1.403(7)
P1-S1	1.949(4)	P2-S3	1.997(4)

---

**Table 36:** Bond angles (°) for complex **92**

C2-C1-S2	112.4(7)	C2-C1-H1A	109.1
S2-C1-H1A	109.1	C2-C1-H1B	109.1
S2-C1-H1B	109.1	H1A-C1-H1B	107.9
C3-C2-C1	116.0(8)	C3-C2-P1	112.2(7)
C1-C2-P1	106.6(6)	C3-C2-H2	107.2
C1-C2-H2	107.2	P1-C2-H2	107.2
C4-C3-C8	117.7(9)	C4-C3-C2	121.1(9)
C8-C3-C2	121.2(9)	C5-C4-C3	122.5(10)
C5-C4-H4	118.8	C3-C4-H4	118.8
C6-C5-C4	118.8(10)	C6-C5-H5	120.6
C4-C5-H5	120.6	C5-C6-C7	120.5(10)

C5-C6-H6	119.7	C7-C6-H6	119.7
C8-C7-C6	119.9(10)	C8-C7-H7	120.1
C6-C7-H7	120.1	C7-C8-C3	120.6(9)
C7-C8-H8	119.7	C3-C8-H8	119.7
C14-C9-C10	118.5(9)	C14-C9-P1	117.8(8)
C10-C9-P1	123.7(7)	C11-C10-C9	120.9(9)
C11-C10-H10	119.5	C9-C10-H10	119.5
C10-C11-C12	120.0(10)	C10-C11-H11	120.0
C12-C11-H11	120.0	C13-C12-C11	119.5(10)
C13-C12-H12	120.3	C11-C12-H12	120.3
C12-C13-C14	120.8(9)	C12-C13-H13	119.6
C14-C13-H13	119.6	C9-C14-C13	120.2(9)
C9-C14-H14	119.9	C13-C14-H14	119.9
C16-C15-C20	119.5(9)	C16-C15-P1	122.2(8)
C20-C15-P1	118.2(8)	C17-C16-C15	120.2(11)
C17-C16-H16	119.9	C15-C16-H16	119.9
C16-C17-C18	121.3(12)	C16-C17-H17	119.4
C18-C17-H17	119.4	C17-C18-C19	119.1(11)
C17-C18-H18	120.4	C19-C18-H18	120.4
C18-C19-C20	119.7(11)	C18-C19-H19	120.2
C20-C19-H19	120.2	C15-C20-C19	120.2(11)
C15-C20-H20	119.9	C19-C20-H20	119.9
C22-C21-S4	112.3(7)	C22-C21-H21A	109.1
S4-C21-H21A	109.1	C22-C21-H21B	109.1
S4-C21-H21B	109.1	H21A-C21-H21B	107.9
C23-C22-C21	113.3(8)	C23-C22-P2	117.1(7)
C21-C22-P2	103.7(6)	C23-C22-H22	107.4
C21-C22-H22	107.4	P2-C22-H22	107.4
C24-C23-C28	118.5(10)	C24-C23-C22	123.2(10)
C28-C23-C22	118.3(9)	C23-C24-C25	120.5(12)
C23-C24-H24	119.8	C25-C24-H24	119.8
C26-C25-C24	121.0(12)	C26-C25-H25	119.5
C24-C25-H25	119.5	C25-C26-C27	120.7(11)
C25-C26-H26	119.6	C27-C26-H26	119.6
C26-C27-C28	118.8(12)	C26-C27-H27	120.6

C28-C27-H27	120.6	C23-C28-C27	120.3(12)
C23-C28-H28	119.8	C27-C28-H28	119.8
C30-C29-C34	122.6(10)	C30-C29-P2	121.7(8)
C34-C29-P2	115.5(8)	C29-C30-C31	117.5(10)
C29-C30-H30	121.3	C31-C30-H30	121.3
C32-C31-C30	119.3(11)	C32-C31-H31	120.4
C30-C31-H31	120.4	C31-C32-C33	120.5(10)
C31-C32-H32	119.7	C33-C32-H32	119.7
C34-C33-C32	121.0(11)	C34-C33-H33	119.5
C32-C33-H33	119.5	C33-C34-C29	119.1(11)
C33-C34-H34	120.5	C29-C34-H34	120.5
C40-C35-C36	121.0(11)	C40-C35-P2	119.9(9)
C36-C35-P2	119.0(10)	C37-C36-C35	119.5(14)
C37-C36-H36	120.2	C35-C36-H36	120.2
C36-C37-C38	121.1(15)	C36-C37-H37	119.4
C38-C37-H37	119.4	C39-C38-C37	120.0(12)
C39-C38-H38	120.0	C37-C38-H38	120.0
C38-C39-C40	119.4(14)	C38-C39-H39	120.3
C40-C39-H39	120.3	C35-C40-C39	118.9(12)
C35-C40-H40	120.5	C39-C40-H40	120.5
C15-P1-C9	107.1(4)	C15-P1-C2	107.7(4)
C9-P1-C2	105.2(4)	C15-P1-S1	113.1(4)
C9-P1-S1	112.6(3)	C2-P1-S1	110.6(3)
C29-P2-C35	106.7(5)	C29-P2-C22	108.7(5)
C35-P2-C22	102.6(5)	C29-P2-S3	112.7(4)
C35-P2-S3	113.2(4)	C22-P2-S3	112.3(3)
O1-S2-O2	120.0(6)	O1-S2-F1	106.9(6)
O2-S2-F1	105.0(5)	O1-S2-C1	111.0(5)
O2-S2-C1	113.3(5)	F1-S2-C1	97.6(4)
O4-S4-O3	120.8(5)	O4-S4-F2	106.6(4)
O3-S4-F2	105.6(5)	O4-S4-C21	112.5(5)
O3-S4-C21	110.9(5)	F2-S4-C21	97.4(4)



## References

1. Cope, A. C.; Siekman, R. W., Formation of Covalent Bonds from Platinum or Palladium to Carbon by Direct Substitution. *J. Am. Chem. Soc.* **1965**, *87* (14), 3272-3273.
2. Cope, A. C.; Friedrich, E. C., Electrophilic aromatic substitution reactions by platinum(II) and palladium(II) chlorides on N,N-dimethylbenzylamines. *J. Am. Chem. Soc.* **1968**, *90* (4), 909-913.
3. Vicente, J.; Saura-Llamas, I., ORTHO-PALLADATION OF PRIMARY AMINES: THE MYTH DISPELLED. *Comments Inorg. Chem.* **2007**, *28* (1-2), 39-72.
4. Frutos-Pedreño, R.; García-Sánchez, E.; Oliva-Madrid, M. J.; Bautista, D.; Martínez-Viviente, E.; Saura-Llamas, I.; Vicente, J., C-H Activation in Primary 3-Phenylpropylamines: Synthesis of Seven-Membered Palladacycles through Orthometalation. Stoichiometric Preparation of Benzazepinones and Catalytic Synthesis of Ureas. *Inorg. Chem.* **2016**, *55* (11), 5520-5533.
5. Dunina, V. V.; Gorunova, O. N.; Zykov, P.; Kochetkov, K. A., Cyclopalladated complexes in enantioselective catalysis. *Russian Chemical Reviews* **2011**, *80* (1), 51.
6. Chen, H. J.; Hong Xiang Teo, R.; Li, Y.; Pullarkat, S. A.; Leung, P.-H., Stereogenic Lock in 1-Naphthylethanamine Complexes for Catalyst and Auxiliary Design: Structural and Reactivity Analysis for Cycloiridated Pseudotetrahedral Complexes. *Organometallics* **2018**, *37* (1), 99-106.
7. Ryabov, A. D., Mechanisms of intramolecular activation of carbon-hydrogen bonds in transition-metal complexes. *Chem. Rev.* **1990**, *90* (2), 403-424.
8. Ryabov, A. D.; Sakodinskaya, I. K.; Yatsimirsky, A. K., Kinetics and mechanism of ortho-palladation of ring-substituted NN-dimethylbenzylamines. *J. Chem. Soc., Dalton Trans.* **1985**, (12), 2629-2638.
9. Clark, P. W.; Dyke, S. F., Cyclopalladated primary, secondary and tertiary benzylamines, and benzalimines. A new method of synthesis. *J. Organomet. Chem.* **1983**, *259* (2), C17-C19.
10. Holton, R. A.; Davis, R. G., Regiocontrolled aromatic palladation. *J. Am. Chem. Soc.* **1977**, *99* (12), 4175-4177.
11. De Vaal, P.; Dedieu, A., The insertion of acetylene into the palladium carbon bond of square planar Pd (II) complexes: a theoretical investigation. *J. Organomet. Chem.* **1994**, *478* (1-2), 121-129.

12. Macgregor, S. A.; Wenger, E., Theoretical Studies on the Insertions of Unsymmetrical Alkynes into the Metal– Carbon Bond of Phosphanickelacycles: Electronic Factors. *Organometallics* **2002**, *21* (6), 1278-1289.
13. Niu, S.; Hall, M. B., Theoretical studies on reactions of transition-metal complexes. *Chem. Rev.* **2000**, *100* (2), 353-406.
14. Musaev, D. G.; Morokuma, K., Ab Initio Molecular Orbital Study of the Mechanism of HH, CH, NH, OH and Si-H Bond Activation on Transient Cyclopentadienylcarbonylrhodium. *J. Am. Chem. Soc.* **1995**, *117* (2), 799-805.
15. Dedieu, A., Theoretical studies in palladium and platinum molecular chemistry. *Chem. Rev.* **2000**, *100* (2), 543-600.
16. Bosque, R.; Maseras, F., A theoretical assessment of the thermodynamic preferences in the cyclopalladation of amines. *Eur. J. Inorg. Chem.* **2005**, *2005* (20), 4040-4047.
17. Omae, I., Intramolecular five-membered ring compounds and their applications. *Coord. Chem. Rev.* **2004**, *248* (11), 995-1023.
18. Dupont, J.; Consorti, C. S.; Spencer, J., The Potential of Palladacycles: More Than Just Precatalysts. *Chem. Rev.* **2005**, *105* (6), 2527-2572.
19. Gorunova, O. N.; Novitskiy, I. M.; Grishin, Y. K.; Gloriov, I. P.; Roznyatovsky, V. A.; Khrustalev, V. N.; Kochetkov, K. A.; Dunina, V. V., Determination of the Absolute Configuration of CN-Palladacycles by  $^31\text{P}\{^1\text{H}\}$  NMR Spectroscopy Using (1R,2S,5R)-Menthylxydiphenylphosphine as the Chiral Derivatizing Agent: Efficient Chirality Transfer in Phosphinite Adducts. *Organometallics* **2016**, *35* (2), 75-90.
20. Yap, J. S. L.; Li, B. B.; Wong, J.; Li, Y.; Pullarkat, S. A.; Leung, P.-H., Development of a novel chiral palladacycle and its application in asymmetric hydrophosphination reaction. *Dalton Trans.* **2014**, *43* (15), 5777-5784.
21. Yap, J. S. L.; Ding, Y.; Yang, X. Y.; Wong, J.; Li, Y.; Pullarkat, S. A.; Leung, P. H., Mechanistic Insights into the PdII-Catalyzed Chemoselective N-Demethylation vs. Cyclometalation Reactivity Pathways in 1-Aryl-N, N-dimethylethanamines. *Eur. J. Inorg. Chem.* **2014**, *2014* (29), 5046-5052.
22. Chen, K.; Pullarkat, S. A.; Ma, M.; Li, Y.; Leung, P.-H., Chiral cyclopalladated complex promoted asymmetric synthesis of diester-substituted P, N-ligands via stepwise hydrophosphination and hydroamination reactions. *Dalton Trans.* **2012**, *41* (17), 5391-5400.
23. Lang, H.; J. Vittal, J.; Leung, P.-H., Metal-template synthesis and co-ordination properties of a palladium complex

containing a novel and stable imidazole-substituted phosphine C-P bidentate chelate. *J. Chem. Soc., Dalton Trans.* **1998**, (13), 2109-2110.

24. Karami, K., Synthesis and characterization of cyclopalladated complexes of benzylamine by IR and NMR spectroscopy studies. *J. Coord. Chem.* **2008**, *61* (16), 2584-2589.

25. Albert, J.; Bosque, R.; Crespo, M.; García, G.; Granell, J.; López, C.; Lovelle, M. V.; Qadir, R.; González, A.; Jayaraman, A.; Mila, E.; Cortés, R.; Quirante, J.; Calvis, C.; Messeguer, R.; Badía, J.; Baldomà, L.; Cascante, M., Cyclopalladated primary amines: A preliminary study of antiproliferative activity through apoptosis induction. *European Journal of Medicinal Chemistry* **2014**, *84*, 530-536.

26. Avshu, A.; O'Sullivan, R. D.; Parkins, A. W.; Alcock, N. W.; Countryman, R. M., Reaction of silver ion with [ML<sub>2</sub>X<sub>2</sub>](L = amine or phosphine; M = Pd or Pt; X = I, Cl, or SCN) leading to orthometallation and catalytic activity. X-ray structure of ab-(2-aminomethyl)phenyl-c-carbonyl-d-iodoplatinum(II). *J. Chem. Soc., Dalton Trans.* **1983**, (8), 1619-1624.

27. Vicente, J.; Saura-Llamas, I.; Jones, P. G., Orthometallated primary amines. Part 1. Facile preparation of the first optically active cyclopalladated primary amines. *J. Chem. Soc., Dalton Trans.* **1993**, (23), 3619-3624.

28. Cleare, M., Coordination Compounds of the Platinum Group Metals. *Platinum Metals Rev* **1974**, *18* (4), 122-129.

29. King, H. J. S., 251. Researches on ammines. Part IX. Diaquo-, hydroxoquo-, and acidohydroxo-diammines of bivalent platinum. *Journal of the Chemical Society (Resumed)* **1938**, (0), 1338-1346.

30. Sabater, S.; Mata, J. A.; Peris, E., Chiral Palladacycles with N-Heterocyclic Carbene Ligands as Catalysts for Asymmetric Hydrophosphination. *Organometallics* **2013**, *32* (4), 1112-1120.

31. Fuchita, Y.; Tsuchiya, H., First ortho-palladation of unsubstituted benzylamine by palladium(II) acetate. *Polyhedron* **1993**, *12* (16), 2079-2080.

32. Fuchita, Y.; Tsuchiya, H.; Miyafuji, A., Cyclopalladation of secondary and primary benzylamines. *Inorg. Chim. Acta* **1995**, *233* (1), 91-96.

33. Albert, J.; Granell, J.; Tavera, R., The cyclopalladation reaction of benzylamine revisited. *Polyhedron* **2003**, *22* (2), 287-291.

34. Dunina, V. V.; Razmyslova, E. D.; Kuz'mina, L. G.; Churakov, A. V.; Rubina, M. Y.; Grishin, Y. K., Synthesis and

resolution of an  $\alpha$ -phenyl substituted ortho-palladated matrix. *Tetrahedron: Asymmetry* **1999**, *10* (16), 3147-3155.

35. Ding, Y.; Zhang, Y.; Li, Y.; Pullarkat, S. A.; Andrews, P.; Leung, P. H., Synthesis of a Chiral Palladacycle and Its Application in Asymmetric Hydrophosphanation Reactions. *Eur. J. Inorg. Chem.* **2010**, *2010* (28), 4427-4437.

36. Li, Y.; Selvaratnam, S.; Vittal, J. J.; Leung, P.-H., A Rational Approach to the Design and Synthesis of Chiral Organopalladium-Amine Complexes. *Inorg. Chem.* **2003**, *42* (10), 3229-3236.

37. Leng, Y. J. S.; Yi, D.; Xiang-Yuan, Y.; Jonathan, W.; Yongxin, L.; A., P. S.; Pak-Hing, L., Mechanistic Insights into the PdII-Catalyzed Chemoselective N-Demethylation vs. Cyclometalation Reactivity Pathways in 1-Aryl-N,N-dimethylethanamines. *Eur. J. Inorg. Chem.* **2014**, *2014* (29), 5046-5052.

38. See Leng Yap, J.; Chen, H. J.; Li, Y.; Pullarkat, S. A.; Leung, P.-H., Synthesis, Optical Resolution, and Stereochemical Properties of a Rationally Designed Chiral C–N Palladacycle. *Organometallics* **2014**, *33* (4), 930-940.

39. Vicente, J.; Saura-Llamas, I.; Palin, M. G.; Jones, P. G., The first orthopalladation of a primary nitrobenzylamine. Synthesis of chiral cyclopalladated complexes derived from (S)-[small alpha]-methyl-4-nitrobenzylamine. *J. Chem. Soc., Dalton Trans.* **1995**, (15), 2535-2539.

40. Smoliakova, I. P.; Wood, J. L.; Stepanova, V. A.; Mawo, R. Y., Solvent-free cyclopalladation on silica gel. *J. Organomet. Chem.* **2010**, *695* (3), 360-364.

41. Fuchita, Y.; Yoshinaga, K.; Ikeda, Y.; Kinoshita-Kawashima, J., Synthesis of optically active cyclopalladated complexes of primary benzylamine derivatives, (R)-(-)-2-phenylglycine methyl ester and (+/-)-1-phenylethylamine. *J. Chem. Soc., Dalton Trans.* **1997**, (14), 2495-2500.

42. Otsuka, S.; Nakamura, A.; Kano, T.; Tani, K., Partial resolution of racemic tertiary phosphines with an asymmetric palladium complex. *J. Am. Chem. Soc.* **1971**, *93* (17), 4301-4303.

43. Ryabov, A. D.; Polyakov, V. A.; Yatsimirsky, A. K., Reaction paths in the cyclopalladated NN-dialkylbenzylamine-substituted styrene system in acetic acid as solvent. The structure of palladated 2-dialkylaminomethylstilbenes. *Journal of the Chemical Society, Perkin Transactions 2* **1983**, (9), 1503-1509.

44. Michel, P., Reactions of cyclopalladated compounds and alkynes: New pathways for organic synthesis? *Recl. Trav. Chim. Pays-Bas* **1990**, 109 (12), 567-576.
45. Vicente, J.; Saura-Llamas, I.; Turpín, J.; Bautista, D.; de Arellano, C. R.; Jones, P. G., Insertion of One, Two, and Three Molecules of Alkyne into the Pd-C Bond of Ortho-palladated Primary and Secondary Arylalkylamines. *Organometallics* **2009**, 28 (14), 4175-4195.
46. Bahsoun, A.; Dehand, J.; Pfeffer, M.; Zinsius, M.; Bouaoud, S.-E.; Le Borgne, G., Reactivity of cyclopalladated complexes. Part 5. Insertion reactions of diphenylacetylene, 1-phenylprop-1-yne, and hexafluorobut-2-yne with cyclopalladated compounds. Crystal and molecular structure of chloro{3-4-[small eta]-4-[(2-dimethylaminomethyl)phenyl]-1,4-dimethyl-2,3-diphenylbuta-1,3-dienyl-C1N}palladium(II) and bromo{3-4-[small eta]-4-[(2-dimethylaminomethyl)phenyl]-2,4-dimethyl-1,3-diphenylbuta-1,3-dienyl-C1N}-palladium(II). *J. Chem. Soc., Dalton Trans.* **1979**, (4), 547-556.
47. Jarvis, A.; Kemmitt, R.; Kimura, B.; Russell, D.; Tucker, P., Addition of hexafluoro-2-butyne to palladium (II)  $\beta$ -diketonato rings: The crystal structure of the adduct Pd (Acac) 2 (C<sub>4</sub>F<sub>6</sub>). *J. Organomet. Chem.* **1974**, 66 (2), C53-C55.
48. Gül, N.; Nelson, J. H.; Willis, A. C.; Rae, A. D., Comparative Study of the Reactions of Two Alkynes and an Alkene with Chiral Cyclopalladated Complexes Derived from N,N-Dimethyl- $\alpha$ -(2-naphthyl)ethylamine and N,N-Dimethyl- $\alpha$ -methylbenzylamine: Insertion or Cycloaddition. *Organometallics* **2002**, 21 (10), 2041-2048.
49. Tao, W.; Silverberg, L. J.; Rheingold, A. L.; Heck, R. F., Alkyne reactions with arylpalladium compounds. *Organometallics* **1989**, 8 (11), 2550-2559.
50. Barr, N.; Dyke, S. F.; Quessy, S. N., Palladium assisted organic reactions: IV. A new isoquinoline ring synthesis. *J. Organomet. Chem.* **1983**, 253 (3), 391-397.
51. Brisdon, B. J.; Nair, P.; Dyke, S. F., Palladium assisted organic reactions-III1Part 1: S.F. Dyke and M. McCartney. *Tetrahedron*: Ortho-aminomethylstilbene derivatives. *Tetrahedron* **1981**, 37 (1), 173-177.
52. Chao, C. H.; Hart, D. W.; Bau, R.; Heck, R. F., Substituted tetralin formation from o-palladated Schiff bases and two equivalents of methyl acrylate. *J. Organomet. Chem.* **1979**, 179 (3), 301-309.

53. Wu, G.; Rheingold, A. L.; Geib, S. J.; Heck, R. F., Palladium-catalyzed annulation of aryl iodides with diphenylacetylene. *Organometallics* **1987**, *6* (9), 1941-1946.
54. Alcock, N. W.; Hulmes, D. I.; Brown, J. M., Contrasting behaviour of related palladium complex-derived resolving agents. 8-H conformational locking of the 1-naphthyl side-chain. *J. Chem. Soc., Chem. Commun.* **1995**, (3), 395-397.
55. Ding, Y.; Li, Y.; Pullarkat, S. A.; Leng Yap, S.; Leung, P. H., Rational Design of a Novel Chiral Palladacycle: Synthesis, Optical Resolution, and Stereochemical Evaluation. *Eur. J. Inorg. Chem.* **2009**, *2009* (2), 267-276.
56. Albrecht, M., Cyclometalation Using d-Block Transition Metals: Fundamental Aspects and Recent Trends. *Chem. Rev.* **2010**, *110* (2), 576-623.
57. Jonathan, C. R.; Pak-Hing, L., Our Odyssey with Functionalized Chiral Phosphines: From Optical Resolution to Asymmetric Synthesis to Catalysis. *The Chemical Record* **2016**, *16* (1), 141-158.
58. Calmuschi, B.; Englert, U., (R)-Di-[mu]-acetato-[kappa]2O:O'-bis{[2-(1-aminoethyl)phenyl]-[kappa]2C1,N]palladium(II)}, (R)-di-[mu]-chloro-bis{[2-(1-aminoethyl)phenyl]-[kappa]2C1,N]palladium(II)} and [SP-4-4]-(R)-[2-(1-aminoethyl)phenyl]-[kappa]2C1,N]chloro(pyridine-[kappa]N)palladium(II). *Acta Crystallographica Section C* **2002**, *58* (11), m545-m548.
59. Albert, J.; Cadena, J. M.; Granell, J., Cyclopalladation of the primary amine (R)-(+)-1-(1-naphthyl) ethylamine: a new resolving agent for monodentate phosphines. *Tetrahedron: Asymmetry* **1997**, *8* (7), 991-994.
60. Dunina, V. V.; Razmyslova, E. D.; Gorunova, O. g. N.; Livantsov, M. V.; Yuri, K. G., New principle for palladacycle resolution: diastereoselective monomer to dimer conversion. *Tetrahedron: Asymmetry* **2005**, *16* (4), 817-826.
61. Dunina, V. V.; Golovan, E. B.; Gulyukina, N. S.; Buyevich, A. V., Enantiomeric discrimination in the complexation of ortho-palladated  $\alpha$ -arylalkylamines with the racemic tert-Butylmethylphenylphosphine. *Tetrahedron: Asymmetry* **1995**, *6* (11), 2731-2746.
62. Yi, D.; Yongxin, L.; Yi, Z.; A., P. S.; Pak-Hing, L., Design, Synthesis, and Stereochemical Evaluation of a Novel Chiral Amine-Palladacycle. *Eur. J. Inorg. Chem.* **2008**, *2008* (11), 1880-1891.

63. Liu, X.; Mok, K.; Leung, P.-H., Metal template promoted hydroamination of ethynylphosphines and aniline. Asymmetric synthesis, coordination chemistry, and the imine-enamine tautomerism of P-chiral iminophosphines. *Organometallics* **2001**, *20* (18), 3918-3926.
64. Aw, B.-H.; Leung, P.-H., A simple route to an enantiomerically pure diphosphine ligand containing a phosphorus stereogenic centre. *Tetrahedron: Asymmetry* **1994**, *5* (7), 1167-1170.
65. Leung, P.-H.; Loh, S.-K.; Mok, K. F.; White, A. J. P.; Williams, D. J., A simple route to a novel enantiomerically pure P-chiral phosphine ligand containing a tertiary amide functional group. *Chem. Commun.* **1996**, (5), 591-592.
66. He, G.; Loh, S.-K.; Vittal, J. J.; Mok, K. F.; Leung, P.-H., Palladium-Complex-Promoted Asymmetric Synthesis of Stereoisomeric P-Chiral Pyridylphosphines via an Unusual Exo-Endo Stereochemically Controlled Asymmetric Diels-Alder Reaction between 2-Vinylpyridine and Coordinated 3,4-Dimethyl-1-phenylphosphole. *Organometallics* **1998**, *17* (18), 3931-3936.
67. Leung, P.-H., Asymmetric synthesis and organometallic chemistry of functionalized phosphines containing stereogenic phosphorus centers. *Acc. Chem. Res.* **2004**, *37* (3), 169-177.
68. Leung, P.-H.; Loh, S.-K.; J. Vittal, J.; J. P. White, A.; J. Williams, D., Asymmetric synthesis of keto-substituted P-chiral phosphines by means of an unusual exo/endo-stereochemically controlled Diels-Alder reaction. *Chem. Commun.* **1997**, (20), 1987-1988.
69. Leung, P.-H.; Qin, Y.; He, G.; Mok, K. F.; Vittal, J. J., Coordination chemistry, reactivities, and stereoelectronic properties of chelating phosphine ligands containing thioamide substituents. *J. Chem. Soc., Dalton Trans.* **2001**, (3), 309-314.
70. Song, Y.; Mok, K. F.; Leung, P.-H.; Chan, S.-H., A Palladium Complex Promoted Asymmetric Synthesis of a Novel P-Chiral Diphosphine Containing an Ester Functional Group. *Inorg. Chem.* **1998**, *37* (24), 6399-6401.
71. Gül, N.; Nelson, J. H., Use of an Enantiomerically Pure Cyclopalladated Complex of (S)-N,N-Dimethyl- $\alpha$ -(2-naphthyl)ethylamine for an Enantioselective Synthesis of a Chiral Diphosphine by an Intramolecular [4+2] Diels-Alder Cycloaddition. *Tetrahedron* **2000**, *56* (1), 71-78.
72. He, G.; Qin, Y.; Mok, K. F.; Leung, P.-H., Metal ion effects on the asymmetric dimerization of 1-phenyl-3,4-dimethylphosphole. *Chem. Commun.* **2000**, (2), 167-168.

73. Leung, P.-H.; Siah, S.-Y.; J. P. White, A.; J. Williams, D., Asymmetric syntheses, structures and reactions of palladium(II) complexes containing thiolato- and sulfinyl-substituted P chiral phosphines. *J. Chem. Soc., Dalton Trans.* **1998**, (6), 893-900.
74. Gugger, P. A.; Willis, A. C.; Wild, S. B.; Heath, G. A.; Webster, R. D.; Nelson, J. H., Enantioselective synthesis of a conformationally rigid, sterically encumbered, 2-arsino-7-phosphanorbornene. *J. Organomet. Chem.* **2002**, 643-644, 136-153.
75. Leung, P.-H.; He, G.; Lang, H.; Liu, A.; Loh, S.-K.; Selvaratnam, S.; Mok, K. F.; White, A. J. P.; Williams, D. J., Metal Template Synthesis and Coordination Chemistry of Functionalized P-Chiral Phosphanorbornenes. *Tetrahedron* **2000**, 56 (1), 7-15.
76. Li, Y.; Ng, K.-H.; Selvaratnam, S.; Tan, G.-K.; Vittal, J. J.; Leung, P.-H., Synthesis and the Stereoelectronic Properties of Novel Cyclopalladated Complexes Derived from Enantiomerically Pure (R/S)-N,N-Dimethyl-1-(9-phenanthryl)ethylamine. *Organometallics* **2003**, 22 (4), 834-842.
77. Leung, P.-H.; Ng, K.-H.; Li, Y.; J. P. White, A.; J. Williams, D., Designer cyclopalladated-amine catalysts for the asymmetric Claisen rearrangement. *Chem. Commun.* **1999**, (23), 2435-2436.
78. Chooi, S. Y. M.; Leung, P.-h.; Chin Lim, C.; Mok, K. F.; Quek, G. H.; Sim, K. Y.; Tan, M. K., Versatile chiral palladium(II) complexes for enantiomeric purities of 1,2-diamines. *Tetrahedron: Asymmetry* **1992**, 3 (4), 529-532.
79. Dunina, V. V.; Kuz'mina, L. G.; Rubina, M. Y.; Grishin, Y. K.; Veits, Y. A.; Kazakova, E. I., A resolution of the monodentate P\*-chiral phosphine PButC6H4Br-4 and its NMR-deduced absolute configuration. *Tetrahedron: Asymmetry* **1999**, 10 (8), 1483-1497.
80. Valk, J.-M.; Claridge, T. D. W.; Brown, J. M.; Hibbs, D.; Hursthouse, M. B., Synthesis and chemistry of a new P-N chelating ligand; (R) and (S)-6-(2'-diphenylphosphino-1'-naphthyl)phenanthridine. *Tetrahedron: Asymmetry* **1995**, 6 (10), 2597-2610.
81. Joan, A.; Ramon, B.; Magali, C. J.; Sergio, D.; Jaume, G.; Guillermo, M.; I. O. J.; Mercé, F. B.; Xavier, S., Synthesis, Resolution, and Reactivity of Benzylmesitylphenylphosphine: A New P-Chiral Bulky Ligand. *Chemistry – A European Journal* **2002**, 8 (10), 2279-2287.
82. Tani, K.; Brown, L. D.; Ahmed, J.; Ibers, J. A.; Nakamura, A.; Otsuka, S.; Yokota, M., Chiral metal complexes. 4. Resolution of racemic tertiary phosphines with chiral palladium(II) complexes. The

chemistry of diastereomeric phosphine palladium(II) species in solution. *J. Am. Chem. Soc.* **1977**, *99* (24), 7876-7886.

83. Dunina, V. V.; Golovan, E. B., A resolution of monodentate P\* chiral phosphine. *Tetrahedron: Asymmetry* **1995**, *6* (11), 2747-2754.

84. Albert, J.; Cadena, J. M.; Granell, J.; Muller, G.; Ordinas, J. I.; Panyella, D.; Puerta, C.; Sañudo, C.; Valerga, P., Resolution of Benzylcyclohexylphenylphosphine by Palladium(II)–Amine Metallacycles. A New Ligand for Asymmetric Hydrovinylation. *Organometallics* **1999**, *18* (17), 3511-3518.

85. Mai, D. N.; Wolfe, J. P., Asymmetric Palladium-Catalyzed Carboamination Reactions for the Synthesis of Enantiomerically Enriched 2-(Arylmethyl)- and 2-(Alkenylmethyl)pyrrolidines. *J. Am. Chem. Soc.* **2010**, *132* (35), 12157-12159.

86. A. Albisson, D.; B. Bedford, R.; Noelle Scully, P.; E. Lawrence, S., Orthopalladated triaryl phosphite complexes as highly active catalysts in biaryl coupling reactions. *Chem. Commun.* **1998**, (19), 2095-2096.

87. L. Shaw, B., Highly active, stable, catalysts for the Heck reaction; further suggestions on the mechanism. *Chem. Commun.* **1998**, (13), 1361-1362.

88. Nakhla, J. S.; Kampf, J. W.; Wolfe, J. P., Intramolecular Pd-Catalyzed Carboetherification and Carboamination. Influence of Catalyst Structure on Reaction Mechanism and Product Stereochemistry. *J. Am. Chem. Soc.* **2006**, *128* (9), 2893-2901.

89. Tang, W.; Zhang, X., New Chiral Phosphorus Ligands for Enantioselective Hydrogenation. *Chem. Rev.* **2003**, *103* (8), 3029-3070.

90. Dunina, V. V.; Gorunova, O. g. N.; Kuz'mina, L. G.; Livantsov, M. V.; Grishin, Y. K., First optically active P\*-chiral phosphapalladacycle. *Tetrahedron: Asymmetry* **1999**, *10* (20), 3951-3961.

91. Cowen, B. J.; Miller, S. J., Enantioselective [3+ 2]-cycloadditions catalyzed by a protected, multifunctional phosphine-containing  $\alpha$ -amino acid. *J. Am. Chem. Soc.* **2007**, *129* (36), 10988-10989.

92. Smith, S. W.; Fu, G. C., Asymmetric Carbon–Carbon Bond Formation  $\gamma$  to a Carbonyl Group: Phosphine-Catalyzed Addition of Nitromethane to Allenes. *J. Am. Chem. Soc.* **2009**, *131* (40), 14231-14233.

93. Wilson, J. E.; Fu, G. C., Synthesis of functionalized cyclopentenes through catalytic asymmetric [3+ 2] cycloadditions of allenes with enones. *Angew. Chem.* **2006**, *118* (9), 1454-1457.
94. Kagan, H.; Sasaki, M., Optically active phosphines: preparation, uses and chiroptical properties. *Organophosphorus Compounds (1990)* **1990**, 51-102.
95. Pietrusiewicz, K. M.; Zablocka, M., Preparation of scalemic P-chiral phosphines and their derivatives. *Chem. Rev.* **1994**, *94* (5), 1375-1411.
96. Grabulosa, A.; Granell, J.; Muller, G., Preparation of optically pure P-stereogenic trivalent phosphorus compounds. *Coord. Chem. Rev.* **2007**, *251* (1), 25-90.
97. Gibbons, S. K.; Xu, Z.; Hughes, R. P.; Glueck, D. S.; Rheingold, A. L., Chiral Bis(Phospholane) PCP Pincer Complexes: Synthesis, Structure, and Nickel-Catalyzed Asymmetric Phosphine Alkylation. *Organometallics* **2018**.
98. Albert, J.; Cadena, J. M.; Delgado, S.; Granell, J., Synthesis and resolution of a new P-chiral hydroxy phosphine. *J. Organomet. Chem.* **2000**, *603* (2), 235-239.
99. Albert, J.; Cadena, J. M.; Granell, J.; Muller, G.; Panyella, D.; Sañudo, C., Resolution of Secondary Phosphanes Chiral at Phosphorus by Means of Palladium Metallacycles. *Eur. J. Inorg. Chem.* **2000**, *2000* (6), 1283-1286.
100. Ng, J. K.-P.; Tan, G.-K.; Vittal, J. J.; Leung, P.-H., Optical Resolution and the Study of Ligand Effects on the Ortho-Metalation Reaction of Resolved ( $\pm$ )-Diphenyl [1-(1-naphthyl) ethyl] phosphine and Its Arsenic Analogue. *Inorg. Chem.* **2003**, *42* (23), 7674-7682.
101. Ng, J. K.-P.; Li, Y.; Tan, G.-K.; Koh, L.-L.; Vittal, J. J.; Leung, P.-H., Stereochemical Investigations of a Novel Class of Chiral Phosphapalladacycle Complexes Derived from 1-[(2,5-Dimethyl)phenyl]ethyldiphenylphosphine. *Inorg. Chem.* **2005**, *44* (26), 9874-9886.
102. Ng, J. K.-P.; Tan, G.-K.; Vittal, J. J.; Leung, P.-H., Optical Resolution and the Study of Ligand Effects on the Ortho-Metalation Reaction of Resolved ( $\pm$ )-Diphenyl[1-(1-naphthyl)ethyl]phosphine and Its Arsenic Analogue. *Inorg. Chem.* **2003**, *42* (23), 7674-7682.
103. Pullarkat, S. A.; Leung, P.-H., Chiral metal complex-promoted asymmetric hydrophosphinations. In *Hydrofunctionalization*, Springer: 2011; pp 145-166.
104. Pullarkat, S. A., Recent progress in palladium-catalyzed asymmetric hydrophosphination. *Synthesis* **2016**, *48* (4), 493-503.

105. Feng, J.-J.; Chen, X.-F.; Shi, M.; Duan, W.-L., Palladium-Catalyzed Asymmetric Addition of Diarylphosphines to Enones toward the Synthesis of Chiral Phosphines. *J. Am. Chem. Soc.* **2010**, *132* (16), 5562-5563.
106. Huang, Y.; Pullarkat, S. A.; Teong, S.; Chew, R. J.; Li, Y.; Leung, P.-H., Palladacycle-Catalyzed Asymmetric Intermolecular Construction of Chiral Tertiary P-Heterocycles by Stepwise Addition of H–P–H Bonds to Bis(enones). *Organometallics* **2012**, *31* (13), 4871-4875.
107. Xu, C.; Jun Hao Kennard, G.; Hennersdorf, F.; Li, Y.; Pullarkat, S. A.; Leung, P.-H., Chiral Phosphapalladacycles as Efficient Catalysts for the Asymmetric Hydrophosphination of Substituted Methylidenemalonate Esters: Direct Access to Functionalized Tertiary Chiral Phosphines. *Organometallics* **2012**, *31* (8), 3022-3026.
108. Jia, Y.-X.; Li, B.-B.; Li, Y.; Pullarkat, S. A.; Xu, K.; Hirao, H.; Leung, P.-H., Stereoelectronic and Catalytic Properties of Chiral Cyclometalated Phospha-palladium and-platinum Complexes. *Organometallics* **2014**, *33* (21), 6053-6058.
109. Hanley, P. S.; Hartwig, J. F., Intermolecular Migratory Insertion of Unactivated Olefins into Palladium–Nitrogen Bonds. Steric and Electronic Effects on the Rate of Migratory Insertion. *J. Am. Chem. Soc.* **2011**, *133* (39), 15661-15673.
110. Glueck, D. S., Recent advances in metal-catalyzed C–P bond formation. In *CX Bond Formation*, Springer: 2010; pp 65-100.
111. Chiang, M.; Li, Y.; Krishnan, D.; Sumod, P.; Ng, K. H.; Leung, P. H., Synthesis and Characterisation of a Novel Chiral Bidentate Pyridine-N-Heterocyclic Carbene-Based Palladacycle. *Eur. J. Inorg. Chem.* **2010**, *2010* (9), 1413-1418.
112. Yang, X.-Y.; Tay, W. S.; Li, Y.; Pullarkat, S. A.; Leung, P.-H., The synthesis and efficient one-pot catalytic "self-breeding" of asymmetrical NC(sp<sup>3</sup>)E-hybridised pincer complexes. *Chem. Commun.* **2016**, *52* (22), 4211-4214.
113. Tay, W. S.; Yang, X.-Y.; Li, Y.; Pullarkat, S. A.; Leung, P.-H., Efficient and stereoselective synthesis of monomeric and bimetallic pincer complexes containing Pd-bonded stereogenic carbons. *RSC Advances* **2016**, *6* (79), 75951-75959.
114. Yang, X.-Y.; Tay, W. S.; Li, Y.; Pullarkat, S. A.; Leung, P.-H., Versatile Syntheses of Optically Pure PCE Pincer Ligands: Facile Modifications of the Pendant Arms and Ligand Backbones. *Organometallics* **2015**, *34* (8), 1582-1588.

115. Yen Wong, E. H.; Jia, Y.-X.; Li, Y.; Pullarkat, S. A.; Leung, P.-H., Catalytic asymmetric synthesis of Pt- and Pd-PCP pincer complexes bearing a para-N pyridinyl backbone. *J. Organomet. Chem.* **2018**, *862*, 22-27.
116. Yang, X.-Y.; Gan, J. H.; Li, Y.; Pullarkat, S. A.; Leung, P.-H., Palladium catalyzed asymmetric hydrophosphination of [small alpha],[small beta]- and [small alpha],[small beta],[gamma],[small delta]-unsaturated malonate esters - efficient control of reactivity, stereo- and regio-selectivity. *Dalton Trans.* **2015**, *44* (3), 1258-1263.
117. Jia, Y.-X.; Yang, X.-Y.; Tay, W. S.; Li, Y.; Pullarkat, S. A.; Xu, K.; Hirao, H.; Leung, P.-H., Computational and carbon-13 NMR studies of Pt-C bonds in P-C-P pincer complexes. *Dalton Trans.* **2016**, *45* (5), 2095-2101.
118. Li, X.-R.; Yang, X.-Y.; Li, Y.; Pullarkat, S. A.; Leung, P.-H., Efficient access to a designed phosphapalladacycle catalyst via enantioselective catalytic asymmetric hydrophosphination. *Dalton Trans.* **2017**, *46* (4), 1311-1316.
119. Ng, J. K. P.; Chen, S.; Tan, G. K.; Leung, P. H., Substituent Effects on the Stereoelectronic and Chemical Properties of a Novel Phosphapalladacycle. *Eur. J. Inorg. Chem.* **2007**, *2007* (19), 3124-3134.
120. Ng, J. K.-P.; Chen, S.; Li, Y.; Tan, G.-K.; Koh, L.-L.; Leung, P.-H., Cyclopalladation of the Prochiral (Di-tert-butyl)(diphenylmethyl)phosphine: Kinetic Lability of the Corresponding (+)-Phosphapalladacyclic Pd-C Bond and the Reluctance of the Phosphine to Bind in a Monodentate Fashion. *Inorg. Chem.* **2007**, *46* (12), 5100-5109.
121. Pullarkat, S. A.; Tan, K.-W.; Ma, M.; Tan, G.-K.; Koh, L. L.; Vittal, J. J.; Leung, P.-H., Asymmetric synthesis of a P-chiral heteroditopic ligand via chiral metal template promoted cycloaddition between 3,4-dimethyl-1-phenylphosphole and its sulfonated analog. *J. Organomet. Chem.* **2006**, *691* (13), 3083-3088.
122. Tan, K.-W.; Liu, F.; Li, Y.; Tan, G.-K.; Leung, P.-H., Asymmetric synthesis of a chiral arsinophosphine via a metal template promoted asymmetric Diels-Alder reaction between diphenylvinylphosphine and 2-furyldiphenylarsine. *J. Organomet. Chem.* **2006**, *691* (22), 4753-4758.
123. Ma, M.; Pullarkat, S. A.; Li, Y.; Leung, P.-H., Novel Stereochemistry, Reactivity, and Stability of an Arsenic Heterocycle in a Metal-Promoted Asymmetric Cycloaddition Reaction. *Inorg. Chem.* **2007**, *46* (22), 9488-9494.

124. Ma, M.; Pullarkat, S. A.; Li, Y.; Leung, P.-H., Asymmetric synthesis of a chiral hetero-bidentate As–P ligand containing both As and P-stereogenic centres. *J. Organomet. Chem.* **2008**, *693* (20), 3289-3294.
125. Liu, F.; Pullarkat, S. A.; Tan, K.-W.; Li, Y.; Leung, P.-H., Organoplatinum Complex Promoted the Asymmetric Endo Stereochemically Controlled Diels–Alder Reaction between 3-Diphenylphosphinofuran and Diphenylvinylphosphine. *Inorg. Chem.* **2009**, *48* (23), 11394-11398.
126. Ma, M.; Pullarkat, S. A.; Chen, K.; Li, Y.; Leung, P.-H., Template effects on the asymmetric cycloaddition reaction between 3,4-dimethyl-1-phenylarsole and diphenylvinylphosphine and their arsenic elimination reaction. *J. Organomet. Chem.* **2009**, *694* (12), 1929-1933.
127. Ma, M.; Pullarkat, S. A.; Yuan, M.; Zhang, N.; Li, Y.; Leung, P.-H., Metal Effects on the Asymmetric Cycloaddition Reaction between 3,4-Dimethyl-1-phenylarsole and Diphenylvinylphosphine Oxide. *Organometallics* **2009**, *28* (16), 4886-4889.
128. Pullarkat, S. A.; Cheow, Y. L.; Li, Y.; Leung, P. H., Enantioselective, High-Yielding Synthesis of Alcohol-Functionalized Diphosphanes Utilizing Asymmetric Control with a Chiral Auxiliary. *Eur. J. Inorg. Chem.* **2009**, *2009* (16), 2375-2382.
129. Yuan, M.; Pullarkat, S. A.; Yeong, C. H.; Li, Y.; Krishnan, D.; Leung, P.-H., Controllable synthesis of P-chiral 1,2- and 1,3-diphosphines via asymmetric Diels-Alder reactions involving functionalized allylic phosphines as dienophiles. *Dalton Trans.* **2009**, (19), 3668-3670.
130. Ma, M.; Lu, R.; Pullarkat, S. A.; Deng, W.; Leung, P.-H., Steric effects on the control of endo/exo-selectivity in the asymmetric cycloaddition reaction of 3,4-dimethyl-1-phenylarsole. *Dalton Trans.* **2010**, *39* (23), 5453-5461.
131. Ma, M.; Pullarkat, S. A.; Li, Y.; Leung, P. H., Metal Effects on the Asymmetric Synthesis of a New Heterobidentate As/P=S Ligand. *Eur. J. Inorg. Chem.* **2010**, *2010* (12), 1865-1871.
132. Ma, M.; Li, J.; Zhang, N.; Yao, W.; Pullarkat, S. A.; Leung, P.-H., Metal effects on the asymmetric syntheses of chiral P–N bidentate ligands. *J. Organomet. Chem.* **2016**, *824*, 99-103.
133. Tang, L.; Zhang, Y.; Ding, L.; Li, Y.; Mok, K.-F.; Yeo, W.-C.; Leung, P.-H., Asymmetric synthesis of dimethyl-1,2-bis-(diphenylphosphino)-1,2-ethanedicarboxylate by means of a chiral

palladium template promoted hydrophosphination reaction. *Tetrahedron Lett.* **2007**, *48* (1), 33-35.

134. Zhang, Y.; Tang, L.; Ding, Y.; Chua, J.-H.; Li, Y.; Yuan, M.; Leung, P.-H., Base controlled (1, 1)-and (1, 2)-hydrophosphination of functionalized alkynes. *Tetrahedron Lett.* **2008**, *49* (11), 1762-1767.

135. Huang, Y.; Pullarkat, S. A.; Yuan, M.; Ding, Y.; Li, Y.; Leung, P.-H., Palladium Template Promoted Asymmetric Synthesis of 1,2-Diphosphines by Hydrophosphination of Functionalized Allenes. *Organometallics* **2010**, *29* (3), 536-542.

136. Pullarkat, S. A.; Yi, D.; Li, Y.; Tan, G.-K.; Leung, P.-H., A Novel Approach toward Asymmetric Synthesis of Alcohol Functionalized C-Chiral Diphosphines via Two-Stage Hydrophosphination of Terminal Alkynols. *Inorg. Chem.* **2006**, *45* (18), 7455-7463.

137. Yuan, M.; Pullarkat, S. A.; Ma, M.; Zhang, Y.; Huang, Y.; Li, Y.; Goel, A.; Leung, P.-H., Asymmetric Synthesis of Functionalized 1,2-Diphosphine via the Chemoselective Hydrophosphination of Coordinated Allylic Phosphines. *Organometallics* **2009**, *28* (3), 780-786.

138. Zhang, Y.; Pullarkat, S. A.; Li, Y.; Leung, P.-H., Asymmetric Synthesis of Diphosphine Ligands Containing Phosphorus and Carbon Stereogenic Centers by Means of a Chiral Palladium Complex Promoted Hydrophosphination Reaction. *Inorg. Chem.* **2009**, *48* (12), 5535-5539.

139. Zhang, Y.; Tang, L.; Pullarkat, S. A.; Liu, F.; Li, Y.; Leung, P.-H., Asymmetric synthesis of 1,2-bis(diphenylphosphino)-1-phenylethane via a chiral palladium template promoted hydrophosphination reaction. *J. Organomet. Chem.* **2009**, *694* (21), 3500-3505.

140. Yuan, M.; Pullarkat, S. A.; Li, Y.; Lee, Z.-Y.; Leung, P.-H., Novel Synthesis of Chiral 1,3-Diphosphines via Palladium Template Promoted Hydrophosphination and Functional Group Transformation Reactions. *Organometallics* **2010**, *29* (16), 3582-3588.

141. Yuan, M.; Pullarkat, S. A.; Li, Y.; Leung, P.-H., Palladacycle mediated synthesis of cyano-functionalized chiral 1, 2-diphosphine and subsequent functional group transformations. *J. Organomet. Chem.* **2011**, *696* (4), 905-912.

142. Chen, S.; Ng, J. K.-P.; Pullarkat, S. A.; Liu, F.; Li, Y.; Leung, P.-H., Asymmetric Synthesis of New Diphosphines and Pyridylphosphines via a Kinetic Resolution Process Promoted and

Controlled by a Chiral Palladacycle. *Organometallics* **2010**, *29* (15), 3374-3386.

143. Yuan, M.; Zhang, N.; Pullarkat, S. A.; Li, Y.; Liu, F.; Pham, P.-T.; Leung, P.-H., Asymmetric Synthesis of Functionalized 1,3-Diphosphines via Chiral Palladium Complex Promoted Hydrophosphination of Activated Olefins. *Inorg. Chem.* **2010**, *49* (3), 989-996.

144. Liu, F.; Pullarkat, S. A.; Li, Y.; Chen, S.; Yuan, M.; Lee, Z. Y.; Leung, P.-H., Highly Enantioselective Synthesis of (2-Pyridyl)phosphine Based C-Chiral Unsymmetrical P,N-Ligands Using a Chiral Palladium Complex. *Organometallics* **2009**, *28* (13), 3941-3946.

145. Jia, Y.-X.; Jonathan Chew, R.; Li, B.-B.; Zhu, P.; Li, Y.; Pullarkat, S. A.; Soon Tan, N.; Leung, P.-H., Palladacycle promoted base controlled regio- and enantioselective hydrophosphination of 2-pyridylacrylate/amide and the cytotoxicity of their gold complexes. *Dalton Trans.* **2015**, *44* (40), 17557-17564.

146. Yang, X.-Y.; Tay, W. S.; Li, Y.; Pullarkat, S. A.; Leung, P.-H., Asymmetric 1,4-Conjugate Addition of Diarylphosphines to  $\alpha,\beta,\gamma,\delta$ -Unsaturated Ketones Catalyzed by Transition-Metal Pincer Complexes. *Organometallics* **2015**, *34* (20), 5196-5201.

147. Chew, R. J.; Sepp, K.; Li, B. B.; Li, Y.; Zhu, P. C.; Tan, N. S.; Leung, P. H., An Approach to the Efficient Syntheses of Chiral Phosphino- Carboxylic Acid Esters. *Adv. Synth. Catal.* **2015**, *357* (14-15), 3297-3302.

148. Chew, R. J.; Li, X. R.; Li, Y.; Pullarkat, S. A.; Leung, P. H., Pd-Catalyzed Enantiodivergent and Regiospecific phospho-Michael Addition of Diphenylphosphine to 4-oxo-Enamides: Efficient Access to Chiral Phosphinocarboxamides and Their Analogues. *Chemistry—A European Journal* **2015**, *21* (12), 4800-4804.

149. Yang, X.-Y.; Li, Y.; Pullarkat, S. A., A One-Pot Diastereoselective Self Assembly of C-Stereogenic Copper (I) Diphosphine Clusters. *Inorg. Chem.* **2014**, *53* (19), 10232-10239.

150. Chew, R. J.; Teo, K. Y.; Huang, Y.; Li, B.-B.; Li, Y.; Pullarkat, S. A.; Leung, P.-H., Enantioselective phospho-Michael addition of diarylphosphines to  $\beta$ ,  $\gamma$ -unsaturated  $\alpha$ -ketoesters and amides. *Chem. Commun.* **2014**, *50* (63), 8768-8770.

151. Chew, R. J.; Lu, Y.; Jia, Y. X.; Li, B. B.; Wong, E. H. Y.; Goh, R.; Li, Y.; Huang, Y.; Pullarkat, S. A.; Leung, P. H., Palladacycle Catalyzed Asymmetric P H Addition of

Diarylphosphines to N-Enoyl Phthalimides. *Chemistry–A European Journal* **2014**, *20* (44), 14514-14517.

152. Chew, R. J.; Huang, Y.; Li, Y.; Pullarkat, S. A.; Leung, P. H., Enantioselective Addition of Diphenylphosphine to 3-Methyl-4-nitro-5-alkenylisoxazoles. *Adv. Synth. Catal.* **2013**, *355* (7), 1403-1408.

153. Huang, Y.; Chew, R. J.; Pullarkat, S. A.; Li, Y.; Leung, P.-H., Asymmetric Synthesis of Enaminophosphines via Palladacycle-Catalyzed Addition of Ph<sub>2</sub>PH to  $\alpha,\beta$ -Unsaturated Imines. *The Journal of Organic Chemistry* **2012**, *77* (16), 6849-6854.

154. Huang, Y.; Chew, R. J.; Li, Y.; Pullarkat, S. A.; Leung, P.-H., Direct Synthesis of Chiral Tertiary Diphosphines via Pd(II)-Catalyzed Asymmetric Hydrophosphination of Dienones. *Org. Lett.* **2011**, *13* (21), 5862-5865.

155. Li, X.-R.; Chew, R. J.; Li, Y.; Leung, P.-H., Investigation of Functional Group Effects on Palladium Catalysed Asymmetric P-H Addition. *Aust. J. Chem.* **2016**, *69* (5), 499-504.

156. Huang, Y.; Li, Y.; Leung, P.-H.; Hayashi, T., Asymmetric synthesis of P-stereogenic diarylphosphinites by palladium-catalyzed enantioselective addition of diarylphosphines to benzoquinones. *J. Am. Chem. Soc.* **2014**, *136* (13), 4865-4868.

157. Bungabong, M. L.; Tan, K. W.; Li, Y.; Selvaratnam, S. V.; Dongol, K. G.; Leung, P.-H., A Novel Asymmetric Hydroarsination Reaction Promoted by a Chiral Organopalladium Complex. *Inorg. Chem.* **2007**, *46* (11), 4733-4736.

158. Liu, F.; Pullarkat, S. A.; Li, Y.; Chen, S.; Leung, P. H., Novel Enantioselective Synthesis of Functionalized Pyridylarsanes by a Chiral Palladium Template Promoted Asymmetric Hydroarsination Reaction. *Eur. J. Inorg. Chem.* **2009**, *2009* (27), 4134-4140.

159. Cheow, Y. L.; Pullarkat, S. A.; Li, Y.; Leung, P.-H., Asymmetric hydroarsination reactions toward synthesis of alcohol functionalised C-chiral As-P ligands promoted by chiral cyclometallated complexes. *J. Organomet. Chem.* **2012**, *696* (26), 4215-4220.

160. Tay, W. S.; Yang, X.-Y.; Li, Y.; Pullarkat, S. A.; Leung, P.-H., Nickel catalyzed enantioselective hydroarsination of nitrostyrene. *Chem. Commun.* **2017**, *53* (47), 6307-6310.

161. Dupont, J.; Consorti, C. S.; Spencer, J., The potential of palladacycles: more than just precatalysts. *Chem. Rev.* **2005**, *105* (6), 2527-2572.

162. Bruno, N. C.; Tudge, M. T.; Buchwald, S. L., Design and preparation of new palladium precatalysts for C–C and C–N cross-coupling reactions. *Chemical science* **2013**, *4* (3), 916-920.
163. Bedford, R. B.; Cazin, C. S.; Holder, D., The development of palladium catalysts for CC and Cheteroatom bond forming reactions of aryl chloride substrates. *Coord. Chem. Rev.* **2004**, *248* (21-24), 2283-2321.
164. Altenhoff, G.; Goddard, R.; Lehmann, C. W.; Glorius, F., Sterically demanding, bioxazoline-derived N-heterocyclic carbene ligands with restricted flexibility for catalysis. *J. Am. Chem. Soc.* **2004**, *126* (46), 15195-15201.
165. Bedford, R. B.; Hazelwood, S. L.; Limmert, M. E.; Brown, J. M.; Ramdeehul, S.; Cowley, A. R.; Coles, S. J.; Hursthouse, M. B., The role of ligand transformations on the performance of phosphite- and phosphinite-based palladium catalysts in the Suzuki reaction. *Organometallics* **2003**, *22* (7), 1364-1371.
166. Consorti, C. S.; Zanini, M. L.; Leal, S.; Ebeling, G.; Dupont, J., Chloropalladated propargyl amine: A highly efficient phosphine-free catalyst precursor for the Heck reaction. *Org. Lett.* **2003**, *5* (7), 983-986.
167. Schnyder, A.; Indolese, A. F.; Studer, M.; Blaser, H. U., A New Generation of Air Stable, Highly Active Pd Complexes for C–C and C–N Coupling Reactions with Aryl Chlorides. *Angew. Chem. Int. Ed.* **2002**, *41* (19), 3668-3671.
168. Gruber, A. S.; Zim, D.; Ebeling, G.; Monteiro, A. L.; Dupont, J., Sulfur-containing palladacycles as catalyst precursors for the Heck reaction. *Org. Lett.* **2000**, *2* (9), 1287-1290.
169. Thakur, V. V.; Kumar, N. R.; Sudalai, A., Sulfilimine palladacycles: stable and efficient catalysts for carbon–carbon coupling reactions. *Tetrahedron Lett.* **2004**, *45* (14), 2915-2918.
170. Lin, C.-A.; Luo, F.-T., Polystyrene-supported recyclable palladacycle catalyst for Heck, Suzuki and Sonogashira reactions. *Tetrahedron Lett.* **2003**, *44* (41), 7565-7568.
171. Alonso, D. A.; Nájera, C.; Pacheco, M. C., C (sp<sup>2</sup>)-C (sp) and C (sp)-C (sp) Coupling Reactions Catalyzed by Oxime-Derived Palladacycles. *Adv. Synth. Catal.* **2003**, *345* (9-10), 1146-1158.
172. Cassar, D. J.; Ilyashenko, G.; Ismail, M.; Woods, J.; Hughes, D. L.; Richards, C. J., Enantioselective Synthesis and Application to the Allylic Imidate Rearrangement of Amine-Coordinated Palladacycle Catalysts of Cobalt Sandwich Complexes. *Chemistry–A European Journal* **2013**, *19* (52), 17951-17962.

173. Rodrigues, A.; Lee, E. E.; Batey, R. A., Enantioselective Palladium(II)-Catalyzed Formal [3,3]-Sigmatropic Rearrangement of 2-Allyloxypyridines and Related Heterocycles. *Org. Lett.* **2010**, *12* (2), 260-263.
174. Fischer, D. F.; Barakat, A.; Xin, Z. q.; Weiss, M. E.; Peters, R., The Asymmetric Aza-Claisen Rearrangement: Development of Widely Applicable Pentaphenylferrocenyl Palladacycle Catalysts. *Chemistry—A European Journal* **2009**, *15* (35), 8722-8741.
175. Mo, D.-L.; Yuan, T.; Ding, C.-H.; Dai, L.-X.; Hou, X.-L., Palladacycle-Catalyzed Methylenecyclopropanation of Bicyclic Alkenes with Propiolates. *The Journal of Organic Chemistry* **2013**, *78* (22), 11470-11476.
176. Mo, D.-L.; Chen, B.; Ding, C.-H.; Dai, L.-X.; Ge, G.-C.; Hou, X.-L., Switch of addition and ring-opening reactions of oxabicyclic alkenes with terminal alkynes by sp<sup>2</sup>-C, P- and sp<sup>3</sup>-C, P-palladacycle catalysis. *Organometallics* **2013**, *32* (16), 4465-4468.
177. Ge, G.-C.; Mo, D.-L.; Ding, C.-H.; Dai, L.-X.; Hou, X.-L., Palladacycle-catalyzed reaction of bicyclic alkenes with terminal ynones: Regiospecific synthesis of polysubstituted furans. *Org. Lett.* **2012**, *14* (22), 5756-5759.
178. Yuan, K.; Zhang, T. K.; Hou, X. L., A highly efficient palladacycle catalyst for hydrophenylation of C-, N-, and O-substituted bicyclic alkenes under aerobic condition. *The Journal of organic chemistry* **2005**, *70* (15), 6085-6088.
179. Brunel, J. M.; Heumann, A.; Buono, G., Highly efficient phosphapalladacyclic catalysts for the hydroarylation of norbornene. *Angew. Chem.* **2000**, *112* (11), 2022-2025.
180. Koshti, V.; Gaikwad, S.; Chikkali, S. H., Contemporary avenues in catalytic PH bond addition reaction: A case study of hydrophosphination. *Coord. Chem. Rev.* **2014**, *265*, 52-73.
181. Herrmann, W. A.; Brossmer, C.; Öfele, K.; Reisinger, C. P.; Priermeier, T.; Beller, M.; Fischer, H., Palladacycles as structurally defined catalysts for the Heck olefination of chloro- and bromoarenes. *Angewandte Chemie International Edition in English* **1995**, *34* (17), 1844-1848.
182. Pabel, M.; Willis, A. C.; Wild, S. B., First Resolution of a Free Fluorophosphine Chiral at Phosphorus. Resolution and Reactions of Free and Coordinated (±)-Fluorophenylisopropylphosphine. *Inorg. Chem.* **1996**, *35* (5), 1244-1249.
183. Allen, D. G.; McLaughlin, G. M.; Robertson, G. B.; Steffen, W. L.; Salem, G.; Wild, S. B., Resolutions with metal

complexes. Preparation and resolution of (R, S)-methylphenyl (8-quinolyl) phosphine and its arsenic analog. Crystal and molecular structure of (+) 589-[(R)-dimethyl (1-ethyl-. alpha.-naphthyl) aminato-C2, N][(S)-methylphenyl (8-quinolyl) phosphine] palladium (II) hexafluorophosphate. *Inorg. Chem.* **1982**, *21* (3), 1007-1014.

184. Roberts, N. K.; Wild, S. B., Resolutions using metal complexes. Synthesis, separation into diastereoisomers, and resolution of o-phenylenebis (methylphenylphosphine) using palladium complexes containing optically active ortho-metalated dimethyl (. alpha.-methylbenzyl) amines. *J. Am. Chem. Soc.* **1979**, *101* (21), 6254-6260.

185. Wild, S. B., Resolutions of tertiary phosphines and arsines with orthometallated palladium (II)—amine complexes. *Coord. Chem. Rev.* **1997**, *166*, 291-311.

186. Roberts, N. K.; Wild, S. B., Resolutions using metal complexes. Resolution of (RR,SS)-ortho-phenylenebis(methylphenylarsine) using internally diastereoisomeric palladium complexes. *J. Chem. Soc., Dalton Trans.* **1979**, (12), 2015-2021.

187. Chooi, S. Y. M.; Tan, M. K.; Leung, P.-H.; Mok, K. F., Stereochemical Investigation of Bis(bidentate)-Palladium(II) Complexes. Transmission of Ring Chiralities between Chelating Amine Ligands via Their Prochiral N-Methyl Substituents. *Inorg. Chem.* **1994**, *33* (14), 3096-3103.

188. Chooi, S. Y.; Hor, T. A.; Leung, P. H.; Mok, K., Stereochemical investigations of coordinated sulfur stereocenters. X-ray structures of diastereomers of (-) 589-[Pd {(R)-CH<sub>3</sub>CH (1-C<sub>10</sub>H<sub>6</sub>) NMe<sub>2</sub>-C<sub>2</sub>, N}(R/S)-{Ph<sub>2</sub>PCH<sub>2</sub>SMe-P, S}] PF<sub>6</sub>. *Inorg. Chem.* **1992**, *31* (8), 1494-1500.

189. Bergens, S. H.; Leung, P. H.; Bosnich, B.; Rheingold, A. L., Synthesis and structure of a biphenanthrol-palladium complex displaying an unusual bonding mode. *Organometallics* **1990**, *9* (8), 2406-2408.

190. Selander, N.; Szabó, K. J., Catalysis by palladium pincer complexes. *Chem. Rev.* **2010**, *111* (3), 2048-2076.

191. O'Reilly, M. E.; Veige, A. S., Trianionic pincer and pincer-type metal complexes and catalysts. *Chem. Soc. Rev.* **2014**, *43* (17), 6325-6369.

192. Albrecht, M.; van Koten, G., Platinum group organometallics based on "pincer" complexes: sensors, switches, and catalysts. *Angew. Chem. Int. Ed.* **2001**, *40* (20), 3750-3781.

193. Albrecht, M.; Lutz, M.; Spek, A. L.; van Koten, G., Organoplatinum crystals for gas-triggered switches. *Nature* **2000**, *406* (6799), 970.
194. Albrecht, M.; Gossage, R. A.; Lutz, M.; Spek, A. L.; van Koten, G., Diagnostic organometallic and metallodendritic materials for SO<sub>2</sub> gas detection: reversible binding of sulfur dioxide to arylplatinum (II) complexes. *Chemistry—A European Journal* **2000**, *6* (8), 1431-1445.
195. Weaver, J. D.; Recio, A.; Grenning, A. J.; Tunge, J. A., Transition Metal-Catalyzed Decarboxylative Allylation and Benzoylation Reactions. *Chem. Rev.* **2011**, *111* (3), 1846-1913.
196. Rauchfuss, T. B., Functionalized tertiary phosphines and related ligands in organometallic coordination chemistry and catalysis. In *Homogeneous Catalysis with Metal Phosphine Complexes*, Springer: 1983; pp 239-256.
197. Marinetti, A.; Voituriez, A., Enantioselective Phosphine Organocatalysis. *Synlett* **2010**, *2010* (02), 174-194.
198. L., M. J.; R., R. W., Nucleophilic Phosphine Organocatalysis. *Adv. Synth. Catal.* **2004**, *346* (9-10), 1035-1050.
199. Gan, K.; Sadeer, A.; Xu, C.; Li, Y.; Pullarkat, S. A., Asymmetric Construction of a Ferrocenyl Phosphapalladacycle from Achiral Enones and a Demonstration of Its Catalytic Potential. *Organometallics* **2014**, *33* (19), 5074-5076.
200. Xie, J.-H.; Zhu, S.-F.; Zhou, Q.-L., Transition metal-catalyzed enantioselective hydrogenation of enamines and imines. *Chem. Rev.* **2010**, *111* (3), 1713-1760.
201. Wauters, I.; Debrouwer, W.; Stevens, C. V., Preparation of phosphines through C–P bond formation. *Beilstein journal of organic chemistry* **2014**, *10*, 1064.
202. Rosenberg, L., Mechanisms of Metal-Catalyzed Hydrophosphination of Alkenes and Alkynes. *ACS Catalysis* **2013**, *3* (12), 2845-2855.
203. Luehr, S.; Holz, J.; Boerner, A., The synthesis of chiral phosphorus ligands for use in homogeneous metal catalysis. *ChemCatChem* **2011**, *3* (11), 1708-1730.
204. Kolodiazny, O. I., Recent developments in the asymmetric synthesis of P-chiral phosphorus compounds. *Tetrahedron: Asymmetry* **2012**, *23* (1), 1-46.
205. Kolodiazny, O. I.; Kukhar, V. P.; Kolodiazna, A. O., Asymmetric catalysis as a method for the synthesis of chiral organophosphorus compounds. *Tetrahedron: Asymmetry* **2014**, *25* (12), 865-922.

206. S., G. D., Catalytic Asymmetric Synthesis of Chiral Phosphanes. *Chemistry – A European Journal* **2008**, *14* (24), 7108-7117.
207. Staubitz, A.; Robertson, A. P.; Sloan, M. E.; Manners, I., Amine- and phosphine- borane adducts: new interest in old molecules. *Chem. Rev.* **2010**, *110* (7), 4023-4078.
208. Brunel, J. M.; Faure, B.; Maffei, M., Phosphane-boranes: Synthesis, characterization and synthetic applications. *Coord. Chem. Rev.* **1998**, *178*, 665-698.
209. Busacca, C. A.; Raju, R.; Grinberg, N.; Haddad, N.; James-Jones, P.; Lee, H.; Lorenz, J. C.; Saha, A.; Senanayake, C. H., Reduction of tertiary phosphine oxides with DIBAL-H. *The Journal of organic chemistry* **2008**, *73* (4), 1524-1531.
210. Trepohl, V. T.; Mori, S.; Itami, K.; Oestreich, M., Palladium (II)-Catalyzed Conjugate Phosphination of Electron-Deficient Acceptors. *Org. Lett.* **2009**, *11* (5), 1091-1094.
211. Stankevič, M.; Pietrusiewicz, K. M., The synthesis and reactivity of phosphinous acid-boranes. *Synthesis* **2005**, *2005* (08), 1279-1290.
212. Hirohisa, O.; Hideki, Y.; Koichiro, O., Cobalt-Catalyzed syn Hydrophosphination of Alkynes. *Angew. Chem. Int. Ed.* **2005**, *44* (16), 2368-2370.
213. Yang, M.-J.; Liu, Y.-J.; Gong, J.-F.; Song, M.-P., Unsymmetrical Chiral PCN Pincer Palladium (II) and Nickel (II) Complexes with Aryl-Based Aminophosphine-Imidazoline Ligands: Synthesis via Aryl C-H Activation and Asymmetric Addition of Diarylphosphines to Enones. *Organometallics* **2011**, *30* (14), 3793-3803.
214. Lu, J.; Ye, J.; Duan, W.-L., Palladium-catalyzed asymmetric 1, 6-addition of diarylphosphines to  $\alpha$ ,  $\beta$ ,  $\gamma$ ,  $\delta$ -unsaturated sulfonic esters: controlling regioselectivity by rational selection of electron-withdrawing groups. *Chem. Commun.* **2014**, *50* (6), 698-700.
215. Yang, X.-Y.; Gan, J. H.; Li, Y.; Pullarkat, S. A.; Leung, P.-H., Palladium catalyzed asymmetric hydrophosphination of  $\alpha$ ,  $\beta$ - and  $\alpha$ ,  $\beta$ ,  $\gamma$ ,  $\delta$ -unsaturated malonate esters—efficient control of reactivity, stereo- and regio-selectivity. *Dalton Trans.* **2015**, *44* (3), 1258-1263.
216. Dunina, V. V.; Gorunova, O. N., Phosphapalladacycles: forms of existence and reactions. *Russian chemical reviews* **2005**, *74* (10), 871-913.

217. Bedford, R. B., Palladacyclic catalysts in C–C and C–heteroatom bond-forming reactions. *Chem. Commun.* **2003**, (15), 1787-1796.

218. Chinchilla, R.; Nájera, C., The Sonogashira reaction: a booming methodology in synthetic organic chemistry. *Chem. Rev.* **2007**, *107* (3), 874-922.

219. Bellina, F.; Carpita, A.; Rossi, R., Palladium catalysts for the Suzuki cross-coupling reaction: an overview of recent advances. *Synthesis* **2004**, *2004* (15), 2419-2440.

220. Beletskaya, I. P.; Cheprakov, A. V., Palladacycles in catalysis—a critical survey. *J. Organomet. Chem.* **2004**, *689* (24), 4055-4082.

221. Leung, P. H.; Willis, A. C.; Wild, S. B., Resolutions involving metal complexation. Optical resolution and photochemical rearrangement of (.+.-)-(2-mercaptoethyl) methylphenylphosphine. *Inorg. Chem.* **1992**, *31* (8), 1406-1410.

222. Aw, B.-H.; Selvaratnam, S.; Leung, P.-H.; Rees, N. H.; McFarlane, W., NMR assignment of absolute configuration of a P-chiral diphosphine and mechanics of its stereoselective formation. *Tetrahedron: Asymmetry* **1996**, *7* (6), 1753-1762.

223. Huang, Y.; Pullarkat, S. A.; Li, Y.; Leung, P.-H., Palladacycle-Catalyzed Asymmetric Hydrophosphination of Enones for Synthesis of C\*- and P\*-Chiral Tertiary Phosphines. *Inorg. Chem.* **2012**, *51* (4), 2533-2540.

224. Ding, Y.; Chiang, M.; Pullarkat, S. A.; Li, Y.; Leung, P.-H., Synthesis, Coordination Characteristics, Conformational Behavior, and Bond Reactivity Studies of a Novel Chiral Phosphapalladacycle Complex. *Organometallics* **2009**, *28* (15), 4358-4370.

225. Vicente, J.; Arcas, A., Aqua palladium complexes: Synthesis, properties and applications. *Coord. Chem. Rev.* **2005**, *249* (11-12), 1135-1154.

226. Corey, E.; Chaykovsky, M., Dimethyloxosulfonium methylide ((CH<sub>3</sub>)<sub>2</sub>SOCH<sub>2</sub>) and dimethylsulfonium methylide ((CH<sub>3</sub>)<sub>2</sub>SCH<sub>2</sub>). Formation and application to organic synthesis. *J. Am. Chem. Soc.* **1965**, *87* (6), 1353-1364.

227. Pohlhaus, P. D.; Sanders, S. D.; Parsons, A. T.; Li, W.; Johnson, J. S., Scope and Mechanism for Lewis Acid-Catalyzed Cycloadditions of Aldehydes and Donor– Acceptor Cyclopropanes: Evidence for a Stereospecific Intimate Ion Pair Pathway. *J. Am. Chem. Soc.* **2008**, *130* (27), 8642-8650.

228. Skvorcova, M.; Grigorjeva, L.; Jirgensons, A., Tetrahydro-1, 3-oxazepines via intramolecular Amination of Cyclopropylmethyl Cation. *Org. Lett.* **2015**, *17* (12), 2902-2904.

229. Pregosin, P.; Rüedi, R., Reactions of palladium (II) cyclometallated benzylideneaniline Schiff's bases. Some relative rates for the synthesis of ortho-substituted carbomethoxy derivatives via CO insertion. *J. Organomet. Chem.* **1984**, *273* (3), 401-413.

230. Nguyen, H.-K.; Asseline, U.; Dupret, D.; Thuong, N. T., Studies towards the design of a modified GC base pair with stability similar to that of the AT base pair. *Tetrahedron Lett.* **1997**, *38* (23), 4083-4086.

231. Huang, Y.; Pullarkat, S. A.; Li, Y.; Leung, P.-H., Palladium (II)-catalyzed asymmetric hydrophosphination of enones: efficient access to chiral tertiary phosphines. *Chem. Commun.* **2010**, *46* (37), 6950-6952.

232. Michael, F. E.; Cochran, B. M., Room temperature palladium-catalyzed intramolecular hydroamination of unactivated alkenes. *J. Am. Chem. Soc.* **2006**, *128* (13), 4246-4247.

233. Ohff, M.; Ohff, A.; Milstein, D., Highly active PdII cyclometallated imine catalysts for the Heck reaction. *Chem. Commun.* **1999**, (4), 357-358.

234. Nowotny, M.; Hanefeld, U.; van Koningsveld, H.; Maschmeyer, T., Cyclopalladated imine catalysts in Heck arylation: search for the catalytic species Electronic supplementary information (ESI) available: selected spectroscopic data for 1d, 2a and 2b. *Chem. Commun.* **2000**, (19), 1877-1878.

235. Gai, X.; Grigg, R.; Ramzan, M. I.; Sridharan, V.; Collard, S.; Muir, J. E., Pyrazole and benzothiazole palladacycles: stable and efficient catalysts for carbon-carbon bond formation. *Chem. Commun.* **2000**, (20), 2053-2054.

236. V Dunina, V., Chiral Cyclopalladated Compounds: New Structures, Methodologies and Applications. A Personal Account. *Curr. Org. Chem.* **2011**, *15* (18), 3415-3440.

237. Gorunova, O. N.; Livantsov, M. V.; Grishin, Y. K.; Kataeva, N. A.; Kochetkov, K. A.; Churakov, A. V.; Kuz'mina, L. G.; Dunina, V. V., Asymmetric synthesis and absolute configuration of a planar chiral phosphapalladacycle with a ferrocenyl framework. *Polyhedron* **2012**, *31* (1), 37-43.

238. Gorunova, O.; Grishin, Y. K.; Ilyin, M.; Kochetkov, K.; Churakov, A.; Kuz, L.; Dunina, V., Enantioselective catalysis of Suzuki reaction with planar-chiral CN-palladacycles: competition of two catalytic cycles. *Russ. Chem. Bull.* **2017**, *66* (2), 282-292.

239. Wang, H.; Lu, W.; Zhang, J., Ferrocene Derived Bifunctional Phosphine-Catalyzed Asymmetric Oxa-[4+ 2] Cycloaddition of  $\alpha$ -Substituted Allenones with Enones. *Chem. - Eur. J.* **2017**, *23* (55), 13587-13590.
240. Lin, W.-J.; Shia, K.-S.; Song, J.-S.; Wu, M.-H.; Li, W.-T., Synthesis of (E)-oxindolylidene acetate using tandem palladium-catalyzed Heck and alkoxyacylation reactions. *Organic & biomolecular chemistry* **2016**, *14* (1), 220-228.
241. Loubidi, M.; Moutardier, A.; Campos, J. F.; Berteina-Raboin, S., Pd-catalyzed Suzuki/Sonogashira cross-coupling reaction and the direct sp<sup>3</sup> arylation of 7-chloro-5-methyl-[1, 2, 4] triazolo [1, 5-a] pyrimidine. *Tetrahedron Lett.* **2018**, *59* (11), 1050-1054.
242. Castanheiro, T.; Schoenfelder, A.; Suffert, J.; Donnard, M.; Gulea, M., Comparative study on the reactivity of propargyl and alkynyl sulfides in palladium-catalyzed domino reactions. *Comptes Rendus Chimie* **2017**, *20* (6), 624-633.
243. Rizkin, B. A.; Hartman, R. L., Catalytic activity of Pd/hydrophilic phosphine ligand in the interface of an aqueous-phase Cu-free Sonogashira coupling. *Reaction Chemistry & Engineering* **2018**, *3* (3), 251-257.
244. Koukal, P.; Dvořáková, H.; Dvořák, D.; Tobrman, T., Palladium-catalysed Claisen rearrangement of 6-allyloxypurines. *Chemical Papers* **2013**, *67* (1), 3-8.
245. Rodrigues, E. G.; Silva, L. S.; Fausto, D. M.; Hayashi, M. S.; Dreher, S.; Santos, E. L.; Pesquero, J. B.; Travassos, L. R.; Caires, A. C., Cyclopalladated compounds as chemotherapeutic agents: antitumor activity against a murine melanoma cell line. *Int. J. Cancer* **2003**, *107* (3), 498-504.
246. Li, C.; Bian, Q.-L.; Xu, S.; Duan, W.-L., Palladium-catalyzed 1, 4-addition of secondary alkylphenylphosphines to  $\alpha$ ,  $\beta$ -unsaturated carbonyl compounds for the synthesis of phosphorus-and carbon-stereogenic compounds. *Organic Chemistry Frontiers* **2014**, *1* (5), 541-545.
247. Du, D.; Duan, W.-L., Palladium-catalyzed 1,4-addition of diarylphosphines to  $\alpha,\beta$ -unsaturated N-acylpyrroles. *Chem. Commun.* **2011**, *47* (39), 11101-11103.
248. Longmire, J. M.; Zhang, X.; Shang, M., Synthesis and X-ray Crystal Structures of Palladium (II) and Platinum (II) Complexes of the PCP-Type Chiral Tridentate Ligand (1 R, 1 'R)-1, 3-Bis [1-(diphenylphosphino) ethyl] benzene. Use in the Asymmetric Aldol Reaction of Methyl Isocynoacetate and Aldehydes. *Organometallics* **1998**, *17* (20), 4374-4379.

249. Zhu, X.; Chiba, S., Construction of 1-pyrroline skeletons by Lewis acid-mediated conjugate addition of vinyl azides. *Chem. Commun.* **2016**, 52 (12), 2473-2476.
250. Grabulosa, A., *P-Stereogenic ligands in enantioselective catalysis*. Royal Society of Chemistry: 2010.
251. Li, B.-B.; Jia, Y.-X.; Zhu, P.-C.; Chew, R. J.; Li, Y.; Tan, N. S.; Leung, P.-H., Highly selective anti-cancer properties of ester functionalized enantiopure dinuclear gold(I)-diphosphine. *European Journal of Medicinal Chemistry* **2015**, 98, 250-255.
252. Dong, J.; Krasnova, L.; Finn, M. G.; Sharpless, K. B., Sulfur(VI) Fluoride Exchange (SuFEx): Another Good Reaction for Click Chemistry. *Angew. Chem. Int. Ed.* **2014**, 53 (36), 9430-9448.
253. C., K. H.; G., F. M.; Barry, S. K., Click Chemistry: Diverse Chemical Function from a Few Good Reactions. *Angew. Chem. Int. Ed.* **2001**, 40 (11), 2004-2021.
254. Hett, E. C.; Xu, H.; Geoghegan, K. F.; Gopalsamy, A.; Kyne, R. E.; Menard, C. A.; Narayanan, A.; Parikh, M. D.; Liu, S.; Roberts, L.; Robinson, R. P.; Tones, M. A.; Jones, L. H., Rational Targeting of Active-Site Tyrosine Residues Using Sulfonyl Fluoride Probes. *ACS Chemical Biology* **2015**, 10 (4), 1094-1098.
255. Qin, H. L.; Zheng, Q.; Bare, G. A. L.; Wu, P.; Sharpless, K. B., A Heck–Matsuda Process for the Synthesis of  $\beta$ -Arylethenesulfonyl Fluorides: Selectively Addressable Bis-electrophiles for SuFEx Click Chemistry. *Angew. Chem. Int. Ed.* **2016**, 55 (45), 14155-14158.
256. Chapman, C. J.; Frost, C. G.; Mahon, M. F., Structure and reactivity of new phosphine ligands containing the hemi-labile sulfone moiety. *Dalton Trans.* **2006**, (18), 2251-2262.
257. Dai, L.-X.; Hou, X.-L., *Chiral ferrocenes in asymmetric catalysis: synthesis and applications*. John Wiley & Sons: 2010.
258. Fahrney, D. E.; Gold, A. M., Sulfonyl fluorides as inhibitors of esterases. I. Rates of reaction with acetylcholinesterase,  $\alpha$ -chymotrypsin, and trypsin. *J. Am. Chem. Soc.* **1963**, 85 (7), 997-1000.
259. Ohnuma, S.; Chufan, E.; Nandigama, K.; Jenkins, L. M. M.; Durell, S. R.; Appella, E.; Sauna, Z. E.; Ambudkar, S. V., Inhibition of multidrug resistance-linked P-glycoprotein (ABCB1) function by 5'-fluorosulfonylbenzoyl 5'-adenosine: evidence for an ATP analogue that interacts with both drug-substrate-and nucleotide-binding sites. *Biochemistry* **2011**, 50 (18), 3724-3735.

260. Wiksell, E.; Larsson-Raźnikiewicz, M., Affinity labeling of phosphoglycerate kinase by 5'-[p-(fluorosulfonyl) benzoyl]-1, N6-ethenoadenosine. *J. Biol. Chem.* **1987**, *262* (30), 14472-14478.

261. Krutak, J. J.; Burpitt, R. D.; Moore, W. H.; Hyatt, J. A., Chemistry of ethenesulfonyl fluoride. Fluorosulfonylethylation of organic compounds. *The Journal of Organic Chemistry* **1979**, *44* (22), 3847-3858.

262. Pullarkat, S. A.; Leung, P.-H., Chiral Metal Complex-Promoted Asymmetric Hydrophosphinations. In *Hydrofunctionalization*, Ananikov, V. P.; Tanaka, M., Eds. Springer Berlin Heidelberg: Berlin, Heidelberg, 2013; pp 145-166.

## Publications and Conferences

1. **Li Xi-Rui**, Yang Xiang-Yuan, Li Yongxin, Pullarkat, Sumod A., and Leung Pak-Hing\*, “Efficient access to a designed phosphapalladacycle catalyst *via* enantioselective catalytic asymmetric Hydrophosphination”, *Dalton Transactions*, **2017**, 46(4), p: 1311-1316;
2. **Li Xi-Rui**, Chew Renta Jonathan, Li Yongxin, and Leung, Pak-Hing\*, “Investigation of Functional Group Effects on Palladium Catalysed Asymmetric P-H Addition”, *Australian Journal of Chemistry*, **2016**, 69(5), p: 499-504, (In memory of Emeritus Professor Brice Bosnich for his contributions to the field of organophosphorus chemistry and in catalysis);
3. **Li Xi-Rui**, Chen Yu, Pang PiaoXiang Benjamin, Tan Jaeyu, Sumod A. Pullarkat, and Leung Pak-Hing\*, “Efficient Synthesis of Malonate Functionalized Chiral Phosphapalladacycles and their Catalytic Evaluation in Asymmetric Hydrophosphination of Chalcone”, *European Journal of Inorganic Chemistry*, **2018**, 39, p:4385-4390;
4. **Li Xi-Rui**, Chen Houguang Jeremy, Wang weifan, Ma Mengtao, Chen Yu, Li Yongxin, Sumod A. Pullarkat, and Leung Pak-Hing\*, “Asymmetric catalytic P-H addition reaction of  $\alpha,\beta$ -unsaturated sulfonyl fluoride”, manuscript under preparing;
5. Chew Renta Jonathan, **Li Xi-Rui**, Li Yongxin, Pullarkat Sumod A, and Leung, Pak-Hing\*, “Pd-Catalyzed Enantiodivergent and Regiospecific phospho-Michael Addition of Diphenylphosphine to 4-oxo-Enamides: Efficient Access to Chiral Phosphinocarboxamides and Their Analogues”, *Chemistry–A European Journal*, **2015**, 21(12), p: 4800-4804;

6. *Pacificchem 2015*, Hawaii USA, **2015**, “Pd-Catalyzed Enantiodivergent and Regiospecific phospho-Michael Addition of Diphenylphosphine to 4-oxo-Enamides: Efficient Access to Chiral Phosphinocarboxamides and Their Analogues”.
7. *SICS-2016 (Singapore Inorganic Chemistry Symposium 2016)*, NTU Singapore, **2016**, “Efficient access to a designed phosphapalladacycle catalyst *via* enantioselective catalytic asymmetric hydrophosphination”;
8. *ISCOC-ISCIC 2016*, NUS Singapore, **2016**, “Investigation of Functional Group Effects on Palladium Catalysed Asymmetric P–H Addition”;
9. *ICMFC-3(3rd International Conference on Molecular & Functional Catalysis 2017)*, NUS Singapore, **2017**, “Pd-catalyzed asymmetric Michael addition of diphenylphosphine”.